Alma Mater Studiorum - Università di Bologna

School of Engineering

Department of Civil, Chemical, Environmental, and Materials Engineering - DICAM

Second Cycle Degree/Two Year Master in Offshore Engineering

MASTER THESIS
IN
OCEAN ENGINEERING AND MARINE RENEWABLE ENERGIES

WEC-Sim Application for the Assessment of Wave Energy Generation in the Tyrrhenian Sea and the North Sea Through the 2-Body Point Absorber (2BPA) and the Oscillating Surge Wave Energy Converter (OSWEC)

Student:

Babak Shafiei

Matricola: 931676

Supervisor:

Prof. Engr. Renata Archetti

Co-Supervisors:

Engr. Muhammad Ahsan Khan

Academic Year 2021/22

Acknowledgments

This dissertation was completed under the supervision and guidance of Professor Renata Archetti. Her enthusiasm for this dissertation was indicative of the spirit of adventure that made this dissertation possible. A genius's attitude and substance are both present in her, and her guidance and ongoing assistance allowed this dissertation to be completed.

On this occasion, I would like to thank my co-supervisor, Engineer Muhammad Ahsan Khan, for his guidance and constant supervision, for providing information about the thesis, and for his support in completing the thesis.

In closing, I want to acknowledge my parents' consideration and encouragement, which enabled me to complete this dissertation.
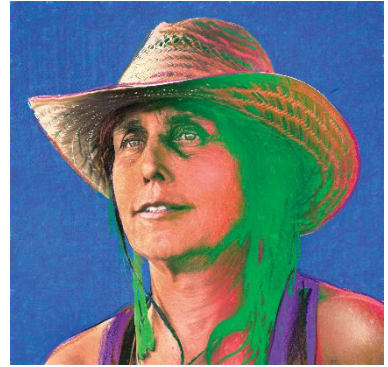
Engr. Babak Shafiei

Abstract

In recent years, developed countries have turned their attention to clean and renewable energy, such as wind energy and wave energy that can be converted to electrical power. Companies and academic groups worldwide are investigating several wave energy ideas today. Accordingly, this thesis studies the numerical simulation of the dynamic response of the wave energy converters (WECs) subjected to the ocean waves.

This study considers a two-body point absorber (2BPA) and an oscillating surge wave energy converter (OSWEC). The first aim is to mesh the bodies of the earlier mentioned WECs to calculate their hydrostatic properties using axiMesh.m and Mesh.m functions provided by NEMOH. The second aim is to calculate the first-order hydrodynamic coefficients of the WECs using the NEMOH BEM solver and to study the ability of this method to eliminate irregular frequencies. The third is to generate a *.h5 file for 2BPA and OSWEC devices, in which all the hydrodynamic data are included. The BEMIO, a pre-and post-processing tool developed by WEC-Sim, is used in this study to create *.h5 files. The primary and final goal is to run the wave energy converter Simulator (WEC-Sim) to simulate the dynamic responses of WECs studied in this thesis and estimate their power performance at different sites located in the Mediterranean Sea and the North Sea.

The hydrodynamic data obtained by the NEMOH BEM solver for the 2BPA and OSWEC devices studied in this thesis is imported to WEC-Sim using BEMIO. Lastly, the power matrices and annual energy production (AEP) of WECs are estimated for different sites located in the Sea of Sicily, Sea of Sardinia, Adriatic Sea, Tyrrhenian Sea, and the North Sea. To this end, the NEMOH and WEC-Sim are still the most practical tools to estimate the power generation of WECs numerically.

Key words: wave energy converters (WECs), two-body point absorber (2BPA), oscillating surge wave energy converter (OSWEC), NEMOH, BEMIO, wave energy converter Simulator (WEC-Sim), power matrices, annual energy production (AEP)

IV

If you're going to spend most of your time in your democracy figuring out how to get oil by intervening in other people's countries and ensuring that you follow it with military might, we think there's an alternative. Which would be renewable energy.

-Winona LaDuke

Contents

Contents

List of Figures

List of Tables

Acronyms

DICAM   Dipartimento di Ingegneria Civile, Chimica, Ambientale e dei Materiali

WECs   Wave Energy Converters

OEE   Ocean Energy Europe

MW   Megawatt

TW   Terawatts

kWh   Kilowatt-hour

PTO   Power Take-Off

Bref-HB   Small Bottom-Referenced Heaving Buoy

Bref-SHB   Bottom-Referenced Submerged Heave-Buoy

F-2HB   Floating Two-Body Heaving Converter

2BPA   Two-body point absorber

B-HBA   Bottom-Fixed Heave-Buoy Array

F-HBA   Floating Heave-Buoy Array

OSWEC   Oscillating Surge Wave Energy Converter

B-OF   Bottom-Fixed Oscillating Flap

F-3OF   Floating Three-Body- Oscillating Flap Device

F-OWC   Floating Oscillating Water Column

WEC-Sim   Wave Energy Converter Simulator

RM3   Reference Model 3

FPS   Floating Power System

NREL   National Renewable Energy Lab.

CFD   Computational Fluid Dynamics

PCC   Power Conversion Chain

FEA   Finite Element Analysis

PG&E   Pacific Gas and Electric Company

OES   Ocean Energy System

RM5   Reference Model 5

BEM   Boundary Element Methods

LHEEA   LABORATOIRE DE RECHERCHE EN HYDRODYNAMIQUE,
                              ÉNERGETIQUE ET ENVIRONNEMENT ATMOSPHERIQUE

PM   Pierson–Moskowitz

AEP   Annual Energy Production

HDF5	Hierarchical Data Format version 5
COB	Center of Buoyancy
COG	Center of Mass
SWL	Still Water Level
IRF	Impulse Response Function
CAD	Computer-Aided Design
DOF	Degree of Freedom
FPS	Floating Power System
NDBC	National Data Buoy Center
CDIP	Coastal Data Information Program
CFD	Computational Fluid Dynamics
W2W	Waves to Weather
BVP	Boundary Value Problem
FOSWEC	Floating Oscillating Surge Wave Energy Converter
CIC	Convolution Integral Calculator
CMEMS	Copernicus Monitoring Environment Marine Service

1.

Introduction

1.1 Wave Energy Converters (WECs)

Sea waves' kinetic energy and potential energy are turned into mechanical or electrical energy by wave energy converters (WECs). The WECs can produce pure energy to run the electrical network and several other uses such as motive force for ocean transports or pumping seawater desalination. Even though wave power has been explored since at least 1890, it isn't widely used at this time [1]. Ocean Energy Europe (OEE) is a global comprehensive ocean energy network of experts. Over 120 companies, including Europe's best utilities, manufacturers, and investigation institutes, grant OEE to serve the benefits of Europe's ocean energy sector. According to the OEE's yearly Ocean Energy Europe Conference & Exhibition report in 2020 [2], there were 23.3 megawatts (MW) of wave energy cumulative installations worldwide, while Europe's share of wave energy cumulative installations was 12 MW, of which 1.1 MW is currently in the water. However, the values mentioned earlier are significantly less than the world's total wave resource, expected to be two terawatts (TW) of energy, equal to the world's electricity consumption [3]. An essential reason is the production prices per kilowatt-hour (kWh), which were in 2020 about a factor of ten that is more high-priced than offshore wind farms [4]. Considering the facts discussed above, the predictions for 2021 appear to be 3.1 MW of capacity for wave energy projects planned for development [2].

Plenty of innovative techniques for wave energy conversion has been revealed in the last three decades, ending in thousands of patents over the current years. Today, several various wave energy ideas are being studied by companies and academic research groups worldwide. Although many functional devices have been produced and tested by modeling and wave tank tests, few have progressed to sea testing. Substantial cost reductions, which are only feasible with a sharp increase in global application, might allow wave plants to compete well with conventional power plants in the future [5].

1.1.1 Point Absorber Wave Energy Converter

Point absorbers derive energy by the relative motion within a body that moves in response to wave forcing and fixed body or motionless structures. The moving body may be on the water surface or submerged, and the fixed body may be on the seabed or a different structure less influenced by wave activity. Their primary dimension is small relative to the length of waves.

Electricity is produced via a hydraulic power take-off (PTO) system. There are different types of point absorbers based on their working principles, such as [6]:

- Small bottom-referenced heaving buoy (Bref-HB)
- Bottom-referenced submerged heave-buoy (Bref-SHB)
- Floating two-body heaving converter (F-2HB) or two-body point absorber (2BPA)
- Bottom-fixed heave-buoy array (B-HBA)
- Floating heave-buoy array (F-HBA)

The 2BPA is the focus of this study. This device is an axisymmetric, self-reacting two-body system, operating in the heave mode [6]. When equipped with a hydraulic PTO system, a 2BPA uses the relative movement between a float and a spar with a heave plate to drive the pushrod and convert wave energy [7].

1.1.2 Oscillating Surge Wave Energy Converter (OSWEC)

Using horizontal fluid particles flow generated by wave motion in a coastal area with a water depth of 10 to 20 meters, an OSWEC converts wave energy into electricity [8]. An OSWEC has at least one flap and a base. When the wave hits the flap, it pitches about the y axis, then converted into electricity using a PTO. An OSWEC utilizes either linear or rotational PTO based on its design. The main models for this kind of WEC are listed below [6]:

- Bottom-fixed oscillating flap (B-OF)
- Floating three-body- oscillating flap device (F-3OF)
- Floating oscillating water column (F-OWC)

This thesis studies a bottom-fixed oscillating flap for given sea wave data. Devices like this oscillate about a fixed axis near the seafloor and are suitable for shallow or intermediate water depths [6].

1.2 Wave Energy Converter Simulator (WEC-Sim)

Wave energy converter Simulator (WEC-Sim) is a free source code used for simulating WECs. The software is performed in MATLAB/SIMULINK, applying the multi-body dynamics solver Simscape Multibody. WEC-Sim was developed and financed by the Office of Water Power Technologies, Dept. of Energy, through a partnership between National Renewable Energy Lab. (NREL) and Sandia. In addition to numerous new features and publications since 2013, WEC-Sim has continued to advance since 2013. Therefore, research is increasingly relying on numerical simulation of WECs using WEC-Sim to simulate the dynamic response of WECs to ocean waves. WEC-Sim was used by Ruehl and colleagues [9] to model Reference Model 3 (RM3) point absorb in one and three degrees of freedom (DOF) and simulate its behavior using WEC-Sim. They simulated the RM3 point absorber for regular wave, ran the simulation including and excluding

1. Introduction

PTO, and compared the motion and moorings tension results obtained via WEC-Sim code with commercial codes ANSYS-AQWA, WaveDyn, and OrcaFlex. A WEC coupled with moorings is also being studied by researchers using WEC-Sim.

For example, Srinivas and his colleagues checked and validated the coupled WEC-Sim and MoorDyn codes for a floating power system (FPS) [10]. A study on the performance evaluation of an FPS [11] provided the experimental data used for validation in Reference [10]. The study was conducted at the Beaufort Research Wave Basin in Ireland. In this thesis, the RM3 point absorber is simulated using WEC-Sim. RM3 was named and developed by Sandia National Laboratories. There are other projects illustrated and developed by this laboratory. This link provides access to the six reference models: https://energy.sandia.gov/programs/renewable-energy/water-power/projects/reference-model-project-rmp/. In this thesis, the heave, surge, and pitch motions of the 2BPA and pitch motion of the OSWEC are simulated by WEC-Sim for both regular and irregular wave conditions. In addition, the device's power performance and its dynamic behavior are obtained using the same approach. WEC-Sim has all the needed codes and functions to represent the governing equations and formulas of the system. This simulator uses the hydrostatic and hydrodynamic results previously calculated by NEMOH, WAMIT, or AQWA-ANSYS to simulate the motion of the offshore device. Moreover, the WEC-Sim input file provides the possibility to define the sea state both for regular or irregular waves. Hence, there will be no need to implement any equation or formula.

The main report for the RM3 two-body point absorber can be found in Ref [12]. Berg [13] and Previsic [14] represented the reference site resource for the model mentioned above. The reference sites for the earlier mentioned model studied by Berg and Previsis are National Data Buoy Center (NDBC) and Coastal Data Information Program (CDIP) stations near Eureka in Humboldt County, California. The performance of the RM3 was studied by Vincent S. Neary and his colleagues [15]. The RM3 mechanical power matrix was calculated by ReVision Consulting using a time-domain radiation and diffraction method. An optimal velocity-dependent damping term was determined using an iterative approach for each sea state. The power performance results were validated by NREL using a similar method and computational fluid dynamics (CFD). In addition, a series of wave tank tests for analyzing the operational wave condition RM3 design power performance was carried out at Scripps in San Diego by ReVision Consulting and NREL to validate the models further.

Further, the materials specifications and structural analysis of the RM3 were studied by Vincent S. Neary [15]. To study the extreme wave load estimation of the RM3, Vincent S. Neary and his colleagues selected the UC Berkeley wave tank to measure the load and analyze the structural performance of the RM3. The device was subjected to an extreme event based on the 100-year return sea states estimated from the NDBC buoy near Humboldt Bay. Then, they used the Finite Element Analysis (FEA) method to perform the stress analysis. Other investigations on RM3 point absorber such as Power Conversion Chain (PCC) design and mooring design were also studied in Ref [15].

1. Introduction

An OSWEC is another type of WEC used in oceans to convert the potential and kinetic energy of an incident ocean wave into beneficial mechanical or electrical energy, using one or more PTOs. An OSWEC comprises at least one flap and a base where the whole structure is mounted on it. The WEC-Sim can simulate the pitching motion of the flap where the OSWEC is subjected to the incident wave in the ocean. By using WEC-Sim, researchers in Ref [16] modeled the hydrodynamic response of an OSWEC and calculated the corresponding power performance for Humboldt Bay located on the rugged North Coast of California. As well, the hydrodynamic response of the device was simulated for the Reference Model 5 (RM5) design in Ref [17], which involved a flap, supported by a steel frame, using WEC-Sim at Humboldt Bay, where the Pacific Gas and Electric Company (PG&E) conducted several tests for the WEC during 2008-2011 [18]. Ref [19] also offers an analytical and empirical investigation of the OSWEC, which correlates the analytical results obtained by WEC-Sim with van't Hoff's experimental study [20].

According to the annual report published in 2020 by Ocean Energy System (OES) [21], there is increasing interest exploitation of wave and tidal energy in Italy. Italy has four fully operational projects in its seas till today. Hence, in the first place, the engineers need to study the hydrodynamic response of different WECs for Italian sea wave conditions. Not too many articles have been published on calculating hydrodynamic and motion responses of a WEC in the Italian sea. Nevertheless, some good works are listed in Refs [22-24]. However, for the studies above, the hydrodynamic responses of the WECs designed for Italian seas were obtained using the governing formulas. Moreover, the motion responses of the WECs were not calculated using WEC-Sim in the earlier mentioned studies. Since the WEC-Sim can calculate all the hydrodynamic forces and the dynamic motion of a WEC when subjected to the incident wave, it is more promising to use this simulator as a comprehensive method.

1.3 NEMOH

The NEMOH code uses the Boundary Element Methods (BEM) to calculate the loads and coefficients of first-order waves, such as the added mass and radiation damping coefficients, the excitation force, and the phase response. NEMOH also calculates the Froude-Krylov forces for each diffraction problem for the offshore structures, far-field coefficients (Kochin function), free surface elevation, and pressure field. Researchers have developed it at Ecole Centrale de Nantes for 30 years. It is regularly used to estimate floating structures' dynamic response or evaluate wave energy converters' performance. Three steps have to be done to obtain hydrodynamic coefficients of floating or submerged bodies in the water. Defining a working folder to contain characteristics of a meshed body, for example, hydrostatic properties of a floating structure is the first step. So, the body must be meshed using axiMesh.m or Mesh.m MATLAB functions to use NEMOH, and the working folder will be created by defining a directory name by the user. These functions are used for meshing structures defined as 1-body or multibody. axiMesh.m can mesh only one cylindrical axisymmetric body while Mesh.m can mesh several when calling these functions in the MATLAB software. These functions are located inside the Nemoh for Matlab zip file, which can be downloaded from: https://box.lheea.ec-nantes.fr/index.php/s/sKLWx6pVGBo7H7Y that is presented by Research Laboratory in Hydrodynamics, Energetics & Atmospheric Environment

1. Introduction

(LHEEA) located in France. The general information about this research laboratory can be found here: https://lheea.ec-nantes.fr/english-version.

After meshing the bodies using axiMesh.m or Mesh.m functions, a Nemoh.cal file will be created for each time that the mesh is generated for each body. The Nemoh.cal file is one of the needed data for bemio.m MATLAB function for reading data from a NEMOH working folder and creating the *.h5 file for the present case. The bemio.m function is located inside the *WEC-Sim\source\functions* folder. The WEC-Sim can be downloaded from: https://github.com/WEC-Sim/WEC-Sim. The Nemoh.cal file contains the number of nodes and panels as the characteristics of the mesh for NEMOH, which are obtained in step one. Additionally, the vertical position of the center of gravity and the directory name for storing the results defined in step one will be recorded in the Nemoh.cal file.

The second step is to define calculation options and lunch computation by calling Nemoh.m MATLAB function inside Nemoh for the Matlab zip file. By defining the input data as vector length of wave frequency (rad/s), wave direction (degree), and water depth (meter), the NEMOH function will obtain added mass coefficients matrix, radiation damping coefficients matrix, and excitation forces (complex values) matrix. The added mass and radiation damping coefficients and excitation force coefficients will be plotted versus wave frequency at the end of this calculation. In the Nemoh.cal file, the number of frequencies and directions previously defined as inputs to the Nemoh.m function will be written. However, it is possible to modify the data of the Nemoh.cal file at the end of step one or step two. More information will be given in other sections of this thesis.

The third step is to call function bemio.m. The purpose is to read data from the NEMOH working folder and create the *.h5 file for the WEC-Sim input file. The *.h5 file contains all the hydrodynamic data of the structure. In this step, the following results will be plotted:

- Normalized added mass
- Normalized radiation damping
- Normalized radiation impulse response functions
- Normalized excitation force magnitude
- Excitation phase
- Normalized excitation impulse response functions

NEMOH is not the only meshing method. WAMIT [25] and ANSYS-AQWA [26] are also viable options. A comparative study for modeling wave energy converter using NEMOH and WAMIT was studied by Penalba and his colleagues [27]. According to their findings, the radiation damping results obtained by NEMOH and WAMIT for a submerged axisymmetric point absorber (SAPA) are almost identical. The significant difference between NEMOH and WAMIT for a two-body point absorber (2BPA) is the frequency shift in their radiation damping versus frequency plot. These spikes are irregular frequencies, which arise due to a fundamental error in the formulation of the NEMOH BEM solver, regardless of the type of solver. WAMIT can remove irregular

frequencies, but in NEMOH, it is not possible at this time. With a BEM, irregular frequencies could appear. Those frequencies correspond to singularities in the system of equations solved. NEMOH does not include additional equations for removing these singularities in the basic version. Penalba concluded for the OSWEC case that the hydrodynamic coefficients calculated using NEMOH and WAMIT matched almost perfectly. However, for the floating oscillating water column (OWC), NEMOH produced negative radiation damping values. Unlike WAMIT, NEMOH uses a MATLAB wrapper (Nemoh.m) to run the simulations, making it much easier for users who know how to use MATLAB. In addition, NEMOH includes MATLAB functions for generating axisymmetric (axiMesh.m) and non-axisymmetric (Mesh.m) meshes. On the other side, WAMIT users can only use the predefined subroutines or specific software, such as Multisurf, to generate meshes [27]. Hence, according to what was said earlier, the author opts for the NEMOH solver in this thesis.

1.4 Scope of the Thesis

The main goals of this Master thesis are briefly described as below:

I. Meshing the Structure Using axiMesh.m and Mesh.m Functions for the Use of NEMOH: 1st Step

The meshes for the bodies are generated using axiMesh.m for the 2BPA, which is considered an axisymmetric structure, and Mesh.m for the OSWEC. As a result of meshing, hydrostatic characteristics such as the center of gravity, the center of buoyancy, water displacement, and waterplane area are obtained.

II. Using NEMOH to Calculate the Hydrodynamic Coefficients: 2nd Step

In this study, Nemoh.m MATLAB function is used to obtain the hydrodynamic results of the 2BPA and OSWEC subjected to the incident waves. The results are:

- Added mass coefficients
- Radiation damping coefficients
- Excitation force and excitation force coefficients
- Diffraction force for the diffraction problems
- Froude-Krylov forces for each of the diffraction problem
- The forces that result from each problem
- Free surface elevation for problem no. XX
- Kochin function for problem no. XX
- Pressure field on body surfaces for problem no. XX

III. Creating a Correct HDF5 (*.h5) File that Will Be Included in WEC-Sim Input File: 3rd Step

Since the input file requires hydrodynamic data of the offshore structure, the data must be converted into a readable *.h5 file. All hydrodynamic data is contained in the *.h5 file, which is created using the bemio.m MATLAB function.

IV. Creating *.stl File for 2BPA and OSWEC Using SOLIDWORKS: 4th Step

The *.stl file is a geometry file used for WEC geometry. Since the WEC-Sim requires a *.stl file, it is necessary to design the offshore structure using solid modeling software. The *.stl file is used to generate Simscape Mechanics Explorer visualization, visualize linear hydrodynamics, and determine the instantaneous wetted surface at each step with the nonlinear buoyancy and Froude-Krylov forces option. In this thesis, the *.stl format geometry files for 2BPA and OSWEC are created via SOLIDWORKS.

V. Creating SIMULINK Models for 2BPA and OSWEC: 5th Step

Apart from the *.stl and *.h5 files, a SIMULINK *.slx file is also required for the WEC-Sim. In MATLAB software, SIMULINK models of 2BPA and OSWEC are created.

VI. Defining an Input File for WEC-Sim for the 2BPA and OSWEC, and Defining the Wave Characteristics for Italian Seas Within it: 6th Step.

In this step, the *.stl, *.h5, and SIMULINK *.slx files for 2BPA and OSWEC are defined in the WEC-Sim input file. The wave class defined for the Italian seas is irregular waves using the Pierson–Moskowitz (PM) spectrum. The significant wave height (Hs) and peak period (Tp) are extracted from the Italian sea state data.

VII. Using WEC-Sim to Simulate the Dynamic Response of a 2BPA and OSWEC: 7th Step

In this thesis, the dynamic responses of a 2BPA and OSWEC are simulated via WEC-Sim. The bodies' surge, heave, and pitch motions are obtained using WEC-Sim in regular and irregular waves. Moreover, the power matrices of each device in different sites located in the Mediterranean Sea and the North Sea are calculated with rated power and annual energy production (AEP).

1.5 Organization of the Thesis

Chapter 1: "Introduction," gives brief information regarding the WECs. The 2BPA and OSWEC are represented in this chapter. The WEC-Sim is represented in this chapter, a technique to simulate the WECs as mentioned above. Also, general information about the NEMOH BEM solver with its meshing functions is explained.

Chapter 2: "Numerical Modeling of Hydrostatic Properties of 2BPA and OSWEC" provides meshing functions which are axisymmetric (axiMesh.m) and non-axisymmetric (Mesh.m) to mesh the 2BPA and OSWEC. In this chapter, the hydrostatic properties are obtained using the MATLAB functions mentioned above.

Chapter 3: "Numerical Modeling of Hydrodynamic Coefficients of 2BPA and OSWEC" studies the first order hydrodynamic coefficients, including added mass coefficient, radiation damping coefficient, excitation force, and excitation force phase response which are calculated by NEMOH preprocessor for 2BPA and OSWEC.

Chapter 4: "Hydrodynamic Data from BEM Solution in Hierarchical Data Format Version 5 (HDF5)" explains BEMIO, which can save and compile all of the results from the NEMOH BEM solver with the data obtained via BEMIO into the HDF5 (*.h5) file.

Chapter 5: "Designing 2BPA and OSWEC Using SOLIDWORKS" explains the procedures to design the 2BPA and OSWEC using SOLIDWORKS software and create *.stl format geometry files needed for WEC-Sim input file.

Chapter 6: "Creating SIMULINK Models in *.slx Format for 2BPA and OSWEC" overviews of WEC-Sim library blocks within SIMULINK and represents the SIMULINK models for 2BPA and OSWEC.

Chapter 7: "WEC-Sim," which is based on two parts. The part one defines an input file for WEC-Sim for the 2BPA and OSWEC devices. Part two simulates the dynamic responses of 2BPA and OSWEC in waves of regular and irregular amplitude and estimates the annual energy production (AEP) in different sites located at the Mediterranean Sea in Italy and the North Sea.

Bibliography: The bibliography includes all the references which are cited in the text

2.

Numerical Modeling of Hydrostatic Properties of 2BPA and OSWEC

2.1 Meshing the Structure Using axiMesh.m and Mesh.m Functions for the Use of NEMOH: 1st step

The first step in modeling and simulation of an offshore structure subjected to the incident ocean waves is to obtain the hydrostatic characteristics of the structure. The hydrostatic properties of a floating or submerged structure are coordinates of the center of buoyancy (COB) and center of mass (COG), hydrostatic stiffness matrix of the body, water displacement, waterplane area, and the information relative to the number of points and panels in the mesh file for NEMOH. These data are calculated when the structure is in motionless water so that the body is not moving. NEMOH includes two MATLAB functions generating axisymmetric (axiMesh.m), and non-axisymmetric (Mesh.m) meshes. These functions can calculate hydrostatic properties of offshore structures such as 2BPA and OSWEC. In this thesis, the hydrostatic data are obtained using axiMesh.m and Mesh.m MATLAB functions.

2.1.1 Meshing RM3 2BPA

The 2BPA in this study is RM3 that Sandia National Laboratories named this model. For an axisymmetric body such as RM3 2BPA, the axiMesh.m function must be used. The axiMesh.m function requires the number of points needed for describing the shape of the rotating curve (generatrix) of the surface of revolution, n, the array of radial coordinates, r, and the array of vertical coordinates, z. The structure dimensions are needed to define the input data mentioned above for a 2BPA. Figure 2.1 shows the dimensions of the 2BPA, which are taken from [9]. Also, Tables 2.1 and 2.2 show the full-scale mass, COG, and moment of inertia of float and spar-plate, respectively. As can be seen from Figure 2.1, a 2BPA consists of a float and spar-plate bodies. The float is 3 m below the still water level (SWL), while the spar-pale is 29 m below SWL. The earlier numbers represent the submerged part of the float and spar-plate bodies. Because the axiMesh meshes only the submerged part of the body, the vertical coordinates of the bodies should be defined from the SWL. However, in the case of describing the vertical coordinates for the whole body, the axiMesh will automatically cut the part of the structure above the SWL. Since axiMesh.m can only mesh one body when calling its function, the float and spar-plate bodies must be meshed by calling the axiMesh.m function for each body.
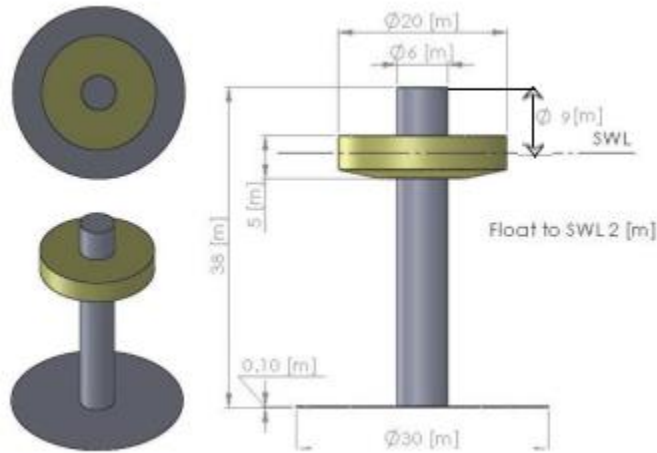
Figure 2.1: 2BPA schematic

COG (m)	Mass (kg)	Moment of inertia ($kg.m^2$)		
0	727010	20,907,301	0	0
0		0	21,306,091	0
-0.72		0	0	37,085,481

Table 2.1: Float full-scale properties

COG (m)	Mass (kg)	Moment of inertia ($kg.m^2$)		
0	878300	94,419,615	0	0
0		0	94,407,091	0
-21.29		0	0	28,542,225

Table 2.2: Spar-plate full-scale properties

Other inputs required for axiMesh.m are the number of points for angular discretization, n_{ad}, directory name for storage results, $dir_{results}$, the vertical position of COG, vp_{COG}, and target number of panels, n_{panel}. Table 2.3 shows all the input data needed for axiMesh.m to mesh the RM3 2BPA. The float geometry illustrated in Figure 2.1 is the reason for naming RM3 for a 2BPA.

2. Numerical Modeling of Hydrostatic Properties of 2BPA and OSWEC

Nevertheless, there are other geometries for float such as 60 ° cone, 90 ° cone, 120 ° cone, hemisphere, and innovative, which can also be considered [28].

Body	n	$r\,(m)$	$z\,(m)$	n_{ad}	$dir_{results}$	$vp_{COG}\,(m)$	n_{panel}
Float	4	[10 10 10 3]	[2 0 -2 -3]	72	*'pointabsorber'*	-0.72	150
Spar-plate	5	[3 3 15 15 0]	[9 -28.90 -28.90 -29 -29]	72	*'pointabsorber'*	-21.29	150

Table 2.3: The axiMesh.m input file for 2BPA.

Now, by having all the data of the 2BPA, the structure can be meshed by calling axiMesh.m function. The MATLAB code for calling this function is shown in Script 2.1. The script was saved inside the *pointabsorber* working folder and named *pointabsorber1*, which indicates the first step carried out for the 2BPA.

```
1   %%% I) Call function axiMesh
2   %%%
3   %%% function [Mass,Inertia,KH,XB,YB,ZB]=axiMesh(r,z,n)
4   %%%
5   %%% Purpose : Mesh generation of an axisymmetric body for use with Nemoh
6   %%%
7   %%% Inputs : description of radial profile of the body
8   %%%    - n        : number of points required for describing the shape of the
9   rotating curve (generatrix) of the surface of revolution (submerged part
10  only)
11  %%%    - r        : array of radial coordinates
12  %%%    - z        : array of vertical coordinates
13  %%%
14  %%% Outputs : hydrostatics
15  %%%    - Mass     : mass of buoy
16  %%%    - Inertia  : inertia matrix (estimated assuming mass is distributed on
17  %%%    wetted surface)
18  %%%    - KH       : hydrostatic stiffness matrix
19  %%%    - XB,YB,ZB : coordinates of buoyancy center
20  %%%
21  %%% Warning : z(i) must be greater than z(i+1)
22  %%%
23  %%% Copyright Ecole Centrale de Nantes 2014
24  %%% Licensed under the Apache License, Version 2.0
25  %%% Written by A. Babarit, LHEEA Lab.
26  %%%
27  %%%%%%%%%%%%%%%%%%%%%%%%%%%%%
28
29  %%% NOTES:
30  %%% Specify mesh file characteristics and mesh the body
31  %%% A vertical cylinder is an axisymettric shape. As a result, the Matlab
32  routine Aximesh.m could
33  %%% be used for the purpose. Only the submerged part needs to be meshed, and
34  because of the % revolution, only 3 points are required.
```

```
35   %%% Aximesh.m can mesh only 1 body, but Mesh.m can mesh several. For more
36   sophisticated
37   %%% bodies, one should use a CAD software and adapt the Mesh file in the good
38   format.
39   %%%%%%%%%%%%%%%%%%%%%%%%%%%
40
41   %%% axiMesh inputs for float body:
42   n=4;
43   r=[10 10 10 3];
44   z=[2 0 -2 -3];
45   [Mass,Inertia,KH,XB,YB,ZB]=axiMesh(r,z,n)     %Call the function axiMesh
46   %%% axiMesh inputs for spar-plate body:
47   n=5;
48   r=[3 3 15 15 0];
49   z=[9 -28.90 -28.90 -29 -29];
50   [Mass,Inertia,KH,XB,YB,ZB]=axiMesh(r,z,n)     %Call the function axiMesh
```

Script 2.1: Call function axiMesh for 2BPA.

Since the axiMesh.m can mesh only one body when calling the function, it is important to rename the files that will appear inside the *pointabsorber/mesh* folder. Because, by calling the axiMesh.m function for float body (line 39 of script 2.1), the result files will be saved with a default name inside the *pointabsorber/mesh* folder. Hence, if we continue to enter the input data for the axiMesh.m function to mesh the spar-plate without renaming the files previously obtained for float, all the data inside the files will be rewritten for the spar, causing the loss of the data for the float. So, to prevent the result files from being rewritten, the float files must be renamed before entering the input data for calling axiMesh.m function for spar-plate. In this study, it is recommended that the number '0' represent float and number '1' indicate spar-plate body.

To mesh float body by entering input data for axiMesh.m function, the result files will be obtained and located inside *pointabsorber/mesh* folder. The files are:

- axisym
- axisym.dat
- axisym.tec
- axisym_info.dat
- Description_Full.tec
- Description_Wetted.tec
- GC_hull.dat
- Hydrostatics.dat
- Inertia_hull.dat
- KH.dat

The files mentioned above must be renamed to:

- float
- float.dat
- float.tec
- float_info.dat
- Description_Full_0.tec
- Description_Full_1.tec
- GC_hull_0.dat
- Hydrostatics_0.dat
- Inertia_hull_0.dat
- KH_0.dat

In addition to the files mentioned above, Nemoh.cal file is also generated for float inside the *pointabsorber* folder. Nemoh.cal will be generated for each time the axiMesh.m function is called for each body. So, to keep the float body data inside the Nemoh.cal and prevent this file from being rewritten when calling axiMesh.m function for spar-plate, the Nemoh.cal file obtained for float must be renamed before proceeding to enter data in Command Window for meshing spar-plate. For the float and spar-plate, Nemoh.cal files generated from their meshing process can be renamed to any arbitrary names such as float.cal and spar.cal. However, since we need only a single Nemoh.cal file containing all the data related to the float and spar, it is necessary to create a single Nemoh.cal manually. The data located inside spar.cal can be copied and pasted into float.cal file. In the end, float.cal file must be renamed to Nemoh.cal, and the spar.cal can be deleted. Now, we have all the data for float and spar-plate inside the single Nemoh.cal file. This procedure must be done when the axiMesh.m function is called for both float and spar bodies and the related result files are renamed. Note that the name of a created single file containing all the data for float and spar must be exactly Nemoh.cal. Because when calling function Nemoh to calculate hydrodynamic coefficients (step 2) plus when calling function bemio to generate *h5 file (step 3), the Nemoh and bemio functions can only identify a single file that is named Nemoh.cal and no other names.

According to what was said earlier, before entering the input data and calling the axiMesh.m function for spar-plate, we need to rename the Nemoh.cal file, which is obtained by calling the axiMesh,m function for float. The float.cal can be the new name for Nemoh.cal. After renaming the result files related to the float and renaming the Nemoh.cal to float.cal, it is possible to continue entering the input data needed for the axiMesh to mesh the spar. Continuing ding to mesh spar-plate by entering input data for axiMesh.m function, the result files will be obtained and located inside *pointabsorber/mesh* folder. The files are:

- axisym
- axisym.dat
- axisym.tec
- axisym_info.dat
- Description_Full.tec
- Description_Wetted.tec

- GC_hull.dat
- Hydrostatics.dat
- Inertia_hull.dat
- KH.dat

The files mentioned above must be renamed to:

- spar
- spar.dat
- spar.tec
- spar_info.dat
- Description_Full_1.tec
- Description_Wetted_1.tec
- GC_hull_1.dat
- Hydrostatics_1.dat
- Inertia_hull_1.dat
- KH_1.dat

The Nemoh.cal file generated for spar-plate at the end of its meshing process is located inside the *pointabsorber* working file. As well as changing the name of the Nemoh.cal obtained for the float to float.cal, the Nemoh.cal created for spar-plate must be renamed to spar.cal. This procedure must be done to make a single Nemoh.cal file out of the data located inside the float.cal and spar.cal files. So, the needed data inside the spar cal file must be copied and pasted into float.cal and the float.cal file must be renamed to Nemoh.cal. In the end, the spar.cal can be deleted since we already created our single Nemoh.cal file containing all the data for float and spar-plate. As a reminder, both float.cal and spar.cal are the renamed files of Nemoh.cal, generated for each float and spar body at the end of their meshing process. The scripts for float.cal and spar.cal obtained at the end of the meshing process for 2BPA are given in Script 2.2 and Script 2.3, respectively.

Further, to create a single Nemoh.cal file, a space between lines 25 and 27 was created by shifting the text written on line 26 (--Load cases to be solved--) to line 27. Then, the scripts written on lines 8 to 25 were copied from spar.cal file and pasted into line 26 in float.cal. In the float.cal file where we added the data for spar from the spar.cal file, the number of bodies in the 7th line is changed from 1 to 2 since we now have the data for float and spar-plate bodies together. Plus, in line 26, the word Body 1 was changed to Body 2 for spar-plate. Then, in the 9th line, the name of the mesh file was changed from axisym.dat to float.dat. Similarly, in line 27, the name of the mesh file was changed from axisym.dat to spar.dat.

```
1    --- Environment ---------------------------------------------------------------
2    1025.000000        *Sea water density(kg/m^3)
3    9.810000           *The gravity acceleration (m/s^2)
4    0.                 *Water depth (m)
5    0.    0.           *Wave measurement point XEFF YEFF (m)
6    --- Description of floating bodies --------------------------------------------
```

```
7    1                      *Count of bodies
8    --- Body 1 -------------------------------------------------------------
9    pointabsorber\mesh\axisym.dat   *The mesh file's name
10   568 142                          *Count of points and panels
11   6                             *DOF
12   1 1.0 0.0 0.0 0.0 0.0 0.0    *Surge
13   1 0.0 1.0 0.0 0.0 0.0 0.0    *Sway
14   1 0.0 0.0 1.0 0.0 0.0 0.0    *Heave
15   2 1.0 0.0 0.0 0.0 0.0 -0.72 *Rolling about this point
16   2 0.0 1.0 0.0 0.0 0.0 -0.72 *Pitching about this point
17   2 0.0 0.0 1.0 0.0 0.0 -0.72 *Yawing about this point
18   6                             *Amount of resulting generalized forces
19   1 1.0 0.0 0.0 0.0 0.0 0.0    *x-direction force
20   1 0.0 1.0 0.0 0.0 0.0 0.0    *y-direction force
21   1 0.0 0.0 1.0 0.0 0.0 0.0    *z-direction force
22   2 1.0 0.0 0.0 0.0 0.0 -0.72 *Moment force about this point in the x-direction
23   2 0.0 1.0 0.0 0.0 0.0 -0.72 *Moment force about this point in the y-direction
24   2 0.0 0.0 1.0 0.0 0.0 -0.72 *Moment force about this point in the z-direction
25   0                             *Number of additional lines of information
26   --- Load cases that have to be solved -----------------------------------
27   1    0.8    0.8              *The number of wave frequencies, the minimum, and
28   the maximum (rad/s)
29   1    0.    0.               *The number of wave directions, minimum, and the
30   maximum (degrees)
31   --- Post processing ----------------------------------------------------
32   260   0.02  5.20.          *Calculation of the IRF (0 is for no calculation),
33   time step, and duration
34   0                      * Pressure
35   0    0.    180.          * Kochin function    Count of directions of
36   calculation (0 is for no calculations), minimum and maximum (degrees)
37   0    50    400. 400.  *Count of points in the x-direction (0 if no
38   calculations) and y-direction, and domain dimensions in x and y-direction
39   ---
```

Script 2.2: float.cal

1

```
1    --- Environment --------------------------------------------------------
2    1025.000000        *Sea water density(kg/m^3)
3    9.810000           *The gravity acceleration (m/s^2)
4    0.                 *Water depth (m)
5    0.    0.           *Wave measurement point XEFF YEFF (m)
6    --- Description of floating bodies -------------------------------------
7    1                *Count of bodies
8    --- Body 1 -------------------------------------------------------------
9    pointabsorber\mesh\axisym.dat   *The mesh file's name
10   1136 284                          *Count of points and panels
11   6                             *DOF
12   1 1.0 0.0 0.0 0.0 0.0 0.0    *Surge
13   1 0.0 1.0 0.0 0.0 0.0 0.0    *Sway
14   1 0.0 0.0 1.0 0.0 0.0 0.0    *Heave
15   2 1.0 0.0 0.0 0.0 0.0 -21.29 *Rolling about this point
```

```
16    2 0.0 1.0 0.0 0.0 0.0 -21.29 *Pitching about this point
17    2 0.0 0.0 1.0 0.0 0.0 -21.29 *Yawing about this point
18    6                            *Amount of resulting generalized forces
19    1 1.0 0.0 0.0 0.0 0.0 0.0    *x-direction force
20    1 0.0 1.0 0.0 0.0 0.0 0.0    *y-direction force
21    1 0.0 0.0 1.0 0.0 0.0 0.0    *z-direction force
22    2 1.0 0.0 0.0 0.0 0.0 -21.29*Moment force about this point in the x-direction
23    2 0.0 1.0 0.0 0.0 0.0 -21.29*Moment force about this point in the y-direction
24    2 0.0 0.0 1.0 0.0 0.0 -21.29*Moment force about this point in the z-direction
25    0                            *Number of additional lines of information
26    --- Load cases that have to be solved -----------------------------------
27    1    0.8   0.8               *The number of wave frequencies, the minimum, and
28    the maximum (rad/s)
29    1    0.    0.                *The number of wave directions, minimum, and the
30    maximum (degrees)
31    --- Post processing ------------------------------------------------------
32    260   0.02  5.20.            *Calculation of the IRF (0 is for no
33    calculation), time step, and duration
34    0                            * Pressure
35    0    0.    180.              * Kochin function    Count of directions of
36    calculation (0 is for no calculations), minimum and maximum (degrees)
37    0     50   400.  400.        *Count of points in the x-direction (0 if no
38    calculations) and y-direction, and domain dimensions in x and y-direction
39    ---
```

Script 2.3: spar.cal

```
1     --- Environment ----------------------------------------------------------
2     1025.000000 *Sea water density(kg/m^3)
3     9.810000    *The gravity acceleration (m/s^2)
4     0.          *Water depth (m)
5     0.    0.    *Wave measurement point XEFF YEFF (m)
6     --- Description of floating bodies ---------------------------------------
7     2          * Count of bodies
8     --- Body 1 ---------------------------------------------------------------
9     pointabsorber\mesh\float.dat    *The mesh file's name
10    568 142                         *Count of points and panels
11    6                               *DOF
12    1 1.0 0.0 0.0 0.0 0.0 0.0   *Surge
13    1 0.0 1.0 0.0 0.0 0.0 0.0   *Sway
14    1 0.0 0.0 1.0 0.0 0.0 0.0   *Heave
15    2 1.0 0.0 0.0 0.0 0.0 -0.72 *Rolling about this point
16    2 0.0 1.0 0.0 0.0 0.0 -0.72 *Pitching about this point
17    2 0.0 0.0 1.0 0.0 0.0 -0.72 *Yawing about this point
18    6                           *Amount of resulting generalized forces
19    1 1.0 0.0 0.0 0.0 0.0 0.0   *x-direction force
20    1 0.0 1.0 0.0 0.0 0.0 0.0   *y-direction force
21    1 0.0 0.0 1.0 0.0 0.0 0.0   *z-direction force
22    2 1.0 0.0 0.0 0.0 0.0 -0.72 *Moment force about this point in the x-direction
23    2 0.0 1.0 0.0 0.0 0.0 -0.72 *Moment force about this point in the y-direction
24    2 0.0 0.0 1.0 0.0 0.0 -0.72 *Moment force about this point in the z-direction
25    0                           *Number of additional lines of information
26    --- Body 2 ---------------------------------------------------------------
27    pointabsorber\mesh\spar.dat     *The mesh file's name
28    1136 284                        *Count of points and panels
```

```
29   6                                    *DOF
30   1 1.0 0.0 0.0 0.0 0.0 0.0     *Surge
31   1 0.0 1.0 0.0 0.0 0.0 0.0     *Sway
32   1 0.0 0.0 1.0 0.0 0.0 0.0     *Heave
33   2 1.0 0.0 0.0 0.0 0.0 -21.29 *Rolling about this point
34   2 0.0 1.0 0.0 0.0 0.0 -21.29 *Pitching about this point
35   2 0.0 0.0 1.0 0.0 0.0 -21.29 *Yawing about this point
36   6                                    *Amount of resulting generalized forces
37   1 1.0 0.0 0.0 0.0 0.0 0.0     *x-direction force
38   1 0.0 1.0 0.0 0.0 0.0 0.0     *y-direction force
39   1 0.0 0.0 1.0 0.0 0.0 0.0     *z-direction force
40   2 1.0 0.0 0.0 0.0 0.0 -21.29*Moment force about this point in the x-direction
41   2 0.0 1.0 0.0 0.0 0.0 -21.29*Moment force about this point in the y-direction
42   2 0.0 0.0 1.0 0.0 0.0 -21.29*Moment force about this point in the z-direction
43   0                                    *Number of additional lines of information
44   --- Load cases that have to be solved --------------------------------------
45   1    0.8     0.8 *The number of wave frequencies, the minimum, and the
46   maximum (rad/s)
47   1    0.      0.   *The number of wave directions, minimum, and the maximum
48   (degrees)
49   --- Post processing -------------------------------------------------------
50   260   0.02  5.20.         *Calculation of the IRF (0 is for no calculation),
51   time step, and duration
52   0                           * Pressure
53   0     0.     180.          * Kochin function    Count of directions of
54   calculation (0 is for no calculations), minimum and maximum (degrees)
55   0     50    400.  400.  *Count of points in the x-direction (0 if no
56   calculations) and y-direction, and domain dimensions in x and y-direction
57   ---
```

Script 2.4: Single Nemoh.cal for 2BPA

In script 2.4, the data written in lines 2 to 5 are for environmental properties where the 2BPA is meant to be simulated. The fluid-specific volume, gravity, water depth, and wave measurement point are the data given in the environment section of the Nemoh.cal. As seen from Nemoh.cal script, the water depth is zero as a default value. For deep water depth, zero is assumed for the depth of the water by Nemoh.cal. However, when calling the Nemoh function in the 2nd step to calculate hydrodynamic coefficients, the water depth can be adjusted to the desired value. In this case, the water depth will be rewritten in Nemoh.cal file to the value defined by the user in the 2nd step. Also, in the 2nd step, it is noted that the zero-depth is exclusively assumed for the deep-water calculations.

The final characteristics of the meshed bodies, including the number of nodes and number of points obtained via axiMesh.m function, are given in lines 10 and 28. The 6DOF is indicated for each body is shown in lines 11 and 29, which means that the simulation of the 2BPA will be carried out for translational (surge, sway, and heave) and rotational (roll, pitch, and yaw) directions. However, since the only surge, heave, and pitch motions are significant to the system, and the hydrodynamic coefficients will be calculated based on those motions, other degrees of freedom are not considered in this study.

2. Numerical Modeling of Hydrostatic Properties of 2BPA and OSWEC

The number 1 written to the left side of lines 12-14 and lines 30-32 indicates the translational movement of the float and spar-plate bodies. Plus, the number 2 written to the left side of the lines 15-17 and lines 33-35 indicates the rotational motion of the float and spar-plate bodies. The following three numbers in those lines are the direction vectors, and the last three numbers are the COG coordinates. For translational motions, only direction vector is defined, while for rotational movements, besides direction vector, COG coordinates of the bodies are defined where rotational motions in x, y, and z directions will be determined about COG.

The number 1 written to the left side of lines 19-21 and 37-39 indicates the forces of the float and spar-plate bodies. The number 2 written on the left side of the lines 22-24 and 40-42 indicates moment force for the float and spar-plate bodies. The following three numbers in those lines are the direction vectors, and the last three numbers are the x, y, and z coordinates of COG. For force, only direction vector is defined, while for moment force, besides direction vector, COG coordinates of the bodies are defined where moment force in x, y, and z directions will be determined about COG.

In Script 2.4, lines 45 and 47 are the wave frequency and wave direction vectors, respectively. At this moment, these values are defined as a default. The vectors of wave frequency and wave direction will be defined in 2nd step by the user. Then, after the Nemoh function is called and the hydrodynamic coefficients are obtained for float and spar-plate bodies, the vector lengths of the wave frequency and wave direction will be corrected in the Nemoh.cal. However, the user can manually enter the values mentioned above in Nemoh.cal script before commencing the 2nd step. Still, again the same values must be defined for the Nemoh function unless the user wants to change them.

Script 2.4 has a post-processing section that post-processes the results to provide relevant quantities in a usual format (added mass, radiation damping, excitation force). A framework is also provided for making relevant calculations. The numbers of calculations for impulse response function (IRF), time step, and duration are indicated in line 50. There is also an indication of the minimum and maximum angle in degrees for each calculation number XX for which the Kochin function will be calculated. The Kochin function expresses the wave kinematics in the far-field [29]. However, in this study, the Kochin function is not considered. More information regarding the Kochin function application to calculate the velocity potential in the far-field can be studied in the following link: https://lheea.ec-nantes.fr/valorisation/logiciels-et-brevets/nemoh-running-1.

At the end of the meshing process for both float and spar-plate bodies, characteristics of discretization of the float and spar-plate bodies are plotted in Figures 2.2 and 2.3, respectively. The plots show the shape of the float and spar with the predefined number of points for angular discretization. The meshed float and spar-plate bodies are obtained as shown in Figures 2.4 and 2.5, respectively. The figures represent half of the bodies since they are symmetrical about the (XOZ) plane. The arrows are the hydrostatic forces applied by the water to the body surface. It is important to note that the direction of the arrows is pointing outside because they show the hydrostatic reaction force that is the force applied by the body to the fluid.

Characteristics of the discretisation
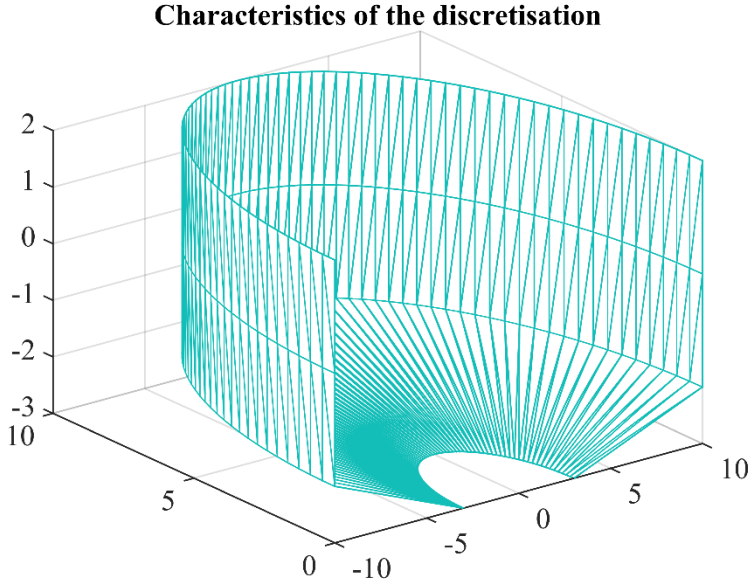
Figure 2.2: Float discretization graph.

Characteristics of the discretisation
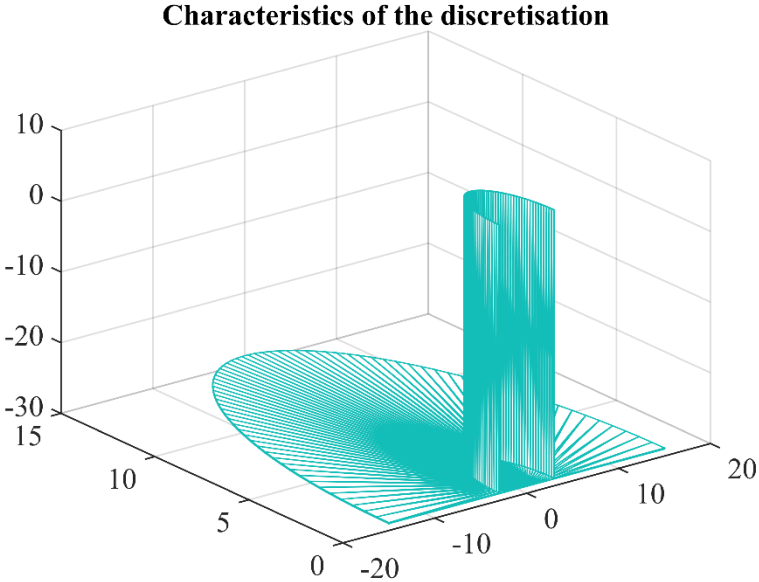
Figure 2.3: Spar-plate discretization graph.

Mesh for Nemoh
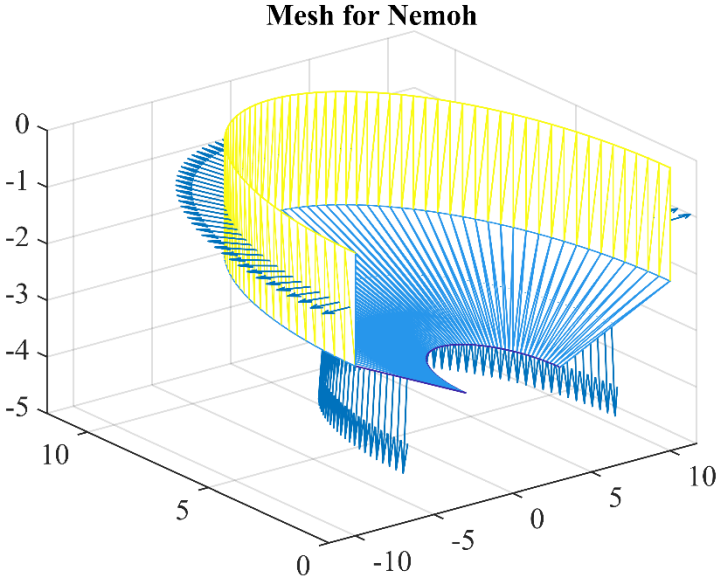
Figure 2.4: Float meshing.

Mesh for Nemoh
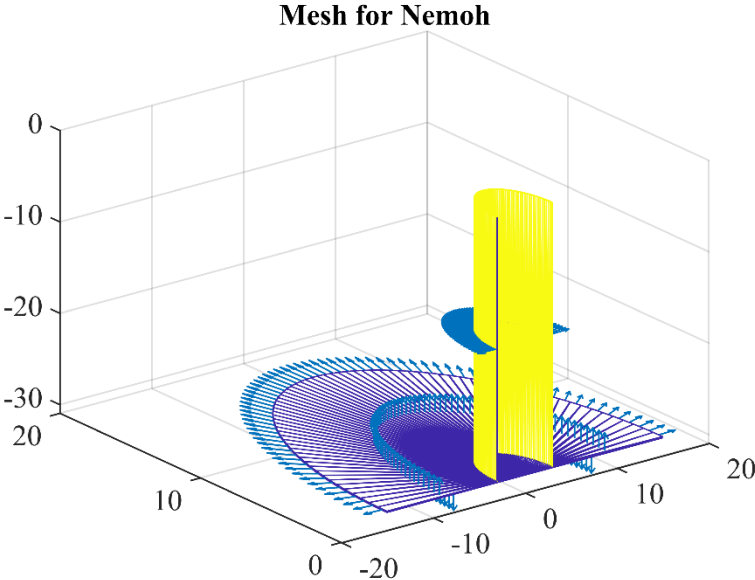
Figure 2.5: Spar-plate meshing.

The hydrostatic data of the float and spar-plate are obtained by meshing the bodies. The *Hydrostatics_0.dat* (for float) and *Hydrostatics_1.dat* (for spar-plate) contain the data for COG and COB of the bodies. Also, they include the data for water displacement and waterplane areas

of float and spar-plate, which are obtained as the output data of the meshing process. The *Hydrostatics_0.dat* and *Hydrostatics_1.dat* files are located inside the *pointabsorber/mesh* folder. In fluid mechanics, the displaced water is the water volume displaced when a body is immersed in it. The body pushes out water to make room for itself. Table 2.4 shows the data for *Hydrostatics_0.dat* and *Hydrostatics_1.dat* obtained for 2BPA.

Body	XF (m)	YF (m)	ZF (M)	XG (M)	YG (M)	ZG (M)	Water displacement (kg)	Waterplane area (m^2)
Float	0.000	0.000	-1.221	0.000	0.000	-0.720	688.8310	285.7917
Spar-plate	0.000	0.000	-15.604	0.000	0.000	-21.290	887.5312	28.2652

Table 2.4: Hydrostatics_0.dat and Hydrostatics_1.dat data obtained for 2BPA

The GC_hull.dat and Inertia_hull.dat files include the coordinates of the gravity center of the body and inertia matrix. These values are obtained by the assumption that the body's mass is the same as its water displacement and that the mass is distributed on the body's surface. The gravity center of the float and spar-plate obtained via calling the axiMesh.m function are given in GC_hull_0.dat and GC_hull_1.dat, respectively. For float, the COG obtained via axiMesh is: $x_G = -1.4270 \times 10^{-7}$ m, $y_G = 0.0000$ m, and $z_G = -2.0451$ m. Plus, for the spar-plate, the COG obtained via axiMesh is: $x_G = 3.1476 \times 10^{-8}$ m, $y_G = 0.0000$ m, and $z_G = -24.8776$ m. As can be seen from the values, the COG of float and spar calculated by axiMesh are different from the COG given in Table 2.4, which the user-defined. As it was mentioned earlier, axiMesh calculates the center of gravity by assuming that the mass is equal to the mass of displaced water and that the mass is distributed on the surface equally. As shown in Table 2.4, the displaced water in float is 688.8310 kg which is 38.1790 kg less than the mass of the float expressed in Table 2.1. The difference between these two values gives us a 5.2515 % percentage error which is acceptable.

Further, the displaced water in the spar is 887.5312 kg which is 9.2312 kg more than the mass of the spar given in Table 2.2. Hence, for the 2BPA, we can conclude that difference between the COG values obtained via axiMesh and the one defined by the problem is not affected by assuming that the masses of float and spar are equal to their displaced water. The difference between these two values gives a 1.0510 % of percentage error which is acceptable.

The second assumption that axiMesh considers calculating the COG of a body is that the mass is uniformly distributed on the body surface equally. However, masses of the float and the spar-plate in this study are not distributed equally on their body surface. Because, when checking the user-defined inertia matrix for float and spar-plate indicated in Tables 2.1 and 2.2 and the inertia matrix obtained via axiMesh given in Inertia_hull_0.dat and Inertia_hull_1.dat. The inertia is strongly dependent on the body's mass and its mass distribution. Since we have a low percentage error in terms of mass and displaced water for float and spar, this does not cause the difference between the inertia values given by the problem and the one calculated via axiMesh.

2. Numerical Modeling of Hydrostatic Properties of 2BPA and OSWEC

The difference between the inertia values given by the user and the one calculated via axiMesh is created because the masses of the float and spar-plate given by the problem are not distrusted equally on their surface. Equations (2.1) and (2.2) show the moment of inertia tensors for float and spar, respectively, obtained by axiMesh.

$$Inertia_0 = \begin{bmatrix} 0.2142321E + 08 & -0.7714844E - 01 & -0.5859375E - 01 \\ -0.7714844E - 01 & 0.2142321E + 08 & 0.4985178E + 06 \\ -0.5859375E - 01 & 0.4985178E + 06 & 0.4217511E + 08 \end{bmatrix} \tag{2.1}$$

$$Inertia_1 = \begin{bmatrix} 0.6249110E + 08 & -0.8740234E + 00 & 0.1125000E + 01 \\ -0.8740234E + 00 & 0.6249110E + 08 & -0.8940837E + 07 \\ 0.1125000E + 01 & -0.8940837E + 07 & 0.4769662E + 08 \end{bmatrix} \tag{2.2}$$

It is important to note that the problem's float and spar inertia matrices only include the diagonal elements. Hence, the masses of float and spa-plate represented by the problem are distributed in a way that the I_{XY}, I_{XZ}, and I_{YZ} are equal to zero. Here, the diagonal elements are:

- I_{XX}: The moment of inertia around the X-axis when the float and spar are rotated around the X-axis

- I_{YY}: The moment of inertia around Y-axis when the float and spar are rotated around the Y-axis

- I_{ZZ}: The moment of inertia around Z-axis when the float and spar are rotated around Z-axis

Further, the off-diagonal elements in moment of inertia tensors are:

- I_{XY}: The moment of inertia around the Y-axis when the float and spar are rotated around X-axis

- I_{XZ}: The moment of inertia around Z-axis when the float and spar are rotated around X-axis

- I_{YZ}: The moment of inertia around Z-axis when the float and spar are rotated around Y-axis

The mass, COG, and moment of inertia tensors calculated by axiMesh have no role in further calculations in the following steps. Because, for the mass, the user can define the mass of a body in the WEC-Sim input file. In case of having a low percentage error in terms of mass and displaced water of a body, the user can define the user-defined mass as equilibrium. Also, the COG

calculated by the axiMesh has no task in subsequent steps since the COG is previously defined in Nemoh.cal. Finally, the user can also define the moment of inertia in the WEC-Sim input file; that is why the NEMOH did not include GC_hull.dat and Inertia_hull.dat files obtained via its meshing functions for its examples.

Further, the hydrostatic stiffness matrix of float (*KH_0.dat*) and spar-plate (*KH_1.dat*) are obtained by meshing the bodies. Equations (2.1) and (2.2) represent the hydrostatic stiffness matrix for float and spar, respectively. The hydrostatic stiffness matrix describes how the net weight plus buoyancy load changes with variations from the datum position. The stiffness elements are solely defined for the heave, roll, and pitch degrees of freedom; the stiffness equals zero for the other degrees of freedom.

$$
KH_0 = \begin{bmatrix}
0 & 0 & 0 & 0 & 0 & 0 \\
0 & 0 & 0 & 0 & 0 & 0 \\
0 & 0 & 0.2873707E+07 & 0 & 0.3750000E+00 & 0 \\
0 & 0 & 0 & 0.5720900E+08 & 0 & 0 \\
0 & 0 & 0.3750000E+00 & 0 & 0.5720899E+08 & 0 \\
0 & 0 & 0 & 0 & 0 & 0
\end{bmatrix}
\tag{2.1}
$$

$$
KH_1 = \begin{bmatrix}
0 & 0 & 0 & 0 & 0 & 0 \\
0 & 0 & 0 & 0 & 0 & 0 \\
0 & 0 & 0.2842112E+06 & 0 & 0.6250000E-01 & 0 \\
0 & 0 & 0 & 0.1297135E+09 & 0 & 0 \\
0 & 0 & 0.6250000E-01 & 0 & 0.1297136E+09 & 0 \\
0 & 0 & 0 & 0 & 0 & 0
\end{bmatrix}
\tag{2.2}
$$

2.1.2 Meshing OSWEC

Mesh.m function is used to mesh the OSWEC. This function is suitable for non-axisymmetric bodies, or they do not have curves in their geometric structure. For more sophisticated geometries, one should use Computer-Aided Design (CAD) software and adapt the files resulting from the meshing process in a suitable format.

The dimensions of the OSWEC, which are considered in this study, are shown in Figure 2.6. The height of the OSWEC below the SWL is 13 m which indicates the device is located in shallow water. The part of the flap above the SWL is 3 m. The length and width of the flap and base are 2 m and 26 m, respectively. The COG is 2.74 m below SWL. The earlier mentioned quantities are taken from Ref [30].
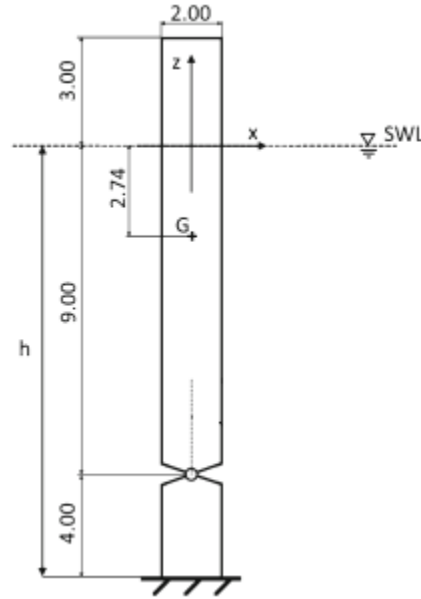
Figure 2.6: OSWEC schematic

The Mesh.m can mesh several bodies when calling its function. However, in this study, flap and base are meshed separately by calling the Mesh.m function for each of them. This approach is also correct since it helps the user easily rename the result files inside the working folder. The user can decide to mesh the flap and base via calling Mesh.m function for a single time. The inputs that are required for Mesh.m function are:

- nBodies: Number of bodies
- n(nBodies): Number of panels
- X (nBodies, n, 4, 3): Coordinates of nodes of each panel
- tX (nBodies): Translations
- CG (nBodies, 3): Position of gravity center
- Nfobj (nBodies): Target number of panels for Aquaplus mesh

Like the axiMesh.m function, the mesh,m function also needs one working folder. OSWEC meshing results are stored in a working folder called *oswec*. The name of the working folder will be asked when the mesh.m function is called for each body. Also, it is essential to note that the result files must be renamed for each body at the end of their meshing process. Hence, all the result files and also Nemoh.cal files for each body must be renamed inside the working folder to prevent data loss for the first body after continuing to mesh the second body.

The MATLAB code for calling mesh.m function is shown in Script 2.5. The script was saved inside the *oswec* working folder and named *oswec1*, which indicates the first step carried out for the 2BPA.

```
1    % Meshing for the oscillating surge wave energy converter (OSWEC)
2    % FLAP
3    nBodies=1;
4    n=7;
5
6    X(1,1,:,:)=[-1 -13 3;-1 -13 -8;1 -13 -8;1 -13 3];
7    X(1,2,:,:)=[-1 0 3;-1 -13 3;1 -13 3;1 0 3];
8    X(1,3,:,:)=[1 0 3;1 -13 3;1 -13 -8;1 0 -8];
9    X(1,4,:,:)=[-1 0 3;-1 0 -8;-1 -13 -8;-1 -13 3];
10   X(1,5,:,:)=[-1 -13 -8;-1 0 -8;0 0 -9;0 -13 -9];
11   X(1,6,:,:)=[0 -13 -9;0 0 -9;1 0 -8;1 -13 -8];
12   X(1,7,:,:)=[-1 -13 -8;0 -13 -9;1 -13 -8;1 -13 -8];
13
14   tX(1)=0;
15   CG(1,:)=[0. 0. -2.74];
16   nfobj(1)=400;
17   [Mass,Inertia,KH,XB,YB,ZB]=Mesh(nBodies,n,X,tX,CG,nfobj)
18
19   %%
20   % BASE
21   nBodies=1;
22   n=7;
23
24   X(1,1,:,:)=[-1 -13 -13;-1 0 -13;1 0 -13;1 -13 -13];
25   X(1,2,:,:)=[-1 -13 -10;0 -13 -9;0 0 -9;-1 0 -10];
26   X(1,3,:,:)=[0 -13 -9;1 -13 -10;1 0 -10;0 0 -9];
27   X(1,4,:,:)=[-1 -13 -13;1 -13 -13;1 -13 -10;-1 -13 -10];
28   X(1,5,:,:)=[-1 -13 -10;1 -13 -10;0 -13 -9;-1 -13 -10];
29   X(1,6,:,:)=[1 0 -10;1 -13 -10;1 -13 -13;1 0 -13];
30   X(1,7,:,:)=[-1 0 -10;-1 0 -13;-1 -13 -13;-1 -13 -10];
31
32   tX(1)=0;
33   CG(1,:)=[0 0 -13];
34   nfobj(1)=400;
35   [Mass,Inertia,KH,XB,YB,ZB]=Mesh(nBodies,n,X,tX,CG,nfobj)
```

Script 2.5: Call function Mesh for OSWEC.

First, we decided to mesh flap, and we considered the number '0' to represent this body. So, after calling the Mesh.m function for the flap, the results files for this body are obtained and saved inside *oswec/mesh*. The files are:

- mesh1
- mesh1.dat
- mesh1.tec
- mesh1_info.dat
- Description_Full.tec
- Description_Wetted.tec
- GC_hull.dat

- Hydrostatics.dat
- Inertia_hull.dat
- KH.dat

The files mentioned above were renamed to:

- flap
- flap.dat
- flap.tec
- flap_info.dat
- Description_Full_0.tec
- Description_Full_1.tec
- GC_hull_0.dat
- Hydrostatics_0.dat
- Inertia_hull_0.dat
- KH_0.dat

Then, the Nemoh.cal file for flap was renamed to flap.cal inside the *oswec* folder.

Second, we proceeded to mesh base, and we considered number '1' to represent this body. So, after calling Mesh.m function for the base, the results files for this body are obtained and saved inside *oswec/mesh*. The files are:

- mesh1
- mesh1.dat
- mesh1.tec
- mesh1_info.dat
- Description_Full.tec
- Description_Wetted.tec
- GC_hull.dat
- Hydrostatics.dat
- Inertia_hull.dat
- KH.dat

The files mentioned above were renamed to:

- base
- base.dat
- base.tec
- base_info.dat
- Description_Full_1.tec
- Description_Wetted_1.tec
- GC_hull_1.dat
- Hydrostatics_1.dat

2. Numerical Modeling of Hydrostatic Properties of 2BPA and OSWEC

- Inertia_hull_1.dat
- KH_1.dat

Then, the Nemoh.cal file for the base was renamed to base.cal inside *the oswec* folder.

The flap.cal and base.cal are given in Script 2.6 and 2.7, respectively. Further, a single Nemoh.cal file containing all the data for flap and base was created following the steps provided in section 2.1.1 and shown in Script 2.8. As mentioned in section 2.1.1, the wave frequency data can be modified manually in the Nemoh.cal or defined in the 2nd step. For OSWEC, the Kochin function was neglected as well as 2BPA.

```
1    --- Environment -----------------------------------------------------------
2    1025.000000        *Sea water density(kg/m^3)
3    9.810000           *The gravity acceleration (m/s^2)
4    0.                 *Water depth (m)
5    0.    0.           *Wave measurement point XEFF YEFF (m)
6    --- Description of floating bodies ----------------------------------------
7    1                  *Count of bodies
8    --- Body 1 ----------------------------------------------------------------
9    oswec\mesh\mesh1.dat  *The mesh file's name
10   498 392               *Count of points and panels
11   6                          *DOF
12   1 1.0 0.0 0.0 0.0 0.0 0.0   *Surge
13   1 0.0 1.0 0.0 0.0 0.0 0.0   *Sway
14   1 0.0 0.0 1.0 0.0 0.0 0.0   *Heave
15   2 1.0 0.0 0.0 0.0 0.0 -2.74 *Rolling about this point
16   2 0.0 1.0 0.0 0.0 0.0 -2.74 *Pitching about this point
17   2 0.0 0.0 1.0 0.0 0.0 -2.74 *Yawing about this point
18   6                          *Amount of resulting generalized forces
19   1 1.0 0.0 0.0 0.0 0.0 0.0   *x-direction force
20   1 0.0 1.0 0.0 0.0 0.0 0.0   *y-direction force
21   1 0.0 0.0 1.0 0.0 0.0 0.0   *z-direction force
22   2 1.0 0.0 0.0 0.0 0.0 -2.74 *Moment force about this point in the x-direction
23   2 0.0 1.0 0.0 0.0 0.0 -2.74 *Moment force about this point in the y-direction
24   2 0.0 0.0 1.0 0.0 0.0 -2.74 *Moment force about this point in the z-direction
25   0                          *Number of additional lines of information
26   --- Load cases that have to be solved -------------------------------------
27   1    0.8    0.8            *The number of wave frequencies, the minimum, and
28   the maximum (rad/s)
29   1    0.    0.             *The number of wave directions, minimum, and the
30   maximum (degrees)
31   --- Post processing -------------------------------------------------------
32   1    0.1    10.          *Calculation of the IRF (0 is for no calculation),
33   time step, and duration
34   0                          * Pressure
35   0    0.    180.          * Kochin function    Count of directions of
36   calculation (0 is for no calculations), minimum and maximum (degrees)
37   0    50    400.  400.   *Count of points in the x-direction (0 if no
38   calculations) and y-direction, and domain dimensions in x and y-direction
39   ---
```

Script 2.6: flap.cal

27

2. Numerical Modeling of Hydrostatic Properties of 2BPA and OSWEC

```
1   --- Environment ------------------------------------------------------------
2   1025.000000        *Sea water density(kg/m^3)
3   9.810000           *The gravity acceleration (m/s^2)
4   0.                 *Water depth (m)
5   0.    0.           *Wave measurement point XEFF YEFF (m)
6   --- Description of floating bodies -----------------------------------------
7   1                  *Count of bodies
8   --- Body 1 -----------------------------------------------------------------
9   oswec\mesh\mesh1.dat   *The mesh file's name
10  514 382                *Count of points and panels
11  6                             *DOF
12  1 1.0 0.0 0.0 0.0 0.0 0.0     *Surge
13  1 0.0 1.0 0.0 0.0 0.0 0.0     *Sway
14  1 0.0 0.0 1.0 0.0 0.0 0.0     *Heave
15  2 1.0 0.0 0.0 0.0 0.0 -13.00 *Rolling about this point
16  2 0.0 1.0 0.0 0.0 0.0 -13.00 *Pitching about this point
17  2 0.0 0.0 1.0 0.0 0.0 -13.00 *Yawing about this point
18  6                             *Amount of resulting generalized forces
19  1 1.0 0.0 0.0 0.0 0.0 0.0     *x-direction force
20  1 0.0 1.0 0.0 0.0 0.0 0.0     *y-direction force
21  1 0.0 0.0 1.0 0.0 0.0 0.0     *z-direction force
22  2 1.0 0.0 0.0 0.0 0.0 -13.00 *Moment force about this point in the x-
23  direction
24  2 0.0 1.0 0.0 0.0 0.0 -13.00 *Moment force about this point in the y-
25  direction
26  2 0.0 0.0 1.0 0.0 0.0 -13.00 *Moment force about this point in the z-
27  direction
28  0                             *Number of additional lines of information
29  --- Load cases that have to be solved --------------------------------------
30  1    0.8    0.8              *The number of wave frequencies, the minimum, and
31  the maximum (rad/s)
32  1    0.    0.               *The number of wave directions, minimum, and the
33  maximum (degrees)
34  --- Post processing --------------------------------------------------------
35  1    0.1   10.        *Calculation of the IRF (0 is for no calculation),
36  time step, and duration
37  0                        * Pressure
38  0    0.    180.         * Kochin function    Count of directions of
39  calculation (0 is for no calculations), minimum and maximum (degrees)
40  0    50    400.  400.  *Count of points in the x-direction (0 if no
41  calculations) and y-direction, and domain dimensions in x and y-direction
42  ---
```

Script 2.7: base.cal

```
1   --- Environment ------------------------------------------------------------
2   1025.000000 *Sea water density(kg/m^3)
3   9.810000    *The gravity acceleration (m/s^2)
4   0.          *Water depth (m)
5   0.    0.    *Wave measurement point XEFF YEFF (m)
6   --- Description of floating bodies -----------------------------------------
7   2          * Count of bodies
8   --- Body 1 -----------------------------------------------------------------
9   oswec\mesh\flap.dat    *The mesh file's name
10  498 392                    *Count of points and panels
```

```
11   6                                       *DOF
12   1 1.0 0.0 0.0 0.0 0.0 0.0    *Surge
13   1 0.0 1.0 0.0 0.0 0.0 0.0    *Sway
14   1 0.0 0.0 1.0 0.0 0.0 0.0    *Heave
15   2 1.0 0.0 0.0 0.0 0.0 -2.74 *Rolling about this point
16   2 0.0 1.0 0.0 0.0 0.0 -2.74 *Pitching about this point
17   2 0.0 0.0 1.0 0.0 0.0 -2.74 *Yawing about this point
18   6                                       *Amount of resulting generalized forces
19   1 1.0 0.0 0.0 0.0 0.0 0.0    *x-direction force
20   1 0.0 1.0 0.0 0.0 0.0 0.0    *y-direction force
21   1 0.0 0.0 1.0 0.0 0.0 0.0    *z-direction force
22   2 1.0 0.0 0.0 0.0 0.0 -2.74 *Moment force about this point in the x-direction
23   2 0.0 1.0 0.0 0.0 0.0 -2.74 *Moment force about this point in the y-direction
24   2 0.0 0.0 1.0 0.0 0.0 -2.74 *Moment force about this point in the z-direction
25   0                                       *Number of additional lines of information
26   --- Body 2 -------------------------------------------------------------
27   oswec\mesh\base.dat            *The mesh file's name
28   514 382                        *Count of points and panels
29   6                              *DOF
30   1 1.0 0.0 0.0 0.0 0.0 0.0    *Surge
31   1 0.0 1.0 0.0 0.0 0.0 0.0    *Sway
32   1 0.0 0.0 1.0 0.0 0.0 0.0    *Heave
33   2 1.0 0.0 0.0 0.0 0.0 -13.00 *Rolling about this point
34   2 0.0 1.0 0.0 0.0 0.0 -13.00 *Pitching about this point
35   2 0.0 0.0 1.0 0.0 0.0 -13.00 *Yawing about this point
36   6                              *Amount of resulting generalized forces
37   1 1.0 0.0 0.0 0.0 0.0 0.0    *x-direction force
38   1 0.0 1.0 0.0 0.0 0.0 0.0    *y-direction force
39   1 0.0 0.0 1.0 0.0 0.0 0.0    *z-direction force
40   2 1.0 0.0 0.0 0.0 0.0 -13.00*Moment force about this point in the x-direction
41   2 0.0 1.0 0.0 0.0 0.0 -13.00*Moment force about this point in the y-direction
42   2 0.0 0.0 1.0 0.0 0.0 -13.00*Moment force about this point in the z-direction
43   0                                       *Number of additional lines of information
44   --- Load cases that have to be solved ----------------------------------------
45   239    0.6283     12.5283 *The number of wave frequencies, the minimum, and
46   the maximum (rad/s)
47   1    0.       0.               *The number of wave directions, minimum, and the
48   maximum (degrees)
49   --- Post processing -----------------------------------------------------------
50   1    0.1   10.           *Calculation of the IRF (0 is for no calculation),
51   time step, and duration
52   0                            * Pressure
53   0    0.    180.          * Kochin function    Count of directions of
54   calculation (0 is for no calculations), minimum and maximum (degrees)
55   0    50   400.  400.  *Count of points in the x-direction (0 if no
56   calculations) and y-direction, and domain dimensions in x and y-direction

     ---
```

Script 2.8: Single Nemoh.cal for OSWEC

In Script 2.8, the data written in lines 2 to 5 are the environmental properties where the OSWEC is simulated. The fluid-specific volume, gravity, water depth, and wave measurement point are the data given in the environment section of the Nemoh.cal. Nemoh.cal script shows that the water depth is zero as a default value. For deep water depth, the value of the water depth is assumed to

be zero by Nemoh.cal. However, when calling the Nemoh function in the 2nd step to calculate hydrodynamic coefficients, it is possible to change the water depth to the desired value. In this case, the water depth will be rewritten in Nemoh.cal file to the value defined by the user in the 2nd step. Also, in the 2nd step, it is noted that the zero-depth is exclusively assumed for the deep-water calculations.

Lines 10 and 28 provide the final properties of the meshed bodies, including the number of nodes and points obtained via the Mesh.m function. The 6DOF is indicated for each body is shown in lines 11 and 29, which means that the simulation of the OSWEC will be carried out for translational (surge, sway, and heave) and rotational (roll, pitch, and yaw) directions. However, since only pitch motion is significant to the system, and the hydrodynamic coefficients will be calculated based on this motion, other degrees of freedom are not considered in this study.

The number 1 written to the left side of lines 12-14 and lines 30-32 indicates the translational movement of the flap and base. Plus, the number 2 corresponding to the left side of the lines 15-17 and lines 33-35 indicate rotational motion of the flap and base bodies. The following three numbers in those lines are the direction vectors, and the last three numbers are the COG coordinates. For translational motions, only direction vector is defined, while for rotational movements, besides direction vector, COG coordinates of the bodies are defined where rotational motions in x, y, and z directions will be determined about COG.

The number 1 written to the left side of lines 19-21 and 37-39 indicates force for the flap and base bodies. The number 2 corresponds to the left side of the lines 22-24 and 40-42, indicating moment force for the flap and base bodies. The following three numbers in those lines are the direction vectors, and the last three numbers are the x, y, and z coordinates of COG. For force, only direction vector is defined, while for moment force, besides direction vector, COG coordinates of the bodies are defined where moment force in x, y, and z directions will be determined about COG.

In Script 2.8, lines 45 and 47 are the wave frequency and wave direction vectors, respectively. At this moment, these values are defined as a default. The vectors of wave frequency and wave direction will be defined in 2nd step by the user. Then, after the Nemoh function is called and the hydrodynamic coefficients are obtained for flap and base bodies, the vector lengths of the wave frequency and wave direction will be corrected in the Nemoh.cal. However, the user can manually enter the values mentioned above in Nemoh.cal script before commencing the 2nd step. Still, again the same values must be defined for the Nemoh function unless the user wants to change them.

Script 2.8 has a post-processing section that post-processes the results to provide relevant quantities in a usual format (added mass, radiation damping, excitation force). A framework is also provided for making relevant calculations. Line 50 of Script 2.8 indicates the numbers of calculations for impulse response function (IRF), time step, and duration. There is also an indication of the minimum and maximum angle in degrees for each calculation number XX for which the Kochin function will be calculated. The Kochin function expresses the wave kinematics in the far-field [29]. However, in this study, the Kochin function is not considered.

2. Numerical Modeling of Hydrostatic Properties of 2BPA and OSWEC

The meshed flap and base bodies are obtained as shown in Figure 2.7 and Figure 2.8, respectively. The figures represent half of the bodies since they are symmetrical about the (XOZ) plane. The arrows are the hydrostatic forces applied by the water to the body surface. It is important to note that the direction of the arrows is pointing outside because they show the hydrostatic reaction force that is the force applied by the body to the fluid.
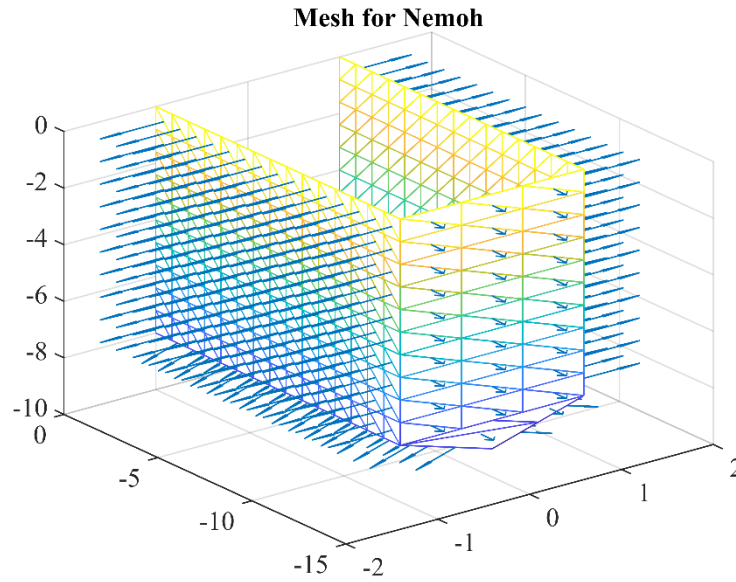
Figure 2.7: Flap meshing
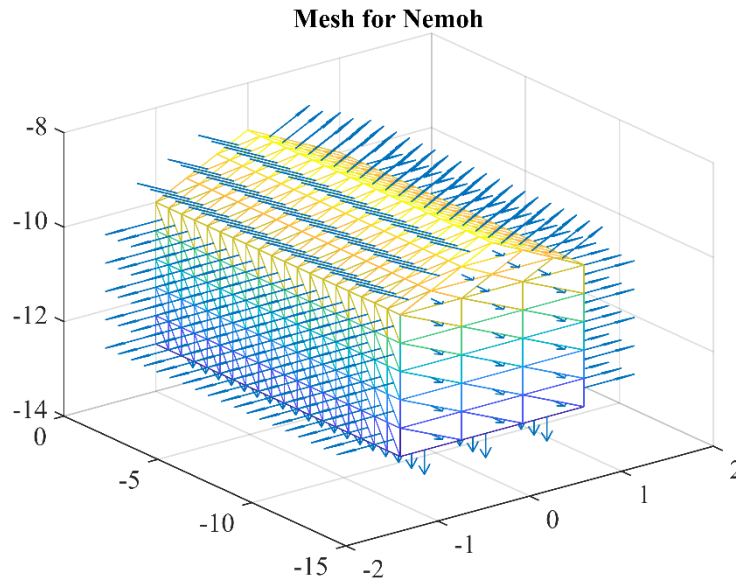
Figure 2.8: Base meshing

31

2. Numerical Modeling of Hydrostatic Properties of 2BPA and OSWEC

The hydrostatic properties of the flap and base are obtained by meshing the bodies. The *Hydrostatics_0.dat* (for the flap) and *Hydrostatics_1.dat* (for base) contain the data for COG and COB of the bodies. Also, they include the data for water displacement and waterplane areas of flap and base, which are obtained as the output data of the meshing process. The *Hydrostatics_0.dat* and *Hydrostatics_1.dat* files are located inside the *oswec/mesh* folder. Table 2.4 shows the data for *Hydrostatics_0.dat* and *Hydrostatics_1.dat* obtained for OSWEC.

Body	XF (m)	YF (m)	ZF (M)	XG (M)	YG (M)	ZG (M)	Water displacement (m³)	Waterplane area (m²)
Flap	0.000	0.000	-4.255	0.000	0.000	-2.740	442	52
Base	0.000	0.000	-11.238	0.000	0.000	-13.000	182.0001	0.000

Table 2.4: Hydrostatics_0.dat and Hydrostatics_1.dat data obtained for OSWEC

Like the 2BPA, the GC_hull.dat and Inertia_hull.dat files obtained by Mesh for OSWEC include the coordinates of the body's gravity center and moment of inertia tensors. These files are not considered the results file since they do not affect the calculations in further steps. The mass, COG, and moment of inertia of OSWEC can be defined by the user in the WEC-Sim input file. However, it is essential to note that a high difference between the total mass of the OSWEC and OSWEC's total displaced water leads to a high percentage error. Hence, it is recommended that the user define the device mass as it is defined by the problem, which is 150000 kg. Plus, the user must note that the base is fixed on the sea bed, which causes the flap to have only pitch motion and pitch moment of inertia. So, the base has no moment of inertia, and the Inertia_hull_1.dat obtained by Mesh.m is not considered. Subsequently, the moment of inertia of flap given in Inertia_hull_0.dat that Mesh.m obtains is incorrect since the flap has only a pitch moment of inertia. These differences in earlier mentioned values are because in the axiMesh and Mesh.m there is no possibility of defining a fixed structure.

Further, the hydrostatic stiffness matrix of the flap (*KH_0.dat*) and base (*KH_1.dat*) are obtained by meshing the bodies. Equations (2.3) and (2.4) show the hydrostatic stiffness matrix for flap and base, respectively.

$$
KH_0 = \begin{bmatrix}
0 & 0 & 0 & 0 & 0 & 0 \\
0 & 0 & 0 & 0 & 0 & 0 \\
0 & 0 & 0.5228732E+06 & 0 & -0.5859375E-02 & 0 \\
0 & 0 & 0 & 0.2268958E+08 & 0 & 0 \\
0 & 0 & -0.5859375E-02 & 0 & -0.6569473E+07 & 0 \\
0 & 0 & 0 & 0 & 0 & 0
\end{bmatrix}
\tag{2.3}
$$

$$KH_1 = \begin{bmatrix} 0 & 0 & 0 & 0 & 0 & 0 \\ 0 & 0 & 0 & 0 & 0 & 0 \\ 0 & 0 & 0.5400391E+00 & 0 & 0.4010010E-01 & 0 \\ 0 & 0 & 0 & 0.3224496E+07 & 0 & 0 \\ 0 & 0 & 0.4010010E-01 & 0 & 0.3209970E+07 & 0 \\ 0 & 0 & 0 & 0 & 0 & 0 \end{bmatrix} \qquad (2.4)$$

3.

Numerical Modeling of Hydrodynamic Coefficients of 2BPA and OSWEC

3.1 Using NEMOH to Calculate the Hydrodynamic Coefficients: 2nd Step

In the second step, we need to calculate the hydrodynamic coefficients of our RM3 2BPA and OSWEC. In this thesis, the first-order hydrodynamic coefficients, including added mass coefficient, radiation damping coefficient, excitation force, and excitation force phase response, are numerically obtained by running the NEMOH preprocessor successfully. With the help of the NEMOH Solver and the NEMOH Postprocessor, we can calculate Froude-Krylov forces that result from each diffraction problem, along with forces associated with each problem. In addition, we can calculate the Kochin function, diffraction force, the free surface elevation, and the pressure field on the body surfaces. The function Nemoh is used as a MATLAB wrapper to calculate hydrodynamic coefficients of 2BPA and OSWEC. The incident wave characteristics were defined as input data for Nemoh.m function to plot the added mass and radiation damping coefficients, excitation force coefficients, and phase excitation response versus wave frequency.

3.1.1 Hydrodynamic Coefficients of RM3 2BPA

In this section, the hydrodynamic coefficients of previously meshed 2BPA are numerically modeled using open-source BEM solver NEMOH. BEM codes based on linear potential flow theory are still extensively applied for wave-structure interactions in numerical waves to weather (W2W) models for WECs [31]. The BEM solver NEMOH is an open-source code used to compute hydrodynamic coefficients, while other BEM solvers such as WAMIT, Diodore, DIFFRACT, Hydrostar, Aquaplus are expensive, and they were developed a long time ago.

For each vector of body condition, BEM solver NEMOH solves the linear Boundary Value Problem (BVP) for the potential and calculates pressure field, hydrodynamic coefficients, far-field coefficients, and wave elevation. In this thesis, the motivation of using the NEMOH solver is to analyze the capability of this solver to represent the interaction between float and spar bodies. NEMOH solver is yet widely used to model the offshore structures' hydrodynamic coefficients numerically. For example, Penalba [27] used the NEMOH solver to numerically model the hydrodynamic coefficients of a 2BPA and analyze this solver's capability to represent the interaction between float and spar bodies. Bingyong Guo and his colleagues [32] obtained the hydrodynamic coefficients of a heaving absorber for wave energy conversion using the NEMOH solver.

3. Numerical Modeling of Hydrodynamic Coefficients of 2BPA and OSWEC

In this study, by calling the Nemoh.m function in MATLAB, the hydrodynamic coefficients of 2BPA are obtained. Script 2.9 is the MATLAB code for calling function Nemoh. The script was saved inside the *pointabsorber* folder and named *pointabsorber2*, which indicates the second step carried out for the 2BPA. Note that the function Nemoh is located inside the *matlab routines* folder in *Nemoh for Matlab* zip file, which can be downloaded from: https://box.lheea.ec-nantes.fr/index.php/s/sKLWx6pVGBo7H7Y.

```matlab
1    %%% II) Call function Nemoh
2    %%%
3    %%% function [A,B,Fe]=Nemoh(w, dir, depth)
4    %%%
5    %%% Purpose: Matlab wrapper for calculation of hydrodynamic coefficients
6    using Nemoh
7    %%%
8    %%% Inputs :
9    %%% - w     : Vector length(w) of wave frequencies (rad/s)
10   %%% - dir   : Wave direction (degrees).
11   %%% - depth : water depth (m), 0 for deep water.
12   %%%
13   %%% Outputs :
14   %%% - A: Matrix (6xnBodies)x(6xnBodies)xlength(w) of added mass coefficients
15   %%% - B: Matrix (6xnBodies)x(6xnBodies)xlength(w) of radiation damping
16   coefficients
17   %%% - Fe : Matrix (6xnBodies)xlength(w) of exciation forces (complex values)
18   %%%
19   %%% Copyright Ecole Centrale de Nantes 2014
20   %%% Licensed under the Apache License, Version 2.0
21   %%% Written by A. Babarit, LHEEA Lab.
22   %%%
23   %%%%%%%%%%%%%%%%%%%%%%%%%%%%%%%%%
24
25   %%% Nemoh inputs:
26
27   w=0.02:0.02:5.20;    %% Vector length(w) of wave frequencies (rad/s)
28   dir=0;               %% Wave direction (degrees). Towards positive x.
29   h=70;                %% Water depth (m), 0 for deep water approximation.
30   [A,B,Fe]=Nemoh(w, dir, h);    %% Call function Nemoh
31
32
33   %%% Plot results (added mass and radiation damping coefficients)
34
35   %%% Float:
36   A11(1,:)=A(1,1,:); %% Surge mode
37   B11(1,:)=B(1,1,:); %% Surge mode
38   A33(1,:)=A(3,3,:); %% Heave mode
39   B33(1,:)=B(3,3,:); %% Heave mode
40   A55(1,:)=A(5,5,:); %% Pitch mode
41   B55(1,:)=B(5,5,:); %% Pitch mode
42
43   figure;
44   plot(w,A11,'r',w,B11,'b'); %% Added mass and radiation damping coefficients
45   for surge mode of the 2BPA float
46   xlabel('wave frequency (rad/s)');
47   ylabel('Added mass (kg) & Radiation damping (N*s/m) coefficients');
```

```matlab
48    legend ('Added mass','Radiation damping')
49    grid on
50
51    figure;
52    plot(w,A33,'r',w,B33,'b'); %% Added mass and radiation damping coefficients
53    for heave mode of the 2BPA float
54    xlabel('wave frequency (rad/s)');
55    ylabel('Added mass (kg) & Radiation damping (N*s/m) coefficients');
56    legend ('Added mass','Radiation damping')
57    grid on
58
59    figure;
60    plot(w,A55,'r',w,B55,'b'); %% Added mass and radiation damping coefficients
61    for pitch mode of the 2BPA float
62    xlabel('wave frequency (rad/s)');
63    ylabel('Added mass (kg) & Radiation damping (N*s/m) coefficients');
64    legend ('Added mass','Radiation damping')
65    grid on
66
67    %%% Spar:
68    A77(1,:)=A(7,7,:);
69    B77(1,:)=B(7,7,:);
70    A99(1,:)=A(9,9,:);
71    B99(1,:)=B(9,9,:);
72    A1111(1,:)=A(11,11,:);
73    B1111(1,:)=B(11,11,:);
74
75    figure; %% Added mass and radiation damping coefficients for surge mode of
76    the 2BPA spar
77    plot(w,A77,'r',w,B77,'b');
78    xlabel('wave frequency (rad/s)');
79    ylabel('Added mass (kg) & Radiation damping (N*s/m) coefficients');
80    legend ('Added mass','Radiation damping')
81    grid on
82
83    figure;
84    plot(w,A99,'r',w,B99,'b'); %% Added mass and radiation damping coefficients
85    for heave mode of the 2BPA spar
86    xlabel('wave frequency (rad/s)');
87    ylabel('Added mass (kg) & Radiation damping (N*s/m) coefficients');
88    legend ('Added mass','Radiation damping')
89    grid on
90
91    figure;
92    plot(w,A1111,'r',w,B1111,'b'); %% Added mass and radiation damping
93    coefficients for pitch mode of the 2BPA spar
94    xlabel('wave frequency (rad/s)');
95    ylabel('Added mass (kg) & Radiation damping (N*s/m) coefficients');
96    legend ('Added mass','Radiation damping')
97    grid on
98
99    %%% Plot results (excitation force)
100   %%% Fe1 (excitation force in surge mode), Fe3 (excitation force in heave
101   mode), and Fe5 (excitation force in pitch mode):
102
103   %%% FLOAT:
104   Fe1(1,:)=Fe(:,1);   %% Heave mode
```

```matlab
105    Fe3(1,:)=Fe(:,3);   %% Surge mode
106    Fe5(1,:)=Fe(:,5);   %% Pitch mode
107
108    figure;
109    subplot(3,1,1), plot(w,abs(Fe1),'r'); xlabel('wave frequency (rad/s)');
110    ylabel('Amplitude excitation response (N)');
111    title('Excitation force for surge mode of 2BPA float')
112    grid on
113    subplot(3,1,2), plot(w,abs(Fe3),'b'); xlabel('wave frequency (rad/s)');
114    ylabel('Amplitude excitation response (N)');
115    title('Excitation force for heave mode of 2BPA float')
116    grid on
117    subplot(3,1,3), plot(w,abs(Fe5),'g'); xlabel('wave frequency (rad/s)');
118    ylabel('Amplitude excitation response (N)');
119    title('Excitation force for pitch mode of 2BPA float')
120    grid on
121
122    %%% SPAR:
123    Fe7(1,:)=Fe(:,7);    %% Heave mode
124    Fe9(1,:)=Fe(:,9);    %% Surge mode
125    Fe11(1,:)=Fe(:,11);  %% Pitch mode
126
127    figure;
128    subplot(3,1,1), plot(w,abs(Fe7),'r'); xlabel('wave frequency (rad/s)');
129    ylabel('Amplitude excitation response (N)');
130    title('Excitation force for surge mode of 2BPA spar')
131    grid on
132    subplot(3,1,2), plot(w,abs(Fe9),'b'); xlabel('wave frequency (rad/s)');
133    ylabel('Amplitude excitation response (N)');
134    title('Excitation force for heave mode of 2BPA spar')
135    grid on
136    subplot(3,1,3), plot(w,abs(Fe11),'g'); xlabel('wave frequency (rad/s)');
137    ylabel('Amplitude excitation response (N)');
138    title('Excitation force for pitch mode of 2BPA spar')
139    grid on
140
141    %%% Plot results (excitation force coefficients)
142    %%% Fe1 & Phase:
143
144    %%% Float:
145    figure;
146    subplot(2,1,1); plot(w, abs(Fe(:,1)),'r'); xlabel('wave frequency (rad/s)');
147    ylabel('Amplitude excitation response (N)');
148    title('Float excitation force in surge mode')
149    grid on
150    subplot(2,1,2); plot(w, angle(Fe(:,1)),'r'); xlabel('wave frequency
151    (rad/s)'); ylabel('Phase excitation response (rad)');
152    title('Float excitation phase response in surge mode')
153    grid on
154
155    figure;
156    subplot(2,1,1); plot(w, abs(Fe(:,3)),'b'); xlabel('wave frequency (rad/s)');
157    ylabel('Amplitude excitation response (N)');
158    title('Float excitation force in heave mode')
159    grid on
160    subplot(2,1,2); plot(w, angle(Fe(:,3)),'b'); xlabel('wave frequency
161    (rad/s)'); ylabel('Phase excitation response (rad)');
```

```
162    title('Float excitation phase response in heave mode')
163    grid on
164
165    figure;
166    subplot(2,1,1); plot(w, abs(Fe(:,5)),'g'); xlabel('wave frequency (rad/s)');
167    ylabel('Amplitude excitation response (N)');
168    title('Float excitation force in pitch mode')
169    grid on
170    subplot(2,1,2); plot(w, angle(Fe(:,5)),'g'); xlabel('wave frequency
171    (rad/s)'); ylabel('Phase excitation response (rad)');
172    title('Float excitation phase response in pitch mode')
173    grid on
174
175    %%% Spar:
176    figure;
177    subplot(2,1,1); plot(w, abs(Fe(:,7)),'r'); xlabel('wave frequency (rad/s)');
178    ylabel('Amplitude excitation response (N)');
179    title('Spar excitation force in surge mode')
180    grid on
181    subplot(2,1,2); plot(w, angle(Fe(:,7)),'r'); xlabel('wave frequency
182    (rad/s)'); ylabel('Phase excitation response (rad)');
183    title('Spar excitation phase response in surge mode')
184    grid on
185
186    figure;
187    subplot(2,1,1); plot(w, abs(Fe(:,9)),'b'); xlabel('wave frequency (rad/s)');
188    ylabel('Amplitude excitation response (N)');
189    title('Spar excitation force in heave mode')
190    grid on
191    subplot(2,1,2); plot(w, angle(Fe(:,9)),'b'); xlabel('wave frequency
192    (rad/s)'); ylabel('Phase excitation response (rad)');
193    title('Spar excitation phase response in heave mode')
194    grid on
195
196    figure;
197    subplot(2,1,1); plot(w, abs(Fe(:,11)),'g'); xlabel('wave frequency (rad/s)');
198    ylabel('Amplitude excitation response (N)');
199    title('Spar excitation force in pitch mode')
200    grid on
201    subplot(2,1,2); plot(w, angle(Fe(:,11)),'g'); xlabel('wave frequency
202    (rad/s)'); ylabel('Phase excitation response (rad)');
203    title('Spar excitation phase response in pitch mode')
204    grid on
```

Script 2.9: Call function Nemoh for 2BPA

In Script 2.9, the Nemoh function input data are vector length (w) of wave frequencies (rad/s), wave direction (degrees) towards positive x, and water depth (m). For our 2BPA, the minimum wave frequency defined is 0.02 (rad/s), the maximum wave frequency is 5.20 (rad/s), and the frequency step between these two values is 0.02 (rad/s). The hydrodynamic coefficients of the 2BPA will be obtained for the defined frequency vector. Also, in the WEC-Sim input file, the wave period must be defined between the range of 1.2083 seconds up to 314.1592 seconds, which

corresponds to the frequency range mentioned earlier. Any wave period that does not fall into the period range discussed above will cause the WEC-Sim to be unable to simulate the problem.

The wave direction for 2BPA is assumed to be 0 degrees. In this case, the direction of the incident wave is perpendicular to the device's surface. Finally, the depth at which the 2BPA is chosen to be implemented is 70 (m). Figures 2.9-2.22 show the hydrodynamic coefficients obtained for the 2BPA.
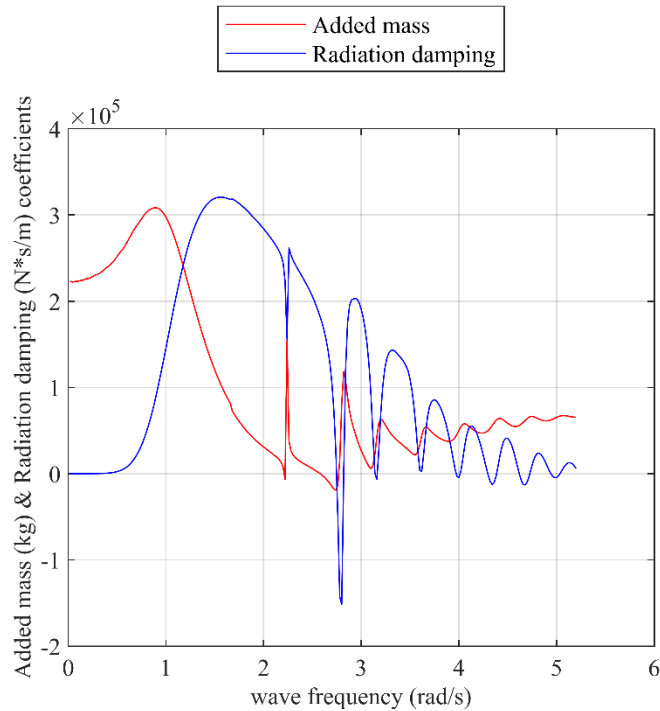
Figure 2.9: Added mass and radiation damping coefficients for surge mode of the 2BPA float
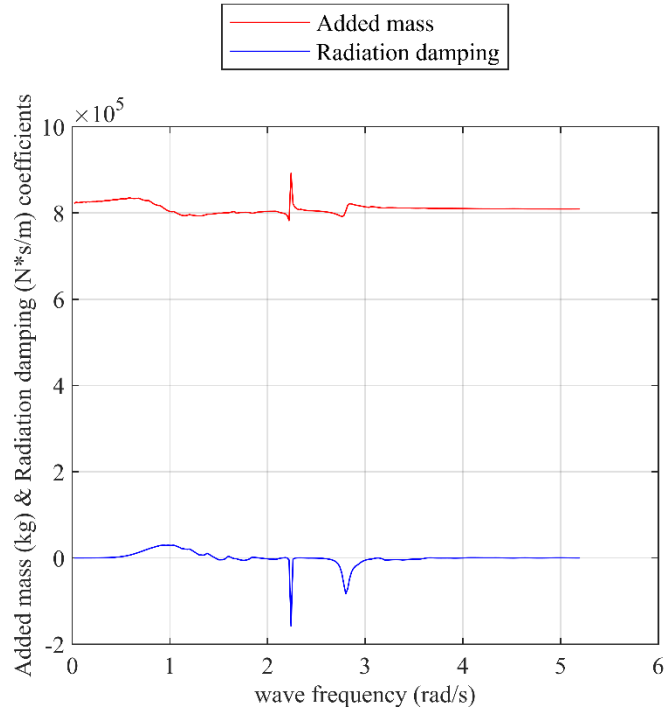
Figure 2.10: Added mass and radiation damping coefficients for surge mode of the 2BPA spar
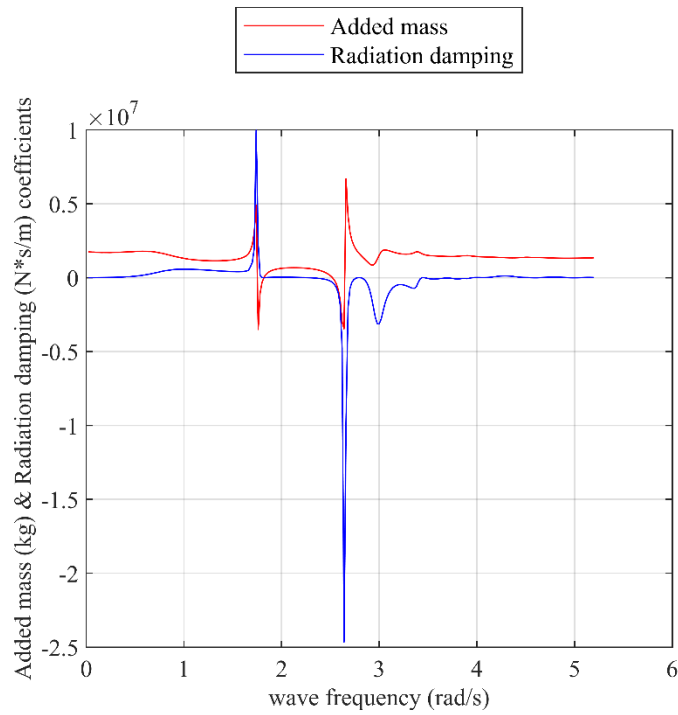
Figure 2.11: Added mass and radiation damping coefficients for heave mode of the 2BPA float

40
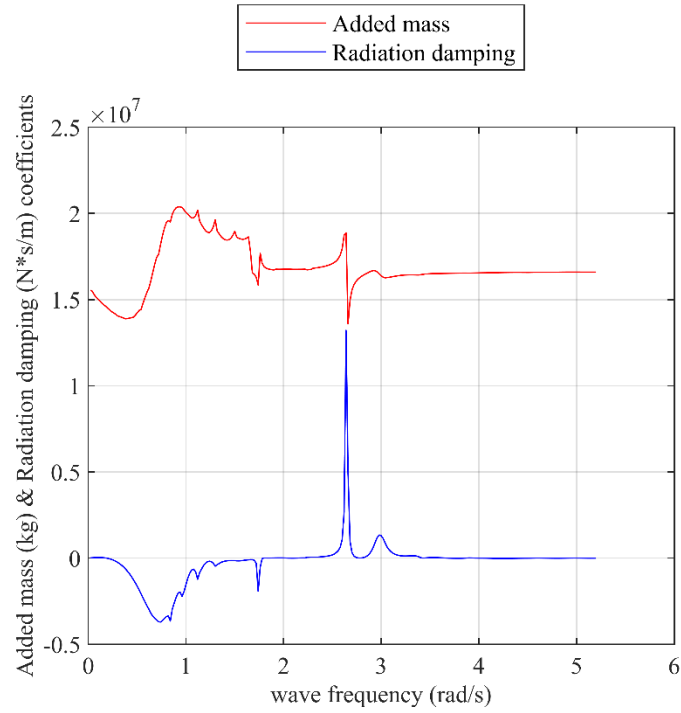
Figure 2.12: Added mass and radiation damping coefficients for heave mode of the 2BPA spar
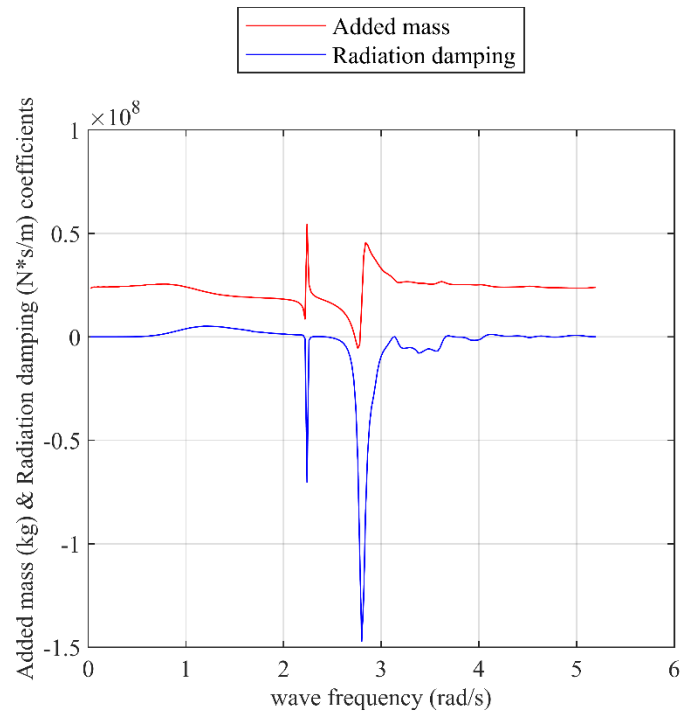
Figure 2.13: Added mass and radiation damping coefficients for pitch mode of the 2BPA float

41
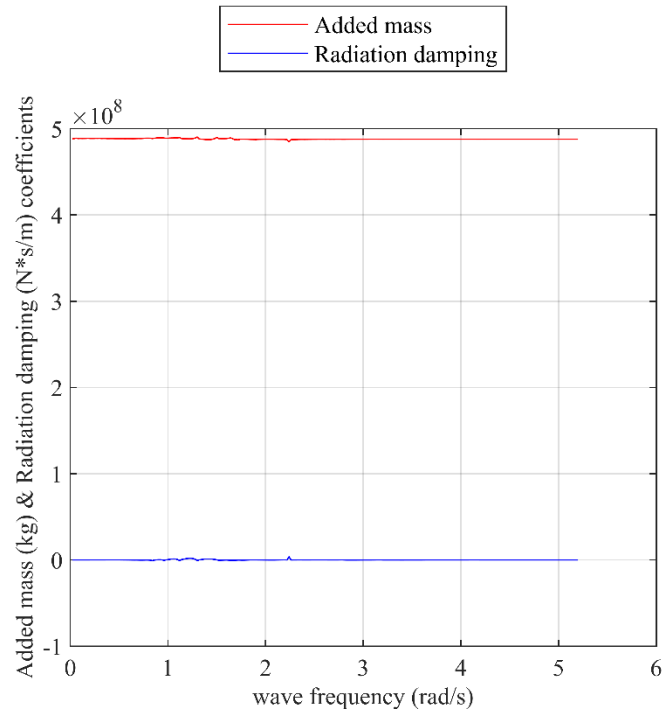
Figure 2.14: Added mass and radiation damping coefficients for pitch mode of the 2BPA spar
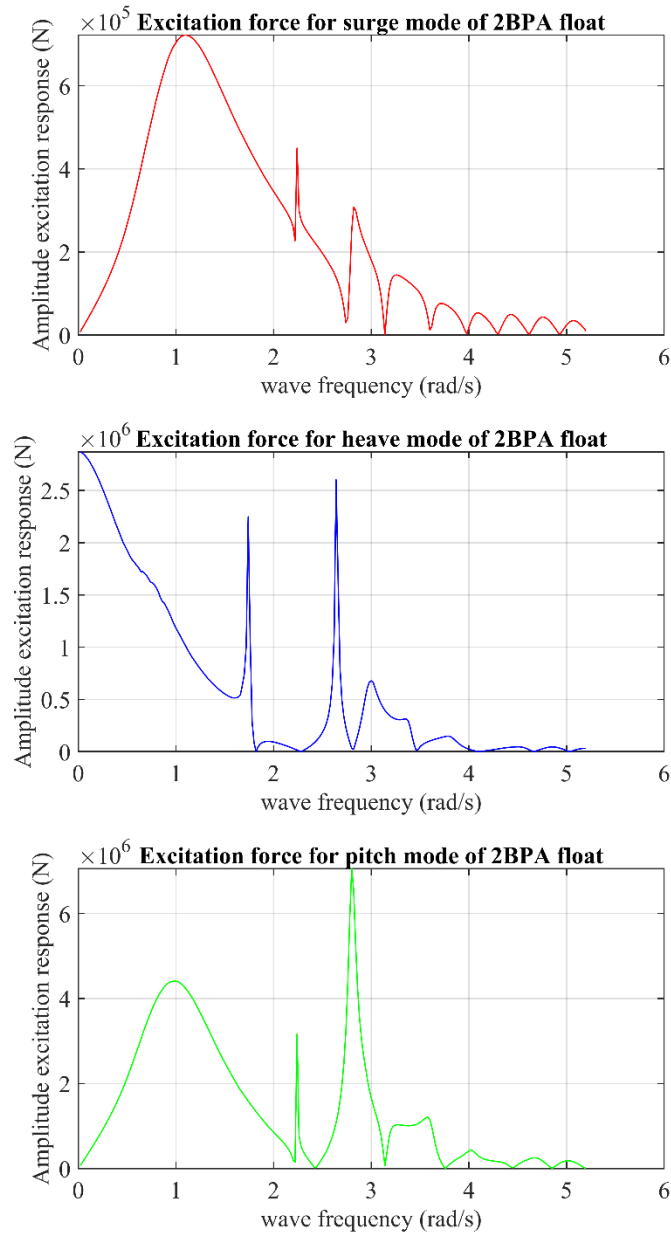
Figure 2.15: Excitation force for surge, heave, and pitch modes of 2BPA float
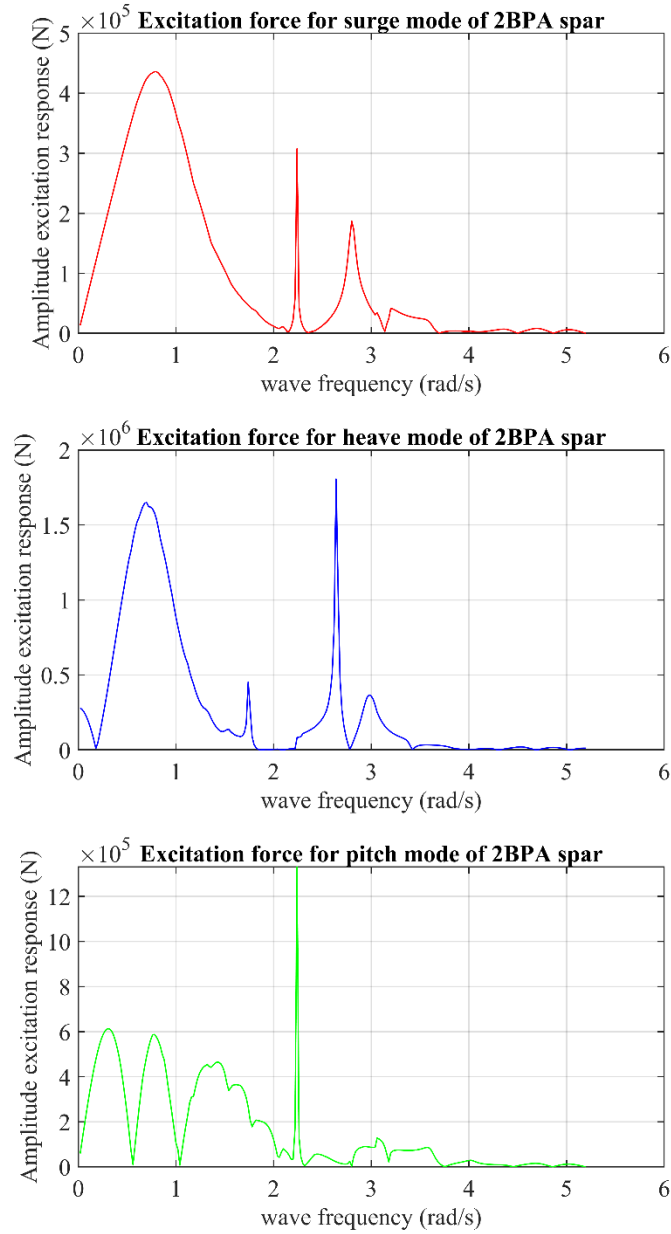
Figure 2.16: Excitation force for surge, heave, and pitch modes of 2BPA spar
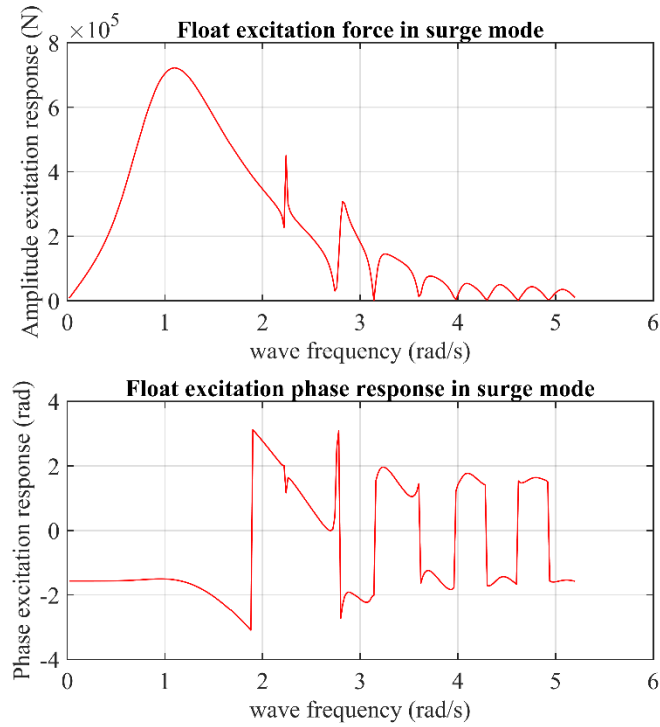
Figure 2.17: Excitation force and phase excitation response for surge mode of 2BPA float
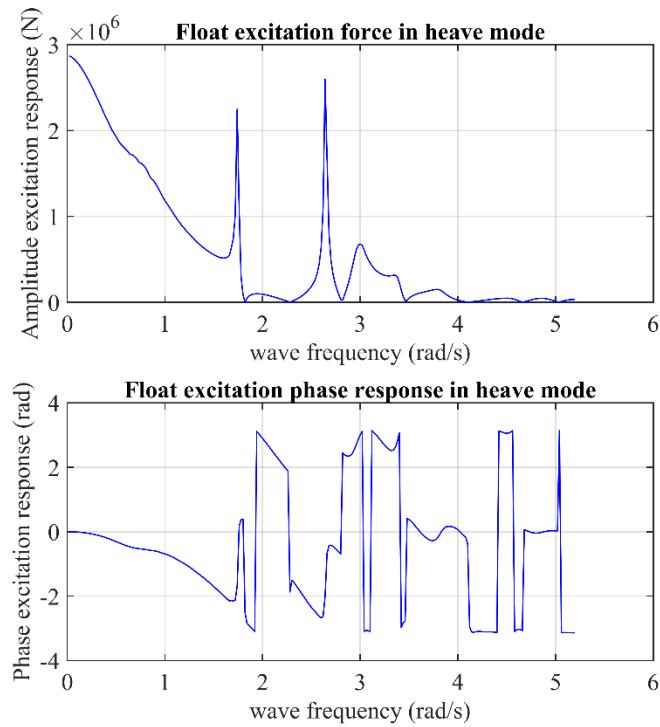
Figure 2.18: Excitation force and phase excitation response for heave mode of 2BPA float
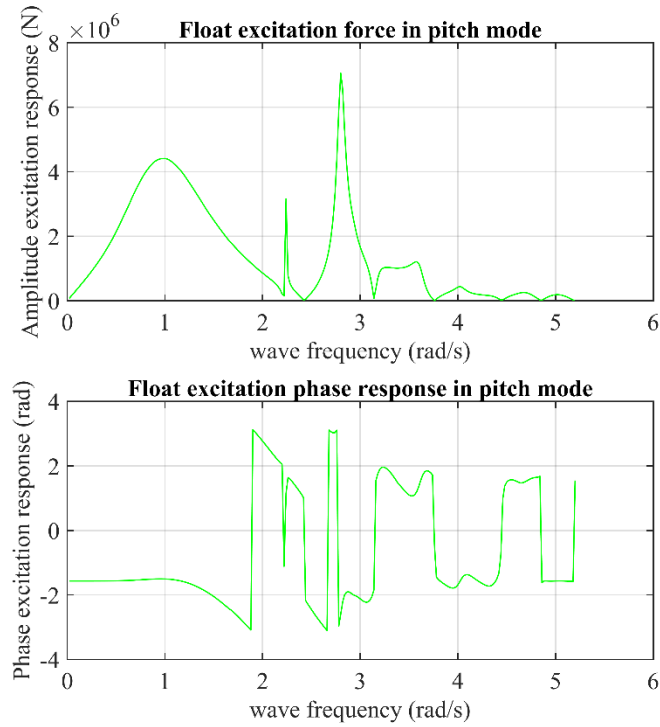
Figure 2.19: Excitation force and phase excitation response for pitch mode of 2BPA float
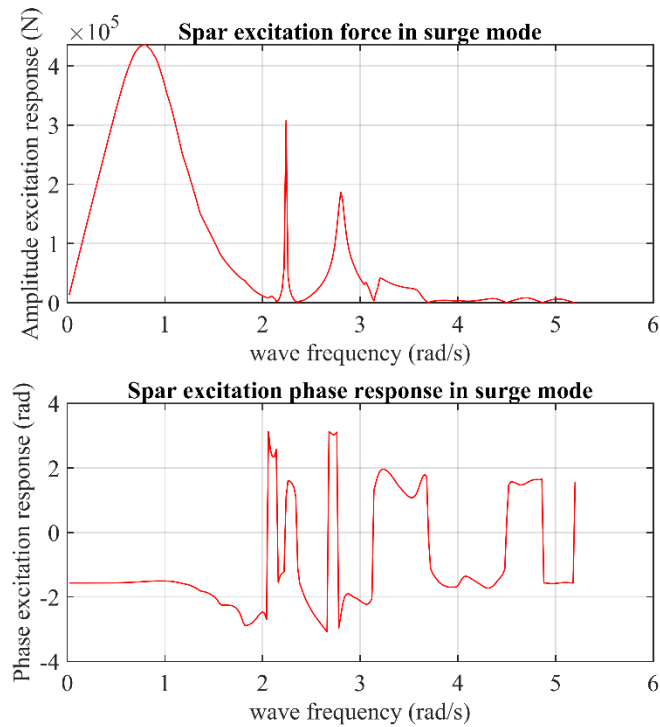
Figure 2.20: Excitation force and phase excitation response for surge mode of 2BPA spar
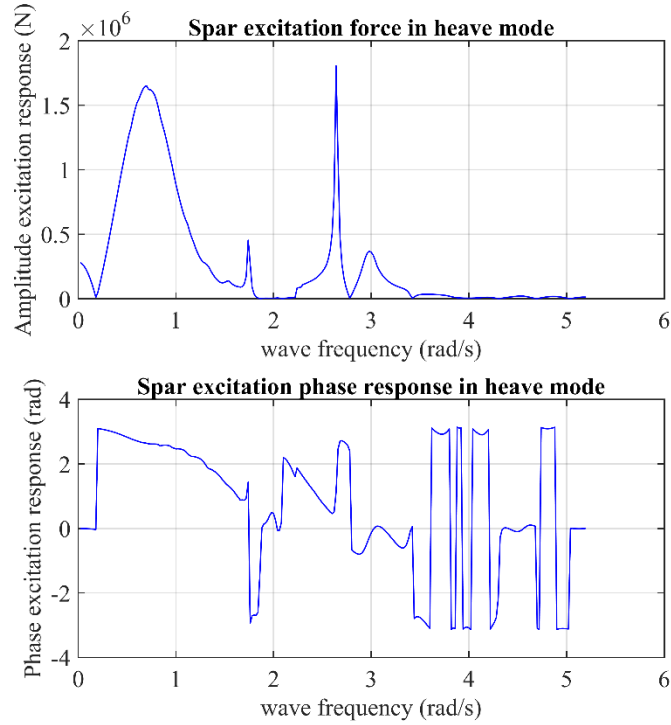
Figure 2.21: Excitation force and phase excitation response for heave mode of 2BPA spar
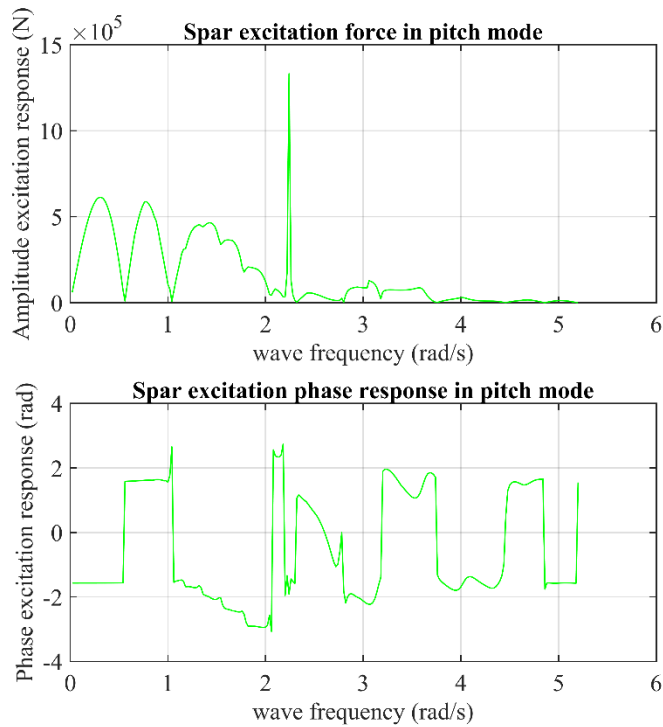
Figure 2.22: Excitation force and phase excitation response for pitch mode of 2BPA spar

The added mass force is an inertia force relating to the mass of water entrained with the body motion [33]. In simple terms, the added mass coefficient is instead an equivalent quantity determining how big the fluid inertia force becomes when the body accelerates [33]. In general, the added mass is a second-order tensor, relating the fluid acceleration vector to the resulting force vector on the body [34]. Figures 2.9-2.14 show the added mass coefficient versus wave frequency for each BVP problem solved by BEM solver NEMOH.

On the opposite side, radiation resistance (or wave damping) force is almost linked to the average power transferred within the sea and the body [33]. This force results from outgoing waves created when the body moves [33]. The radiation resistance coefficient is equivalent to how large the outgoing waves become when the body's velocity varies [33]. Since these waves interfere with the incoming waves, the radiation resistance also obliquely tells how much power we can derive from the incoming waves [33]. Figures 2.9-2.14 show the radiation damping coefficient versus wave frequency for each BVP problem solved by BEM solver NEMOH. In Figures 2.9-2.13, the radiation damping coefficient shows a negative value for specific wave frequencies. In a similar result obtained by Penalba [27], these irregular spikes arise due to a fundamental error in the formulation of the NEMOH BEM solver. The irregular frequencies correspond to singularities in the system of equations solved. The latest version of the NEMOH solver used in this thesis is v2.03 which does not include the additional equations for removing these singularities. However, the ability to remove the irregular frequencies will be included in the future version of NEMOH [31].

Wave exciting forces are created via the direct action of the incident waves on the body [35]. In linear theory, these forces are straightly proportional to the wave amplitude, which is supposed to be small [35]. Therefore, the leading-order interactions among the exciting forces and the radiation forces, which are proportional to the small body motions, are expected to be the product of the wave and body motion amplitudes [35]. Therefore, these interactions can be neglected in linear theory so that the body can be assumed to be fixed in its equilibrium position to evaluate the exciting forces [35]. The excitation force for surge, heave, and pitch of float and spar-plate are plotted in Figures 2.15-2.22, where Figures 2.17-2.22 include the excitation force phase responses. As can be seen from the plots, the curve of excitation force does not regularly descend when the wave frequency increases. The irregular spikes that NEMOH cannot remove are why the reason for having such an irregular curve for excitation force.

As previously mentioned in sections 2.1.1 and 2.1.2, after the Nemoh.m function is called and the hydrodynamic coefficients are obtained for each body, the vector lengths of the wave frequency and wave direction will be updated in scripts 2.3 and 2.7. In script 2.10, the final Nemoh.cal is shown where the wave frequency and wave direction data are updated for 2BPA in lines 45 and 47. This last modified Nemoh.cal will be used by function bemio to create *.h5 file.

```
1    --- Environment ---------------------------------------------------------
2    1025.000000 *Sea water density(kg/m^3)
3    9.810000    *The gravity acceleration (m/s^2)
4    70.000000   *Water depth (m)
5    0.   0.     *Wave measurement point XEFF YEFF (m)
6    --- Description of floating bodies ------------------------------------
7    2           * Count of nodes
```

```
8    --- Body 1 -----------------------------------------------------------
9    pointabsorber\mesh\float.dat      *The mesh file's name
10   568 142                            *Count of points and panels
11   6                                  *DOF
12   1 1.0 0.0 0.0 0.0 0.0 0.0   *Surge
13   1 0.0 1.0 0.0 0.0 0.0 0.0   *Sway
14   1 0.0 0.0 1.0 0.0 0.0 0.0   *Heave
15   2 1.0 0.0 0.0 0.0 0.0 -0.72 *Rolling about this point
16   2 0.0 1.0 0.0 0.0 0.0 -0.72 *Pitching about this point
17   2 0.0 0.0 1.0 0.0 0.0 -0.72 *Yawing about this point
18   6                                  *Amount of resulting generalized forces
19   1 1.0 0.0 0.0 0.0 0.0 0.0   *x-direction force
20   1 0.0 1.0 0.0 0.0 0.0 0.0   *y-direction force
21   1 0.0 0.0 1.0 0.0 0.0 0.0   *z-direction force
22   2 1.0 0.0 0.0 0.0 0.0 -0.72 *Moment force about this point in the x-direction
23   2 0.0 1.0 0.0 0.0 0.0 -0.72 *Moment force about this point in the y-direction
24   2 0.0 0.0 1.0 0.0 0.0 -0.72 *Moment force about this point in the z-direction
25   0                                  *Number of additional lines of information
26   --- Body 2 -----------------------------------------------------------
27   pointabsorber\mesh\spar.dat       *The mesh file's name
28   1136 284                           *Count of points and panels
29   6                                  *DOF
30   1 1.0 0.0 0.0 0.0 0.0 0.0    *Surge
31   1 0.0 1.0 0.0 0.0 0.0 0.0    *Sway
32   1 0.0 0.0 1.0 0.0 0.0 0.0    *Heave
33   2 1.0 0.0 0.0 0.0 0.0 -21.29 *Rolling about this point
34   2 0.0 1.0 0.0 0.0 0.0 -21.29 *Pitching about this point
35   2 0.0 0.0 1.0 0.0 0.0 -21.29 *Yawing about this point
36   6                                  *Amount of resulting generalized forces
37   1 1.0 0.0 0.0 0.0 0.0 0.0    *x-direction force
38   1 0.0 1.0 0.0 0.0 0.0 0.0    *y-direction force
39   1 0.0 0.0 1.0 0.0 0.0 0.0    *z-direction force
40   2 1.0 0.0 0.0 0.0 0.0 -21.29*Moment force about this point in the x-direction
41   2 0.0 1.0 0.0 0.0 0.0 -21.29*Moment force about this point in the y-direction
42   2 0.0 0.0 1.0 0.0 0.0 -21.29*Moment force about this point in the z-direction
43   0                                  *Number of additional lines of information
44   --- Load cases that have to be solved ----------------------------------
45   260 0.020000 5.200000 *The number of wave frequencies, the minimum, and the
46   maximum (rad/s)
47   1 0.000000 0.000000   *The number of wave directions, minimum, and the
48   maximum (degrees)
49   --- Post processing ----------------------------------------------------
50   260   0.02  5.20.        *Calculation of the IRF (0 is for no calculation),
51   time step, and duration
52   0                         * Pressure
53   0    0.    180.          * Kochin function    Count of directions of
54   calculation (0 is for no calculations), minimum and maximum (degrees)
55   0    50   400. 400.   *Count of points in the x-direction (0 if no
56   calculations) and y-direction, and domain dimensions in x and y-direction
57   ---
```

Script 2.10: The final modified Nemoh.cal of 2BPA for function bemio

3. Numerical Modeling of Hydrodynamic Coefficients of 2BPA and OSWEC

In general, NEMOH is a preprocessor, solver, and postprocessor. For each calculation case (radiation and diffraction), the preprocessor prepares the mesh and generates the body conditions. Nemoh.cal is the input file that defines the computation cases. The files that were created by running the preprocessor and saved inside the working folder *pointabsorber* are:

- pointabsorber/mesh/L12.dat
- pointabsorber/mesh/L10.dat
- pointabsorber/mesh/Mesh.tec

  ➢ Tables of nodes and connectivities are included in the top one, and additional geometrical information such as symmetry about the (XOZ) plane, number of nodes, number of panels, number of bodies, panel to body belonging, panel centers, panel's normal vectors, and panel areas is included in the second one. For visualization purposes, the last one is in Tecplot format.

- pointabsorber/Normalvelocities.dat

  ➢ In this file the user will find the body requirements for each radiation and diffraction problem described in the Nemoh.cal file.

- pointabsorber/mesh/Integration.dat file

  ➢ This file contains instructions on how to integrate the pressure over the body surfaces to obtain the requested forces (as specified in the Nemoh.cal file).

- pointabsorber/results/FKForce.dat
- pointabsorber/results/FKForce.tec

  ➢ Here are Froude-Krylov forces for each of the diffraction problems. The second file can be used to visualize the Froude-Krylov forces with Tecplot.

- pointabsorber/results/Kochin.dat

  ➢ This file contains data related to the Kochin function calculation for a given angle.

- pointabsorber/results/index.dat

  ➢ This table is a correlation between force ID numbers with body ID numbers for the bodies on which it applies and the numbers of the Nemoh.cal files. It also gives correlations between the radiation problem ID number and the body ID number, and the number of DOF.

The solver reads parameters from the file input.txt, in the *pointabsorber* working folder, to solve linear BVP for each problem defined in the file Normalvelocities.dat. Once the calculation is successful, the files below are created and stored in the working folder:

- pointabsorber/results/Forces.dat

➢ In this file, the user will find all of the forces associated with each problem.

• pointabsorber/results/freesurface.XX.dat

➢ For problem no. XX, this file provides the free surface elevation.

• pointabsorber/results/Kochin.XX.dat

➢ The Kochin function for problem no. XX is contained in this file. Additional information on the Kochin function can be found at the following link: https://lheea.ec-nantes.fr/valorisation/logiciels-et-brevets/nemoh-running-1.

• pointabsorber/results/Pressure.XX.dat

➢ In this file, the user can find the pressure field on body surfaces for problem no. XX.

Upon processing the results, the postprocessor tries to provide the relevant quantities (added mass, radiation damping, excitation force) in the usual format. A framework is also provided to make appropriate calculations. In the *pointabsorber* working folder, the following results files are created upon successful run:

• pointabsorber/results/RadiationCoefficients.tec

➢ The user will find the added mass plus damping forces for the radiation problems in this file.

• pointabsorber/results/DiffractionForce.tec

➢ In this file, the user can find the diffraction force for the diffraction problems.

• pointabsorber/results/ExcitationForce.tec

➢ In this file, the user can find the excitation force for the diffraction problems.

• pointabsorber/results/IRF.tec

➢ This file consists of the infinite frequency added mass and the impulse response function for the radiation force.

3.1.2 Hydrodynamic Coefficients of OSWEC

In this section, the hydrodynamic coefficients of previously meshed OSWEC are numerically modeled using open-source BEM solver NEMOH. The reason for including OSWEC, such as the Oyster device by Aquamarine Power Ltd. [36], arises from the fundamental difference in the mode of operation of such a device compared to any point absorber. OSWECs only use the pitch mode to extract energy from ocean waves, so only pitch coefficients are studied.

3. Numerical Modeling of Hydrodynamic Coefficients of 2BPA and OSWEC

Penalba [27] concluded that the hydrodynamic coefficients of an OSWEC obtained by NEMOH and WAMIT solvers match almost perfectly. The only difference between the coefficients obtained from these two solvers is the magnitudes of the peak values, which are always slightly higher in NEMOH.

In this study, by calling the Nemoh.m function in MATLAB, the hydrodynamic coefficients of the OSWEC are obtained. Script 2.11 is the MATLAB code for calling function Nemoh. The script was saved inside the *oswec* folder and named *oswec2*, which indicates the second step carried out for the OSWEC.

```
1   %%% II) Call function Nemoh
2   %%%
3   %%% function [A,B,Fe]=Nemoh(w, dir, depth)
4   %%%
5   %%% Purpose: Matlab wrapper for calculation of hydrodynamic coefficients
6   using Nemoh
7   %%%
8   %%% Inputs :
9   %%% - w     : Vector length(w) of wave frequencies (rad/s)
10  %%% - dir   : Wave direction (degrees).
11  %%% - depth : water depth (m), 0 for deep water.
12  %%%
13  %%% Outputs :
14  %%% - A: Matrix (6xnBodies)x(6xnBodies)xlength(w) of added mass coefficients
15  %%% - B: Matrix (6xnBodies)x(6xnBodies)xlength(w) of radiation damping
16  coefficients
17  %%% - Fe: Matrix (6xnBodies)xlength(w) of exciation forces (complex values)
18  %%%
19  %%% Copyright Ecole Centrale de Nantes 2014
20  %%% Licensed under the Apache License, Version 2.0
21  %%% Written by A. Babarit, LHEEA Lab.
22  %%%
23  %%%%%%%%%%%%%%%%%%%%%%%%%%%%%%
24
25  %%% Nemoh inputs:
26
27  w=0.6283:0.05:12.5664;  %% Vector length(w) of wave frequencies (rad/s)
28  dir=0;                  %% Wave direction (degrees). Towards positive x.
29  h=13;                   %% Water depth (m), 0 for deep water approximation.
30  [A,B,Fe]=Nemoh(w, dir, h) %% Call function Nemoh
31
32
33  %%% Plot results (added mass and radiation damping coefficients)
34
35  %%% Flap:
36  A55(1,:)=A(5,5,:); %% Pitch mode
37  B55(1,:)=B(5,5,:); %% Pitch mode
38
39  figure;
40  plot(w,A55,'r',w,B55,'b'); %% Added mass and radiation damping coefficients
41  for pitch mode of the OSWEC flap
42  xlabel('wave frequency (rad/s)');
43  ylabel('Added mass (kg) & Radiation damping (N*s/m) coefficients');
44  legend ('Added mass','Radiation damping')
```

```
45   grid on
46
47   %%% Plot results (excitation force)
48   %%% Fe5 (excitation force in pitch mode):
49
50   %%% FLAP:
51   Fe5(1,:)=Fe(:,5);   %% Pitch mode
52
53   figure;
54   plot(w,abs(Fe5),'g'); xlabel('wave frequency (rad/s)'); ylabel('Amplitude
55   excitation response (N)');
56   title('Excitation force for pitch mode of OSWEC flap')
57   grid on
58
59   %%% Plot results (excitation force coefficients)
60   %%% Fe1 & Phase:
61
62   %%% Flap:
63   figure;
64   subplot(2,1,1); plot(w, abs(Fe(:,5)),'g'); xlabel('wave frequency (rad/s)');
65   ylabel('Amplitude excitation response (N)');
66   title('Flap excitation force in pitch mode')
67   grid on
68   subplot(2,1,2); plot(w, angle(Fe(:,5)),'g'); xlabel('wave frequency
69   (rad/s)'); ylabel('Phase excitation response (rad)');
70   title('Flap excitation phase response in pitch mode')
71   grid on
```

Script 2.11: Call function Nemoh for OSWEC

In Script 2.11, the Nemoh function input data are vector length (w) of wave frequencies (rad/s), wave direction (degrees) towards positive x, and water depth (m). For our 2BPA, the minimum wave frequency defined is 0.6283 (rad/s), the maximum wave frequency is 12.5664 (rad/s), and the frequency step between these two values is 0.05 (rad/s). The hydrodynamic coefficients of the OSWEC will be obtained for the defined frequency vector. Also, in the WEC-Sim input file, the wave period must be defined between the range of 0.5 seconds up to 10 seconds, which corresponds to the frequency range mentioned earlier. Any wave period that does not fall into the period range discussed above will cause the WEC-Sim to be unable to simulate the problem.

The wave direction for OSWEC is assumed to be 0 degrees. In this case, the direction of the incident wave is perpendicular to the device's surface. Finally, the depth at which the OSWEC is chosen to be implemented is 13 (m). Figures 2.23-2.25 show the hydrodynamic coefficients obtained for the OSWEC. Note that only pitch motion is considered since the flap is mounted on the base.
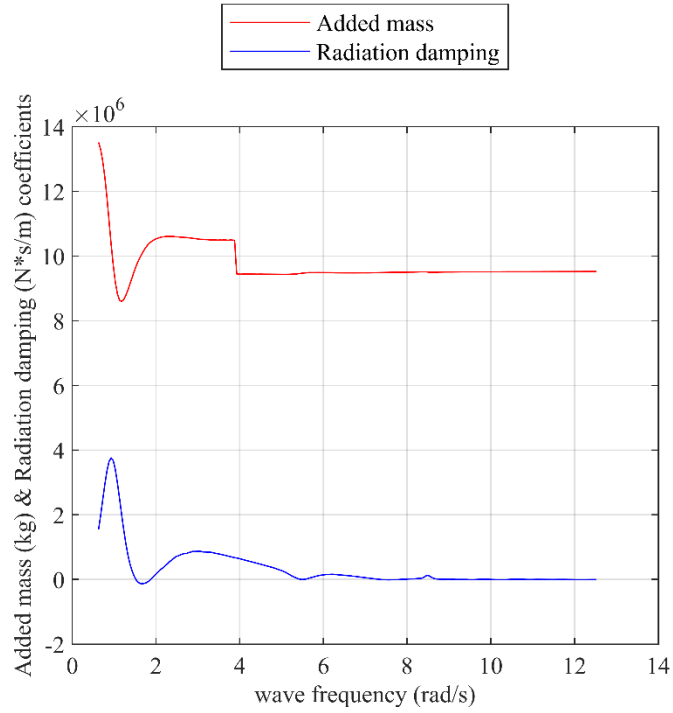
Figure 2.23: Added mass and radiation damping coefficients for pitch mode of the OSWEC flap
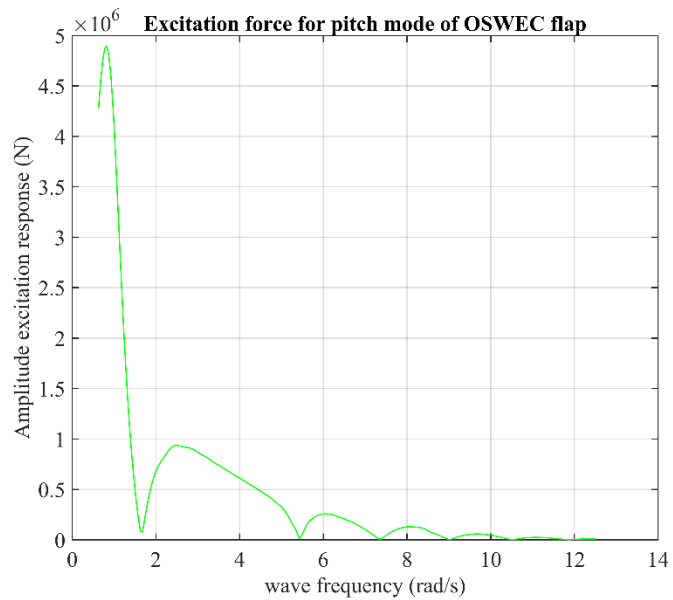
Figure 2.24: Excitation force for pitch modes of OSWEC flap
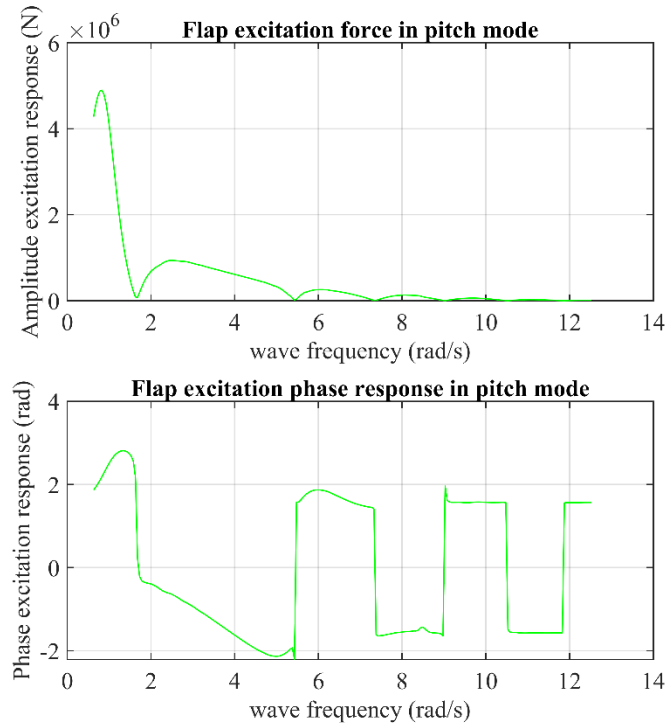
Figure 2.25: Excitation force and phase excitation response for pitch mode of OSWEC flap

In script 2.12, the final Nemoh.cal is shown where the data for wave frequency and wave direction are updated for OSWEC in lines 45 and 47. This last modified Nemoh.cal will be used by function bemio to create the *.h5 file.

```
1    --- Environment ---------------------------------------------------------------
2    1025.000000 *Sea water density(kg/m^3)
3    9.810000    *The gravity acceleration (m/s^2)
4    13.000000   *Water depth (m)
5    0.    0.    *Wave measurement point XEFF YEFF (m)
6    --- Description of floating bodies -------------------------------------------
7    2           * Count of nodes
8    --- Body 1 -------------------------------------------------------------------
9    oswec\mesh\flap.dat    *The mesh file's name
10   498 392                        *Count of points and panels
11   6                              *DOF
12   1 1.0 0.0 0.0 0.0 0.0 0.0    *Surge
13   1 0.0 1.0 0.0 0.0 0.0 0.0    *Sway
14   1 0.0 0.0 1.0 0.0 0.0 0.0    *Heave
15   2 1.0 0.0 0.0 0.0 0.0 -2.74 *Rolling about this point
16   2 0.0 1.0 0.0 0.0 0.0 -2.74 *Pitching about this point
17   2 0.0 0.0 1.0 0.0 0.0 -2.74 *Yawing about this point
18   6                              *Amount of resulting generalized forces
19   1 1.0 0.0 0.0 0.0 0.0 0.0    *x-direction force
20   1 0.0 1.0 0.0 0.0 0.0 0.0    *y-direction force
```

55

```
21   1 0.0 0.0 1.0 0.0 0.0 0.0    *z-direction force
22   2 1.0 0.0 0.0 0.0 0.0 -2.74 *Moment force about this point in the x-direction
23   2 0.0 1.0 0.0 0.0 0.0 -2.74 *Moment force about this point in the y-direction
24   2 0.0 0.0 1.0 0.0 0.0 -2.74 *Moment force about this point in the z-direction
25   0                           *Number of additional lines of information
26   --- Body 2 ------------------------------------------------------------
27   oswec\mesh\base.dat       *The mesh file's name
28   514 382                        *Count of points and panels
29   6                              *DOF
30   1 1.0 0.0 0.0 0.0 0.0 0.0    *Surge
31   1 0.0 1.0 0.0 0.0 0.0 0.0    *Sway
32   1 0.0 0.0 1.0 0.0 0.0 0.0    *Heave
33   2 1.0 0.0 0.0 0.0 0.0 -13.00 *Rolling about this point
34   2 0.0 1.0 0.0 0.0 0.0 -13.00 *Pitching about this point
35   2 0.0 0.0 1.0 0.0 0.0 -13.00 *Yawing about this point
36   6                              *Amount of resulting generalized forces
37   1 1.0 0.0 0.0 0.0 0.0 0.0    *x-direction force
38   1 0.0 1.0 0.0 0.0 0.0 0.0    *y-direction force
39   1 0.0 0.0 1.0 0.0 0.0 0.0    *z-direction force
40   2 1.0 0.0 0.0 0.0 0.0 -13.00*Moment force about this point in the x-direction
41   2 0.0 1.0 0.0 0.0 0.0 -13.00*Moment force about this point in the y-direction
42   2 0.0 0.0 1.0 0.0 0.0 -13.00*Moment force about this point in the z-direction
43   0                           *Number of additional lines of information
44   --- Load cases that have to be solved ----------------------------------
45   239 0.6283 12.5283    *The number of wave frequencies, the minimum, and the
46   maximum (rad/s)
47   1 0.000000 0.000000   *The number of wave directions, minimum, and the
48   maximum (degrees)
49   --- Post processing ---------------------------------------------------
50   1    0.1   10.         *Calculation of the IRF (0 is for no calculation),
51   time step, and duration
52   0                      * Pressure
53   0    0.    180.        * Kochin function    Count of directions of
54   calculation (0 is for no calculations), minimum and maximum (degrees)
55   0    50   400.  400.  *Count of points in the x-direction (0 if no
56   calculations) and y-direction, and domain dimensions in x and y-direction
57   ---
```

Script 2.11: The final modified Nemoh.cal of OSWEC for function bemio

The files that were created by running the preprocessor and saved inside the working folder *oswec* are:

- oswec/mesh/L12.dat
- oswec/mesh/L10.dat
- oswec/mesh/Mesh.tec

  ➢ Tables of nodes and connectivities are included in the top one, and additional geometrical information such as symmetry about the (XOZ) plane, number of nodes, number of panels, number of bodies, panel to body belonging, panel centers, panel's

normal vectors, and panel areas is included in the second one. For visualization purposes, the last one is in Tecplot format.

- oswec/Normalvelocities.dat

  ➢ In this file, the user will find the body requirements for each radiation and diffraction problem described in the Nemoh.cal file.

- oswec/mesh/Integration.dat file

  ➢ This file contains instructions on how to integrate the pressure over the body surfaces to obtain the requested forces (as specified in the Nemoh.cal file).

- oswec/results/FKForce.dat
- oswec/results/FKForce.tec

  ➢ Here are Froude-Krylov forces for each of the diffraction problems. The second file can be used to visualize the Froude-Krylov forces with Tecplot.

- oswec/results/Kochin.dat

  ➢ This file contains data related to the Kochin function calculation for a given angle.

- oswec/results/index.dat

  ➢ This table is a correlation between force ID numbers with body ID numbers for the bodies on which it applies and the numbers of the Nemoh.cal files. It also gives correlations between the radiation problem ID number and the body ID number, and the number of DOF.

Using parameters read from input.txt, located in the *oswec* working folder, the solver solves linear BVP for each problem defined in the file Normalvelocities.dat. Once the calculation is successful, the files below are created and stored in the working folder:

- oswec/results/Forces.dat

  ➢ In this file, the user will find all of the forces associated with each problem.

- oswec/results/freesurface.XX.dat

  ➢ For problem no. XX, this file provides the free surface elevation.

- oswec/results/Kochin.XX.dat

  ➢ The Kochin function for problem no. XX is contained in this file. Additional information on the Kochin function can be found at the following link: https://lheea.ec-nantes.fr/valorisation/logiciels-et-brevets/nemoh-running-1.

- oswec/results/Pressure.XX.dat

  ➢ In this file, the user can find the pressure field on body surfaces for problem no. XX.

Following the results have been processed, the postprocessor provides the relevant quantities (added mass, radiation damping, excitation force) in the usual format. A framework is also provided to make appropriate calculations. In the *oswec* working folder, the following results files are created upon successful run:

- oswec/results/RadiationCoefficients.tec

  ➢ In this file, the user will find the added mass plus damping forces for the radiation problems.

- oswec/results/DiffractionForce.tec

  ➢ In this file, the user can find the diffraction force for the diffraction problems.

- oswec/results/ExcitationForce.tec

  ➢ In this file, the user can find the excitation force for the diffraction problems.

- oswec/results/IRF.tec

  ➢ This file consists of the infinite frequency added mass and the impulse response function for the radiation force.

4.

Hydrodynamic Data from BEM Solution in Hierarchical Data Format Version 5 (HDF5)

4.1 Creating HDF5 (*.h5) File for 2BPA and OSWEC Using BEMIO: 3rd Step

The third step is to generate a *.h5 file for each 2BPA and OSWEC device. A *.h5 file contains all the hydrodynamic data from the BEM solution (2nd step). The *.h5 file is created via BEMIO, a pre-and post-processing tool developed by WEC-Sim. In pre-processing, BEMIO calculates the radiation and excitation impulse response functions (IRFs) and calculates the state-space realization coefficients from the hydrodynamic output data from WAMIT, NEMOH, and ANSYS-AQWA [28]. In post-processing, BEMIO saves and compiles all of the results from above mentioned BEM solvers with the data obtained via BEMIO into the .h5 file, which is required to operate WEC-Sim [28].

In this study, the *.h5 files for 2BPA and OSWEC devices are created using BEMIO code (bemio.m MATLAB function). The bemio.m function reads, views, and converts between mesh formats used by BEM codes. Specifically, the bemio.m function can read STL, VTK, WAMIT, and NEMOH mesh formats and convert between them. The function bemio also reads NEMOH, WAMIT, and AQWA simulation output files and saves the data in a standardized readable bemio format that uses the Hierarchical Data Format version 5 (HDF5) or (*.h5) file format. The calculations of the wave excitation and radiation impulse response functions (IRFs) and state-space realization coefficients that represent the IRFs are also carried out using the bemio.m function.

4.1.1 Creating HDF5 (*.h5) File for 2BPA Using bemio.m MATLAB Function

The bemio.m MATLAB function is widely used to read the output data from WAMIT, NEMOH, and ANSYS-AQWA. For example, in McKie's thesis [28], once the hydrodynamic coefficients were obtained via NEMOH, the function bemio calculated the normalized, excitation, and state-space realization of the radiation IRFs and created a *.h5 file for WEC-Sim. In Ref [37], several researchers simulated an attenuator style WEC in which the device meshing and definition of the environment were done in AQWA's subsequent functions via a Graphical User Interface. Then, the resulting hydrodynamic coefficients were post-processed with the help of BEMIO code and

used for the time domain simulation with WEC-Sim. A Novi Ocean WEC, a point absorber type WEC, was investigated by Kanagaraj [38]. Kanagaraj's work analyzed the hydrodynamic

interaction between the float and the waves using the WAMIT. Then, the BEMIO code was used to convert the hydrodynamic data from WAMIT to the *.h5 file.

In this thesis, for 2BPA, the bemio.m function calculated the radiation and excitation IRFs from the hydrodynamic output data from NEMOH and created the *.h5 file. Script 3.1 is the code for calling the bemio.m function in MATLAB. The script was saved inside the *pointabsorber* working folder and named *pointabsorber3*, which indicates the third step carried out for the 2BPA. Note that before calling bemio.m, the location of the *pointabsorber* working folder must be specified in line 27 of Script 3.1.

```
1   %% III) Call function bemio
2   %
3   % Purpose: Reads data from a NEMOH working folder and creates the file *.h5
4   for the present case.
5   %
6   %% hydro = Read_NEMOH(hydro, filedir)
7   %
8   % hydro-data structure
9   % filedir-NEMOH working folder, must include:
10  % • Nemoh.cal
11  % • Mesh/Hydrostatics.dat (or Hydrostatiscs_0.dat, Hydrostatics_1.dat, etc.
12  for multiple bodies)
13  % • Mesh/KH.dat (or KH_0.dat, KH_1.dat, etc. for multiple bodies)
14  % • Results/RadiationCoefficients.tec
15  % • Results/ExcitationForce.tec
16  % • Results/DiffractionForce.tec-If simu.nlHydro= 3 will be used
17  % • Results/FKForce.tec-If simu.nlHydro= 3 will be used
18  %
19  %Source: https://github.com/WEC-Sim/WEC-
20  Sim/tree/master/source/functions/BEMIO
21  %%%%%%%%%%%%%%%%%%%%%%%%%%%%%
22
23  %% bemio inputs:
24
25  hydro = struct();
26
27  hydro = Read_NEMOH(hydro,'C:\Users\Babak Shafiei\Documents\MATLAB\cccc\matlab
28  routines\pointabsorber');
29  hydro = Radiation_IRF(hydro,60,[],[],[],1.9);
30  hydro = Radiation_IRF_SS(hydro,[],[]);
31  hydro = Excitation_IRF(hydro,157,[],[],[],1.9);
32
33  Write_H5(hydro)
34  Plot_BEMIO(hydro)
```

Script 3.1: Call function bemio for 2BPA.

As can be seen from Script 3.1, the function bemio requires Nemoh.cal, Hydrostatics.dat, KH.dat, RadiationCoefficients.tec, ExcitationForce.tec, DiffractionForce.tec, and FKForce.tec output files resulted from the meshing process and BEM solver NEMOH. By having all earlier mentioned files, the function bemio was called and pointabsorber.h5 file was generated

inside *pointabsorber* working folder. Further, the output data resulting from BEMIO were plotted in Figures 3.1-3.6 for 2BPA float and spar. The plots are:

- Normalized added mass for surge, heave, and pitch motions
- Normalized radiation damping for surge, heave, and pitch motions
- Normalized radiation impulse response functions for surge, heave, and pitch motions
- Normalized excitation force magnitude for surge, heave, and pitch motions
- Excitation phase for surge, heave, and pitch motions
- Normalized excitation impulse response functions for surge, heave, and pitch motions

Normalized Added Mass: $\bar{A}_{i,j}(\omega) = \dfrac{A_{i,j}(\omega)}{\rho}$
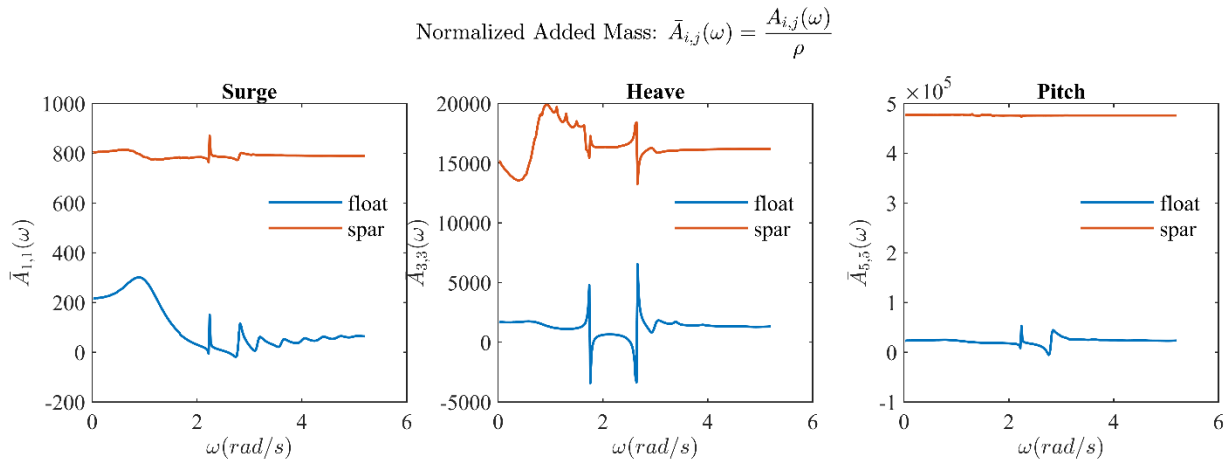
Notes:
- $\bar{A}_{i,j}(\omega)$ should tend towards a constant, A_∞, within the specified ω range.
- Only $\bar{A}_{i,j}(\omega)$ for the surge, heave, and pitch DOFs are plotted here. If another DOF is significant to the system, that $\bar{A}_{i,j}(\omega)$ should also be plotted and verified before proceeding.

Figure 3.1: Normalized added mass for surge, heave, and pitch motions of 2BPA float and spar

4. Hydrodynamic Data from BEM Solution in Hierarchical Data Format Version 5 (HDF5)

Normalized Radiation Damping: $\bar{B}_{i,j}(\omega) = \dfrac{B_{i,j}(\omega)}{\rho\omega}$
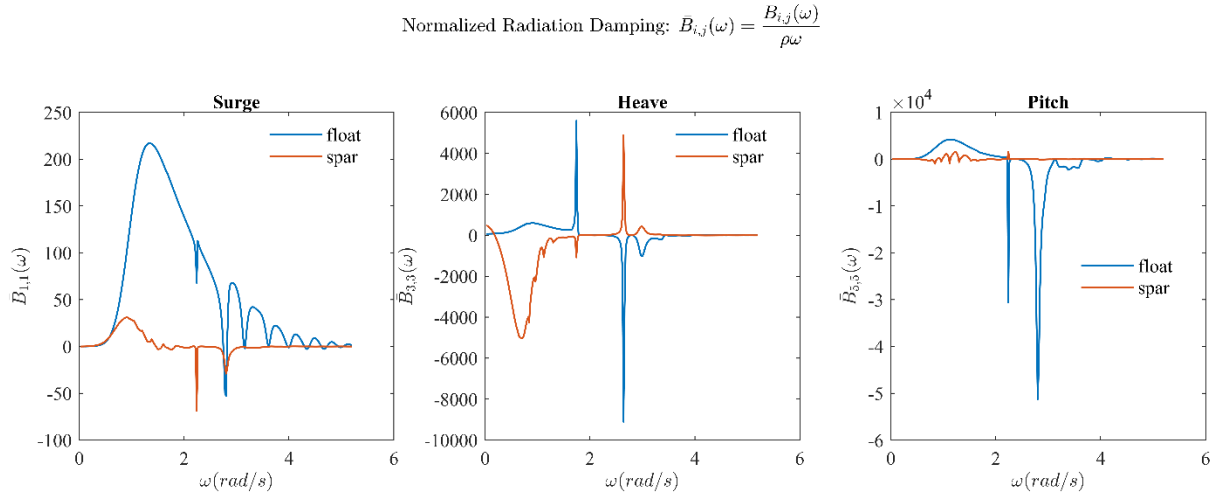
Notes:
- $\bar{B}_{i,j}(\omega)$ should tend towards zero within the specified ω range.
- Only $\bar{B}_{i,j}(\omega)$ for the surge, heave, and pitch DOFs are plotted here. If another DOF is significant to the system that $\bar{B}_{i,j}(\omega)$ should also be plotted and verified before proceeding.

Figure 3.2: Normalized radiation damping for surge, heave, and pitch motions of 2BPA float and spar
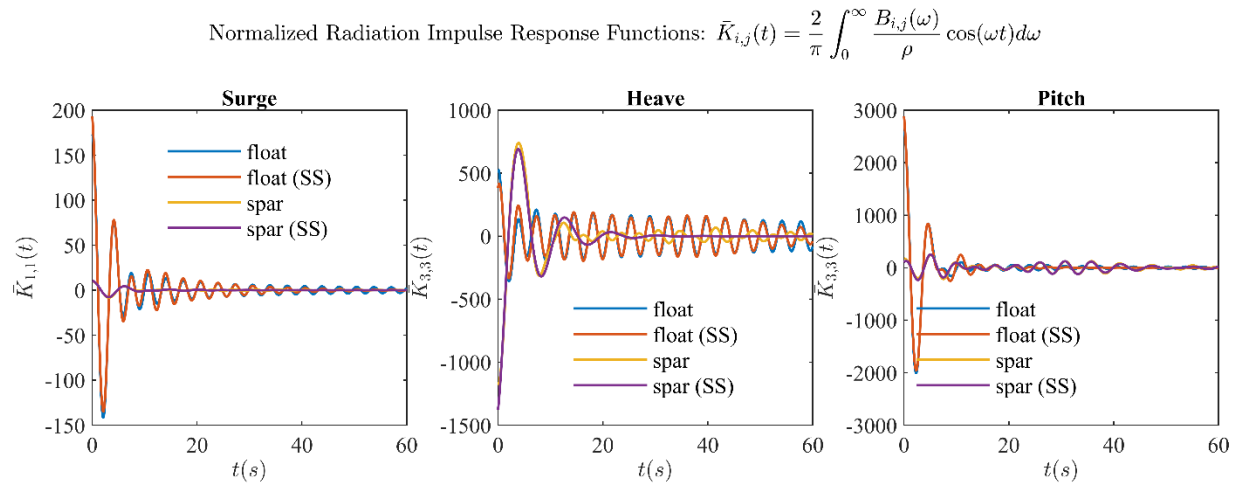
Normalized Radiation Impulse Response Functions: $\bar{K}_{i,j}(t) = \dfrac{2}{\pi} \displaystyle\int_0^\infty \dfrac{B_{i,j}(\omega)}{\rho} \cos(\omega t)d\omega$

Notes:
- The IRF should tend towards zero within the specified timeframe. If it does not, attempt to correct this by adjusting the ω and t range and/or step size used in the IRF calculation.
- Only the IRFs for the surge, heave, and pitch DOFs are plotted here. If another DOF is significant to the system, that IRF should also be plotted and verified before proceeding.

Figure 3.3: Normalized radiation impulse response functions for surge, heave, and pitch motions of 2BPA float and spar

Normalized Excitation Force Magnitude: $\bar{X}_i(\omega, \beta) = \dfrac{X_i(\omega, \beta)}{\rho g}$
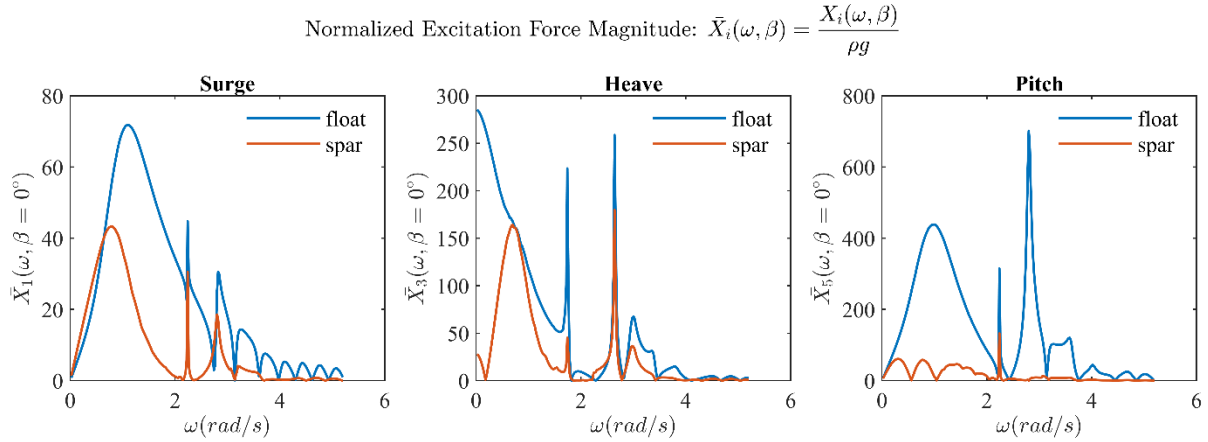
Figure 3.4: Normalized excitation force magnitude for surge, heave, and pitch motions of 2BPA float and spar

Excitation Force Phase: $\phi_i(\omega, \beta)$
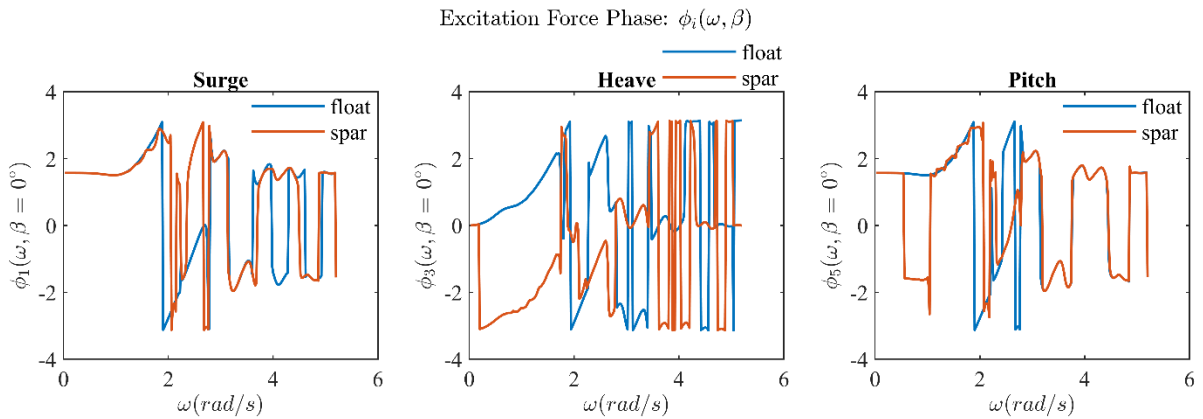
Figure 3.5: Excitation phase for surge, heave, and pitch motions of 2BPA float and spar

4. Hydrodynamic Data from BEM Solution in Hierarchical Data Format Version 5 (HDF5)

Normalized Excitation Impulse Response Functions: $\bar{K}_i(t) = \frac{1}{2\pi}\int_{-\infty}^{\infty}\frac{X_i(\omega,\beta)e^{i\omega t}}{\rho g}d\omega$
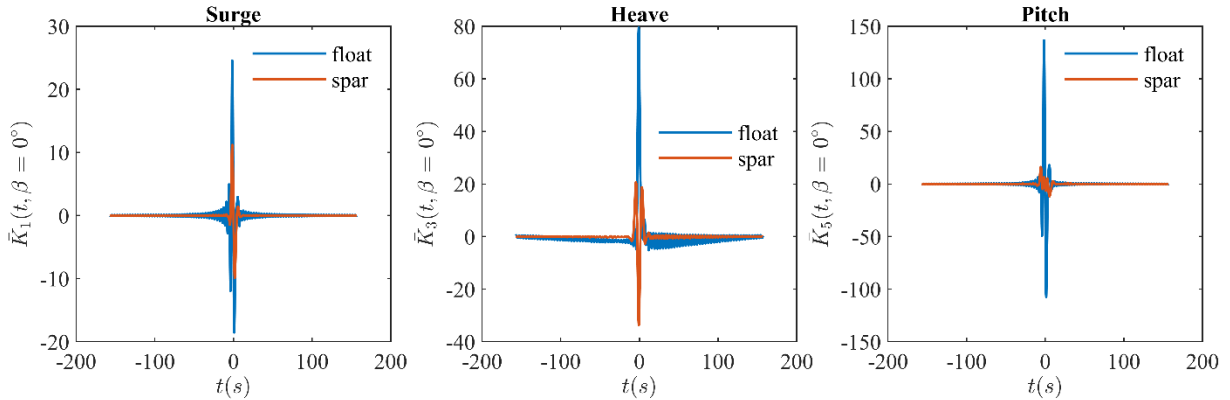
Notes:
- The IRF should tend towards zero within the specified timeframe. If it does not, attempt to correct this by adjusting the ω and t range and/or step size used in the IRF calculation.
- Only the IRFs for the first wave heading, surge, heave, and pitch DOFs are plotted here. If another wave heading or DOF is significant to the system, that IRF should also be plotted and verified before proceeding.

Figure 3.6: Normalized excitation impulse response functions for surge, heave, and pitch motions of 2BPA float and spar

In Figure 3.1, the normalized added mass for surge, heave, and pitch of 2BPA float is negative in specific wave frequencies. This is because the added mass coefficient $A(\omega)$ for float is negative in specific frequencies, as previously shown in Figures 2.8, 2.10, and 2.12. The added-mass coefficient can be interpreted as the fluid mass accelerated by the body and is positive for a deeply submerged body. However, when free-surface effects are essential, this need not be so [39]. Nevertheless, in this thesis, the free-surface effects were not considered for 2BPA (see Script 2.10). In multi-body problems, the added mass takes the form of a matrix, reflecting the fact that the oscillations of one body can create a force on another [39]. The variation with frequency of the off-diagonal terms is invariably oscillatory, taking both positive and negative values [39]. This thesis validated the positive and negative added mass values when NEMOH calculated the added mass matrix in the 2nd step. Also, the diagonal terms tend to be more oscillatory in their frequency variation than for a single body. See, for example, Matsui and Tamaki [40]. A simple physical interpretation of accelerated fluid mass is not appropriate in complicated multi-body problems where interaction effects are essential [39]. So, it is reasonable to state that the interaction effects between float and spar-plate resulting from the creation of force by one body to another are the reason to have negative added mass in specific wave frequencies. However, the irregular spikes in Figure 3.1 must be removed to avoid the singularity of the system. In NEMOH v2.03, it is impossible to remove the irregular spikes, so the author recommends using WAMIT if a researcher wants to remove them.

As extra information regarding added mass, Ogilvie [41] calculated added-mass coefficients for a submerged horizontal cylinder for single body problems, and he noticed that when the depth of submergence is sufficiently small, compared to the diameter of the cylinder, the added mass is negative over a range of frequencies. Experimental confirmation of the behavior was made by

Chung [42] for cylinders with both square and circular cross-sections. The negative added mass has also been found for floating bodies that enclose a region of the free surface; for example, the floating torus described by Newman [43] and the two half-immersed cylinders studied by Wang and Wahab [44] as a model for the motion of a catamaran hull. Similar behavior was obtained when two submerged cylinders were considered. An approximate solution for two vertical spaced rolling plates in two dimensions given by Srokosz and Evans [45] also produced negative added-mass coefficients.

In Figure 3.2, the normalized radiation damping is negative in specific wave frequencies because the radiation damping coefficient $B(\omega)$ is negative in specific wave frequencies, as shown in Figures 2.8-2.12. The radiation damping coefficient measures energy flux in the waves radiating away from the oscillating body [39] and is necessarily non-negative [34]. However, as previously discussed in section 3.1.1, the negative radiation coefficient arises due to a fundamental error in the formulation of the NENOH BEM solver [27].

In Figure 3.4, the curve of normalized excitation force magnitude does not regularly descend when the wave frequency increases. The irregular spikes that NEMOH cannot remove are why such an irregular curve for normalized excitation force magnitude.

Regarding previously mentioned information, the author suggests that the WAMIT BEM solver is also to be utilized in future studies by researchers to remove the irregular frequencies to avoid having singularity in the system and negative radiation damping coefficient. Plus, removing irregular spikes will lead the radiation damping coefficient, normalized radiation damping, excitation force, and normalized excitation force magnitude curves to descend regularly while the wave frequency increases.

4.1.2 Creating HDF5 (*.h5) File for OSWEC Using bemio.m MATLAB Function

BEMIO is also used to import the hydrodynamic output data of an OSWEC obtained via BEM solvers to WEC-Sim. For example, Ref [46] represents a floating oscillating surge wave energy converter (FOSWEC) which its hydrodynamic data was calculated by AQWA-ANSYS software then imported to WEC-Sim by using BEMIO. The hydrodynamic data obtained by NEMOH for the OSWEC studied in this thesis was imported to WEC-Sim using BEMIO. Having all required files for function bemio, bemio.m was called using Script 3.2 and oswec.h5 file was generated inside the *oswec* working folder. Script 3.2 was saved inside the *oswec* working folder and named *oswec3*, indicating the third step carried out for the OSWEC. Note that before calling bemio.m, the location of the *oswec* working folder must be specified in line 27 of Script 3.2.

```
1   %% III) Call function bemio
2   %
3   % Purpose: Reads data from a NEMOH working folder and creates the file *.h5
4   for the present case.
5   %
```

4. Hydrodynamic Data from BEM Solution in Hierarchical Data Format Version 5 (HDF5)

```matlab
6   %% hydro = Read_NEMOH(hydro, filedir)
7   %
8   % hydro-data structure
9   % filedir-NEMOH working folder, must include:
10  % • Nemoh.cal
11  % • Mesh/Hydrostatics.dat (or Hydrostatiscs_0.dat, Hydrostatics_1.dat, etc.
12  for multiple bodies)
13  % • Mesh/KH.dat (or KH_0.dat, KH_1.dat, etc. for multiple bodies)
14  % • Results/RadiationCoefficients.tec
15  % • Results/ExcitationForce.tec
16  % • Results/DiffractionForce.tec-If simu.nlHydro= 3 will be used
17  % • Results/FKForce.tec-If simu.nlHydro= 3 will be used
18  %
19  %Source: https://github.com/WEC-Sim/WEC-
20  Sim/tree/master/source/functions/BEMIO
21  %%%%%%%%%%%%%%%%%%%%%%%%%%%%%%
22
23  %% bemio inputs:
24
25  hydro = struct();
26
27  hydro = Read_NEMOH(hydro,'C:\Users\Babak Shafiei\Documents\MATLAB\cccc\matlab
28  routines\oswec');
29  hydro = Radiation_IRF(hydro,60,[],[],[],1.9);
30  hydro = Radiation_IRF_SS(hydro,[],[]);
31  hydro = Excitation_IRF(hydro,157,[],[],[],1.9);
32
33  Write_H5(hydro)
34  Plot_BEMIO(hydro)
```

Script 3.2: Call function bemio for OSWEC

Further, the output data for the OSWEC flap resulting from BEMIO were plotted in Figures 3.7-3.12. Note that only pitch motion is considered since the flap is mounted on the base. The plots are:

- Normalized added mass for pitch motion
- Normalized radiation damping for pitch motion
- Normalized radiation impulse response functions for pitch motion
- Normalized excitation force magnitude for pitch motion
- Excitation phase for pitch motion
- Normalized excitation impulse response functions for pitch motion

Normalized Added Mass: $\bar{A}_{i,j}(\omega) = \dfrac{A_{i,j}(\omega)}{\rho}$
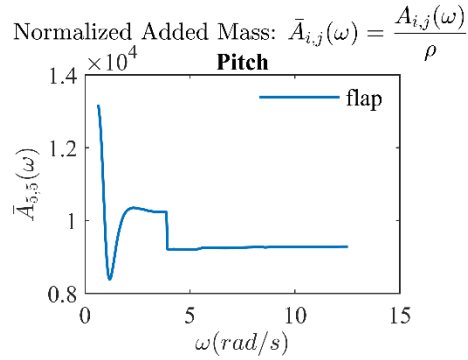
Notes:
- $\bar{A}_{i,j}(\omega)$ should tend towards a constant, A_∞, within the specified ω range.
- Only $\bar{A}_{i,j}(\omega)$ for the pitch DOF is plotted here. If another DOF is significant to the system, that $\bar{A}_{i,j}(\omega)$ should also be plotted and verified before proceeding.

Figure 3.7: Normalized added mass for pitch motion of OSWEC flap

Normalized Radiation Damping: $\bar{B}_{i,j}(\omega) = \dfrac{B_{i,j}(\omega)}{\rho\omega}$
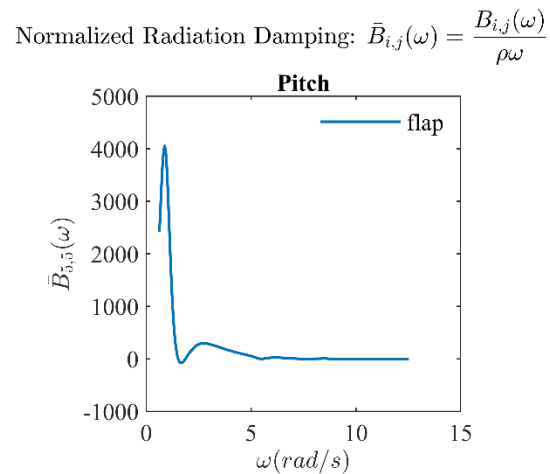
Notes:
- $\bar{B}_{i,j}(\omega)$ should tend towards zero within the specified ω range.
- Only $\bar{B}_{i,j}(\omega)$ for the pitch DOF is plotted here. If another DOF is significant to the system that $\bar{B}_{i,j}(\omega)$ should also be plotted and verified
before proceeding.

Figure 3.8: Normalized radiation damping for pitch motion of OSWEC flap

Normalized Radiation Impulse Response Functions: $\bar{K}_{i,j}(t) = \dfrac{2}{\pi} \displaystyle\int_0^\infty \dfrac{B_{i,j}(\omega)}{\rho} \cos(\omega t)d\omega$
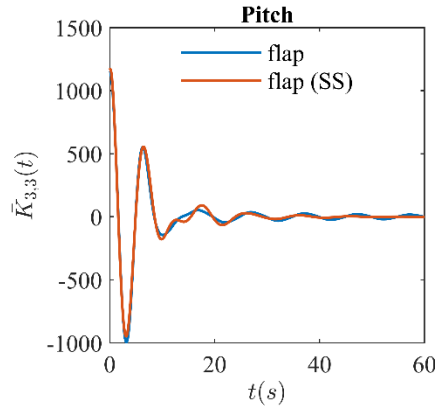
Notes:
• The IRF should tend towards zero within the specified timeframe. If it does not, attempt to correct this by adjusting the ω and t range and/or step size used in the IRF calculation.
• Only the IRFs for the pitch DOF is plotted here. If another DOF is significant to the system, that IRF should also be plotted and verified

Figure 3.9: Normalized radiation impulse response functions for pitch motion of OSWEC flap

Normalized Excitation Force Magnitude: $\bar{X}_i(\omega, \beta) = \dfrac{X_i(\omega, \beta)}{\rho g}$
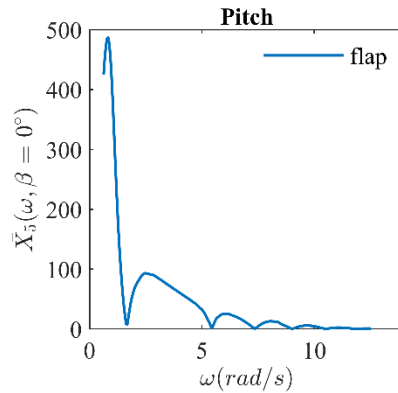
Figure 3.10: Normalized excitation force magnitude for pitch motion of OSWEC flap

68

Excitation Force Phase: $\phi_i(\omega, \beta)$
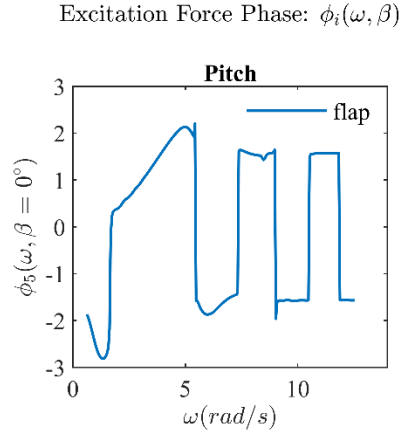
Figure 3.11: Excitation phase for pitch motion of OSWEC flap

Normalized Excitation Impulse Response Functions: $\bar{K}_i(t) = \dfrac{1}{2\pi} \displaystyle\int_{-\infty}^{\infty} \dfrac{X_i(\omega, \beta)e^{i\omega t}}{\rho g} d\omega$

Notes:
- The IRF should tend towards zero within the specified timeframe. If it does not, attempt to correct this by adjusting the ω and t range and/or step size used in the IRF calculation.
- Only the IRFs for the first wave heading, surge, heave, and pitch DOFs are plotted here. If another wave heading or DOF is significant to the system, that IRF should also be plotted and verified before proceeding.

Figure 3.12: Normalized excitation impulse response functions for pitch motion of OSWEC flap

According to the graphs shown above, there are no significant irregular frequencies in normalized added mass, normalized radiation damping, and normalized excitation force, which indicates that the NEMOH works well calculating hydrodynamic coefficients for OSWEC device shown in Figures 2.22-2.24. Moreover, For the OSWEC case, Penalba [27] concluded that the hydrodynamic coefficients solved by NEMOH and WAMIT match almost perfectly.

5.

Designing 2BPA and OSWEC Using SOLIDWORKS

5.1 Creating *.stl File for 2BPA and OSWEC Using SOLIDWORKS: 4th Step

A *.stl file is a geometry file used for WEC geometry. Since the WEC-Sim input file requires a *.stl file, it is necessary to design the offshore structure using solid modeling software. The *.stl file is used to generate Simscape Mechanics Explorer visualization, visualize linear hydrodynamics, and determine the instantaneous wetted surface at each step with the nonlinear buoyancy and Froude-Krylov forces option. In this thesis, the *.stl geometry files for 2BPA and OSWEC are created via SOLIDWORKS.

In Refs [12, 15, and 37], the SOLIDWORKS is used to model and obtain the geometry files. In addition to SOLIDWORKS software, Fusion 360, a product of Autodesk, can be used to model the WECs. For example, Taylor McKie [28] designed the different geometries of float using Fusion 360. Also, FreeCAD, an open-source computer-aided design (CAD) software, can generate a *.stl file for the WEC-Sim input file [38]. FreeCAD can be downloaded by the following link: https://www.freecadweb.org/.

5.1.1 Creating *.stl File for 2BPA

The *.stl files for float and spar-plate bodies were generated using SOLIDWORKS v2018. First, the float and spar-plate were designed. Then, the models were saved as a *.stl file.

5.1.1.1 Designing Float Body

After opening SOLIDWORKS software, on the Welcome-SOLIDWORKS 2018 page, the _Part_ option was selected (arrow No.1 in Figure 5.1). Then, from the _Feature Manager Design Tree_, the _Front Plane_ option was selected in which the _Sketch_ option was chosen (arrow No.2 in Figure 5.2). Next, the _Document Properties_ option was selected from the _System Options – General_ page. Then, inside the _Units_ page, the _MKS (meter, kilogram. second)_ was chosen as a unit system for float (arrows 3-7 in Figure 5.3). A circle was drawn with an arbitrary radius using the _Circle_ option from the _Sketch_ tab to draw the cross-section of the float. Then, from the _Parameters_ section, the X and Y coordinates of the circle's center were defined as zero (Figure 5.4). With the _Smart Dimension_ option, the circle's diameter was defined as 20 m (Figure 5.5).

Further, according to Figure 2.1, the height of the float was drawn (Figure 5.6). The origin point was illustrated on the circle made at the bottom of the float by selecting the _Origin_ option. (Figure 5.7). Then by clicking on the origin point shown on the circle made at the bottom of the float, a plane was selected to make a simple hole through this plane (Figure 5.8). A simple hole was made on the plane, shown earlier in Figure 5.8 (Figures 5.9-5.11). Finally, the design was saved as a *.stl file (Figures 5.12, 5.13).
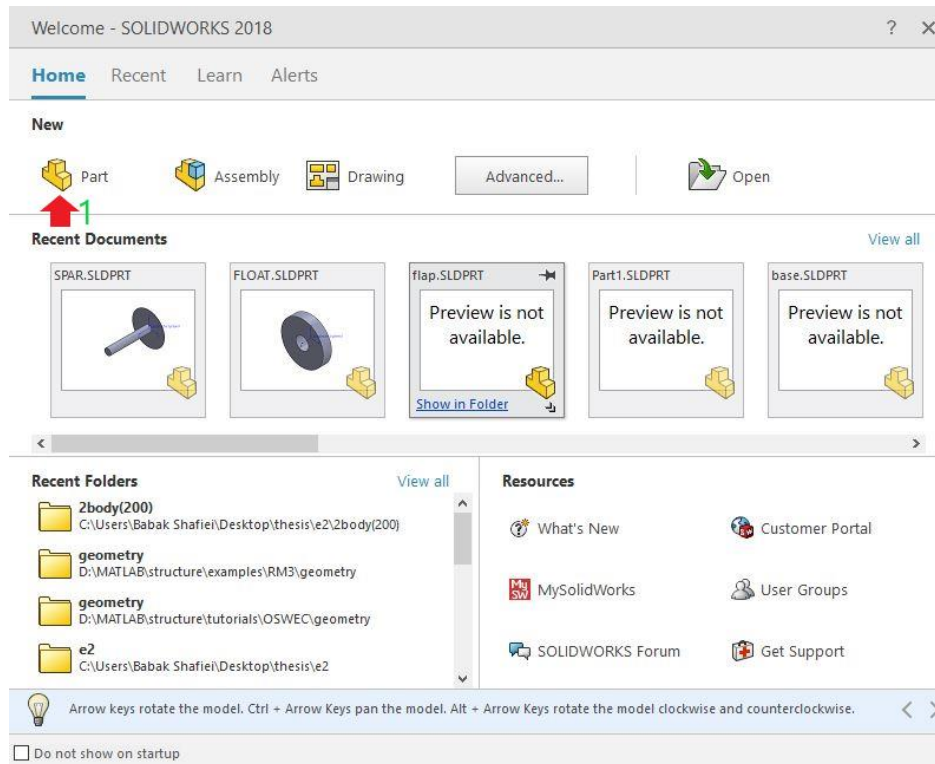
Figure 5.1: _Welcome-SOLIDWORKS 2018_ page
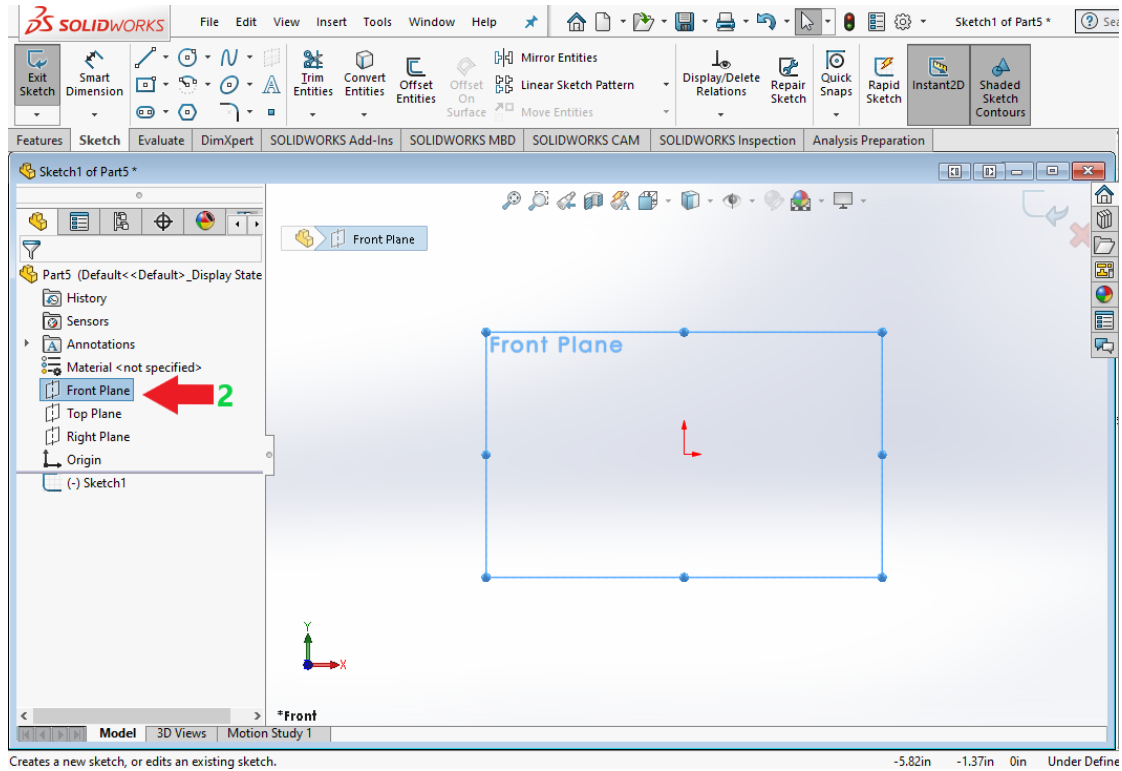
Figure 5.2: Plane selection for float
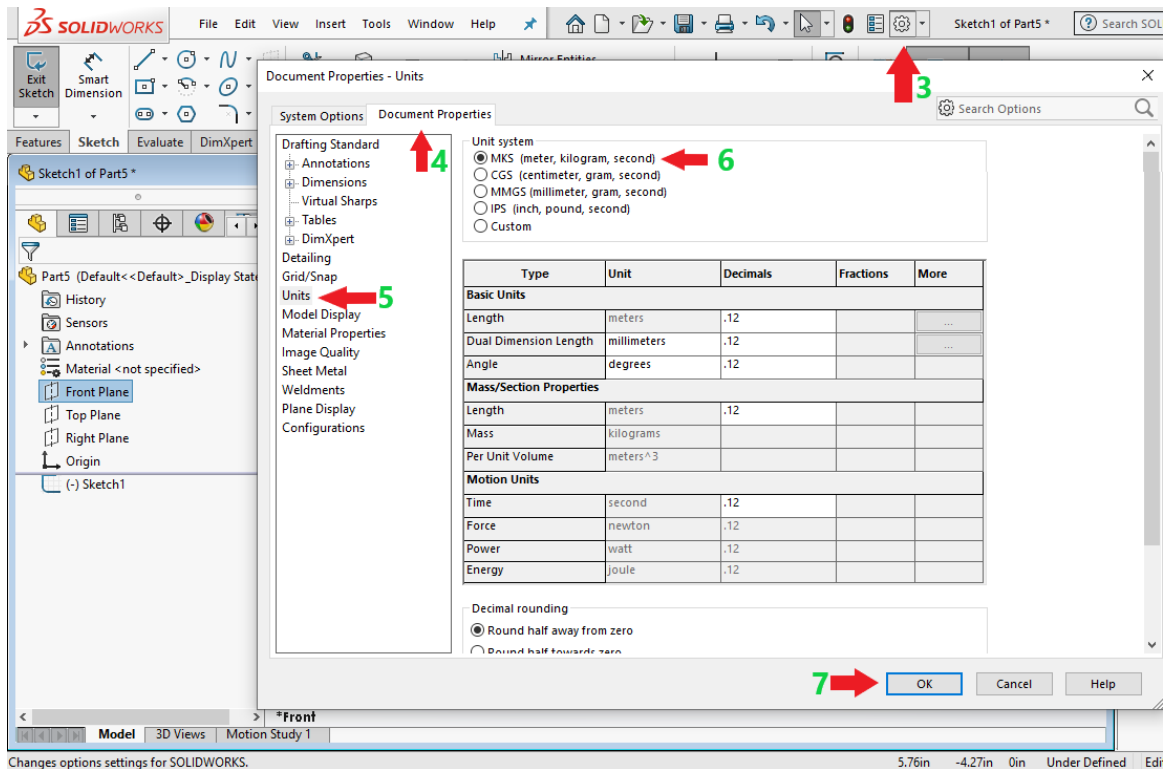
Figure 5.3: Selection of a unit system for float
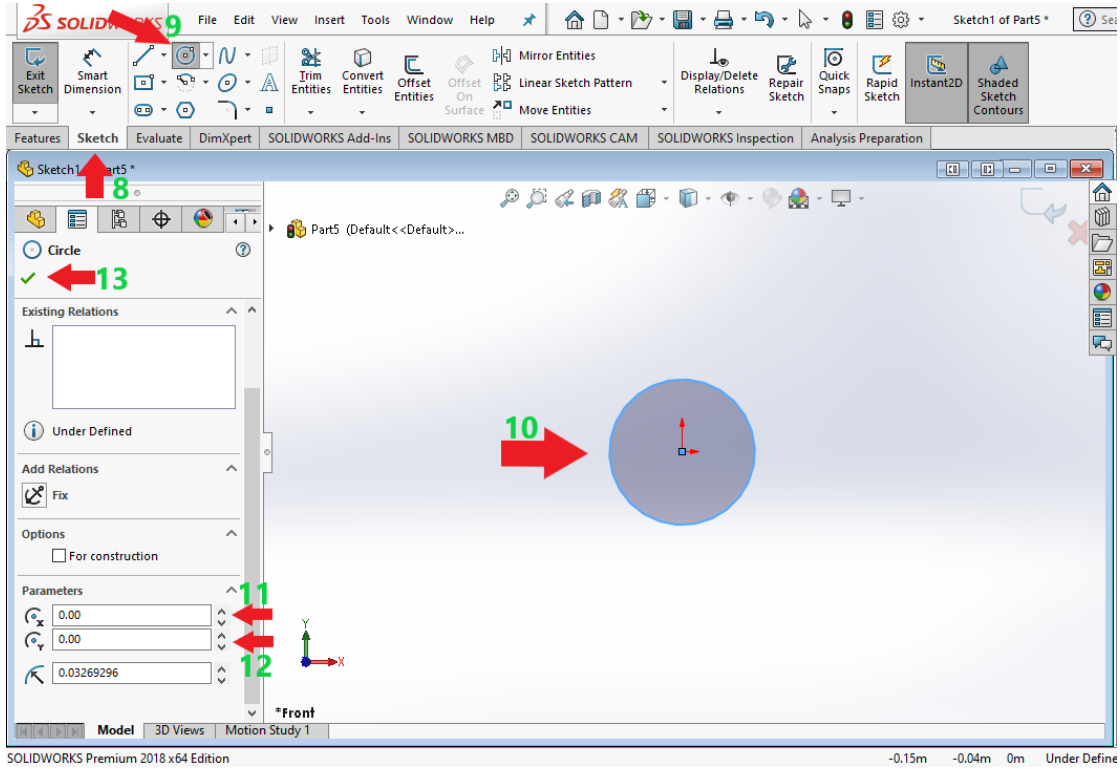
Figure 5.4: Drawing the cross-section of the float
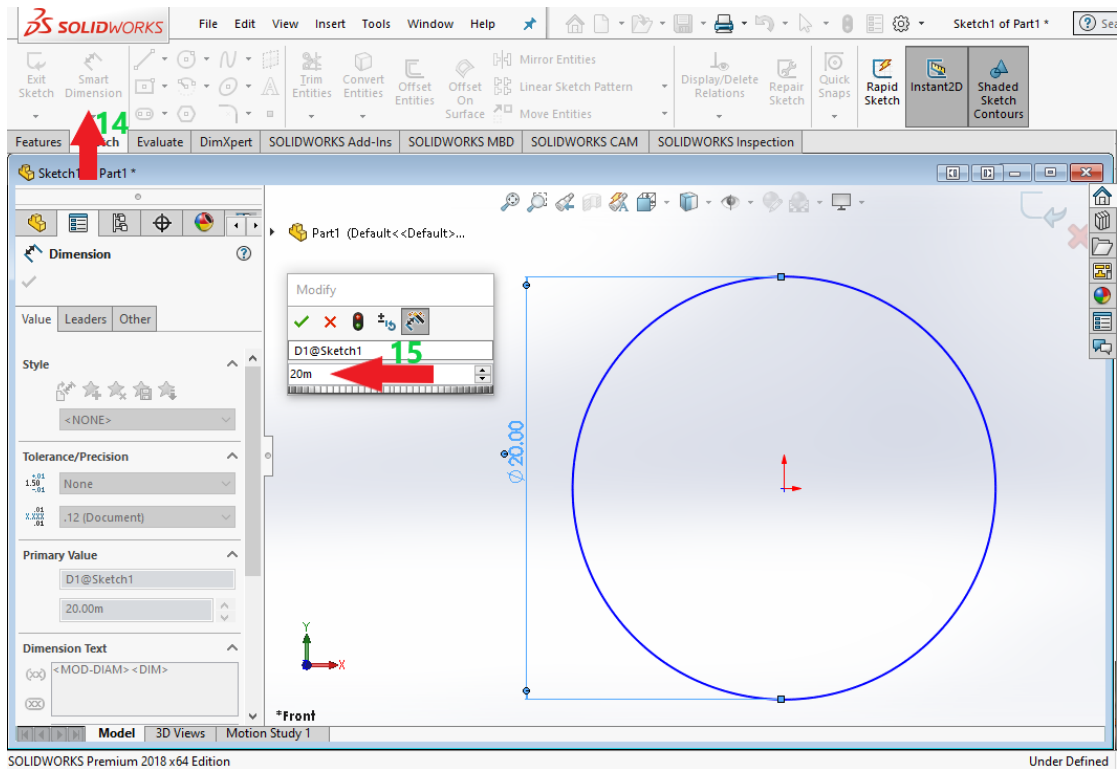
Figure 5.5: Defining the diameter of the float

73
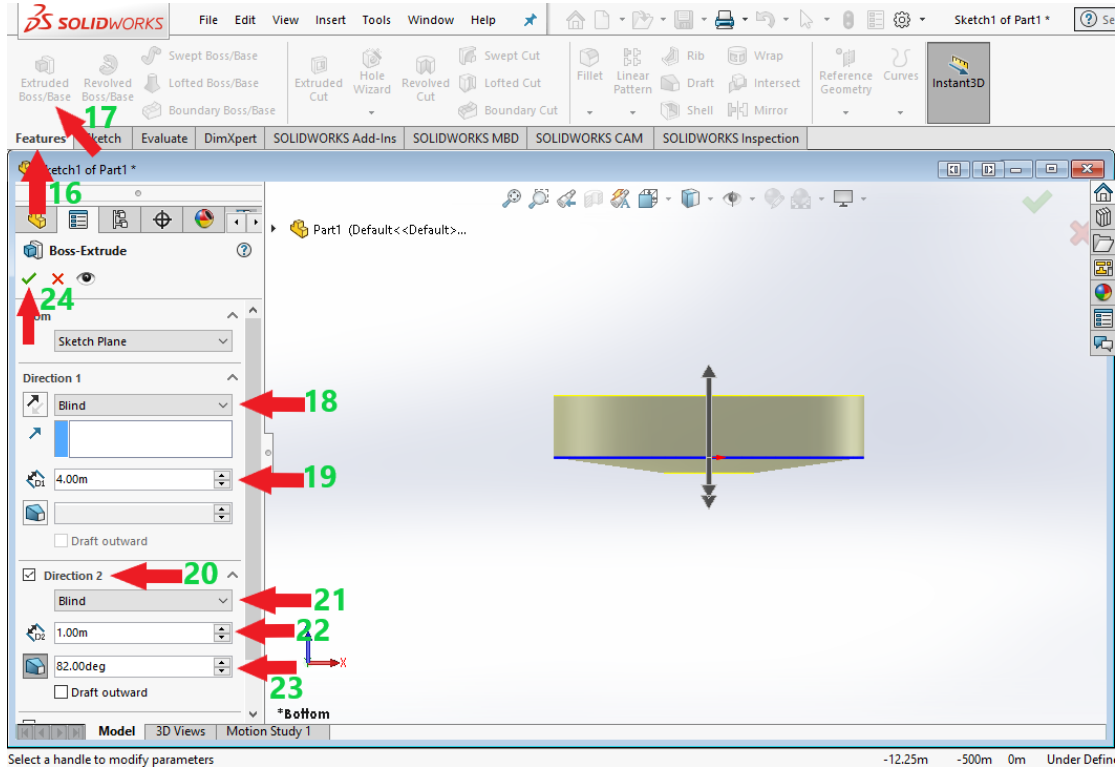
Figure 5.6: Drawing the height of the float
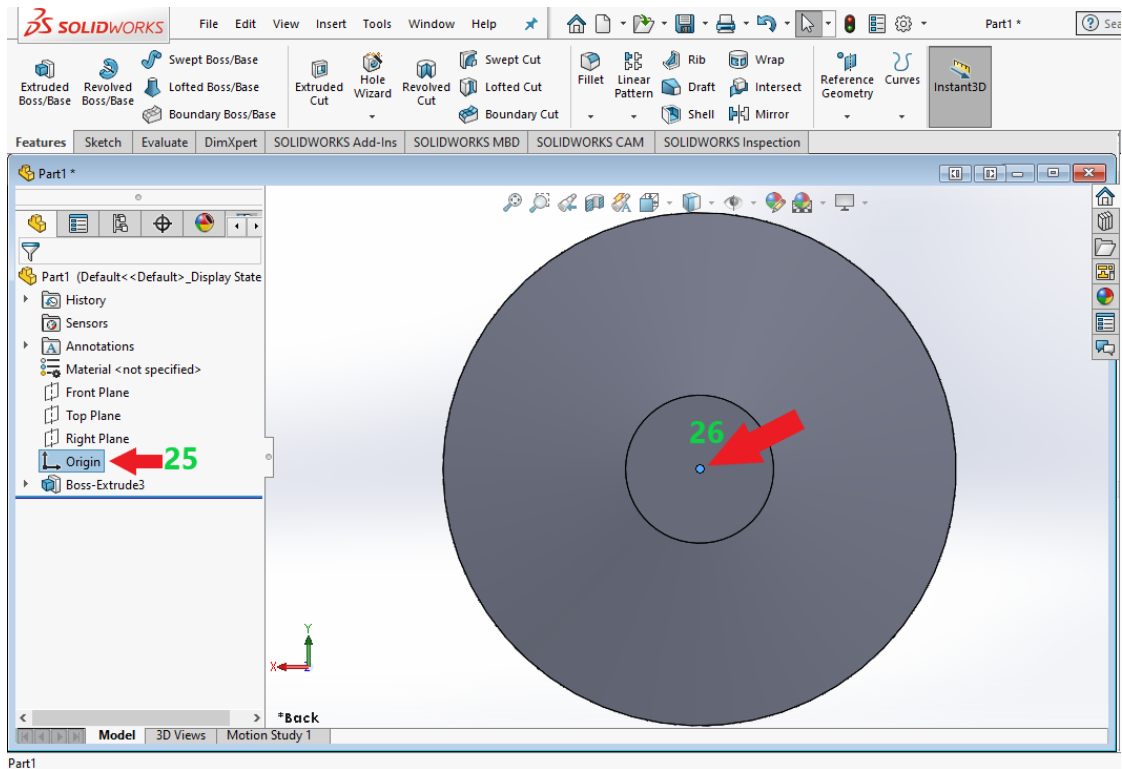
Figure 5.7: Illustrating the origin point on the float

74
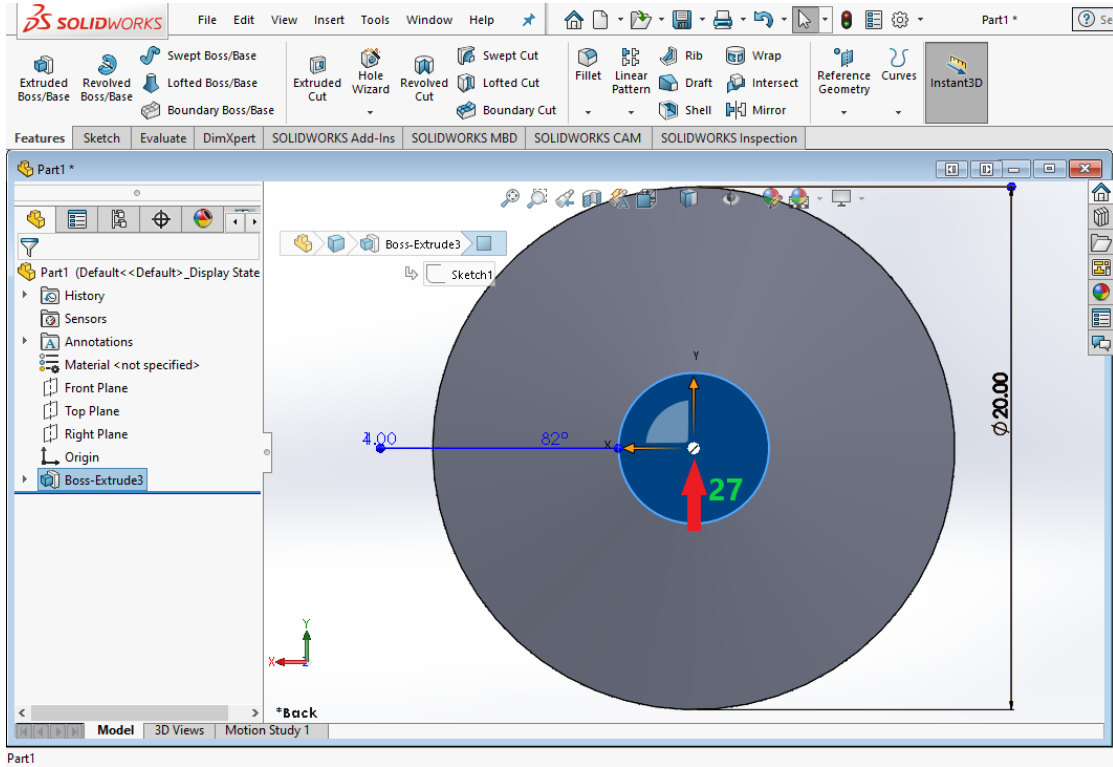
Figure 5.8: Selecting a plane on the float to make a hole
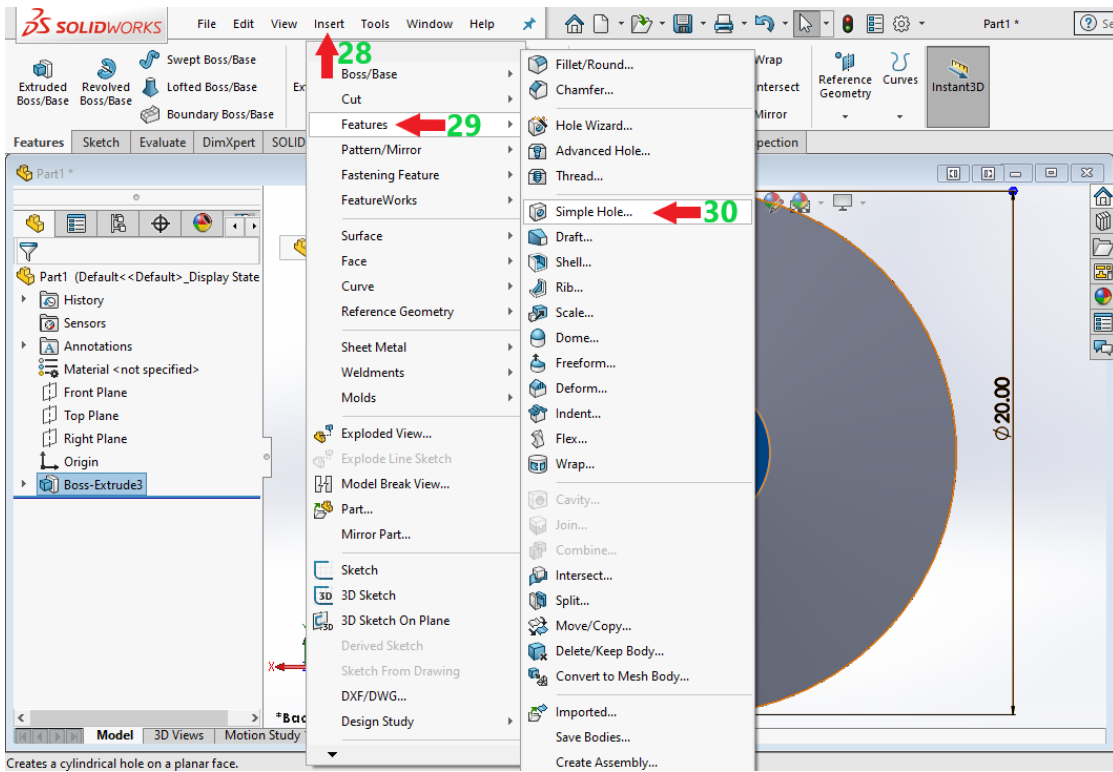
Figure 5.9: Selecting Simple Hole option in SOLIDWORKS for float
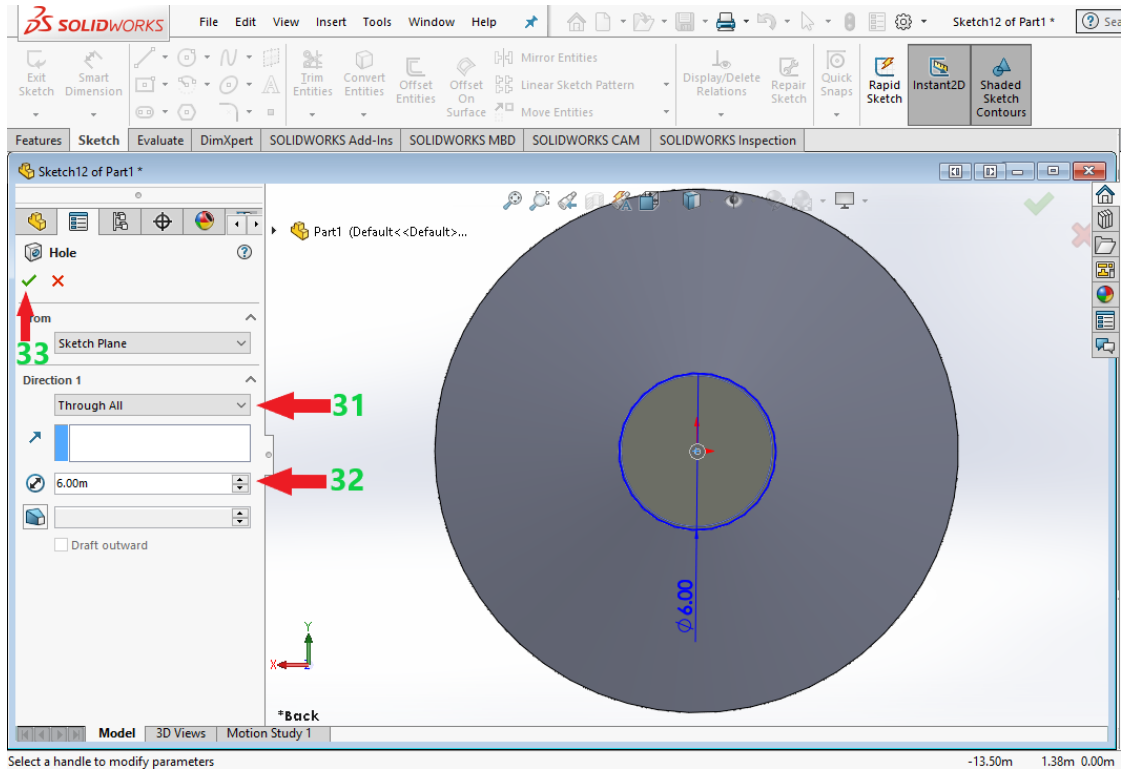
Figure 5.10: Defining the specification of the hole for float
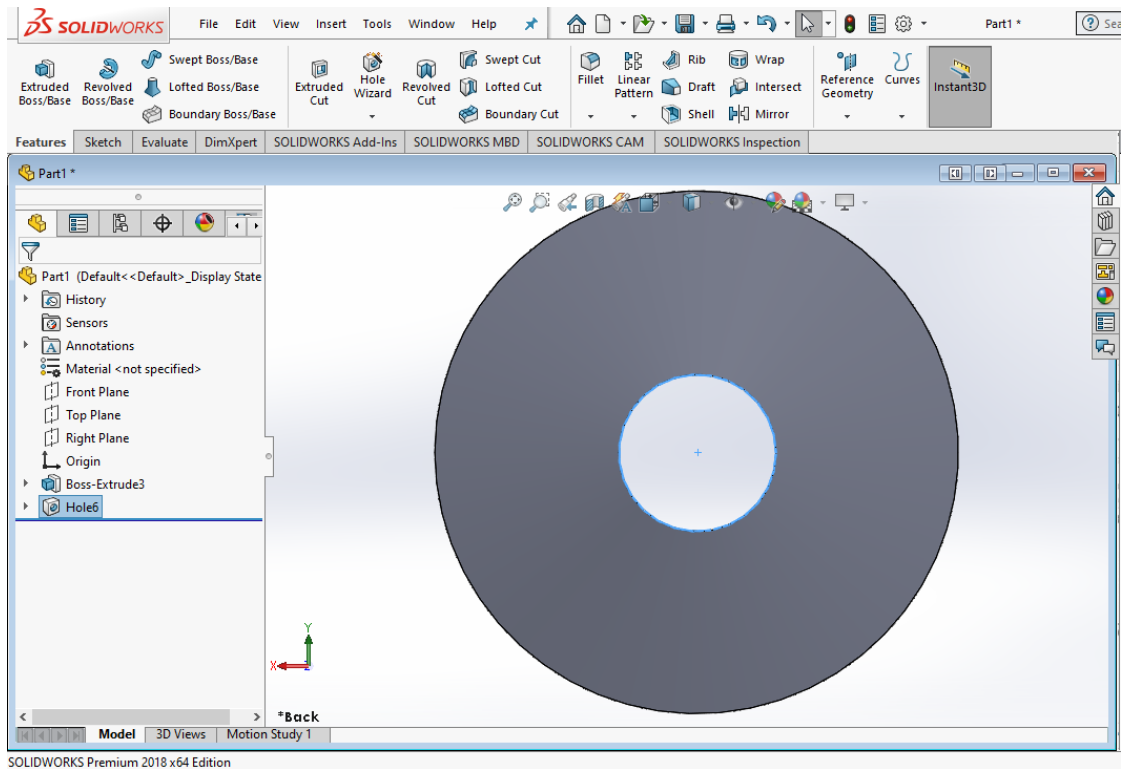
Figure 5.11: A hole made on the float's body
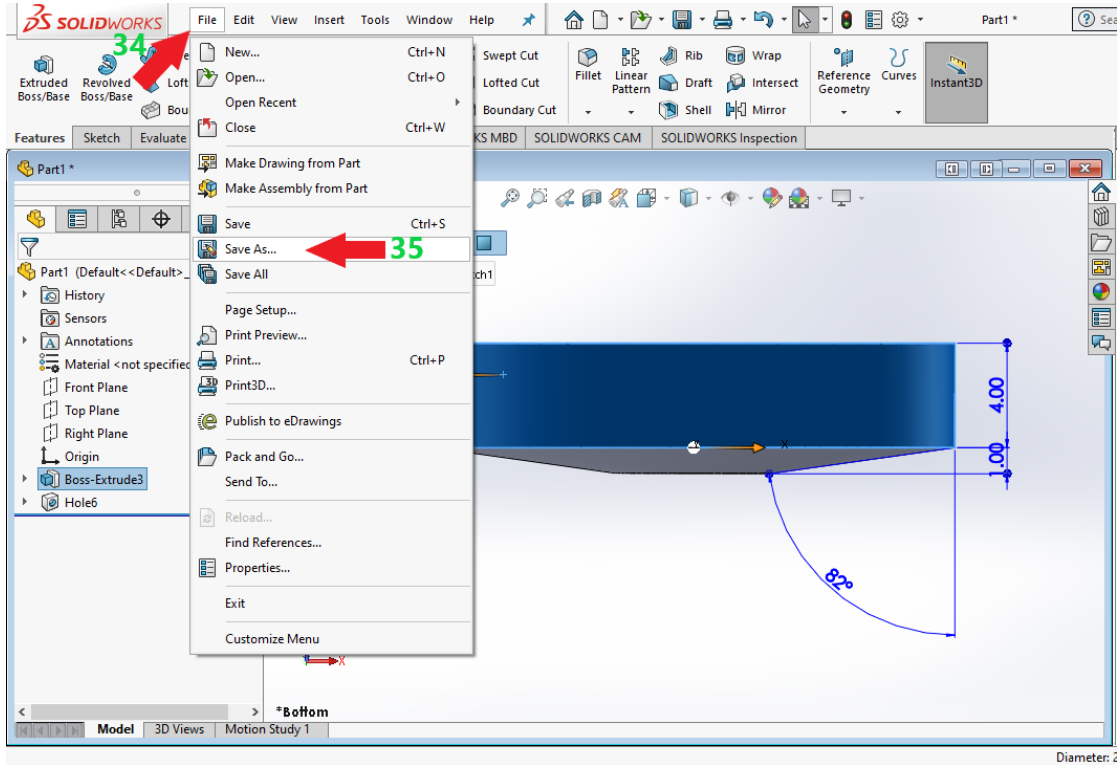
Figure 5.12: *Save As* option to save the float design
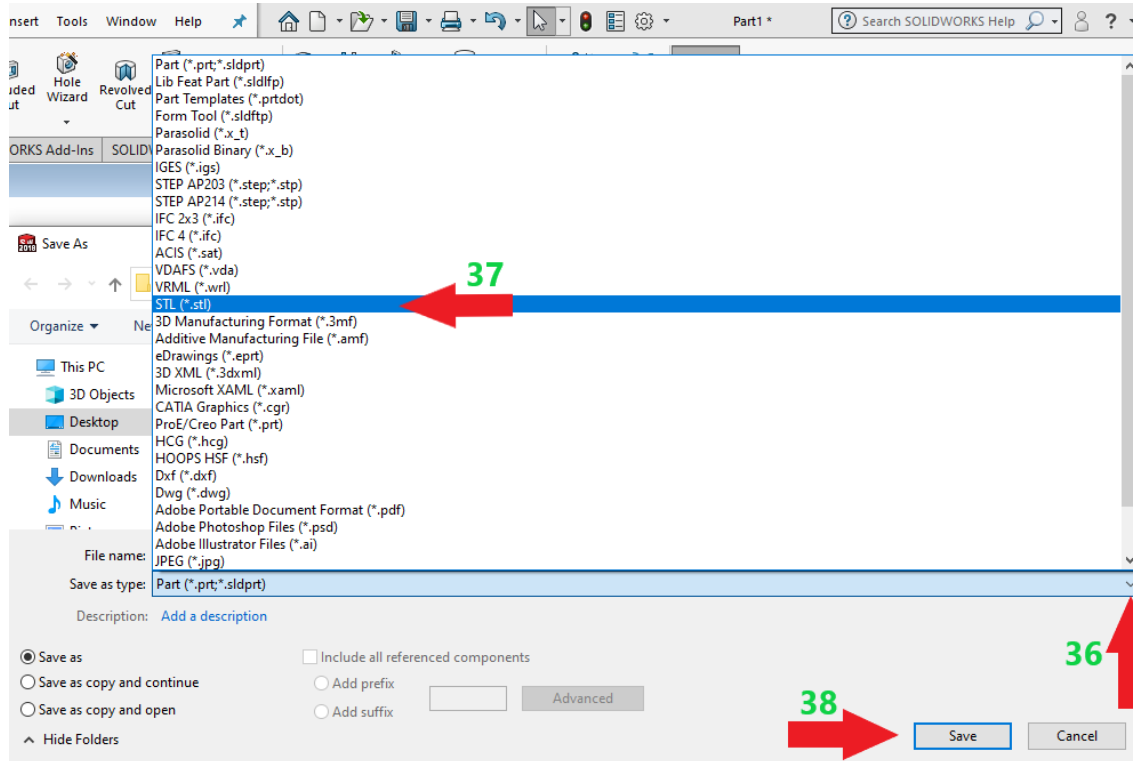
Figure 5.13: Saving the float design as an STL (*.stl) file

77

5.1.1.2 Designing Spar-Plate Body

A new project was opened after the float was designed, as shown in Figure 5.14. Then *Part* option was selected, as shown in Figure 5.15. From *the Feature Manager Design Tree*, the *Front Plane* option was selected in which the *Sketch* option was chosen (arrow No.5 in Figure 5.16). Next, the *Document Properties* option was selected from the *System Options – General* page. Then, inside the *Units* page, the *MKS (meter, kilogram. second)* was chosen as the unit system for spar-plate (arrows 6-10 in Figure 5.17).

A circle was drawn with an arbitrary radius using the *Circle* option from the *Sketch* tab. Then, from the *Parameters* section, the X and Y coordinates of the circle's center were defined as zero (Figure 5.18). Further, to specify the spar diameter, from the *Smart Dimension* option, the circle's diameter was defined as 6 m (Figure 5.19). According to Figure 2.1, the height of the spar, which is 37.90 m, was drawn (Figure 5.20). Then, the bottom side plane of the spar was selected. On this plane, a circle was drawn with an arbitrary radius using the *Circle* option to draw the cross-section of the plate. Then, from the *Parameters* section, the X and Y coordinates of the circle's center were defined as zero (Figure 5.21). With the *Smart Dimension* option, the circle's diameter was defined as 30 m (Figure 5.22). Next, according to Figure 2.1, the height of the plate, that is, 0.10 m, was drawn (Figure 5.23). Finally, the design was saved as a *.stl file (Figures 5.24, 5.25).
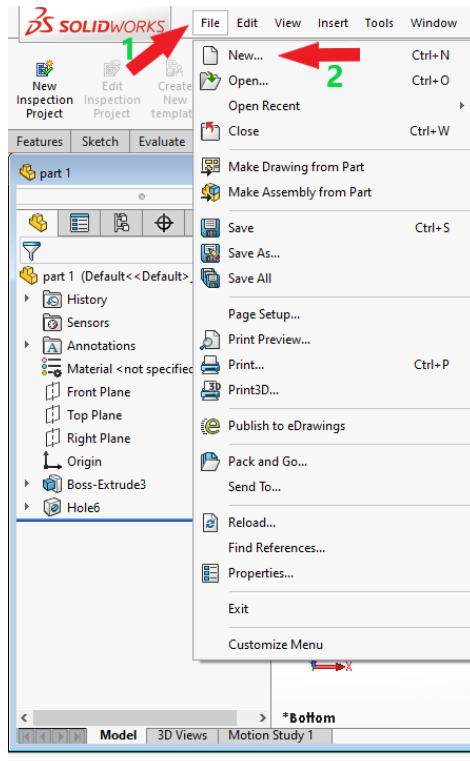
Figure 5.14: Opening a new project for designing spar-plate in SOLIDWORKS
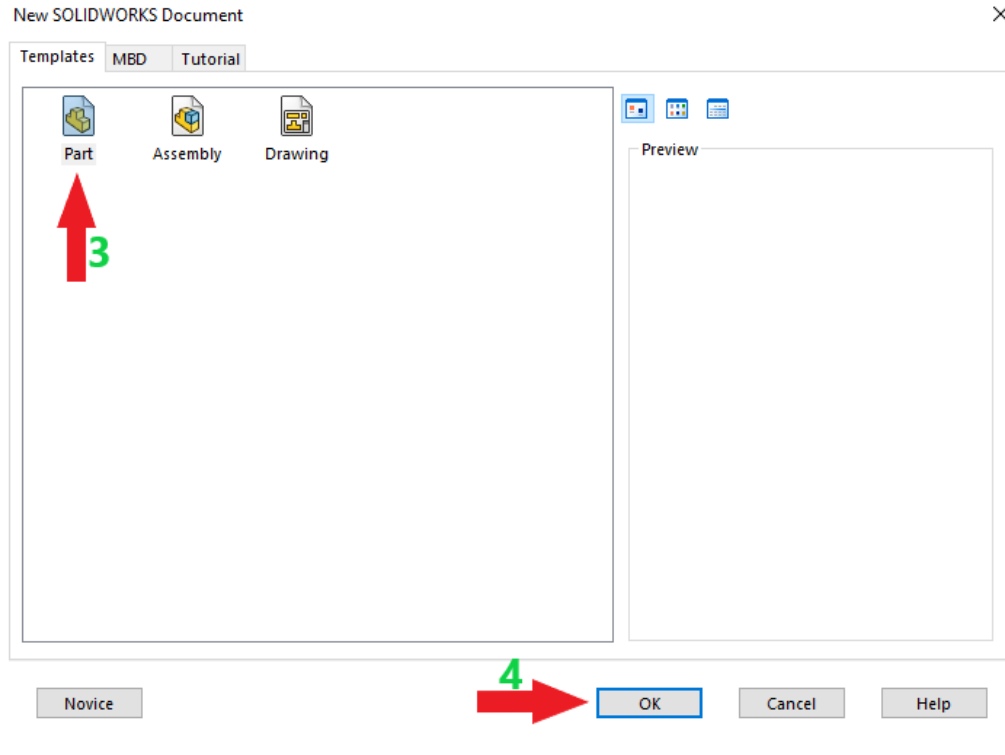
Figure 5.15: New SOLIDWORKS Document page for spar-plate
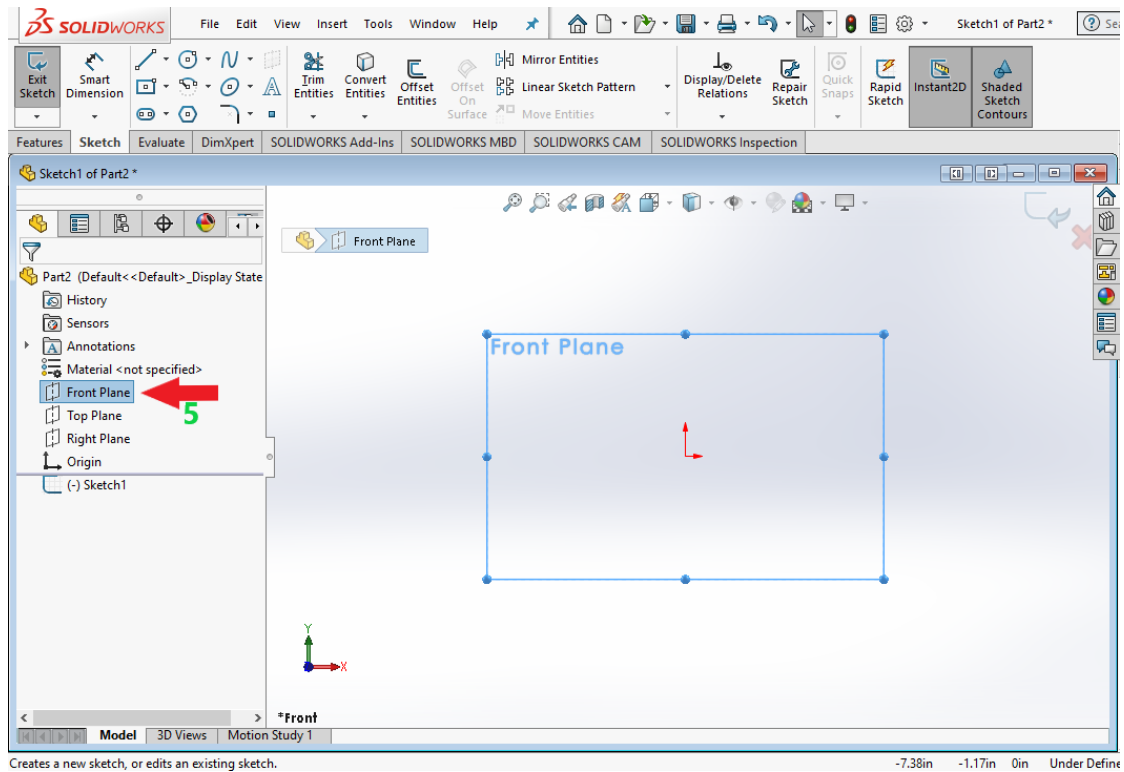
Figure 5.16: Plane selection for spar-plate
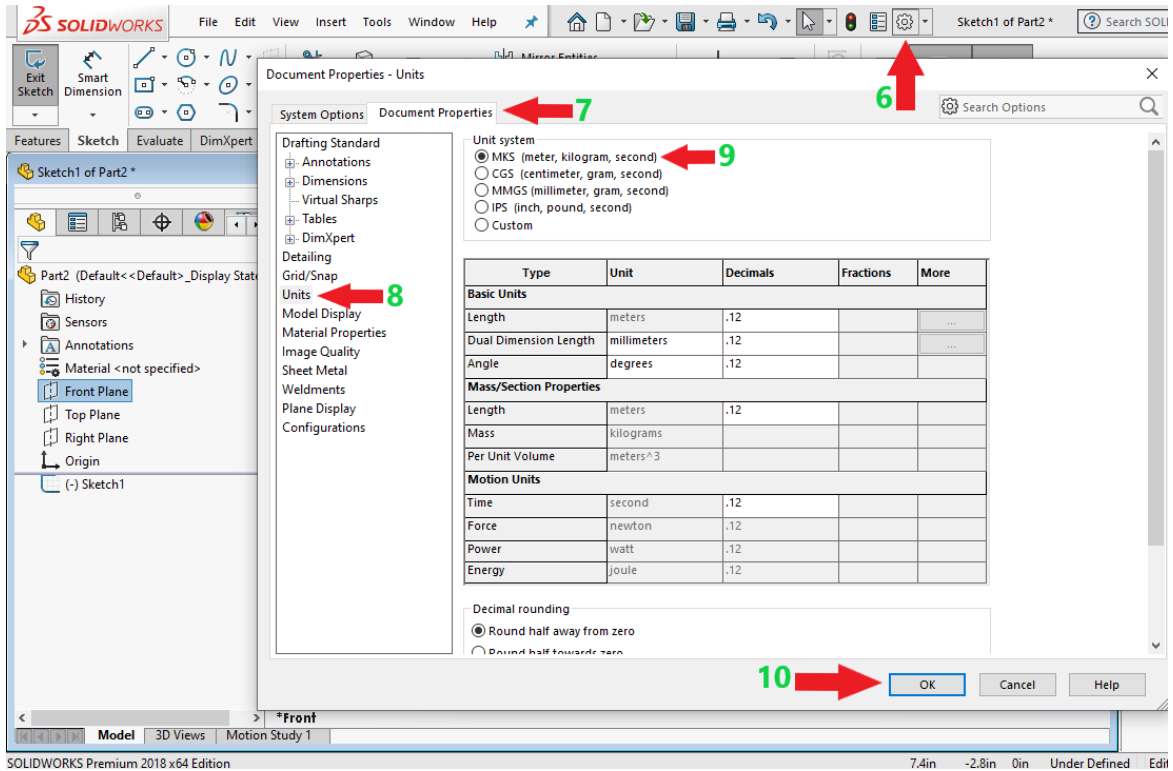
Figure 5.17: Selection of a unit system for spar-plate
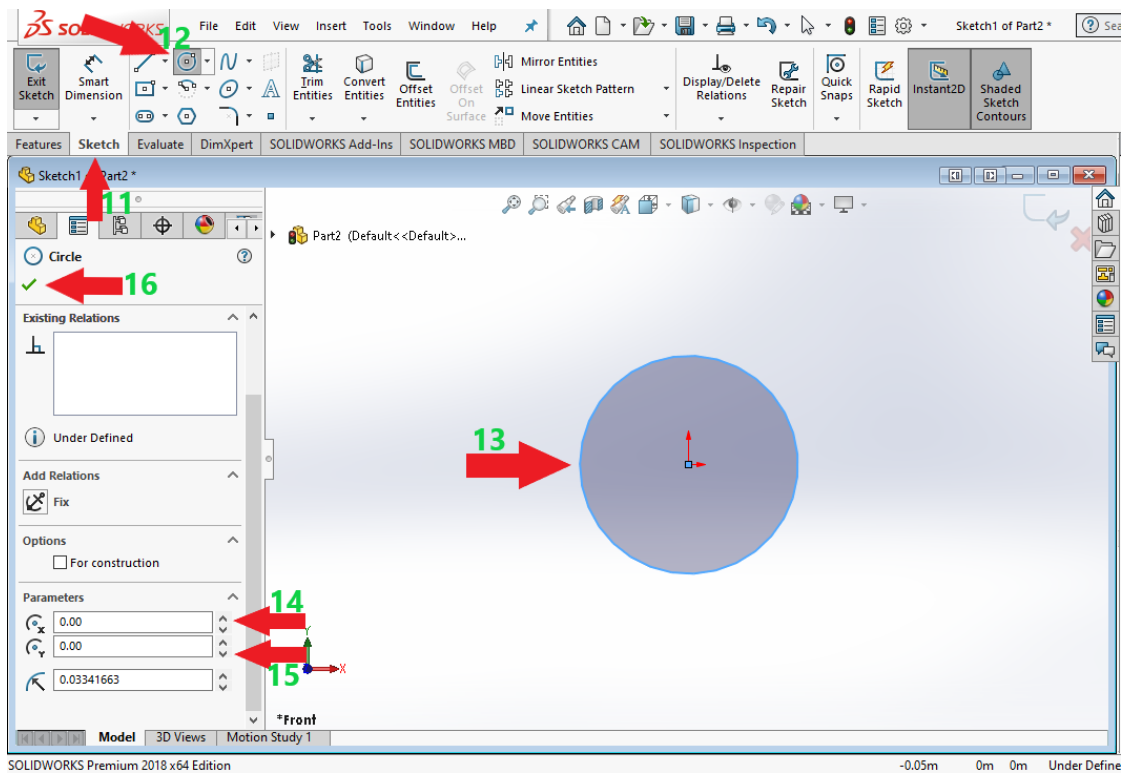
Figure 5.18: Drawing the cross-section of the spar-plate
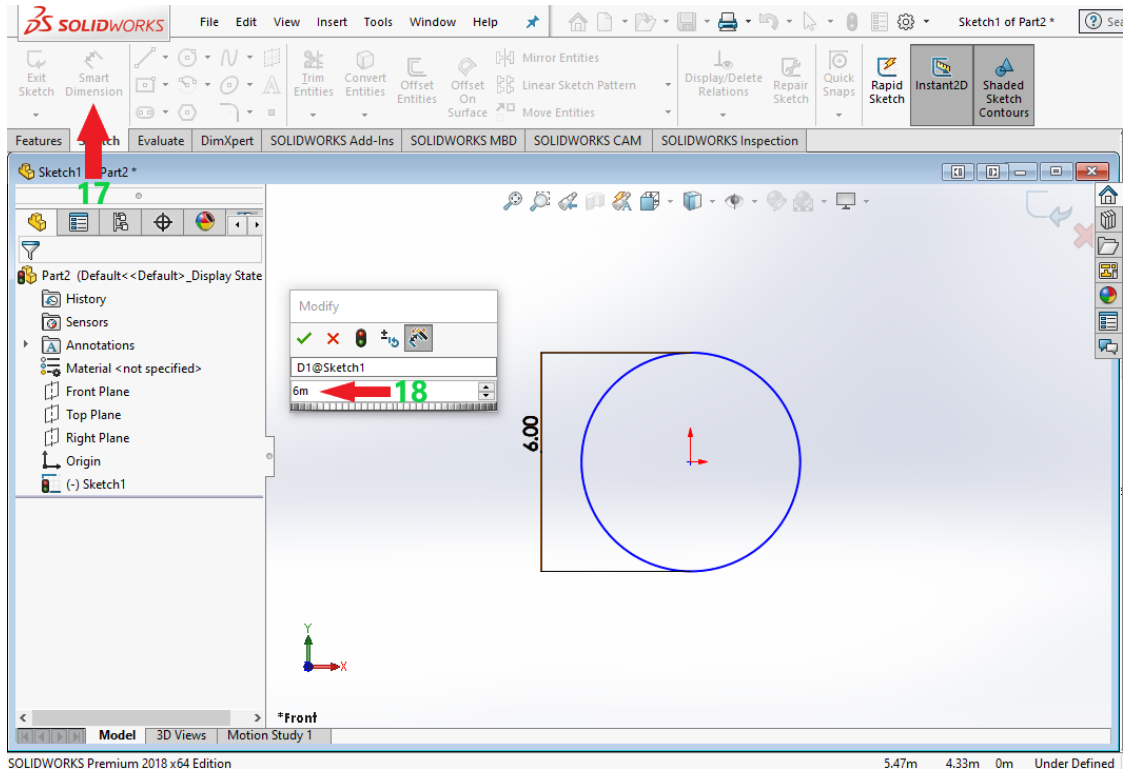
Figure 5.19: Defining the diameter of the spar
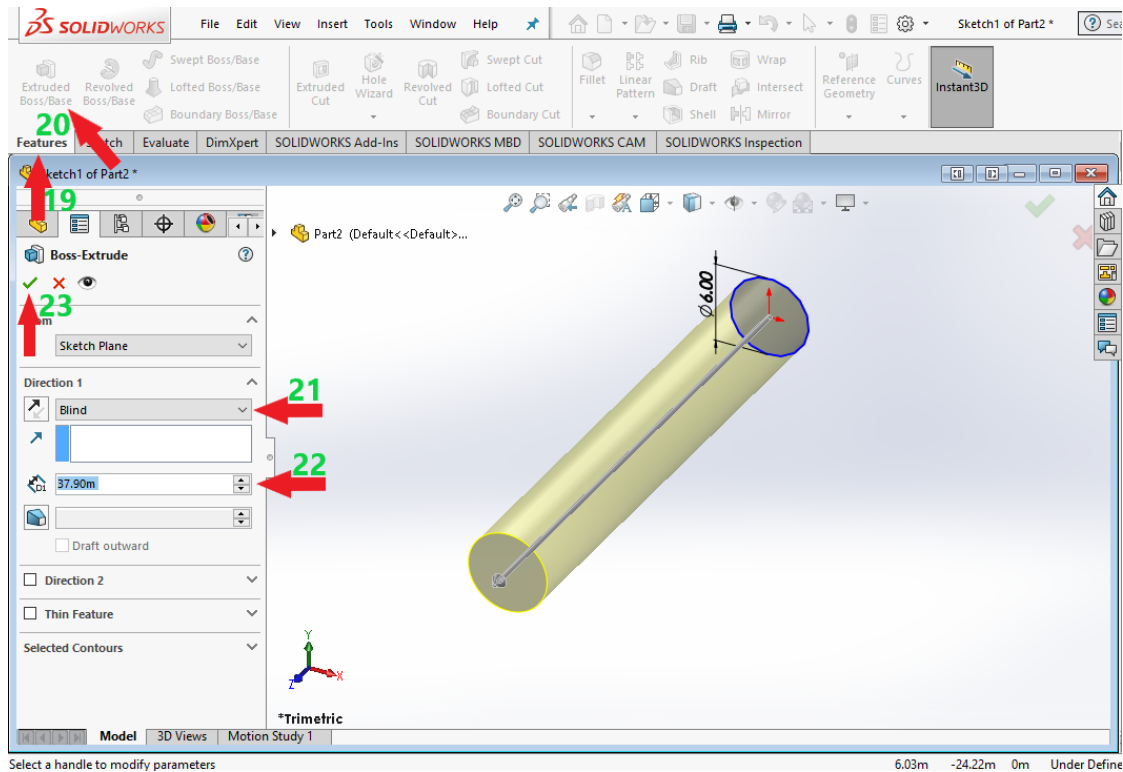
Figure 5.20: Drawing the height of the spar
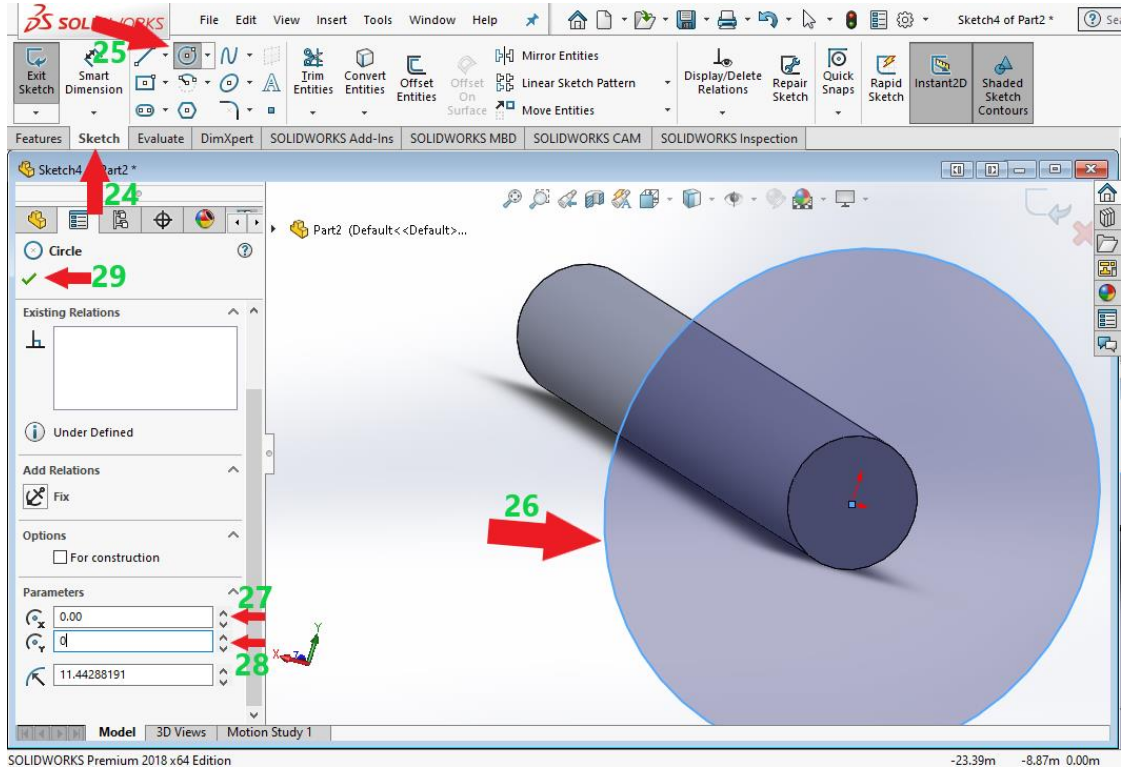
Figure 5.21: Drawing the cross-section of the plate
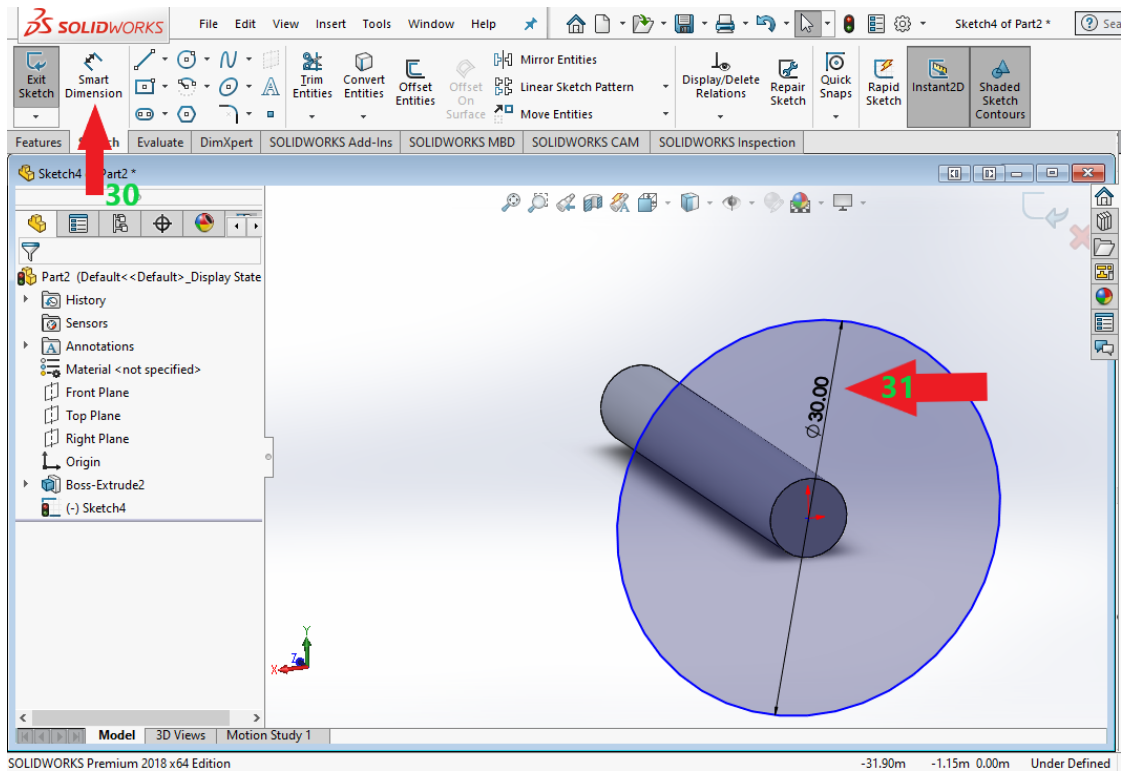
Figure 5.22: Defining the diameter of the plate
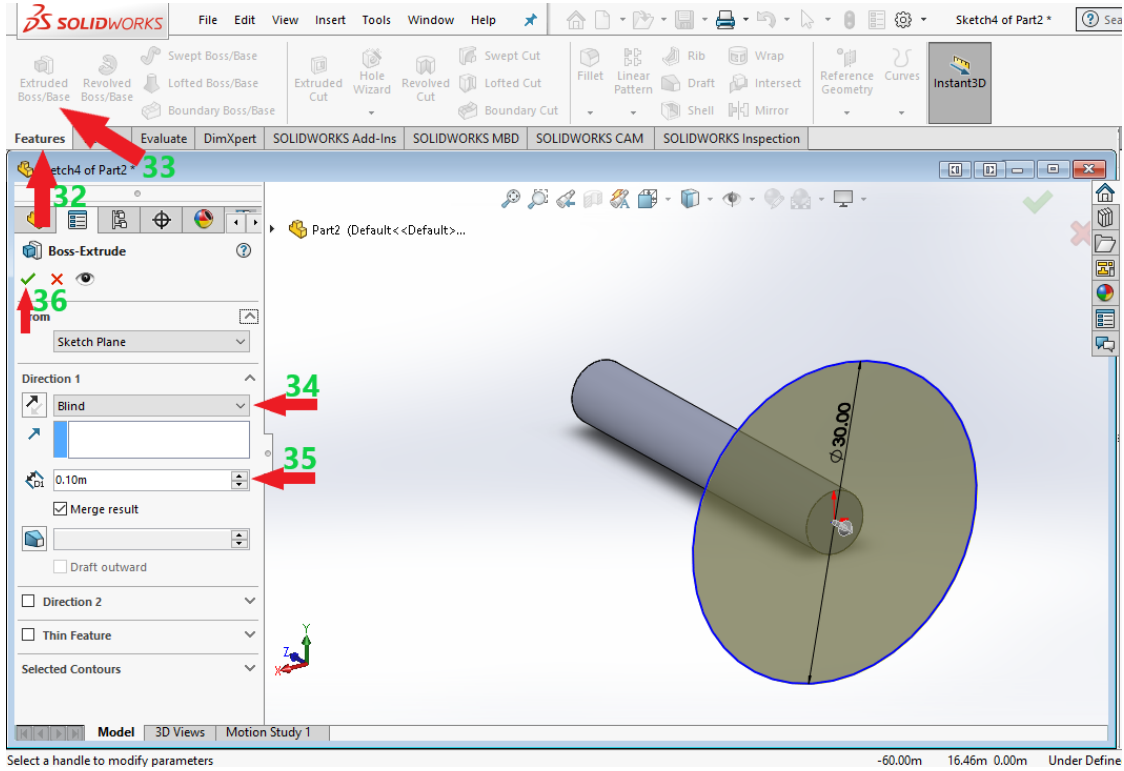
Figure 5.23: Drawing the height of the plate
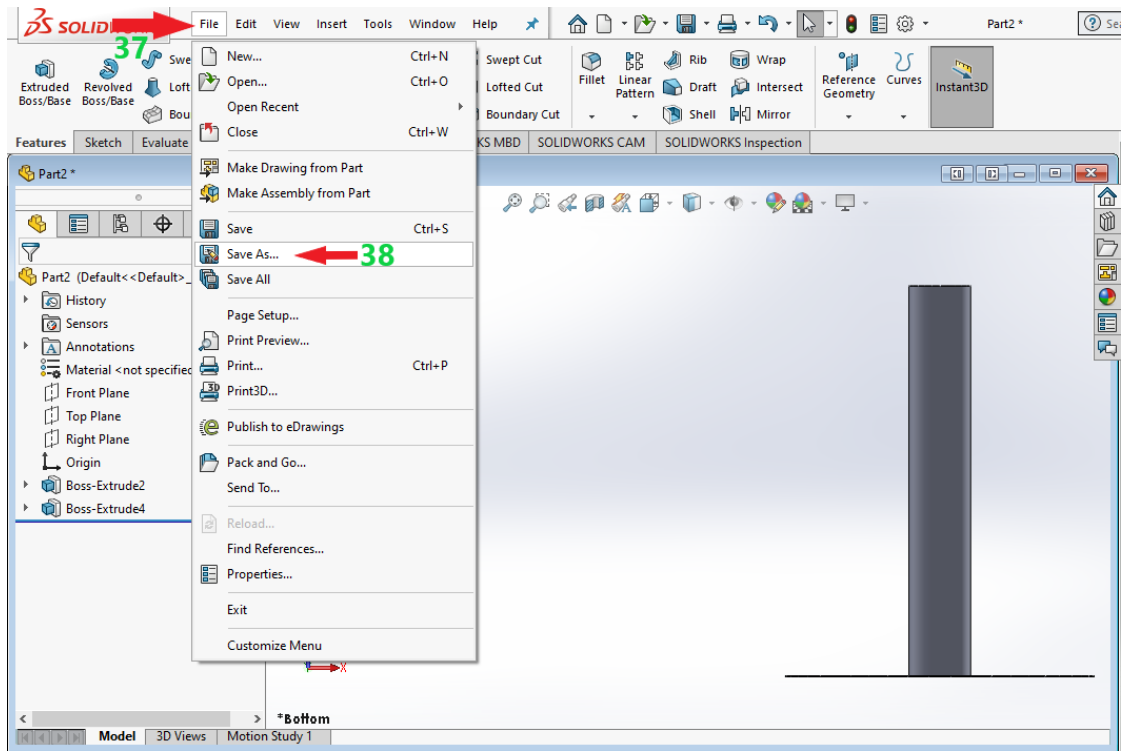
Figure 5.24: *Save As* option to save the spar-plate design
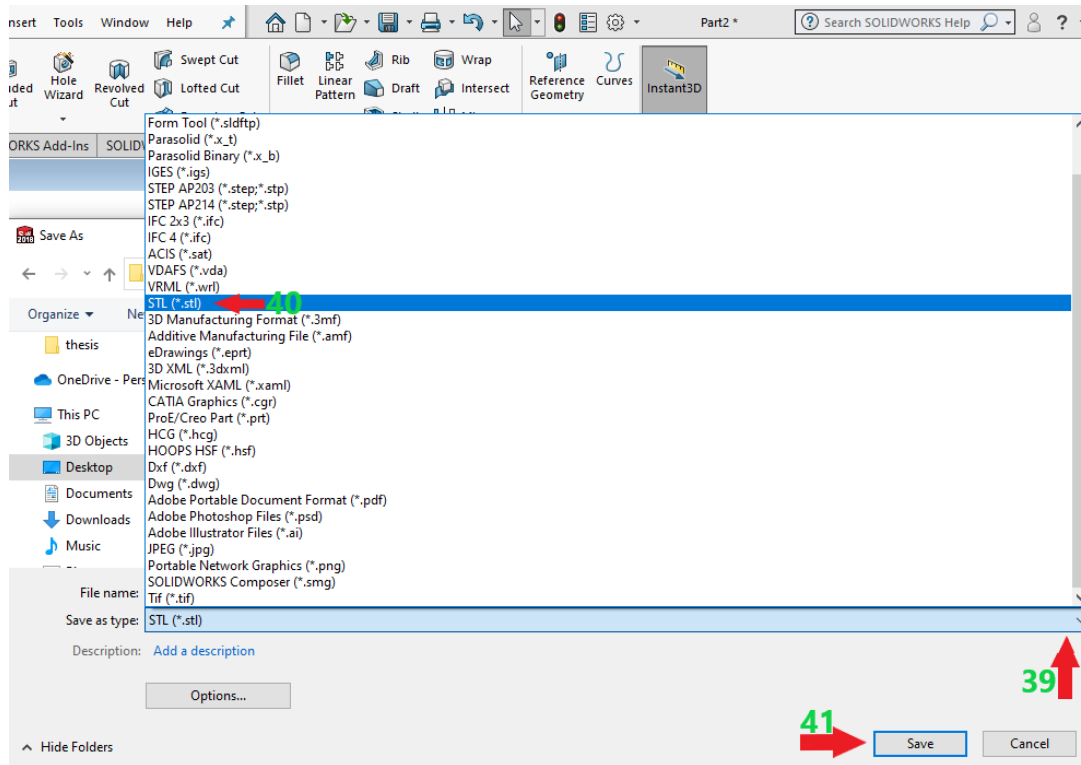
Figure 5.25: Saving the spar-plate design as an STL (*.stl) file

5.1.2 Creating *.stl File for OSWEC

The *.stl files for flap and base bodies were generated using SOLIDWORKS v2018. First, the flap and base were designed. Then, the models were saved as a *.stl file.

5.1.2.1 Designing Flap Body

After the 2BPA was designed, a new project was opened to design the flap of OSWEC (Figures 5.26 and 5.27). From the *Feature Manager Design Tree*, the *Top Plane* option was selected in which the *Sketch* option was chosen (arrow No.5 in Figure 5.28). From the *System Options – General* page, the *Document Properties* option was selected. Then, inside the *Units* page, the *MKS (meter, kilogram. second)* was chosen as the unit system for the flap (arrows 6-10 in Figure 5.29). In the first place, a rectangle was drawn with arbitrary dimensions using the *Center rectangle* option from the Sketch tab (Figure 5.30).

Next, to define the height and length of the flap, from the *Smart Dimension* option, the height and length of the flap were defined as 11 m and 2 m, respectively (Figure 5.31). Then, the X and Y coordinates of the center of the rectangle were both defined as zero (Figure 5.32). The part of the flap where the hinge is located was drawn using the *Line* option from the *Sketch* tab. Then the coordinates of the points on the part drawn were corrected (Figure 5.33). Further, the width of the

flap was defined as 26 m using _Extruded Boss/Base_ option from the _Features_ tab. Finally, the design was saved as a *.stl file (Figures 5.35, 5.36).
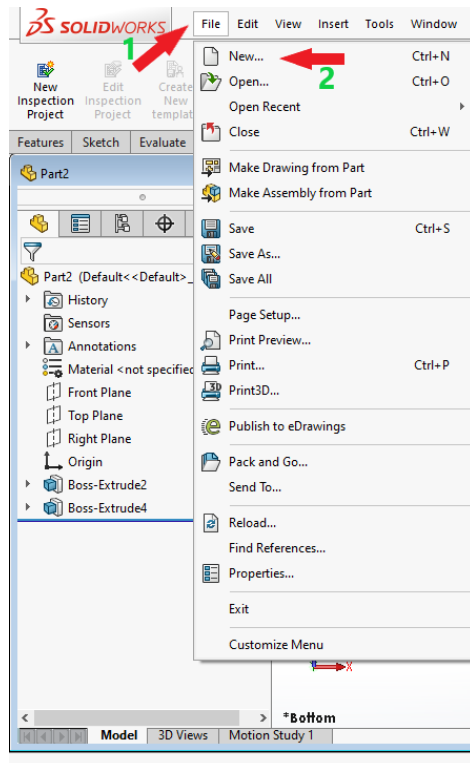
Figure 5.26: Opening a new project for designing flap in SOLIDWORKS

5. Designing 2BPA and OSWEC Using SOLIDWORKS
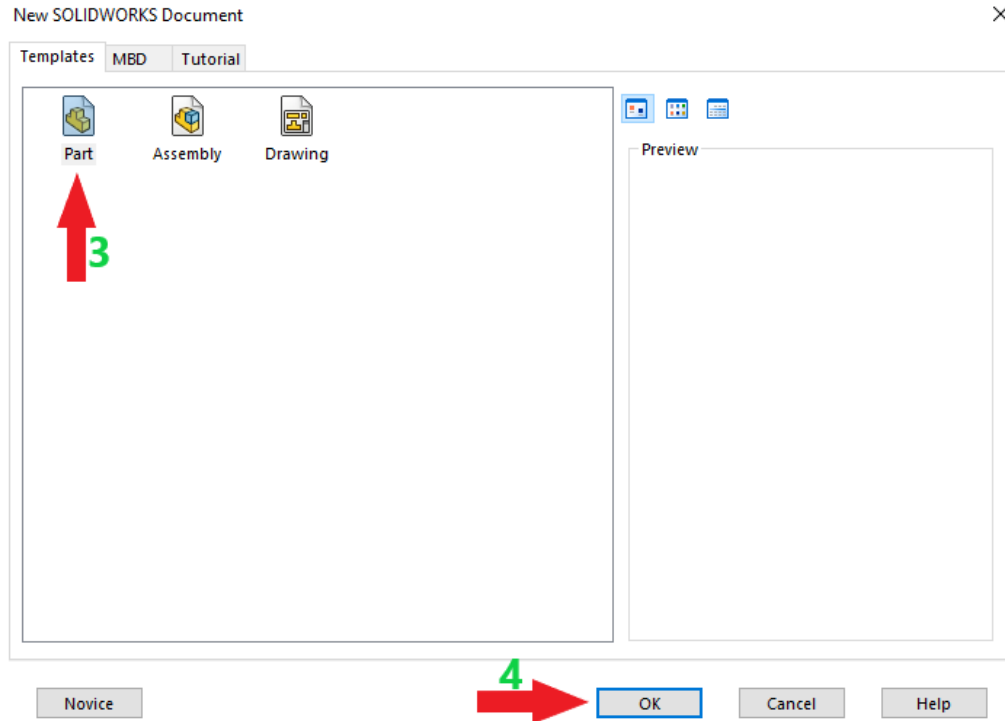
Figure 5.27: New SOLIDWORKS Document page for flap
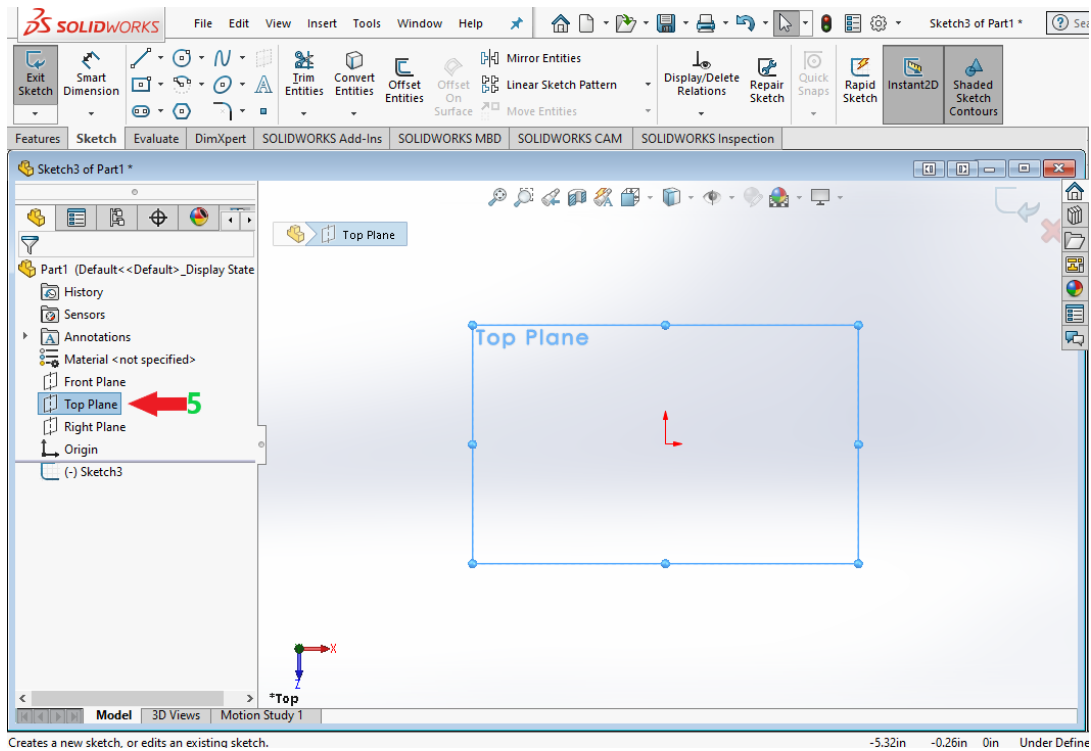
Figure 5.28: Plane selection for flap
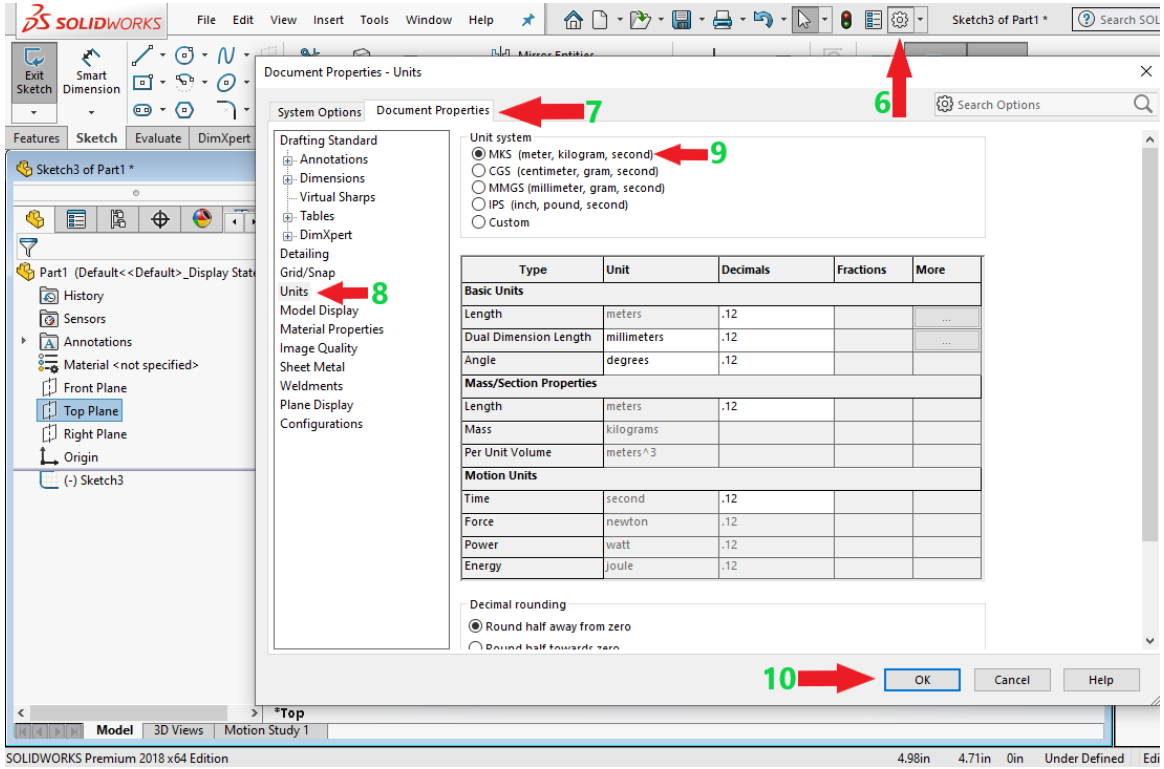
Figure 5.29: Selection of a unit system for flap
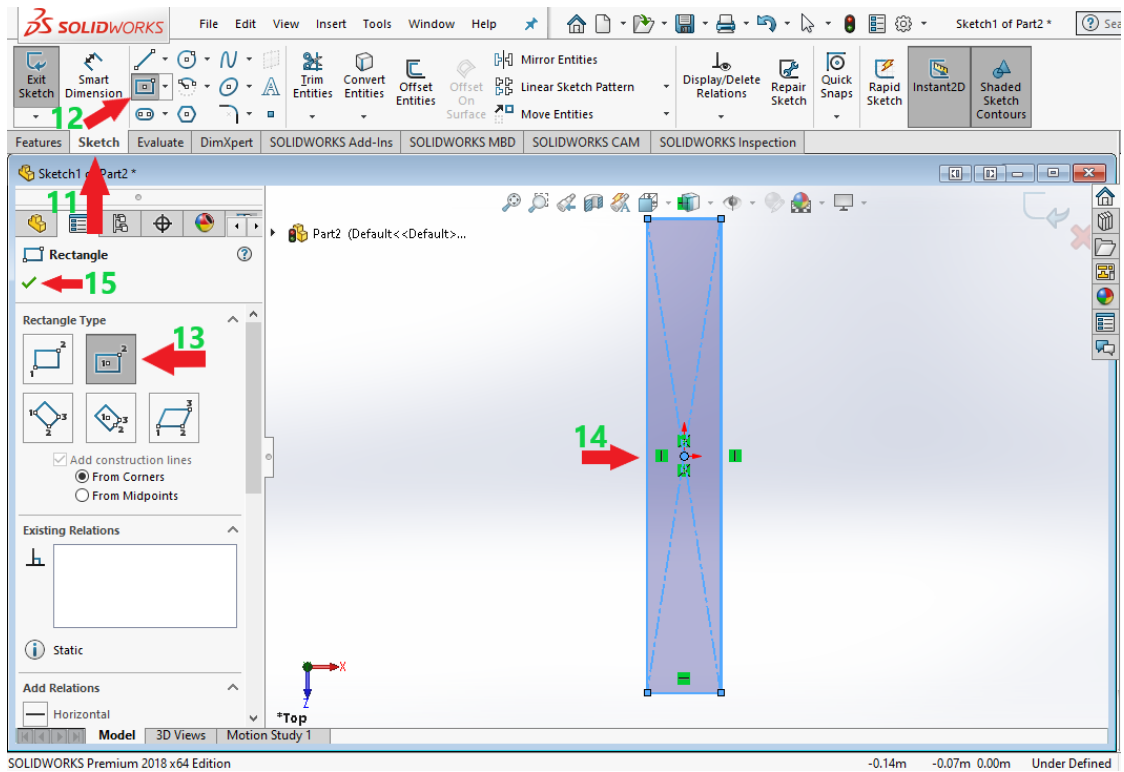
Figure 5.30: Drawing the cross-section of the flap
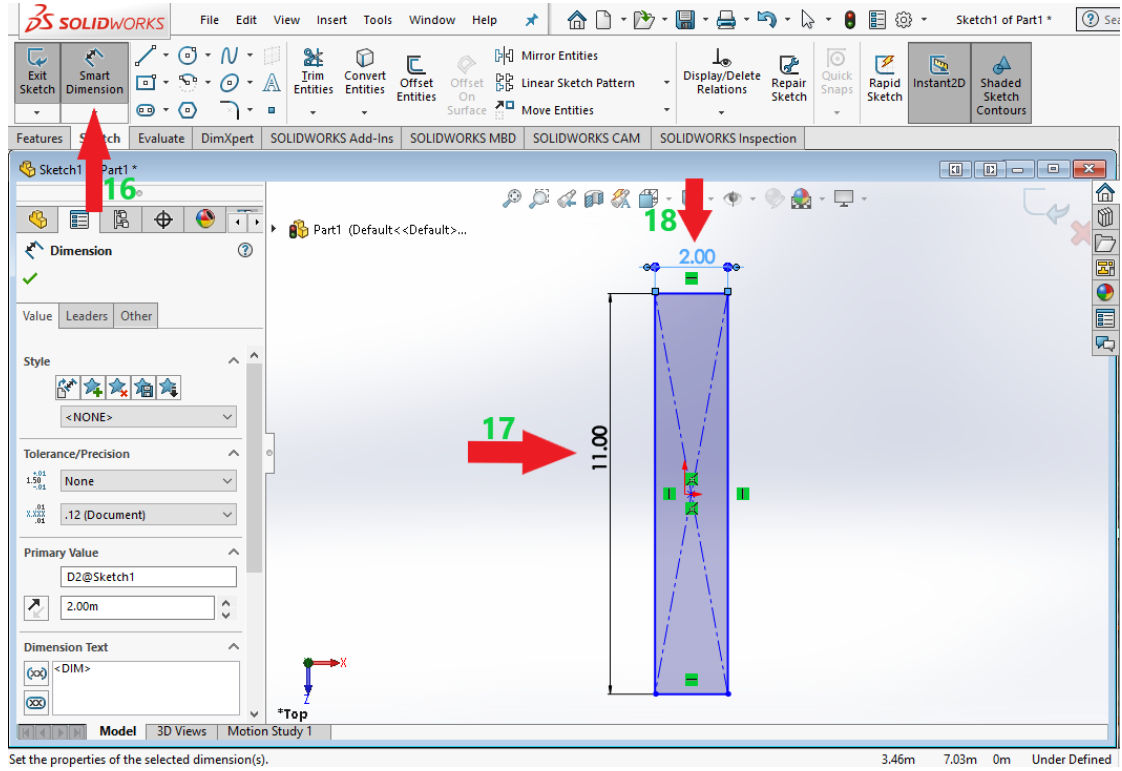
Figure 5.31: Defining the height and length of the flap
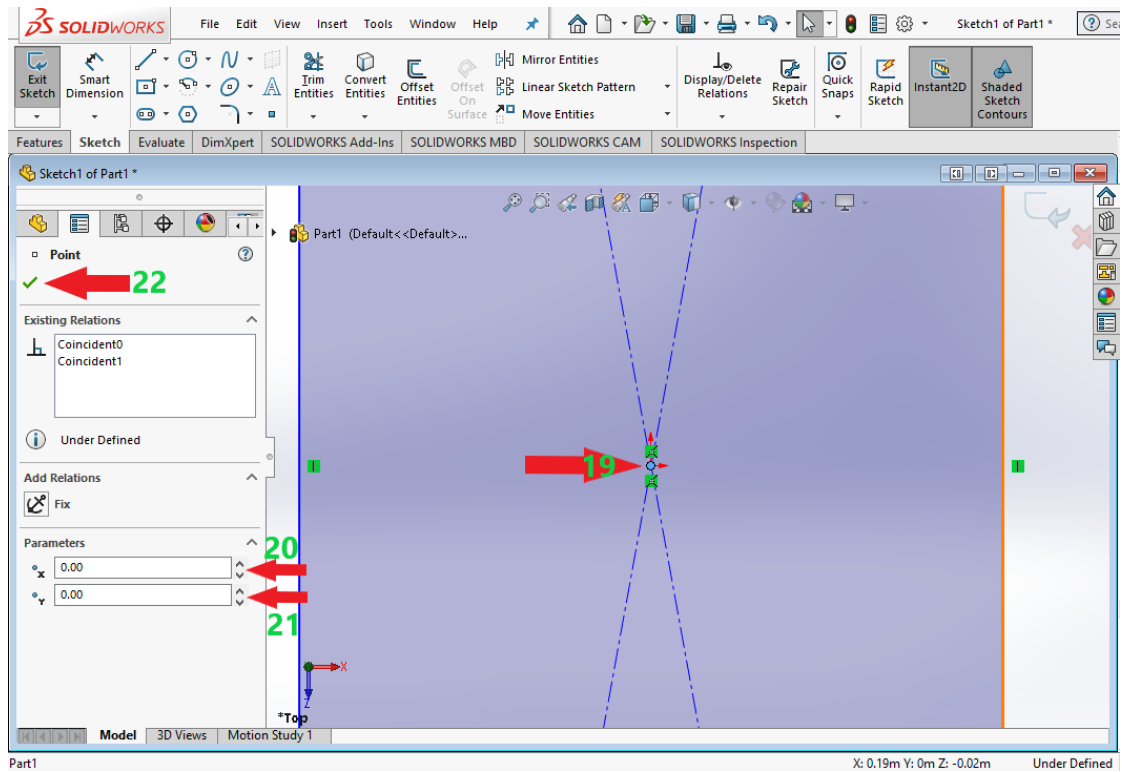
Figure 5.32: The X and Y coordinates of the center of the rectangular part of flap
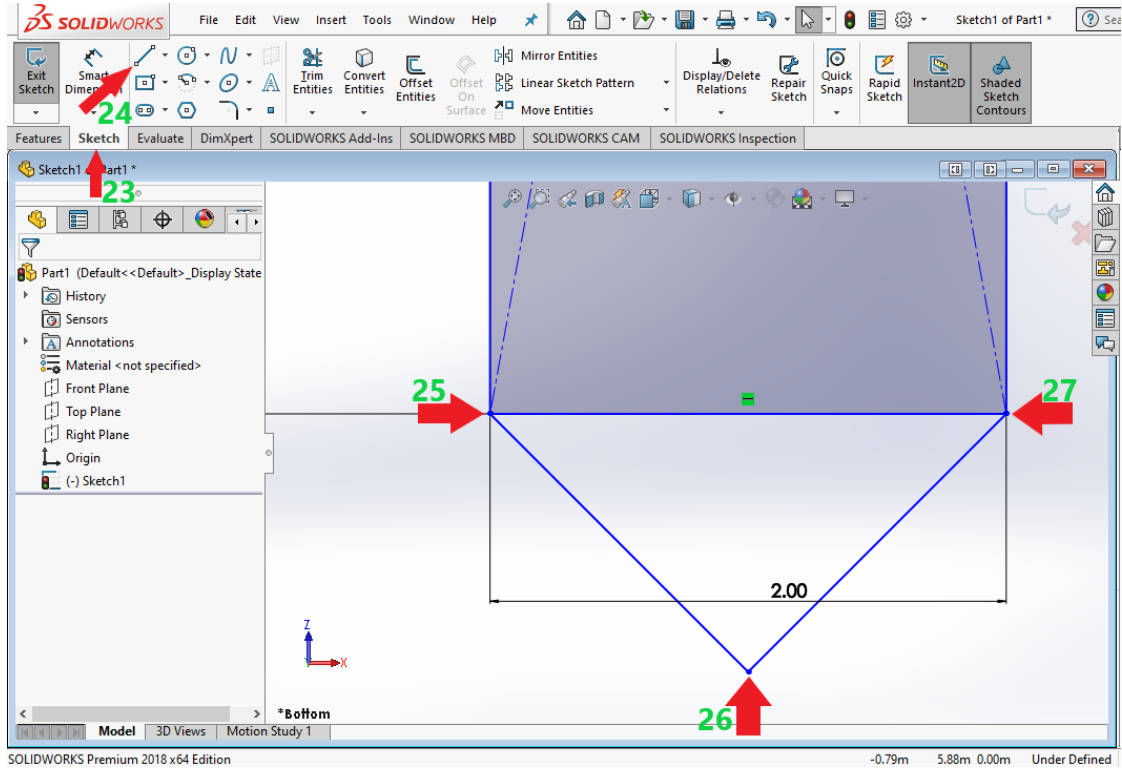
Figure 5.33: Drawing the part of the flap where the hinge is located
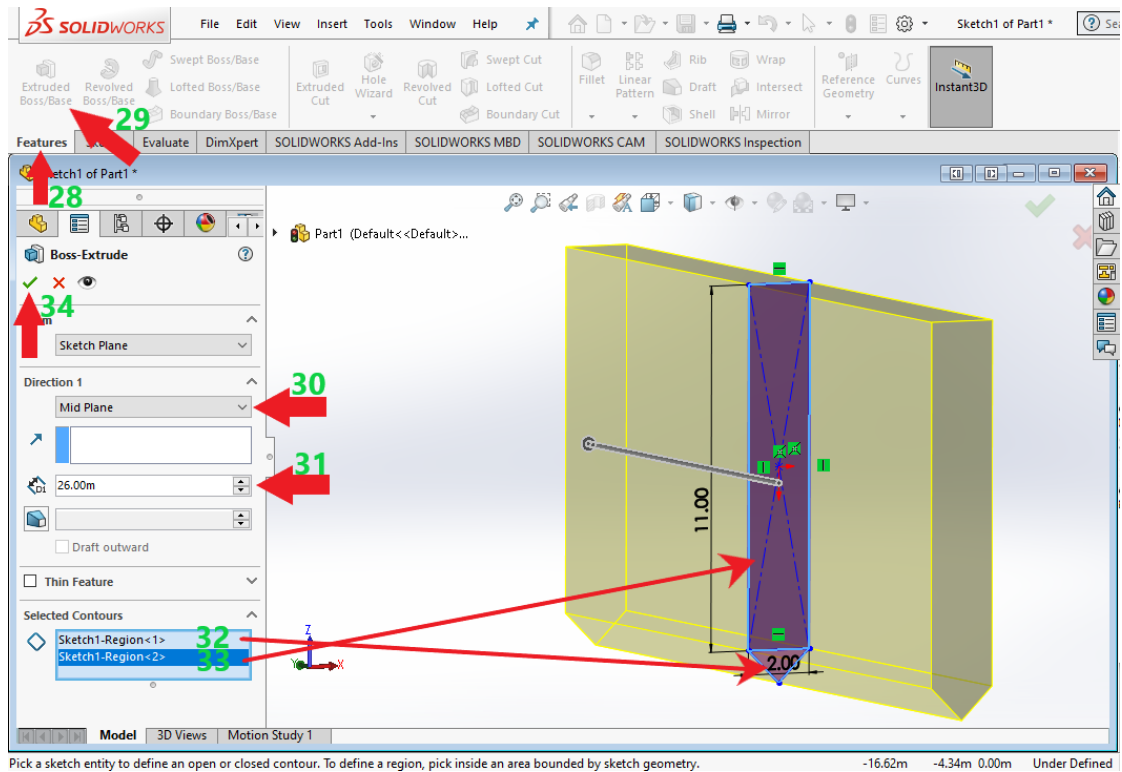
Figure 5.34: Defining the width of the flap
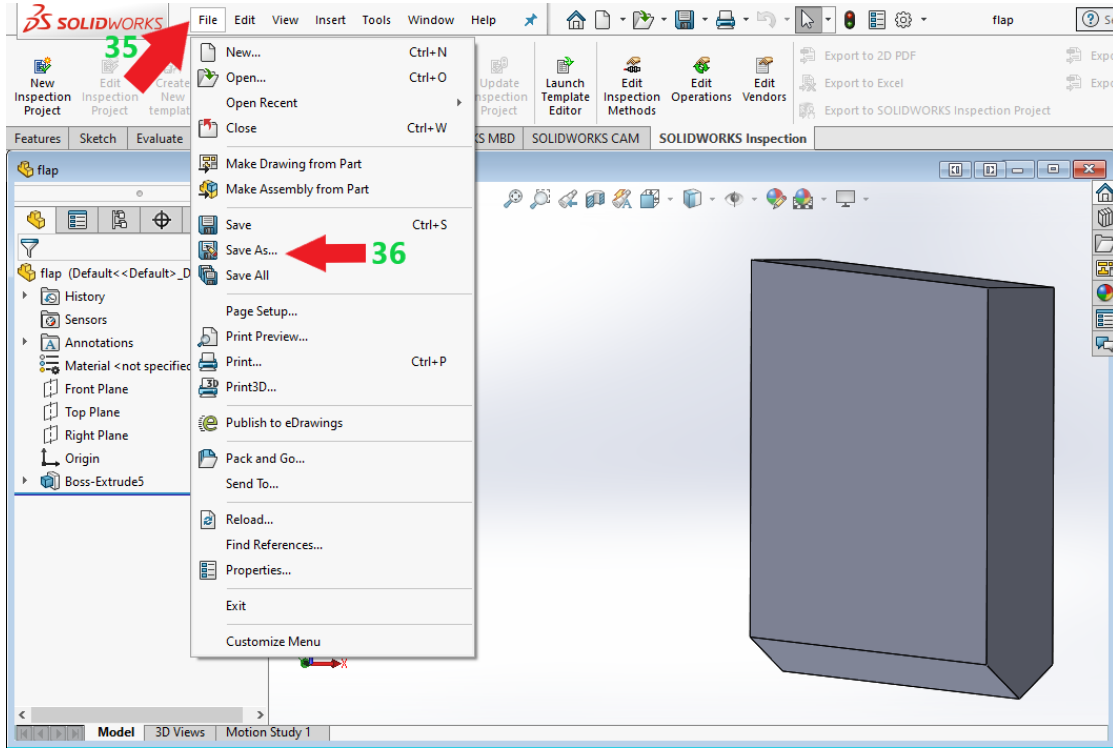
Figure 5.35: *Save As* option to save the flap design
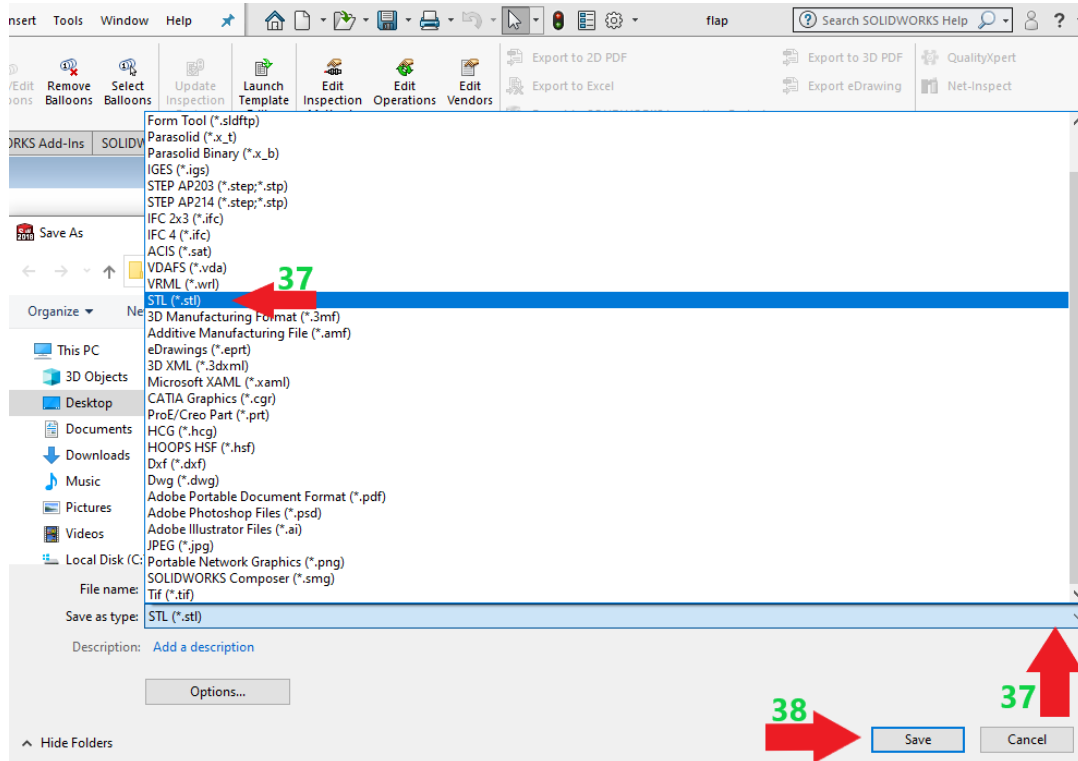
Figure 5.36: Saving the float design as an STL (*.stl) file

5.1.2.2 Designing Base Body

After the flap was designed, a new project was opened to design the base of OSWEC (Figures 5.37 and 5.38). From the *Feature Manager Design Tree*, the *Top Plane* option was selected in which the *Sketch* option was chosen (arrow No.5 in Figure 5.39). From the *System Options – General* page, the *Document Properties* option was selected. Then, inside the *Units* page, the *MKS (meter, kilogram. second)* was chosen as the unit system for the base (arrows 6-10 in Figure 5.40). In the first place, a rectangle was drawn with arbitrary dimensions using the *Center rectangle* option from the *Sketch* tab (Figure 5.41).

Next, to define the height and length of the base, from the *Smart Dimension* option, the height and length of the base were defined as 3 m and 2 m, respectively (Figure 5.42). Then, the X and Y coordinates of the center of the rectangle were both defined as zero (Figure 5.43). The part of the base where the flap is installed was drawn using the *Line* option from the *Sketch* tab. Then the coordinates of the points on the part drawn were corrected (Figure 5.44). Further, the width of the base was defined as 26 m using *Extruded Boss/Base* option from the Features tab. Finally, the design was saved as a *.stl file (Figures 5.45, 5.46).
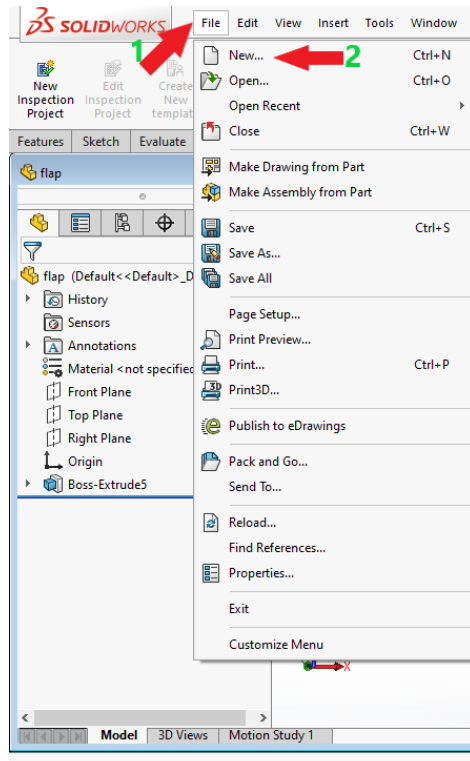
Figure 5.37: Opening a new project for designing base in SOLIDWORKS
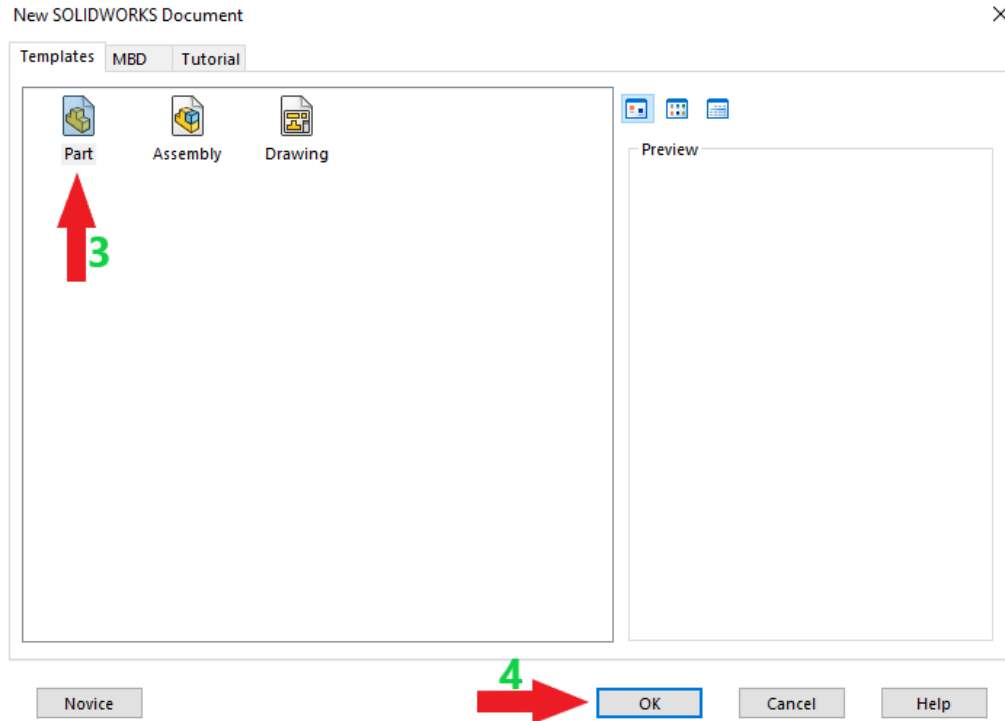
Figure 5.38: New SOLIDWORKS Document page for base
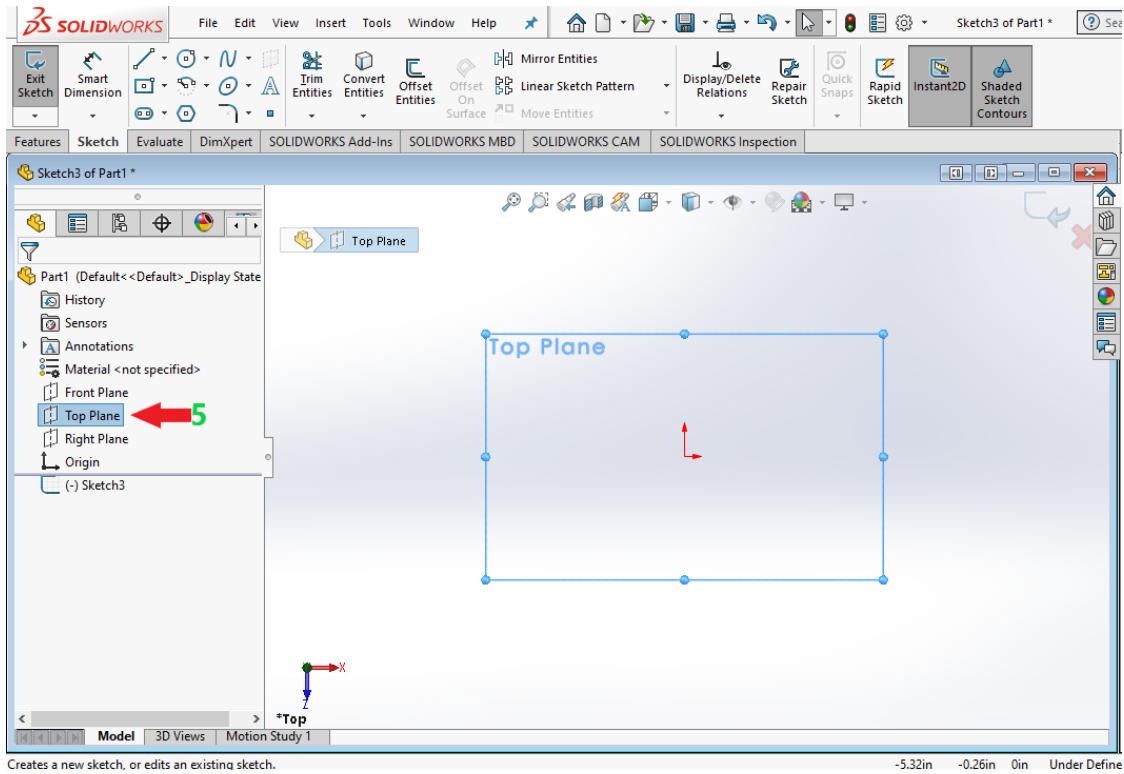
Figure 5.39: Plane selection for spar-plate
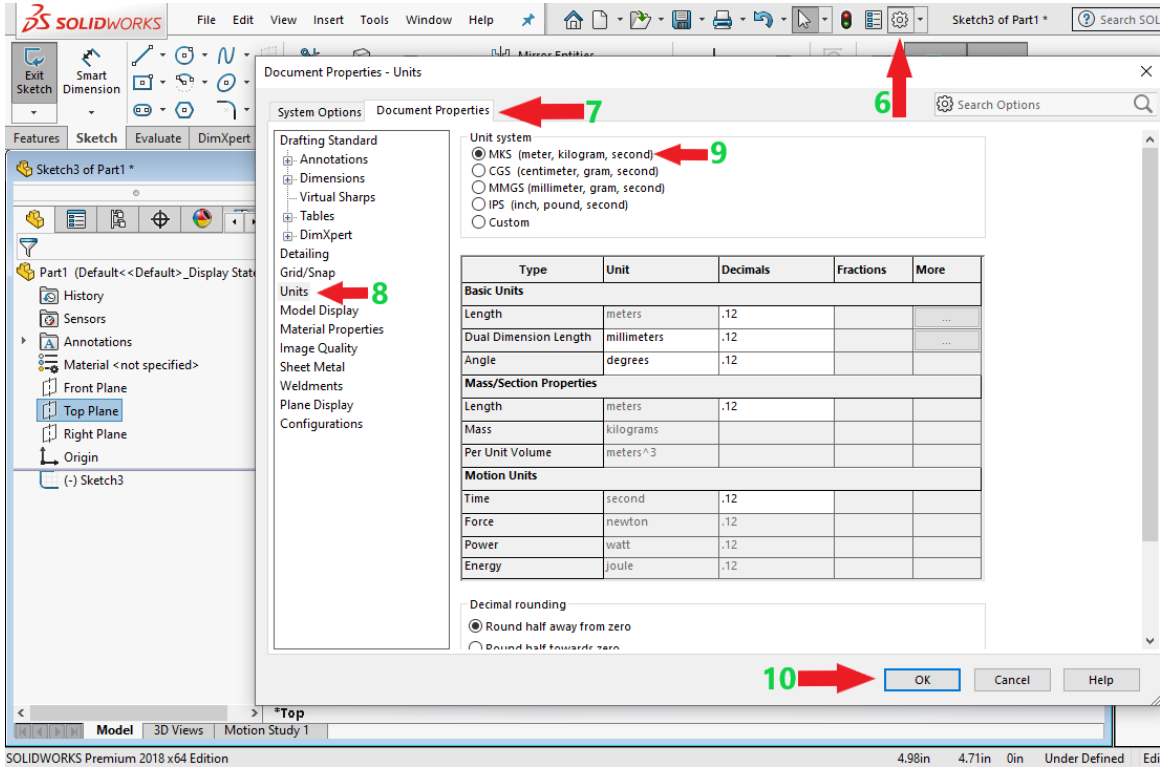
Figure 5.40: Selection of a unit system for flap
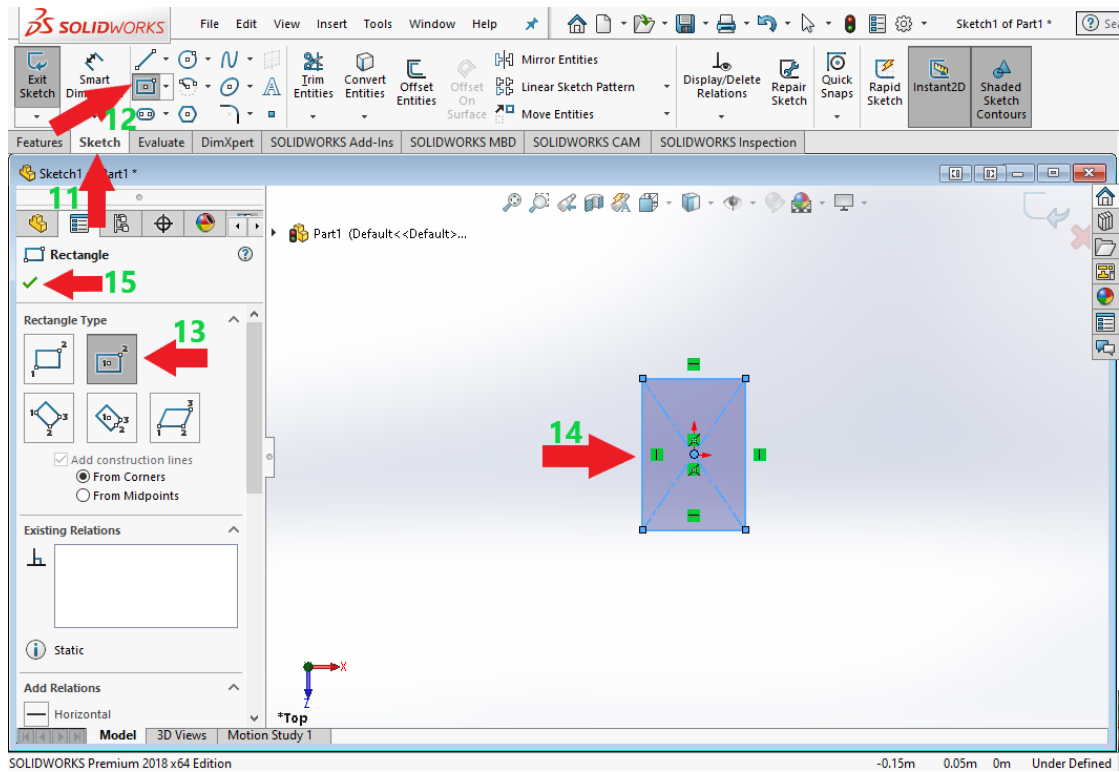
Figure 5.41: Drawing the cross-section of the base

93
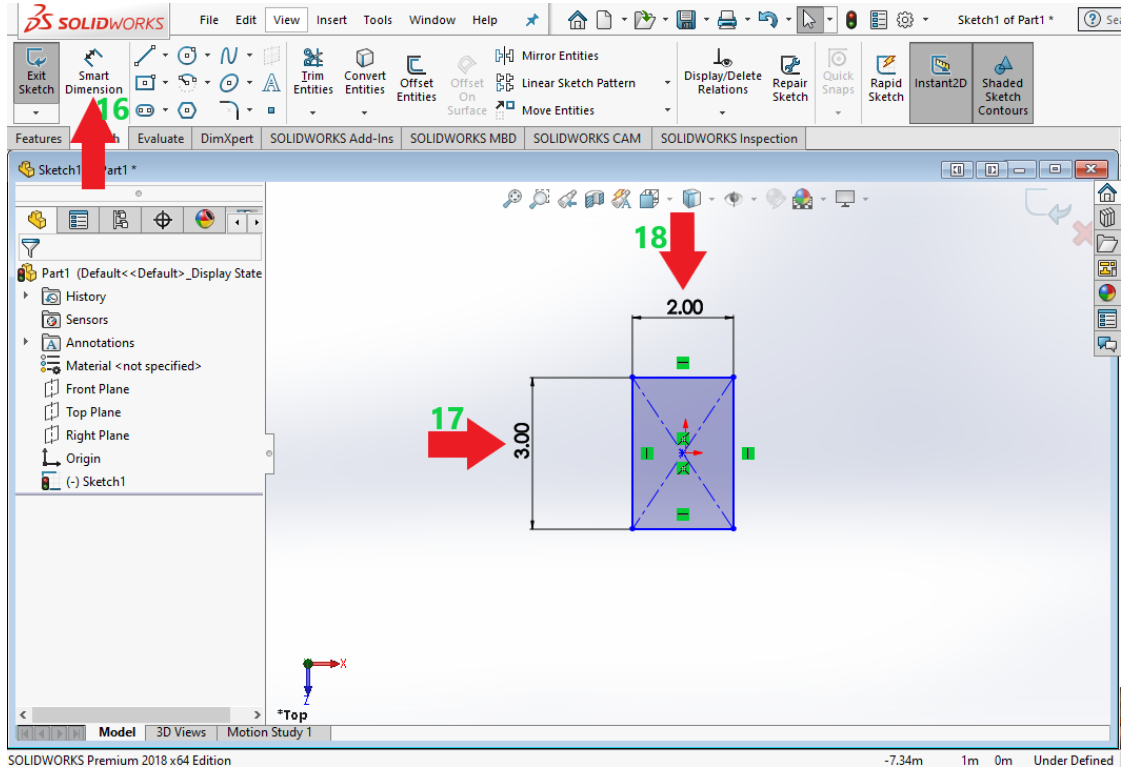
Figure 5.42: Defining the height and length of the base
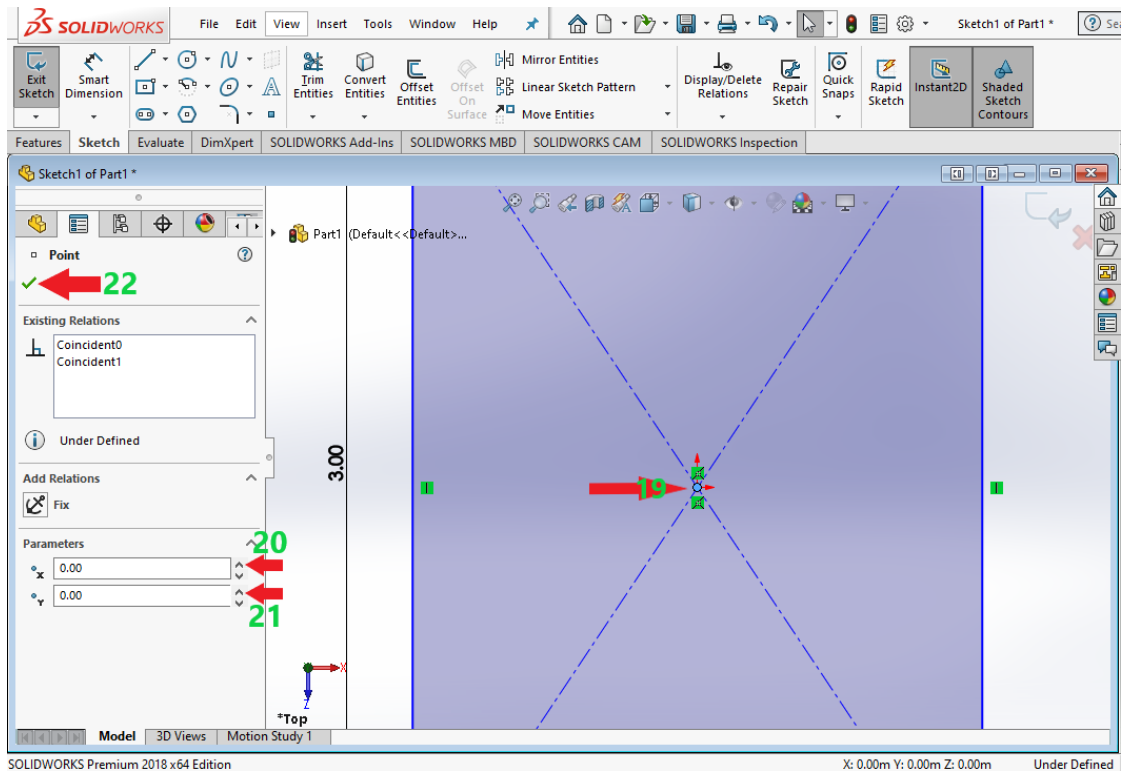
Figure 5.43: The X and Y coordinates of the center of the rectangular part of the base
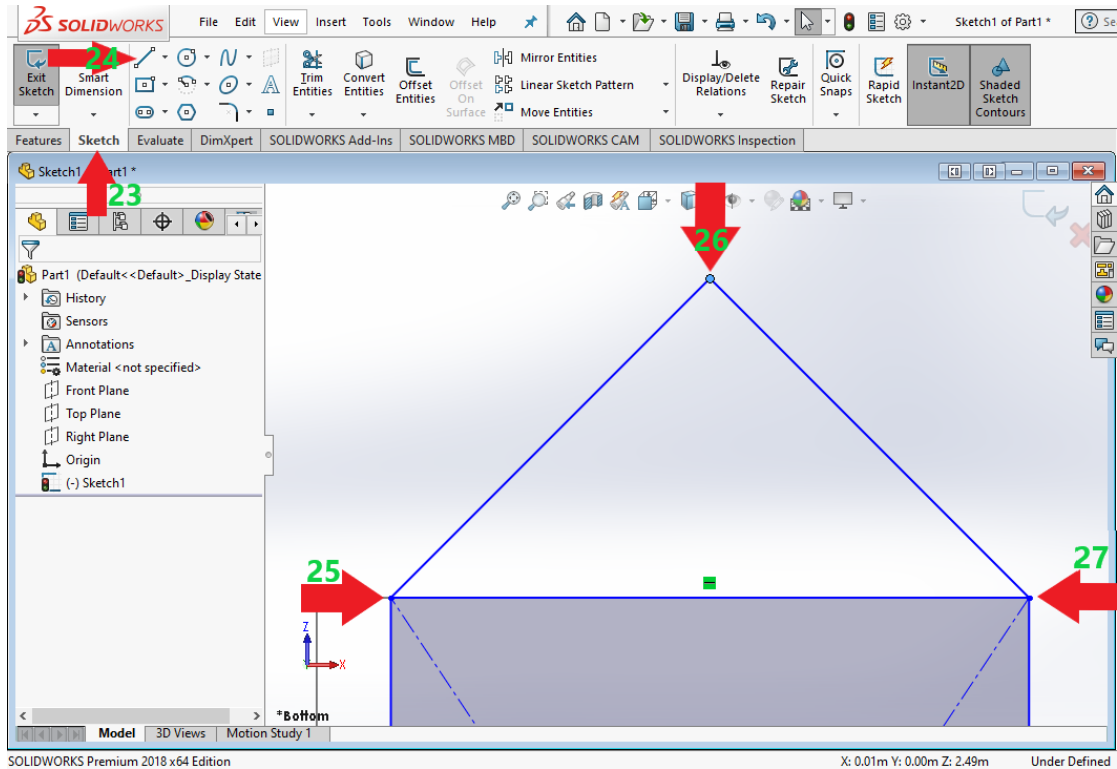
Figure 5.44: Drawing the part of the base where the flap is installed
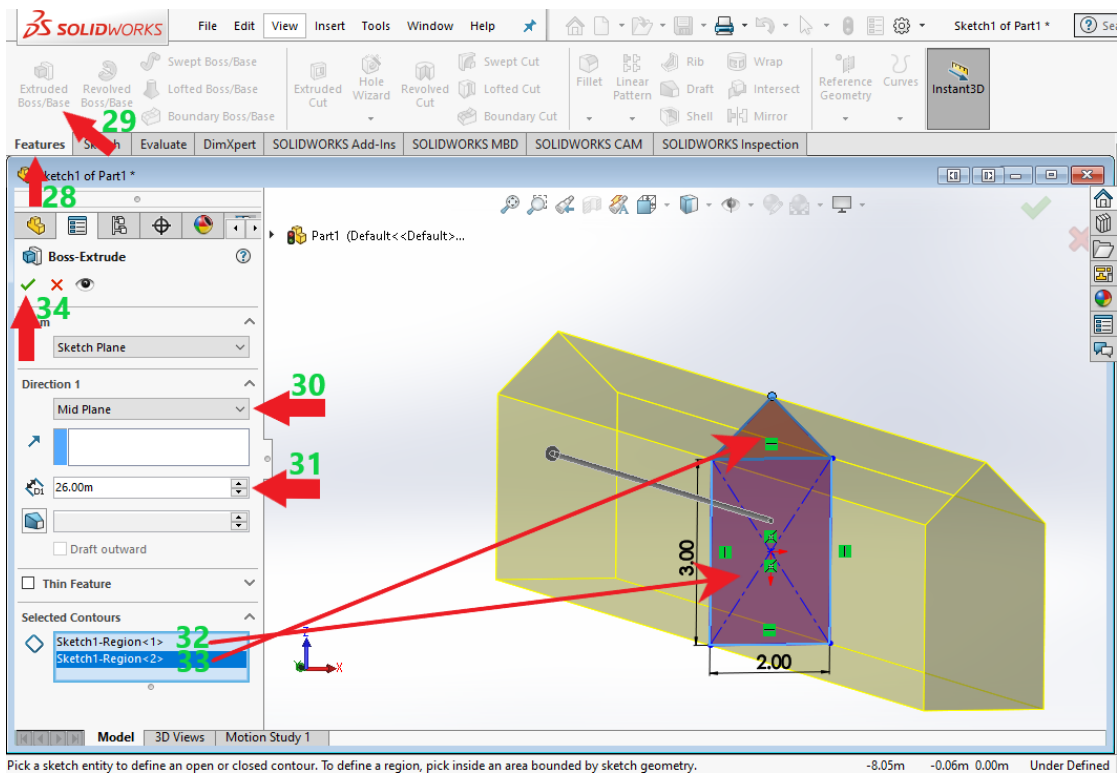
Figure 5.45: Defining the width of the base
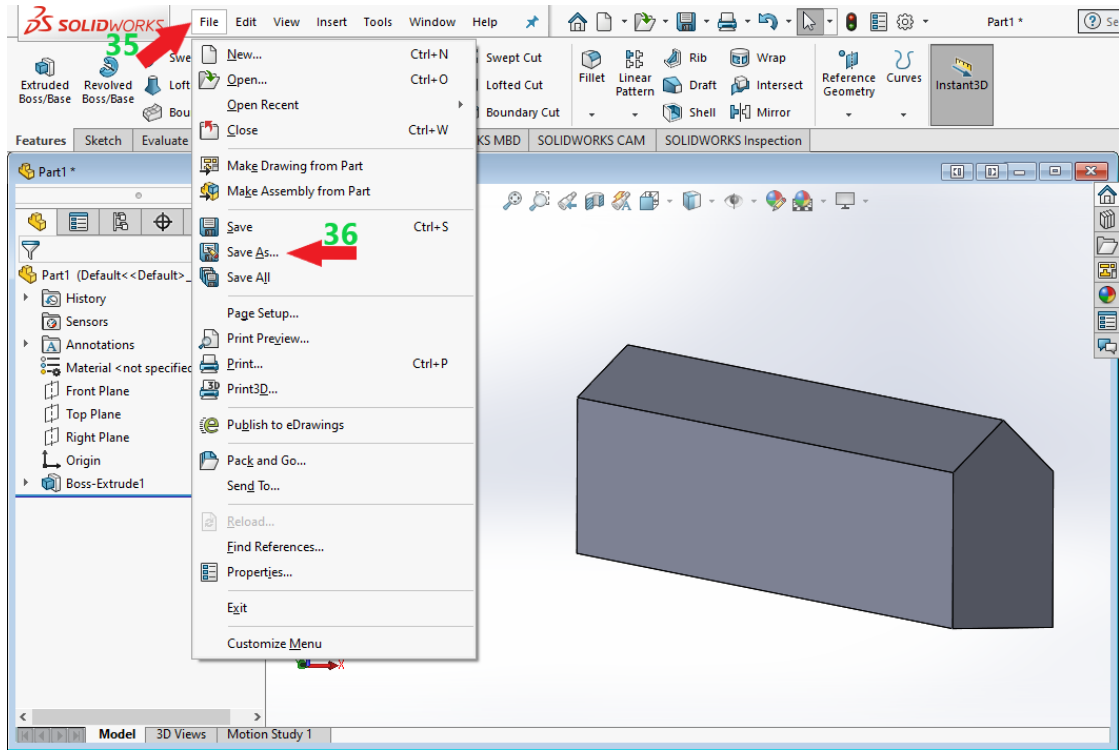
Figure 5.46: *Save As* option to save the base design
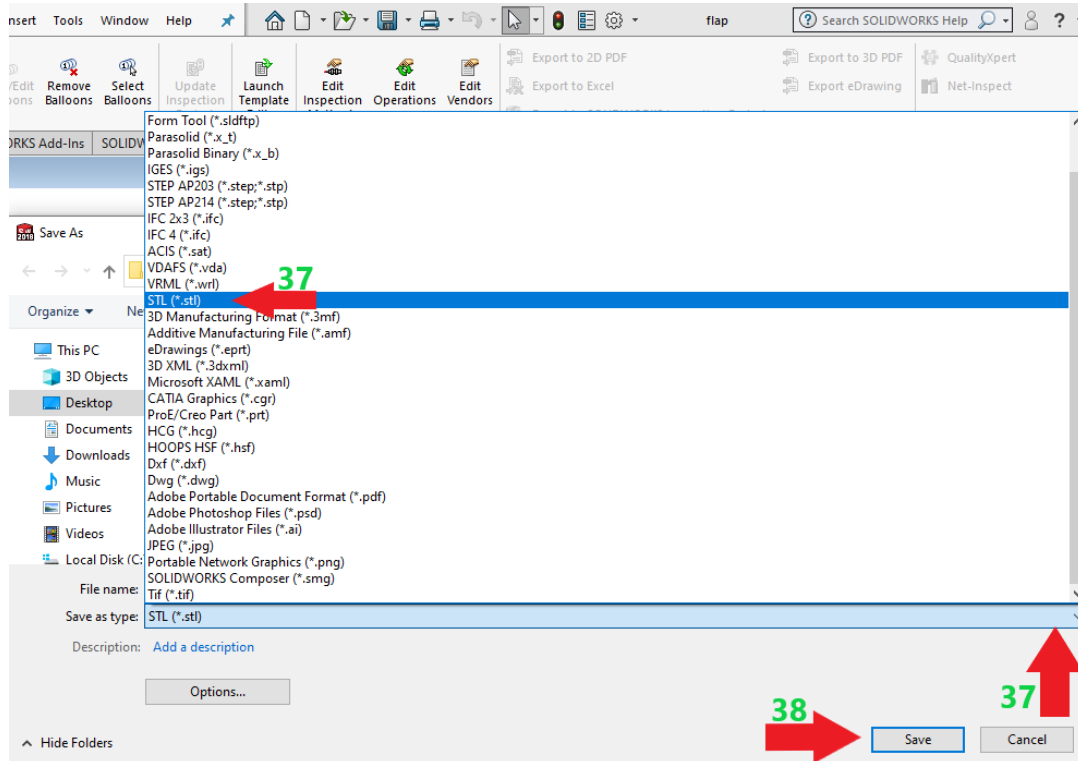
Figure 5.47: Saving the base design as an STL (*.stl) file

5.2 Scaling the 2BPA and OSWEC Designs and Defining Their COG for Visualization Purposes in WEC-Sim Using MeshMagic 3D Modeling Software: 5th Step

In WEC-Sim, the planes of SWL and sea bed have specific dimensions, making it necessary to reduce the geometry of a design to be small enough to fit into those dimensions. Hence, the WECs designed via SOLIDWORKS have to be scaled next. For scaling the WECs, MeshMagic 3D Modeling Software v 2.00 is used. The scale used in this study is 1:1000 for 2BPA and OSWEC. It is important to note that scaling is just for visualization purposes and does not affect the calculations in WEC-Sim. The MeshMagic 3D Modeling Software can be downloaded from: https://www.nchsoftware.com/meshmagic3d/index.html.

Furthermore, the COG of the 2BPA and OSWEC were defined in MeshMagic. The COG of the earlier mentioned WECs must be positioned precisely on the origin of the XYZ coordinate system in MeshMagic software. The STL files for each body obtained via SOLIDWORKS have to be opened in MeshMagic software to define each body's COG in the MeshMagic coordinate system. By correctly defining the COG of the bodies in MeshMagic, the COG points of each body can be visualized in the correct position in WEC-Sim.

For the 2BPA, first, the STL file of the float, which SOLIDWORKS previously obtained, was opened in MeshMagic. The float was scaled after the float was shown on the MeshMagic perspective view screen. In order to scale the float, the whole float body was first selected by pressing Ctrl+A bottoms on the keyboard. Then, the *Object Properties* window was opened by pressing Ctrl+P bottoms. On the opened window, in the *Scale* option, number 0.01 was entered for the X-axis, Y-axis, and Z-axis, which means that for now, the scale of the float is 1:100. We did not enter the number 0.001 that represents the scale of 1:1000 because, in the MeshMagic, we can define the 1:100 scale as a maximum scaling value for the first attempt. Hence, the float STL file was saved in MeshMagic with the 1:100 scale as the first attempt for scaling the float. Then, as for the second attempt, the float STL file was reopened in MeshMagic to further make the float size ten times smaller by entering number 0.1 for XYZ axes in the *Scale* option in the *Object Properties* window. So, by scaling float as 1:100 in the first attempt and 1:10 in the second attempt, the float was scaled as 1:1000.

On the scale of 1:1000, the COG of the float is 0.720 millimeters below the SWL. The COG of the float was positioned on the origin of the MeshMagic coordinate system by entering 0 mm, 0.220 mm, and 0 mm for X-axis, Y-axis, and Z-axis, respectively, in the *Position* option the *Object Properties* window. Finally, the *float.stl* file was saved inside the *pointabsorber* working folder.

Like float, the spar-plate was scaled to 1:1000 according to the earlier procedure. Then, the COG of the spar-plate, which is -21.29 millimeters below SWL in 1:1000 scale, was positioned on the origin of the MeshMagic coordinate system by entering 0 mm, 11.29 mm, and 0 mm for X-axis, Y-axis, and Z-axis, respectively, in the *Position* option in the *Object Properties* window. Finally, the *spar-plate.slt* file was saved inside the *pointabsorber* working folder.

For the OSWEC, the flap was scaled to 1:1000. Then, COG of the body, which is -2.74 millimeters below SWL in 1:1000 scale, was positioned on the origin of the MeshMagic coordinate system by entering 0 mm, -0.260 mm, and 0 mm for X-axis, Y-axis, and Z-axis, respectively, in the *Position* option in the *Object Properties* window. Eventually, the *flap.stl* file was saved inside the *oswec* working folder.

Like flap, the base was scaled to 1:1000. Next, the COG of the base, which is -13 millimeters below SWL in 1:1000 scale, was positioned on the origin of the MeshMagic coordinate system by entering 0 mm, 2 mm, and 0 mm for X-axis, Y-axis, and Z-axis, respectively, in the *Position* option in the *Object Properties* window. Finally, the *base.stl* file was saved inside the *oswec* working folder.

6.

Creating SIMULINK Models in *.slx Format for 2BPA and OSWEC: 6th Step

6.1 An Overview of WEC-Sim Library Blocks Within SIMULINK

Apart from the *.stl and *.h5 files, a SIMULINK *.slx file is also needed for the WEC-Sim. The SIMULINK models of 2BPA and OSWEC are created using the SIMULINK environment in MATLAB software. A SIMULINK model (*.slx) represents the WEC parts and their connections. The SIMULINK model utilizes WEC-Sim library blocks. There must be a 1-to-1 connection within the objects represented in the blocks plus the input file employed in the model represented in Simulink. The corresponding library block for 2BPA and OSWEC are Frames, Body Elements, Constraints, PTOs, and Moorings if we have any mooring lines for our WECs.

Frames library includes a single block: Global Reference Frame block. This block is assumed to be the seafloor in a model. The solver setup, global coordinates, seafloor and SWL definition, simulation period, and additional global settings are all defined by the Global Reference Frame block. The *simu* plus waves classes represented in the input file are employed by the Global Reference Frame block.

The Body Elements library contains two kinds of bodies: Flex Body and Rigid Body. Hydrodynamic bodies with additional degrees of freedom are defined by the Flex Body block. As for the Rigid Body block, it represents hydrodynamic, non-hydrodynamic, and drag bodies. The Flex Body is automatically determined by the DOF in BEM input data. The *body class* is linked with the Body Elements library.

With the Constraints library, constraint blocks are only used to represent the degree of freedom of the body, not to generate force. These constraint blocks consist of a follower (F) and a base (B). For instance, in a single body system, a constraint block limits the movement of a rigid body attached to the follower in relation to the Global Reference Frame attached to the base. The constraint class is linked to the Constraints library.

For the PTO case, for 2BPA and OSWEC, the Translational PTO and Rotational PTO blocks are used. The *pto* class is closely tied to the PTOs library. Care must be taken when connecting the base (B) and follower (F) of PTO to the correct blocks.

Finally, there are two blocks inside the Moorings library for the Mooring case: MoorDyn and MooringMatrix blocks. A MoorDyn block can represent realistic mooring systems using compiled executables and MoorDyn files. According to the position of the follower in relation to the base,

MooringMatrix applies damping and stiffness according to a 6x6 matrix. The Mooring Class is linked to the Moorings library.

6.2 The SIMULINK Model of 2BPA

The Simulink model for 2BPA is shown in Figure 6.1. A Rigid Body block was selected for each float and spar-plate body. The float was named body (1), and the spar-plate was named body (2). Then, the pto (1), constraint (1), and the global reference frame-blocks were added to the system. For 2BPA, the PTO type is translational, and the constraint is fixed. The model was saved in *.slx format inside the *pointabsorber* working folder and named *cylinder_simulink.slx*. For the moored 2BPA, the MoorDyn block is added.
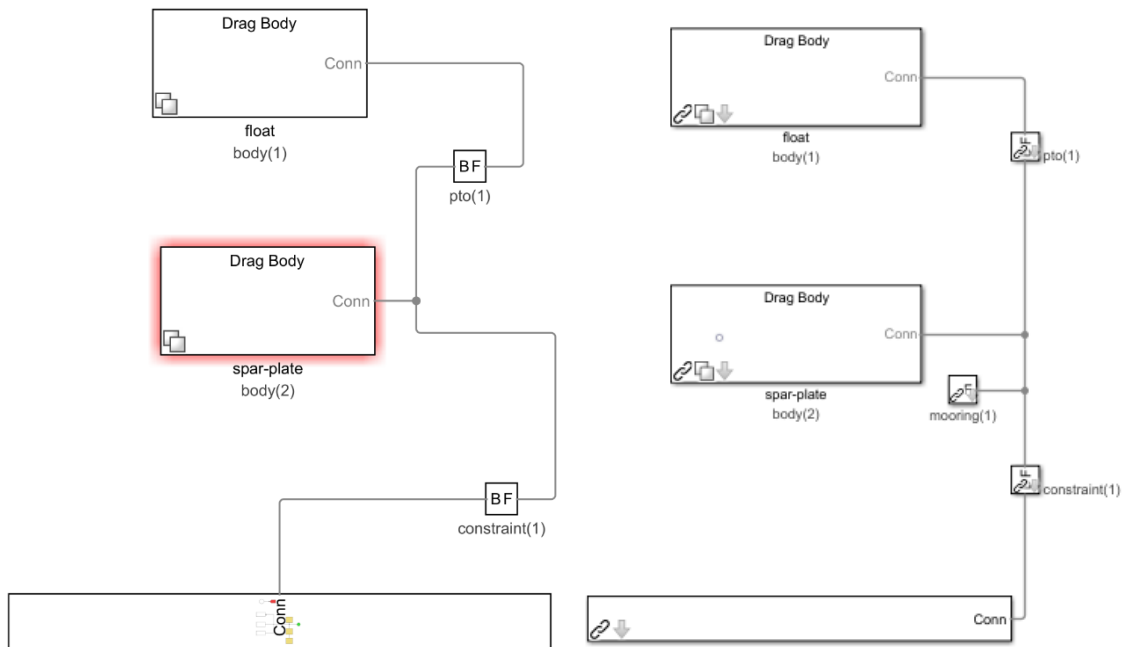
Figure 6.1: The SIMULINK models of unmoored 2BPA (left) and moored 2BPA (right)

6.3 The SIMULINK Model of OSWEC

The Simulink model for OSWEC is illustrated in Figure 6.2. A Rigid Body block was selected for each flap and the base body. The flap was named body (1), and the base was named body (2). Then, the pto (1), constraint (1), and the global reference frame-blocks were added to the system. For OSWEC, the PTO type is rotational, and the constraint is fixed. The model was saved in *.slx format inside the *oswec* working folder and named *oscilliating.slx*.
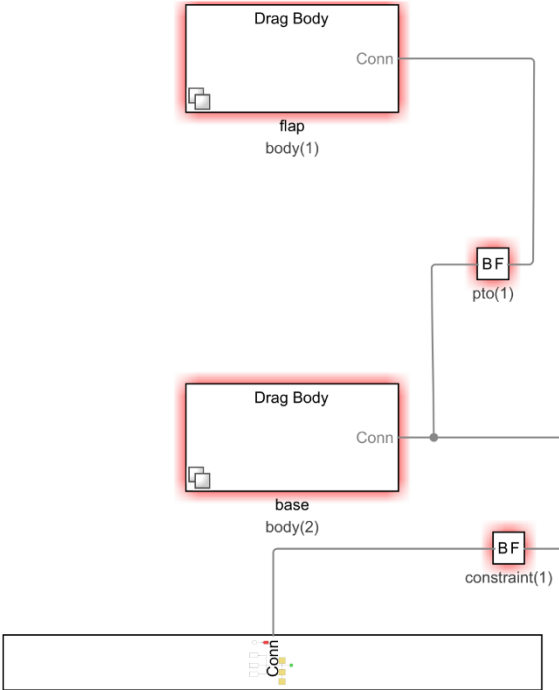
Figure 6.2: The SIMULINK model of OSWEC

7.

WEC-Sim

7.1 Defining an Input File for WEC-Sim for the 2BPA and OSWEC: 7th Step

This section defines an input file for each run for 2BPA and OSWEC. WEC-Sim input file is a MATLAB code that holds simulation data, wave information, body data, PTO and constraint parameters, and Mooring data. The earlier mentioned information is included in the simu, waves, body(i), pto(i), constraint(i), and mooring(i) classes. The interaction between these classes is carried out by wecSimInputFile.m. This file must not be renamed.

7.1.1 WEC-Sim Input File for Unmoored 2BPA

Script 7.1 is the WEC-Sim input file for unmoored 2BPA. The SIMULINK model of unmoored 2BPA, hydrodynamic data in *.h5 format, geometry file of float and spar-plate, and moment of inertia of float and spar-plate are included in this input file. The masses of float and spar-pale are defined equilibrium which means that the masses of the bodies are assumed to be the same as their displaced water. The ode4 solver is selected for fixed-step calculation. The PTO stiffness and damping coefficients are set to $0 \ N/m$ and $1200000 \ N.m/s$, respectively. Finally, the code was saved as *wecSimInputFile.m* inside the *pointabsorber* working folder. It is essential to mention that since there were irregular frequencies in the hydrodynamic coefficients obtained for 2BPA, the Convolution Integral Calculator (CIC) has to be utilized (see line 23 of Script 7.1) to neglect the irregular frequencies and continue the simulation. Otherwise, while running the WEC-Sim for 2BPA, the user will face the following error indicated in Script 7.2 in specific wave state, which can create resonance phenomena.

```
1  %% Simulation Data
2  simu = simulationClass();          % Initialize Simulation Class
3  simu.simMechanicsFile = 'cylinder_simulink.slx'; % Specify Simulink Model
4  File
5  simu.mode = 'normal';              % Specify Simulation Mode
6  ('normal','accelerator','rapid-accelerator')
7  simu.explorer='on';                % Turn SimMechanics Explorer (on/off)
8  simu.startTime = 0;                % Simulation Start Time [s]
```

```
 9   simu.rampTime =100;                % Wave Ramp Time [s]
10   simu.endTime=400;                  % Simulation End Time [s]
11
12   simu.solver = 'ode4';              % simu.solver = 'ode4' for fixed step &
13   simu.solver = 'ode45' for variable step
14   simu.dt = 0.1;                     % Simulation time-step [s]
15   %% Wave Information
16   % % noWaveCIC, no waves with radiation CIC
17   % waves = waveClass('noWaveCIC'); % Initialize Wave Class and Specify Type
18
19   % Regular Waves
20   %waves = waveClass('regular');    % Initialize Wave Class and Specify Type
21   %waves.H =5;                      % Wave Height [m]
22   %waves.T =5;                      % Wave Period [s]
23
24   % % Regular Waves with CIC
25   waves = waveClass('regularCIC');  % Initialize Wave Class and Specify Type
26   waves.H =5;                       % Wave Height [m]
27   waves.T =7.5;                     % Wave Period [s]
28
29   % % Irregular Waves using PM Spectrum
30    %waves = waveClass('irregular'); % Initialize Wave Class and Specify Type
31    %waves.H =8;                     % Significant Wave Height [m]
32    %waves.T =11;                    % Peak Period [s]
33    %waves.spectrumType = 'PM';      % Specify Wave Spectrum Type
34
35   % % Irregular Waves using JS Spectrum with Equal Energy and Seeded Phase
36   % waves = waveClass('irregular'); % Initialize Wave Class and Specify Type
37   % waves.H = ;                     % Significant Wave Height [m]
38   % waves.T = ;                     % Peak Period [s]
39   % waves.spectrumType = 'JS';      % Specify Wave Spectrum Type
40   % waves.freqDisc = 'EqualEnergy'; % Uses 'EqualEnergy' bins (default)
41   % waves.phaseSeed = 1;            % Phase is seeded so eta is the same
42
43   % % Irregular Waves using PM Spectrum with Traditional and State Space
44   % waves = waveClass('irregular'); % Initialize Wave Class and Specify Type
45   % waves.H = ;                     % Significant Wave Height [m]
46   % waves.T = ;                     % Peak Period [s]
47   % waves.spectrumType = 'PM';      % Specify Wave Spectrum Type
48   % simu.ssCalc = 1;                % Turn on State Space
49   % waves.freqDisc = 'Traditional'; % Uses 1000 frequnecies
50
51   % % Irregular Waves with imported spectrum
52   % waves = waveClass('spectrumImport');   % Create the Wave Variable and
53   Specify Type
54   % waves.spectrumDataFile = 'spectrumData.mat'; %Name of User-Defined Spectrum
55   File [:,2] = [f, Sf]
56
57   % % Waves with imported wave elevation time-history
58   % waves = waveClass('etaImport');    % Create the Wave Variable and Specify
59   Type
60   % waves.etaDataFile = 'etaData.mat'; % Name of User-Defined Time-Series File
61   [:,2] = [time, eta]
62
63   %% Body Data
64   % Float
65   body(1) = bodyClass('pointabsorber.h5');
```

```
66      %Create the body(1) Variable, Set Location of Hydrodynamic Data File
67      %and Body Number Within this File.
68   body(1).geometryFile = 'C:\Users\Babak Shafiei\Documents\MATLAB\cccc\matlab
69   routines\pointabsorber\float.stl';     % Location of Geomtry File
70   body(1).mass = 'equilibrium';
71      %Body Mass. The 'equilibrium' Option Sets it to the Displaced Water
72      %Weight.
73   body(1).momOfInertia = [20907301 21306091 37085481];  %Moment of Inertia
74   [kg*m^2]
75
76   % Spar/Plate
77   body(2) = bodyClass('pointabsorber.h5');
78   body(2).geometryFile = 'C:\Users\Babak Shafiei\Documents\MATLAB\cccc\matlab
79   routines\pointabsorber\spar-plate.stl';
80   body(2).mass = 'equilibrium';
81   body(2).momOfInertia = [94419615 94407091 28542225];
82
83   %% PTO and Constraint Parameters
84   % Floating (3DOF) Joint
85   constraint(1) = constraintClass('Constraint1'); % Initialize Constraint Class
86   for Constraint1
87   constraint(1).loc = [0 0 0];                      % Constraint Location [m]
88
89   %Translational PTO
90   pto(1) = ptoClass('PTO1');                        % Initialize PTO Class for
91   PTO1
92   pto(1).k = 0;                                     % PTO Stiffness [N/m]
93   pto(1).c = 1200000;                               % PTO Damping [N/(m/s)]
94   pto(1).loc = [0 0 0];                             % PTO Location [m]
```

Script 7.1: WEC-Sim input file for unmoored 2BPA

```
1    Error using wecSim (line 312)
2    ['cylinder_simulink/Global Reference Frame/Solver Configuration']: Error
3    evaluating equations
4    at time 392.90000000000003.  Stopping simulation.  There may be a singularity
5    in the solution.
6    If not, try reducing the step size (either by reducing the fixed step size or
7    by tightening the
8    error tolerances)
9    Caused by:
10       Error using wecSim (line 312)
11       ['cylinder_simulink/Floating (3DOF)/CONSTRAINT (Planar Joint)']:
12       'cylinder_simulink/Floating (3DOF)/CONSTRAINT (Planar Joint)' has a
13   degenerate mass distribution on its follower side.
```

Script 7.2: Error using WEC-Sim

The user input MATLAB file for post processing is called *userDefinedFunctions.m*. This file plots the responses and forces of a WEC subjected to any wave condition predefined in the WEC-

Sim input file. For unmoored 2BPA, the MATLAB code of user-defined functions is given in Script 7.3.

```matlab
1    %Example of user input MATLAB file for post processing
2    close all
3
4    %Plot waves
5    waves.plotEta(simu.rampTime);
6    grid on
7    try
8        waves.plotSpectrum();
9
10   catch
11   end
12
13   tout=0:0.1:400;
14   %plot surge (x) force for body 1
15   plotForces(output,1,1)
16   grid on
17   ylabel('Force (N)')
18
19
20   %plot heave (z) force for body 1
21   plotForces(output,1,3)
22   grid on
23   ylabel('Force (N)')
24
25
26   %plot pitch (Ry) force for body 1
27   plotForces(output,1,5)
28   grid on
29   ylabel('Torque (N*m)')
30
31
32   %Plot surge (x) response for body 1
33   output.plotResponse(1,1);
34   grid on
35   ylabel('m, m/s, m/s^2')
36
37
38   %plot heave (z) response for body 1
39   output.plotResponse(1,3);
40   grid on
41   ylabel('m, m/s, m/s^2')
42
43
44   %plot pitch (Ry) response for body 1
45   a1=output.bodies(1).position(:,5);
46   a2=(180/pi).*a1;
47   b1=output.bodies(1).velocity(:,5);
48   b2=(180/pi).*b1;
49   c1=output.bodies(1).acceleration(:,5);
50   c2=(180/pi).*c1;
51   figure
52   plot(tout,a2,'blue',tout,b2,'green',tout,c2,'red')
53   grid on
```

```
54    xlabel('Time (s)')
55    ylabel('deg, deg/s, deg/s^2')
56    title('body1 (float) Pitch Response')
57    legend
58
59
60    %plot surge (x) force for body 2
61    plotForces(output,2,1)
62    grid on
63    ylabel('Force (N)')
64
65
66    %plot heave (z) force for body 2
67    plotForces(output,2,3)
68    grid on
69    ylabel('Force (N)')
70
71
72    %plot pitch (Ry) force for body 2
73    plotForces(output,2,5)
74    grid on
75    ylabel('Torque (N*m)')
76
77
78    %Plot surge (x) response for body 2
79    output.plotResponse(2,1);
80    grid on
81    ylabel('m, m/s, m/s^2')
82
83
84
85    %plot heave (z) response for body 2
86    output.plotResponse(2,3);
87    grid on
88    ylabel('m, m/s, m/s^2')
89
90
91    %plot pitch (Ry) response for body 2
92    aa1=output.bodies(2).position(:,5);
93    aa2=(180/pi)*aa1;
94    bb1=output.bodies(2).velocity(:,5);
95    bb2=(180/pi).*bb1;
96    cc1=output.bodies(2).acceleration(:,5);
97    cc2=(180/pi).*cc1;
98    figure
99    plot(tout,a2,'blue',tout,b2,'green',tout,c2,'red')
100   grid on
101   xlabel('Time (s)')
102   ylabel('deg, deg/s, deg/s^2')
103   title('body2 (spar) Pitch Response')
104   legend
105
106
107
108   %plot WEC mechanical and electerical power
109   ref=output.ptos.forceInternalMechanics(:,3);  %PTO reaction force (applied
110   from the PTO to the body)
```

```
111   f=-1*ref; %PTO force (applied from the body to the PTO)
112   pm=(output.ptos.velocity(:,3).*f)/1000; %PTO power (kwatt)
113   figure
114   plot(tout,pm);
115   grid on
116   xlabel('Time (s)')
117   ylabel('Power (kW)')
118   title('Mechanical power')
119   pmmax=max(pm);     %Maximum power (kwatt)
120   pmmean=mean(pm);
121   pe=pm*0.8;
122   pemax=max(pe);
123   pemean=mean(pe);
124   figure
125   plot(tout,pe);
126   grid on
127   xlabel('Time (s)')
128   ylabel('Power (kW)')
129   title('Electrical power')
130
131   %plot Relative displacement of float/spar-plate and wave elevation
132   etha=output.wave.elevation(:,1);
133   X1=-0.72-output.bodies(1).position(:,3);
134   X2=-21.29-output.bodies(2).position(:,3);
135   X3=X1-X2;
136   x3max=max(X3);
137   figure
138   plot(tout,X3,tout,etha)
139   grid on
140   xlabel('Time (s)')
141   ylabel('Displacement & Elevation (m)')
142   legend
```

Script 7.3: User defined functions for unmoored 2BPA

7.1.2 WEC-Sim Input File for Moored 2BPA

Script 7.4 is the WEC-Sim input file, and Script 7.5 is the user-defined function for moored 2BPA. As previously mentioned in Section 7.1.1, the Convolution Integral Calculator (CIC) has to be utilized (see line 22 of Script 7.4) to neglect the irregular frequencies seen previously after obtaining the hydrodynamic coefficients of the 2BPA.

```
1   %% Simulation Data
2   simu = simulationClass();
3   simu.simMechanicsFile = 'RM3MoorDyn.slx'; % Location of Simulink Model File
4   with MoorDyn
5   simu.mode='accelerator';
6   simu.explorer = 'off';
7   simu.rampTime = 100;
8   simu.startTime = 0;
9   simu.endTime=400;
```

```matlab
10    simu.dt = 0.1;
11    simu.dtCITime = 0.05;
12
13    %% Wave Information
14    % % noWaveCIC, no waves with radiation CIC
15    % waves = waveClass('noWaveCIC'); % Initialize Wave Class and Specify Type
16
17    % Regular Waves
18    %waves = waveClass('regular');    % Initialize Wave Class and Specify Type
19    %waves.H =5 ;                     % Wave Height [m]
20    %waves.T =7.5;                    % Wave Period [s]
21
22    % % Regular Waves with CIC
23    waves = waveClass('regularCIC'); % Initialize Wave Class and Specify Type
24    waves.H =5;                       % Wave Height [m]
25    waves.T =7.5;                     % Wave Period [s]
26
27    % % Irregular Waves using PM Spectrum
28    %waves = waveClass('irregular'); % Initialize Wave Class and Specify Type
29    %waves.H =8;                      % Significant Wave Height [m]
30    %waves.T =11;                     % Peak Period [s]
31    %waves.spectrumType = 'PM';       % Specify Wave Spectrum Type
32
33    % % Irregular Waves using JS Spectrum with Equal Energy and Seeded Phase
34    % waves = waveClass('irregular'); % Initialize Wave Class and Specify Type
35    % waves.H = ;                      % Significant Wave Height [m]
36    % waves.T = ;                      % Peak Period [s]
37    % waves.spectrumType = 'JS';       % Specify Wave Spectrum Type
38    % waves.freqDisc = 'EqualEnergy'; % Uses 'EqualEnergy' bins (default)
39    % waves.phaseSeed = 1;             % Phase is seeded so eta is the same
40
41    % % Irregular Waves using PM Spectrum with Traditional and State Space
42    % waves = waveClass('irregular'); % Initialize Wave Class and Specify Type
43    % waves.H = ;                      % Significant Wave Height [m]
44    % waves.T = ;                      % Peak Period [s]
45    % waves.spectrumType = 'PM';       % Specify Wave Spectrum Type
46    % simu.ssCalc = 1;                 % Turn on State Space
47    % waves.freqDisc = 'Traditional'; % Uses 1000 frequnecies
48
49    % % Irregular Waves with imported spectrum
50    % waves = waveClass('spectrumImport');        % Create the Wave Variable and
51    Specify Type
52    % waves.spectrumDataFile = 'spectrumData.mat';%Name of User-Defined Spectrum
53    File [:,2] = [f, Sf]
54
55    % % Waves with imported wave elevation time-history
56    % waves = waveClass('etaImport');    % Create the Wave Variable and Specify
57    Type
58    % waves.etaDataFile = 'etaData.mat'; % Name of User-Defined Time-Series File
59    [:,2] = [time, eta]
60    %% Body Data
61    % Float
62    body(1) = bodyClass('C:\Users\Babak Shafiei\Documents\MATLAB\cccc\matlab
63    routines\pointabsorber\pointabsorber.h5');
64    body(1).geometryFile = 'C:\Users\Babak Shafiei\Documents\MATLAB\cccc\matlab
65    routines\pointabsorber\float.stl';
66    body(1).mass = 'equilibrium';
```

```matlab
67    body(1).momOfInertia = [20907301 21306091 37085481];
68
69    % Spar/Plate
70    body(2) = bodyClass('C:\Users\Babak Shafiei\Documents\MATLAB\cccc\matlab
71    routines\pointabsorber\pointabsorber.h5');
72    body(2).geometryFile = 'C:\Users\Babak Shafiei\Documents\MATLAB\cccc\matlab
73    routines\pointabsorber\spar-plate.stl';
74    body(2).mass = 'equilibrium';
75    body(2).momOfInertia = [94419615 94407091 28542225];
76    body(2).initDisp.initLinDisp = [0 0 -0.3];  % Initial Displacement
77
78    %% PTO and Constraint Parameters
79    % Floating (3DOF) Joint
80    constraint(1) = constraintClass('Constraint1');
81    constraint(1).loc = [0 0 0];
82
83    % Translational PTO
84    pto(1) = ptoClass('PTO1');
85    pto(1).k=0;
86    pto(1).c=1200000;
87    pto(1).loc = [0 0 0];
88
89    %% Mooring
90    % Moordyn
91    mooring(1) = mooringClass('mooring');        % Initialize mooringClass
92    mooring(1).moorDynLines = 6;                 % Specify number of lines
93    mooring(1).moorDynNodes(1:3) = 16;           % Specify number of nodes per
94    line
95    mooring(1).moorDynNodes(4:6) = 6;            % Specify number of nodes per
96    line
97    mooring(1).initDisp.initLinDisp = [0 0 -0.3];     % Initial Displacement
```

Script 7.4: WEC-Sim input file for moored 2BPA

```matlab
1     %Example of user input MATLAB file for post processing
2     close all
3
4     %Plot waves
5     waves.plotEta(simu.rampTime);
6     try
7         waves.plotSpectrum();
8     catch
9     end
10
11    tout=0:0.1:400;
12    %plot surge (x) force for body 1
13    plotForces(output,1,1)
14    grid on
15    ylabel('Force (N)')
16
17
18    %plot heave (z) force for body 1
19    plotForces(output,1,3)
20    grid on
```

```matlab
21   ylabel('Force (N)')
22
23
24   %plot pitch (Ry) force for body 1
25   plotForces(output,1,5)
26   grid on
27   ylabel('Torque (N*m)')
28
29
30   %Plot surge (x) response for body 1
31   output.plotResponse(1,1);
32   grid on
33   ylabel('m, m/s, m/s^2')
34
35
36   %plot heave (z) response for body 1
37   output.plotResponse(1,3);
38   grid on
39   ylabel('m, m/s, m/s^2')
40
41
42   %plot pitch (Ry) response for body 1
43   a1=output.bodies(1).position(:,5);
44   a2=(180/pi).*a1;
45   b1=output.bodies(1).velocity(:,5);
46   b2=(180/pi).*b1;
47   c1=output.bodies(1).acceleration(:,5);
48   c2=(180/pi).*c1;
49   figure
50   plot(tout,a2,'blue',tout,b2,'green',tout,c2,'red')
51   grid on
52   xlabel('Time (s)')
53   ylabel('deg, deg/s, deg/s^2')
54   title('body1 (float) Pitch Response')
55   legend
56
57
58   %plot surge (x) force for body 2
59   plotForces(output,2,1)
60   grid on
61   ylabel('Force (N)')
62
63
64   %plot heave (z) force for body 2
65   plotForces(output,2,3)
66   grid on
67   ylabel('Force (N)')
68
69
70   %plot pitch (Ry) force for body 2
71   plotForces(output,2,5)
72   grid on
73   ylabel('Torque (N*m)')
74
75
76   %Plot surge (x) response for body 2
77   output.plotResponse(2,1);
```

```matlab
 78   grid on
 79   ylabel('m, m/s, m/s^2')
 80
 81
 82
 83   %plot heave (z) response for body 2
 84   output.plotResponse(2,3);
 85   grid on
 86   ylabel('m, m/s, m/s^2')
 87
 88
 89   %plot pitch (Ry) response for body 2
 90   aa1=output.bodies(2).position(:,5);
 91   aa2=(180/pi)*aa1;
 92   bb1=output.bodies(2).velocity(:,5);
 93   bb2=(180/pi).*bb1;
 94   cc1=output.bodies(2).acceleration(:,5);
 95   cc2=(180/pi).*cc1;
 96   figure
 97   plot(tout,a2,'blue',tout,b2,'green',tout,c2,'red')
 98   grid on
 99   xlabel('Time (s)')
100   ylabel('deg, deg/s, deg/s^2')
101   title('body2 (spar) Pitch Response')
102   legend
103
104
105
106   %plot WEC mechanical and electerical power
107   ref=output.ptos.forceInternalMechanics(:,3);  %PTO reaction force (applied
108   from the PTO to the body)
109   f=-1*ref; %PTO force (applied from the body to the PTO)
110   pm=(output.ptos.velocity(:,3).*f)/1000; %PTO power (kwatt)
111   figure
112   plot(tout,pm);
113   grid on
114   xlabel('Time (s)')
115   ylabel('Power (kW)')
116   title('Mechanical power')
117   pmmax=max(pm);     %Maximum power (kwatt)
118   pmmean=mean(pm);
119   pe=pm*0.8;
120   pemax=max(pe);
121   pemean=mean(pe);
122   figure
123   plot(tout,pe);
124   grid on
125   xlabel('Time (s)')
126   ylabel('Power (kW)')
127   title('Electrical power')
128
129
130   etha=output.wave.elevation(:,1);
131   X1=-0.72-output.bodies(1).position(:,3);
132   X2=-0.3-21.29-output.bodies(2).position(:,3);
133   X3=X1-X2;
134   x3max=max(X3);
```

```
135    figure
136    plot(tout,X3,tout,etha)
137    grid on
138    xlabel('Time (s)')
139    ylabel('Displacement & Elevation (m)')
140
141
142    hf=output.mooring.forceMooring(:,3)/1000;
143    figure
144    plot(tout,hf)
145    grid on
146    xlabel('Time (s)')
147    ylabel('Force (kN)')
148    sf=output.mooring.forceMooring(:,1)/1000;
149    figure
150    plot(tout,sf)
151    grid on
152    xlabel('Time (s)')
153    ylabel('Force (kN)')
154    pf=output.mooring.forceMooring(:,5)/1000;
155    figure
156    plot(tout,pf)
157    grid on
158    xlabel('Time (s)')
159    ylabel('Torque (kN*m)')
```

Script 7.5: User defined functions for moored 2BPA

7.1.3 WEC-Sim Input File for OSWEC

Script 7.6 is the WEC-Sim input file for OSWEC. The SIMULINK model of OSWEC, hydrodynamic data of OSWEC in *.h5 format, geometry file of flap and base, and moment of inertia of flap is included in this input file. The mass of the flap is defined as 150000 kg, while the base is fixed to the seabed. The ode4 solver is selected for fixed-step calculation. The PTO stiffness and damping coefficients are set to 6.40×10^6 $N.m/rad$ and 5.70×10^7 $N.s.m/rad$, respectively. The code was saved as *wecSimInputFile.m* inside the *oswec* working folder. Plus, the MATLAB code of user-defined functions (*userDefinedFunctions.m*) for OSWEC is given in Script 7.7.

```
1    %% Simulation Data
2    simu = simulationClass();              % Initialize Simulation Class
3    simu.simMechanicsFile = 'oscilliating.slx';   % Specify Simulink Model File
4    simu.mode = 'normal';                  % Specify Simulation Mode
5    ('normal','accelerator','rapid-accelerator')
6    simu.explorer='on';                    % Turn SimMechanics Explorer (on/off)
7    simu.startTime = 0;                    % Simulation Start Time [s]
8    simu.rampTime = 100;                   % Wave Ramp Time [s]
9    simu.endTime=400;                      % Simulation End Time [s]
```

```matlab
10    simu.solver = 'ode4';                    % simu.solver = 'ode4' for fixed step
11    & simu.solver = 'ode45' for variable step
12    simu.dt = 0.1;                           % Simulation Time-Step [s]
13    simu.CITime = 30;                        % Specify CI Time [s]
14
15    %% Wave Information
16    % % noWaveCIC, no waves with radiation CIC
17    % waves = waveClass('noWaveCIC');    % Initialize Wave Class and Specify Type
18
19    % % Regular Waves
20     waves = waveClass('regular');       % Initialize Wave Class and Specify Type
21     waves.H = 2;                        % Wave Height [m]
22     waves.T = 5;                        % Wave Period [s]
23
24    % % Irregular Waves using PM Spectrum
25     %waves = waveClass('irregular');    % Initialize Wave Class and Specify Type
26     %waves.H = ;                        % Significant Wave Height [m]
27     %waves.T = ;                        % Peak Period [s]
28     %waves.spectrumType = 'PM';         % Specify Wave Spectrum Type
29
30    % % Irregular Waves using PM Spectrum with Directionality
31    %waves = waveClass('irregular');     % Initialize Wave Class and Specify Type
32    %waves.H = ;                         % Significant Wave Height [m]
33    %waves.T = ;                         % Peak Period [s]
34    %waves.spectrumType = 'PM';          % Specify Spectrum Type
35    %waves.waveDir = [0,30,90];          % Wave Directionality [deg]
36    %waves.waveSpread = [0.1,0.2,0.7];   % Wave Directional Spreading [%}
37
38    % % Irregular Waves with imported spectrum
39    % waves = waveClass('spectrumImport');       % Create the Wave Variable and
40    Specify Type
41    % waves.spectrumDataFile = 'spectrumData.mat';  %Name of User-Defined
42    Spectrum File [:,2] = [f, Sf]
43
44    % % Waves with imported wave elevation time-history
45    % waves = waveClass('etaImport');        % Create the Wave Variable and
46    Specify Type
47    % waves.etaDataFile = 'etaData.mat'; % Name of User-Defined Time-Series File
48    [:,2] = [time, eta]
49
50
51    %% Body Data
52    % Flap
53    body(1) = bodyClass('oswec.h5');       % Initialize bodyClass for Flap
54    body(1).geometryFile = 'C:\Users\Babak Shafiei\Documents\MATLAB\cccc\matlab
55    routines\oswec\flap.stl';     % Geometry File
56    body(1).mass =150000;                       % User-Defined mass [kg]
57    body(1).momOfInertia = [8.12e6 8.12e6 8.12e6];  % Moment of Inertia [kg-m^2]
58
59    % Base
60    body(2) = bodyClass('oswec.h5');       % Initialize bodyClass for Base
61    body(2).geometryFile = 'C:\Users\Babak Shafiei\Documents\MATLAB\cccc\matlab
62    routines\oswec\base.stl';     % Geometry File
63    body(2).mass = 'fixed';                       % Creates Fixed Body
64
65    %% PTO and Constraint Parameters
66    % Fixed
```

113

```
67    constraint(1)= constraintClass('Constraint1');   % Initialize ConstraintClass
68    for Constraint1
69    constraint(1).loc = [0 0 -10];                    % Constraint Location [m]
70
71    % Rotational PTO
72    pto(1) = ptoClass('PTO1');                        % Initialize ptoClass for PTO1
73    pto(1).k = 6.4e6;                                 % PTO Stiffness Coeff [Nm/rad]
74    pto(1).c = 50e6;                                  % PTO Damping Coeff [Nsm/rad]
75    pto(1).loc = [0 0 -9];                            % PTO Location [m]
```

Script 7.6: WEC-Sim input file for OSWEC.

```
1     %Example of user input MATLAB file for post processing
2     close all
3
4     %Plot waves
5     waves.plotEta(simu.rampTime);
6     grid on
7     try
8         waves.plotSpectrum();
9     catch
10    end
11
12    tout=0:0.1:400;
13    % Plot RY forces for body 1
14    plotForces(output,1,5)
15    grid on
16    ylabel('Torque (N*m)')
17
18    %Plot RY response for body 1
19    a1=output.bodies(1).position(:,5);
20    a2=(180/pi).*a1;
21    b1=output.bodies(1).velocity(:,5);
22    b2=(180/pi).*b1;
23    c1=output.bodies(1).acceleration(:,5);
24    c2=(180/pi).*c1;
25    figure
26    plot(tout,a2,'blue',tout,b2,'green',tout,c2,'red')
27    grid on
28    xlabel('Time (s)')
29    ylabel('deg, deg/s & deg/s^2')
30    title('body1 (flap) Pitch Response')
31    legend
32
33    %plot WEC mechanical and electerical power
34    ref=output.ptos.forceInternalMechanics(:,5);   %PTO reaction force (applied
35    from the PTO to the body)
36    f=-1*ref; %PTO force (applied from the body to the PTO)
37    pm=(output.ptos.velocity(:,5).*f)/1000; %PTO power (kwatt)
38    figure
39    plot(tout,pm);
40    grid on
41    xlabel('Time (s)')
```

```
42    ylabel('Power (kW)')
43    title('Mechanical power')
44    pmmax=max(pm);      %Maximum power (kwatt)
45    pmmean=mean(pm);
46    pe=pm*0.8;
47    pemax=max(pe);
48    pemean=mean(pe);
49    figure
50    plot(tout,pe);
51    grid on
52    xlabel('Time (s)')
53    ylabel('Power (kW)')
54    title('Electrical power')
```

Script 7.7: User defined functions for OSWEC

7.2 Simulating Dynamic Responses of 2BPA and OSWEC in Regular and Irregular Wave States: 8th Step

In this step, the dynamic responses of 2BPA and OSWEC subjected to regular ocean waves are simulated using WEC-Sim. For 2BPA, the heave, surge, and pitch motions, and for OSWEC, the pitch motion are simulated. Also, the resonance frequencies in which the devices will have the maximum power are founded. The excitation, diffraction, and radiation are calculated by WEC-Sim using the hydrodynamic coefficients obtained via the NEMOH BEM solver in the 2nd step. Other forces such as hydrostatic restoring force, added mass force, viscous force, linear damping force, PTO force are also calculated by WEC-Sim. In most common cases, WEC-Sim simulates the dynamics of the WECs using the following equation [47]:

$$m\ddot{x}(t) = f_{hs}(t) + f_{ex}(t) + f_{rad}(t) + f_v(t) + f_{pto}(t) + f_m(t) \qquad (7.1)$$

where m is the mass matrix, $f_{hs}(t)$ is hydrostatic restoring force, $f_{ex}(t)$ is wave excitation force obtained from NEMOH BEM solver, $f_{rad}(t)$ is the radiation force calculated using added mass and radiation damping coefficients obtained via NEMOH BEM solver, $f_v(t)$ is the viscous force, $f_{pto}(t)$ is the PTO force, and $f_m(t)$ is mooring force.

The $f_{hs}(t)$ is defined as below:

$$f_{hs}(t) = KH \times x(t) \qquad (7.2)$$

where KH is the (6×6) hydrostatic stiffness matrix calculated in the meshing process (1st step) and $x(t)$ is the (6×1) displacement matrix of the body. The hydrostatic stiffness matrix is defined

solely for heave, roll, and pitch motions; the stiffness equals zero for the other degrees of freedom. Hence, there will be no hydrostatic restoring force for the surge mode of 2BPA.

For regular wave, the $f_{ex}(t)$ can be calculated using Equation (7.3). For irregular wave, the $f_{ex}(t)$ is given by Equation (7.4) [47]:

$$f_{ex}(t) = \Re\left[R_f(t) \frac{H}{2} X(\omega, \beta) e^{-i\omega t} \right] \tag{7.3}$$

$$f_{ex}(t) = \Re\left[R_f(t) X(\omega_n, \beta) e^{i(\omega_n t + \phi)} \int_0^\infty \sqrt{2S(\omega_n) d\omega} \right] = \int_{-\infty}^\infty \eta_n(\tau) f_e(t - \tau) d\tau \tag{7.4}$$

where $\Re$ represents the real part of the formula, R_f denotes ramp function, H is wave height, $X(\omega, \beta)$ is the complex excitation force amplitude dependent on wave frequency, ω, and wave direction, β, $X(\omega_n, \beta)$ is the complex excitation force amplitude of n-th wave component that is dependent on wave frequency, ω_n, and wave direction, β, ϕ is randomized phase angle, $S(\omega_n)$ is wave spectrum describing the wave energy distribution over a range of wave frequencies, η_n is the amplitude of the sinusoidal n-th wave component [48], and f_e is excitation IRF calculated by BEMIO in 3rd step.

For regular wave, the $f_{rad}(t)$ is given in Equation (7.5). For irregular wave, the $f_{rad}(t)$ is calculated using Equation (7.6) defined as below [47]:

$$f_{rad}(t) = -A(\omega)\ddot{x} - B(\omega)\dot{x} \tag{7.5}$$

$$f_{rad}(t) = -A_\infty \ddot{x} - \int_0^t f_r(t - \tau)\dot{x}(\tau) d\tau \tag{7.6}$$

where $A(\omega)$ is the added mass matrix, $B(\omega)$ is the radiation damping matrix, A_∞ is the added mass matrix at infinite frequency calculated by NEMOH BEM solver, and f_r is the radiation IRF obtained by BEMIO.

The viscous force, $f_v(t)$ is calculated using Equation (7.7):

$$f_v(t) = -C_v\dot{x} - \frac{C_d \rho A_d}{2} \dot{x}|\dot{x}| = -C_v\dot{x} - C_D\dot{x}|\dot{x}| \tag{7.7}$$

where C_v denotes linear viscous damping coefficient, C_d denotes the quadratic drag coefficient, ρ represents the fluid density, and A_d indicates the characteristic area for drag calculation. Alternatively, one can define C_D directly.

The PTO force, $f_{pto}(t)$ is calculated using Equation (7.8) [49]:

$$f_{pto}(t) = -K_{pto}x_{rel} - C_{pto}\dot{x}_{rel} \tag{7.8}$$

where K_{pto} is the PTO stiffness coefficient, C_{pto} is PTO damping coefficient, and x_{rel} and $\dot{x}_{rel}$ are relative displacement and velocity between two bodies.

The mooring force, $f_m(t)$, is represented in Equation given below:

$$f_m(t) = -K_m x - C_m \dot{x} \tag{7.9}$$

Where K_m and C_m are the stiffness and damping matrices respectively for mooring system, and x and $\dot{x}$ are displacement and velocity of the body, respectively.

7.2.1 Dynamic Response of Unmoored 2BPA in Regular Wave State

Now that all the needed data for WEC-Sim is obtained, the 2BPA can be simulated in regular wave conditions. In this study, the wave height is defined as 5 m, and the wave period is 7.5 seconds for a regular wave. The wave period has been chosen so that the amplitude of the relative displacement of the float/spar-plate is close to the amplitude of the wave elevation to obtain the resonance phenomena to gain maximum electrical power. The simulation ending times were 400 and 5000 seconds in the WEC-Sim input file. To start simulating the dynamic behavior of the device, we typed wecSim in the MATLAB Command Window. The plots resulting from the 400 seconds of simulation are shown in Figures 7.1-7.16.

For 5000 seconds of simulation for un-moored 2BPA, only surge response of spar is shown in Figure 7.11 because the heave and pith responses did not change as the simulation time increased from 400 to 5000 seconds. As shown in Figure 7.11 (right), it is evident that the device moves along the x-axis because it is not moored. According to the graphical visualization shown by WEC-Sim, the displacement was in a negative direction of the x-axis. After 5000 seconds, the device moved 100 meters in the negative direction of the x-axis. In 400 seconds, the movement was not recognizable, but in 5000 seconds, the displacement was evident.
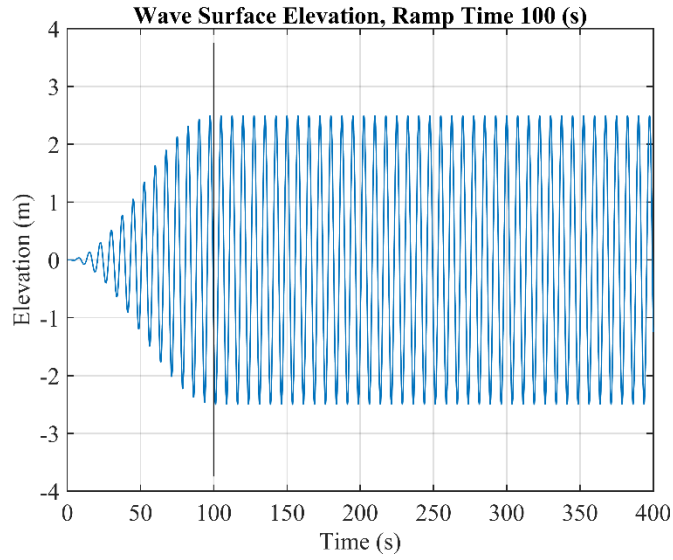
Figure 7.1: Regular wave surface elevation in unmoored 2BPA
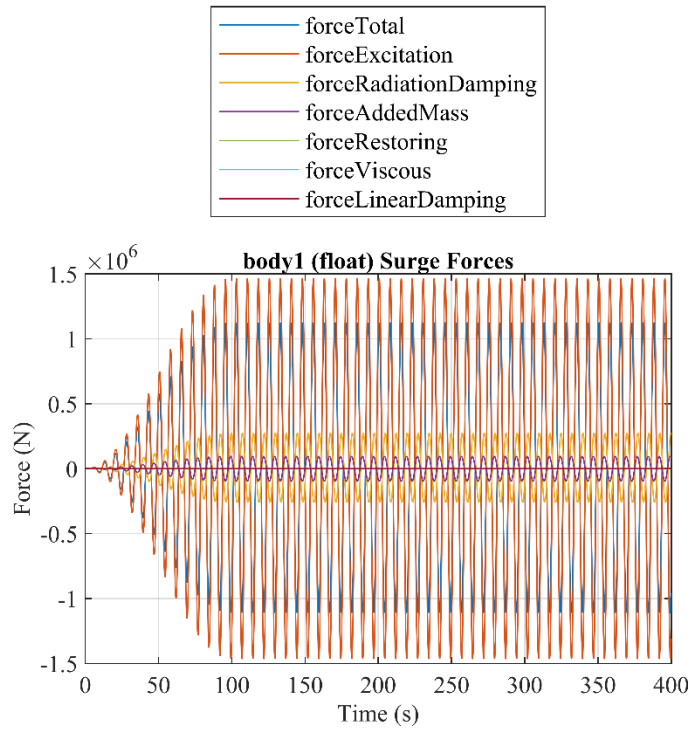
Figure 7.2: Float surge forces in regular wave state for unmoored case
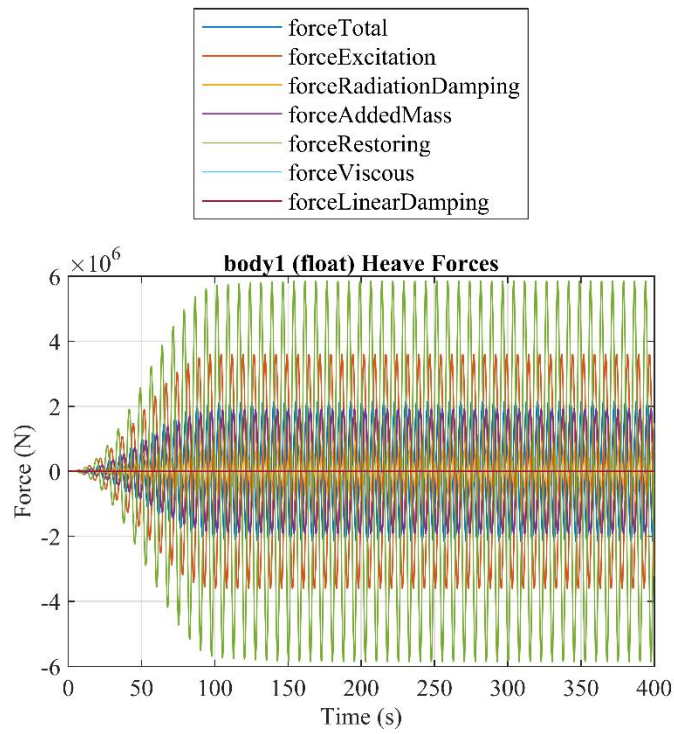
Figure 7.3: Float heave forces in regular wave state for unmoored case
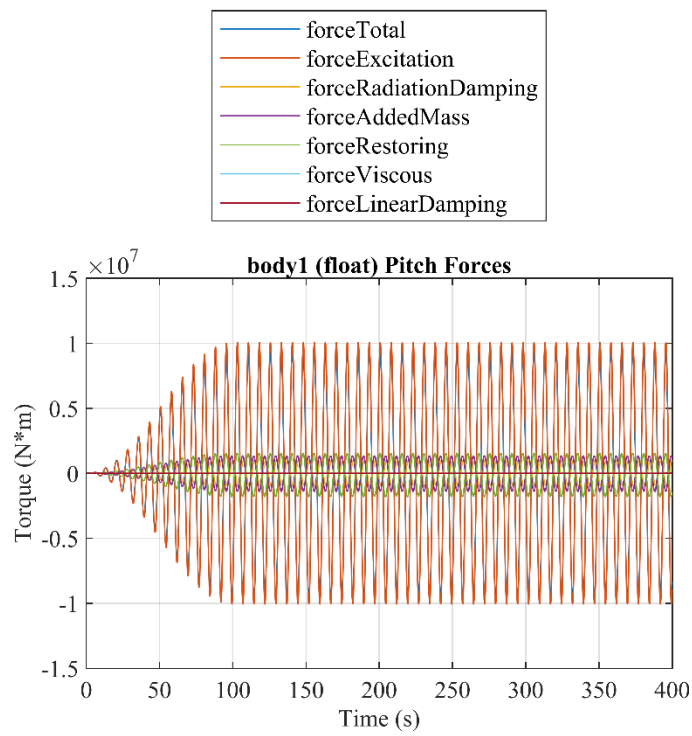
Figure 7.4: Float pitch forces in regular wave state for unmoored case
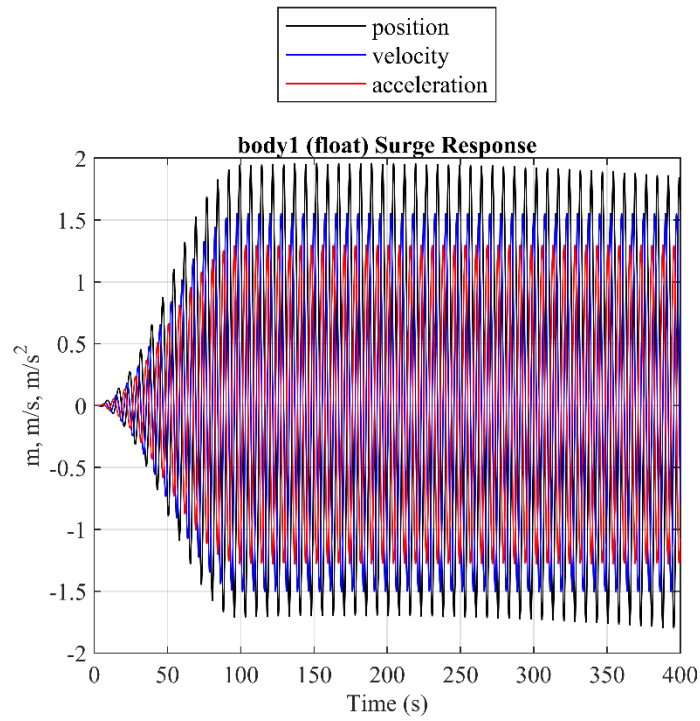
Figure 7.5: Float surge response in regular wave state for unmoored case
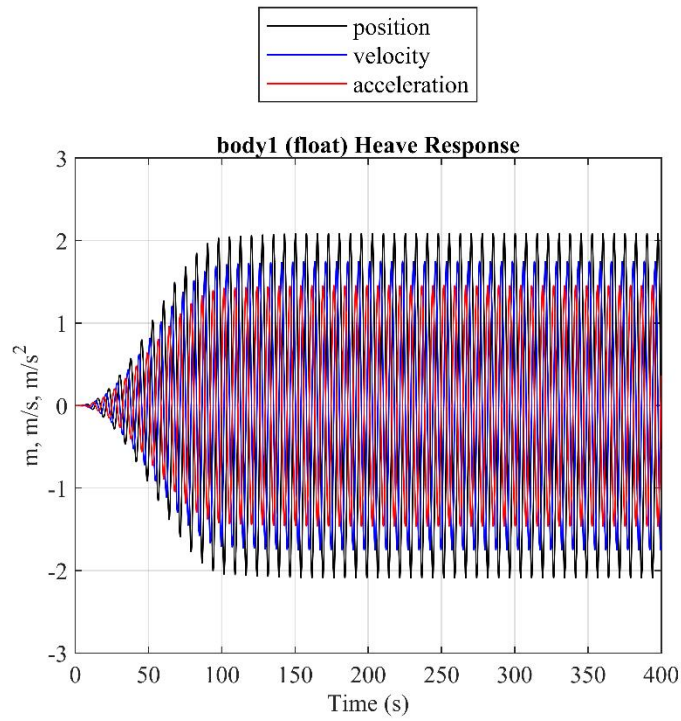
Figure 7.6: Float heave response in regular wave state for unmoored case
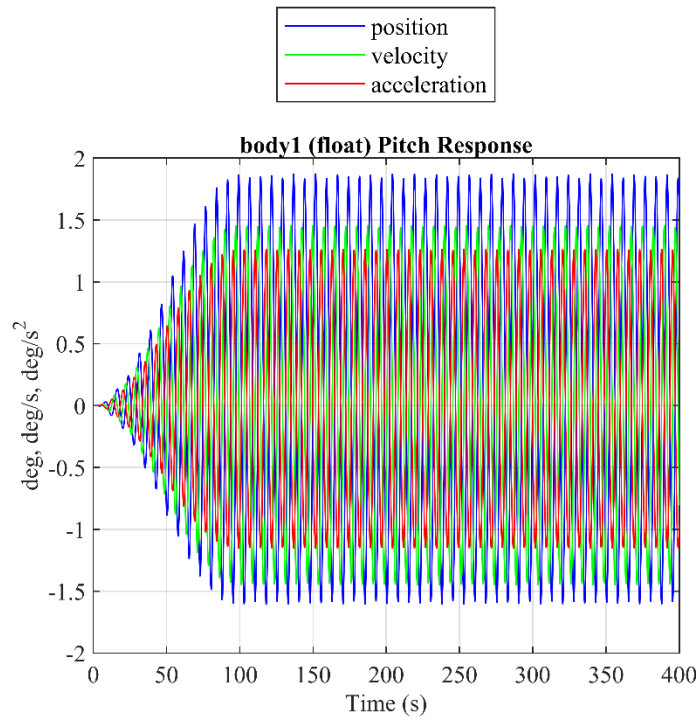
Figure 7.7: Float pitch response in regular wave state for unmoored case
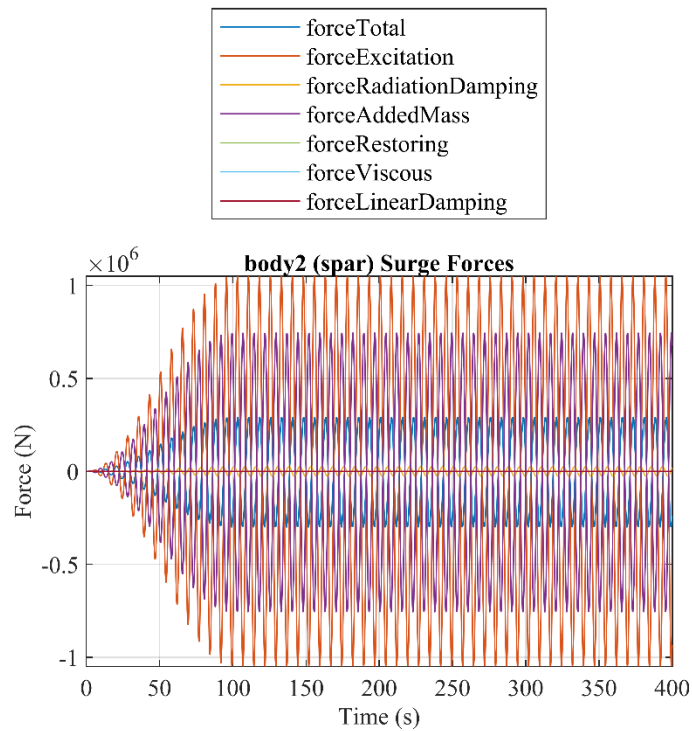
Figure 7.8: Spar surge forces in regular wave state for unmoored case
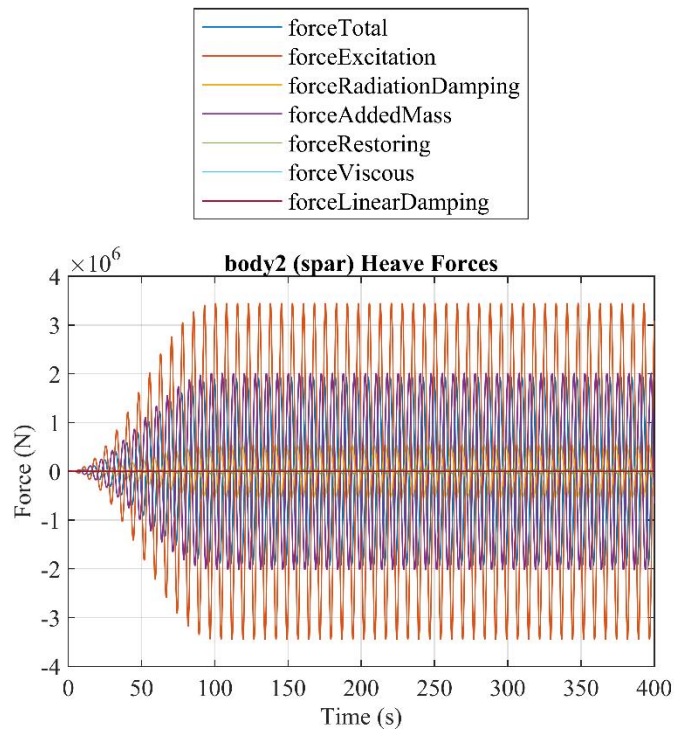
Figure 7.9: Spar heave forces in regular wave state for unmoored case
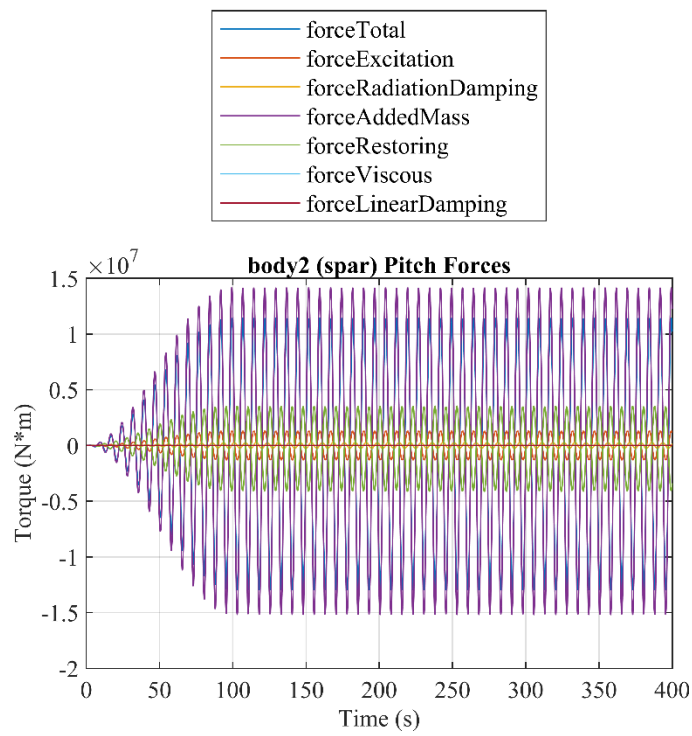
Figure 7.10: Spar pitch forces in regular wave state for unmoored case
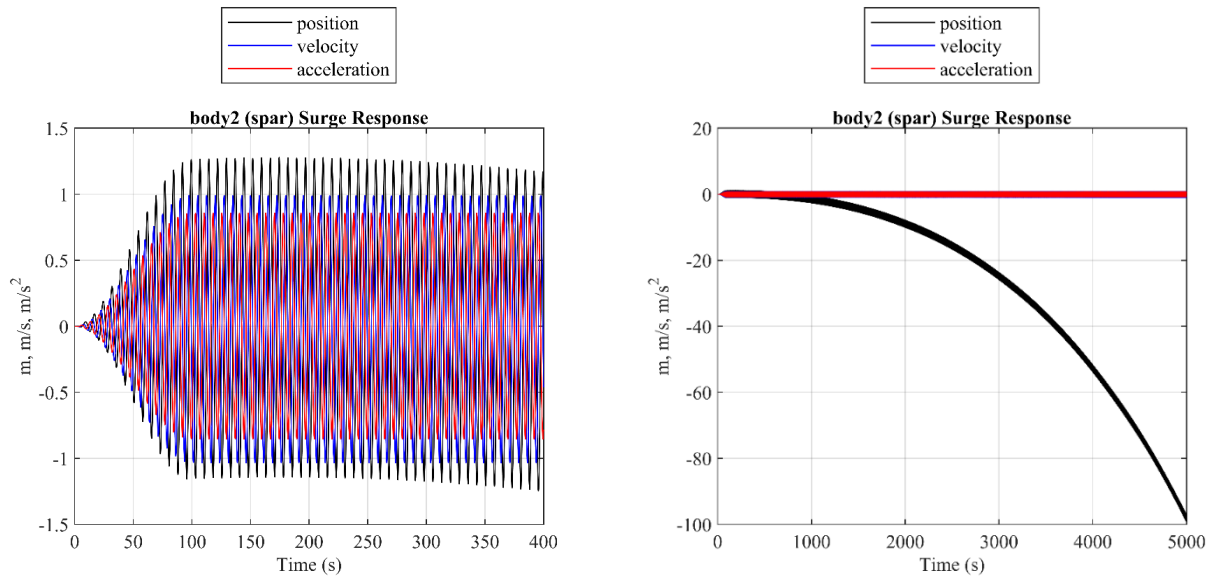
Figure 7.11: Unmoored case: Spar surge response in regular wave state for 400 seconds of simulation (left) and spar surge response in regular wave state for 500 seconds of simulation (right)
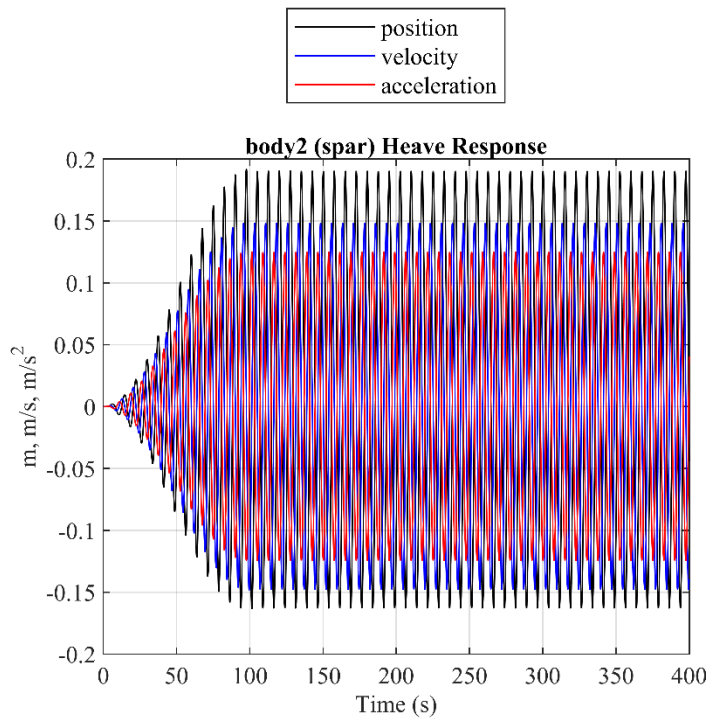
Figure 7.12: Spar heave response in regular wave state for unmoored case
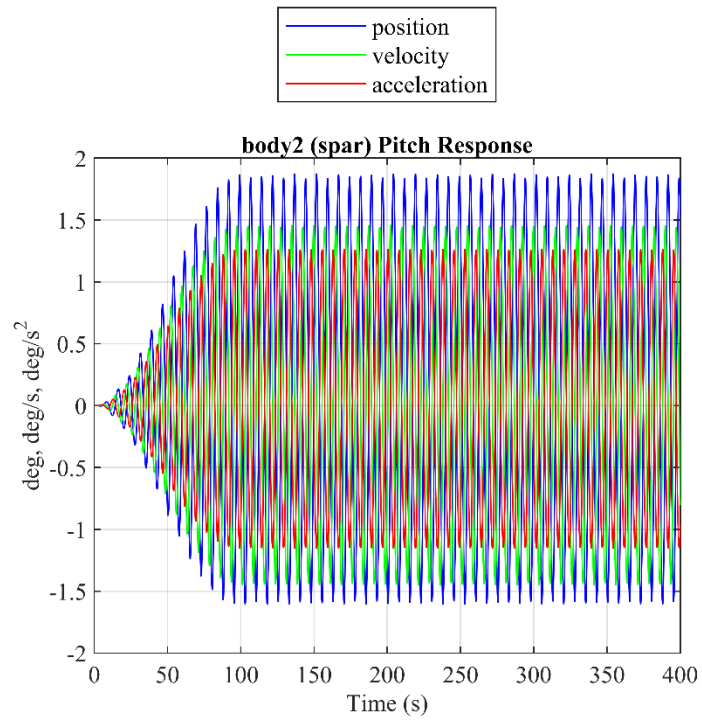
Figure 7.13: Spar pitch response in regular wave state for unmoored case
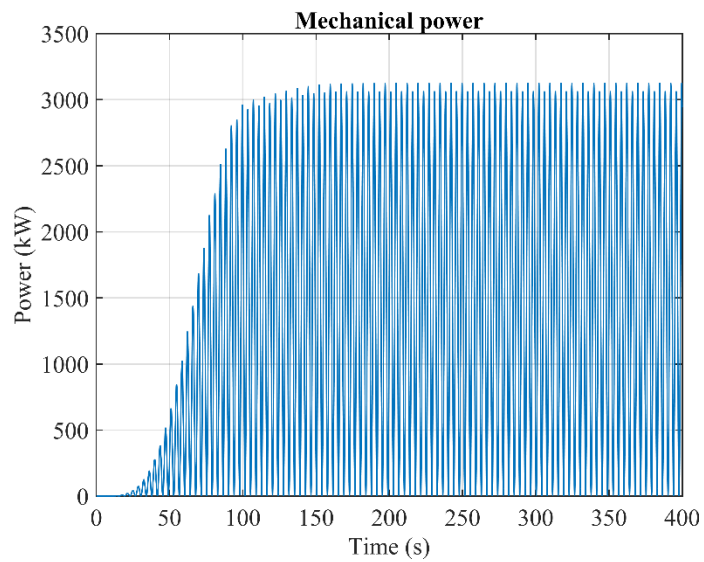
Figure 7.14: 2BPA mechanical power in regular wave state for unmoored case
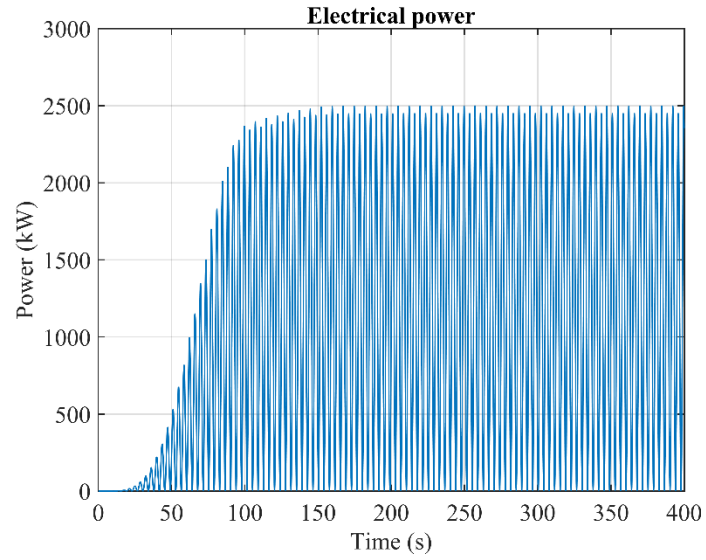
Figure 7.15: 2BPA electrical power in regular wave state for unmoored case
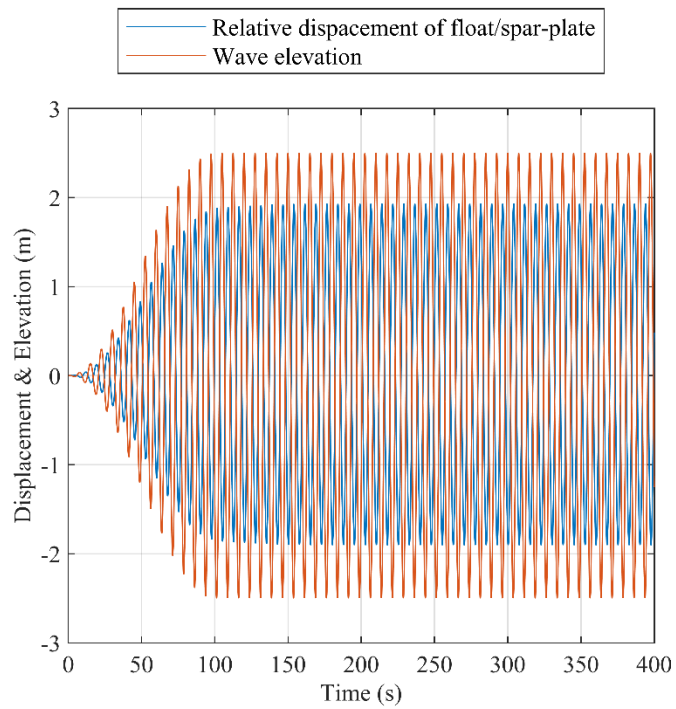
Figure 7.16: Relative displacement of float/spar-plate and wave elevation in regular wave state for unmoored case

7.2.2 Dynamic Response of Moored 2BPA in Regular Wave State

For 2BPA, three mooring lines were considered to keep the device in its location. Mooring lines are of the chain type. All mooring lines data are given in the MoorDyn input file lines.txt. This file is located inside the MoorDyn\mooring folder. In this thesis, the mooring lines data in lines.txt were not changed and remained the default. The WEC-Sim input file used to simulate the moored 2BPA was previously given in Script 7.4.

In order to simulate the mooring lines, an external code was used called MoorDyn. Also, a MinGW-w64 compiler is needed to run the moored WEC simulation using WEC-Sim. The WEC-Sim input file used to simulate the moored 2BPA was previously given in Script 7.4.

The sea state is: $H_s = 5\ m$ and $T_p = 7.5\ sec$, and the water depth is -70 m. The simulation ending times were 400 and 5000 seconds in the WEC-Sim input file. The plots resulting from the 400 seconds of simulation are shown in Figures 7.17-7.35. It was concluded that the float and spar-plate heave and pitch responses, float heave forces, and float and spar-plate surge and pitch forces in both moored and unmoored cases were identical. But, to see the effect of the mooring line on the surge response, the simulation time was increased up to 5000 seconds. In 5000 seconds, it was concluded that the surge response of moored 2BPA showed improvement so that the device was fixed in its location and it was not moving along the x-axis. Please compare Figure 7.11(right) with Figure 7.27 (right).

Furthermore, the power performance of the device remained the same, and there were no changes in mechanical and electrical power. In addition, it was concluded that the mooring lines did not affect the resonance phenomena of the system since the relative displacement of the float/spar-plate in both moored and un-moored cases remained unchanged. Note that the initial displacement of the spar and mooring line is -0.3 meters, given in Script 7.4. Hence, the initial location of the COG of the spar-plate is 21.59 meters below SWL. It was concluded from Figure 7.25 that the restoring force gained an initial value because of the initial displacement of the spar. So, the total force that caused the spar to heave had an initial value.
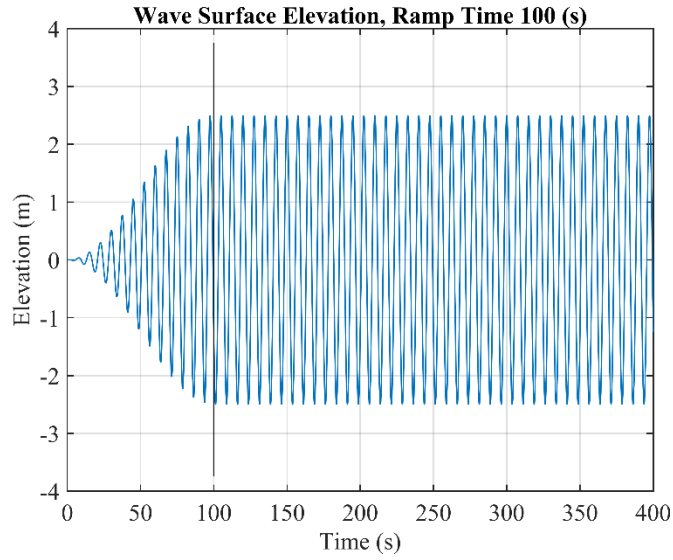
Figure 7.17: Regular wave surface elevation in moored 2BPA
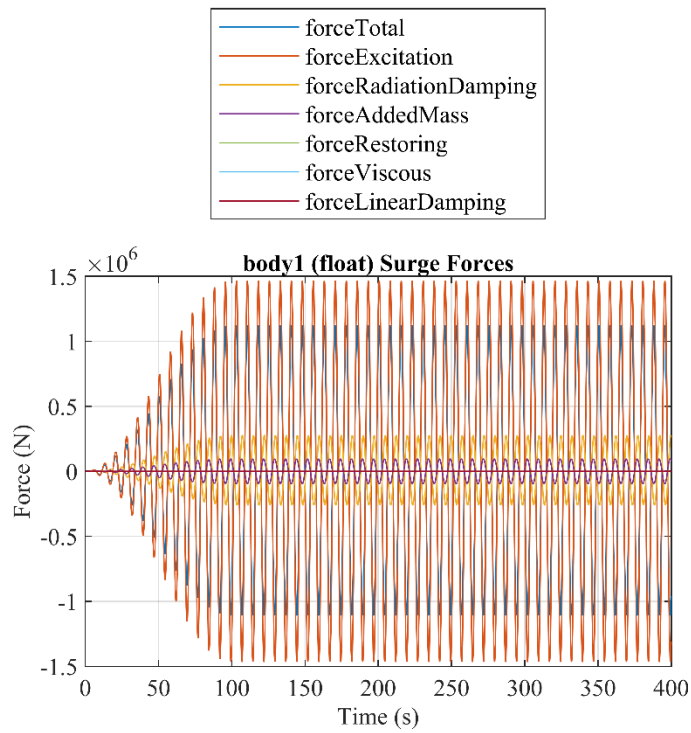
Figure 7.18: Float surge forces in regular wave state for moored case
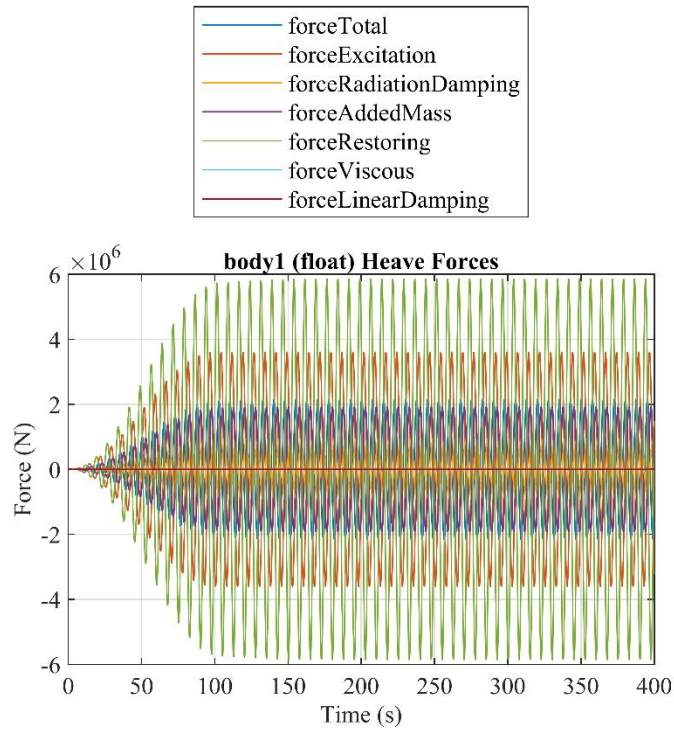
Figure 7.19: Float heave forces in regular wave state for moored case
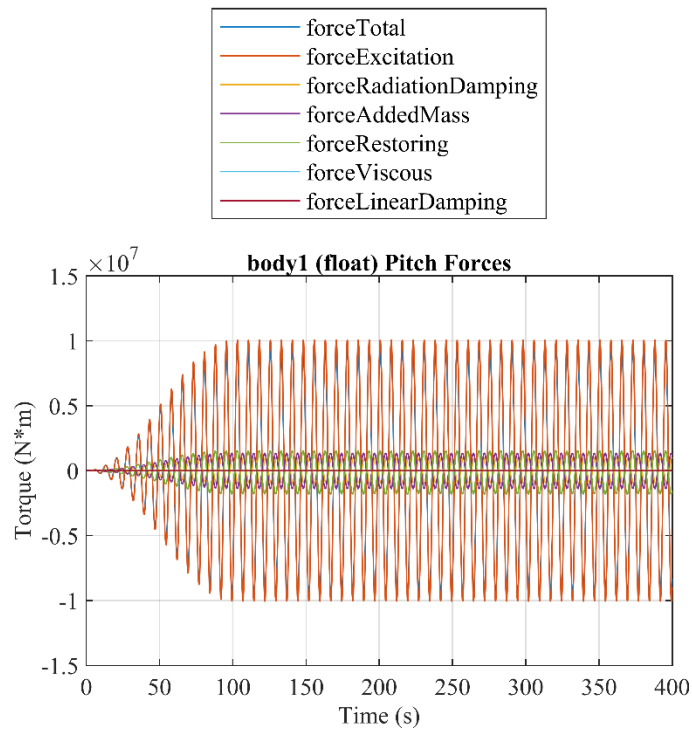
Figure 7.20: Float pitch forces in regular wave state for moored case
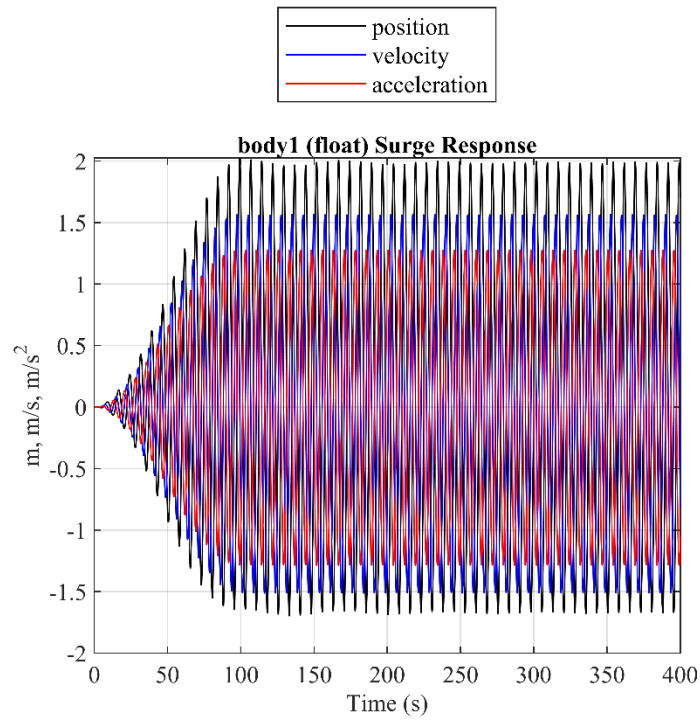
Figure 7.21: Float surge response in regular wave state for moored case
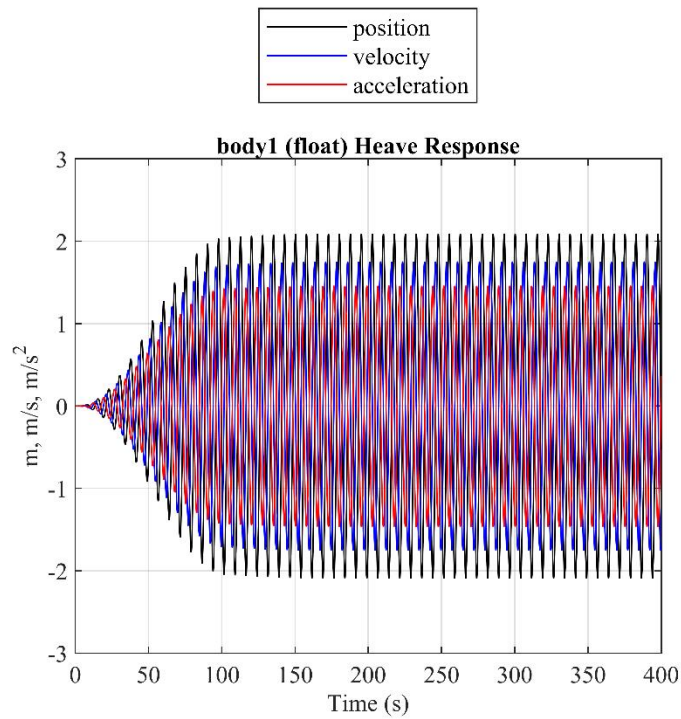
Figure 7.22: Float heave response in regular wave state for moored case
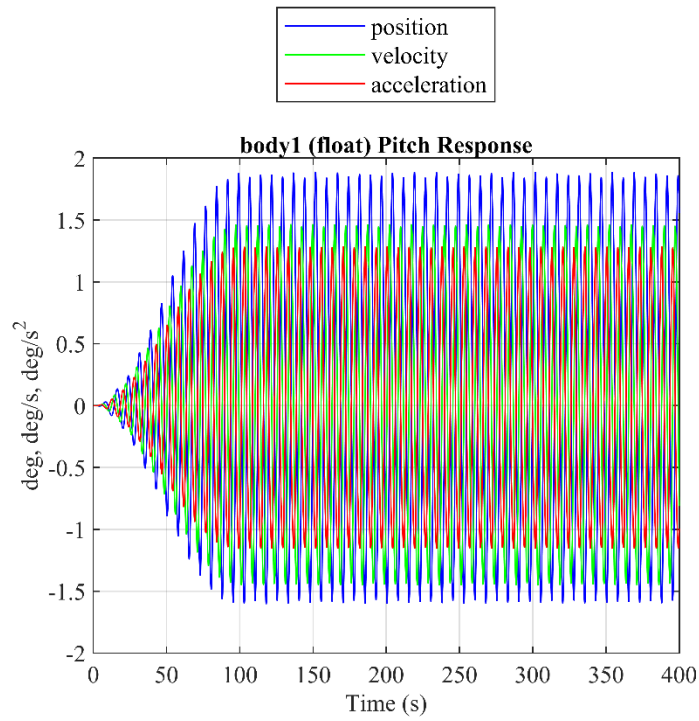
Figure 7.23: Float pitch response in regular wave state for moored case
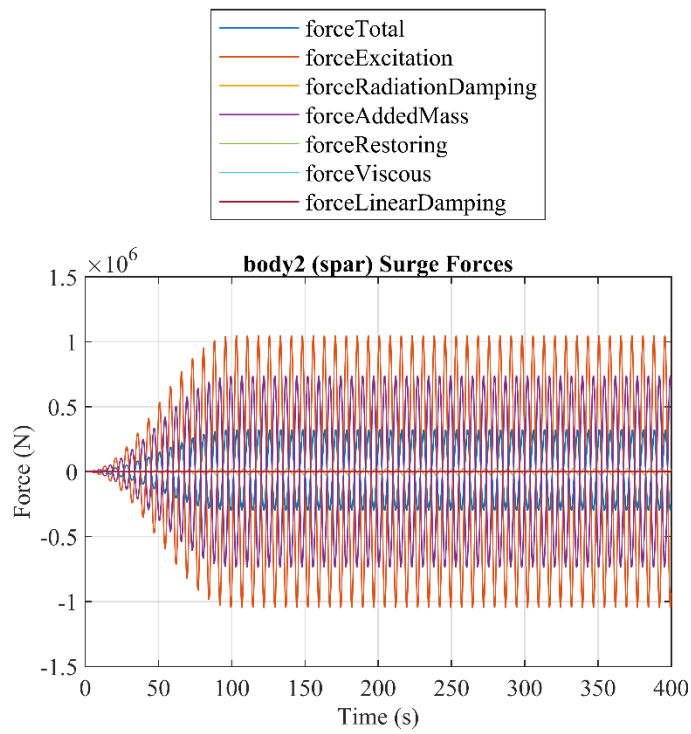
Figure 7.24: Spar surge forces in regular wave state for moored case
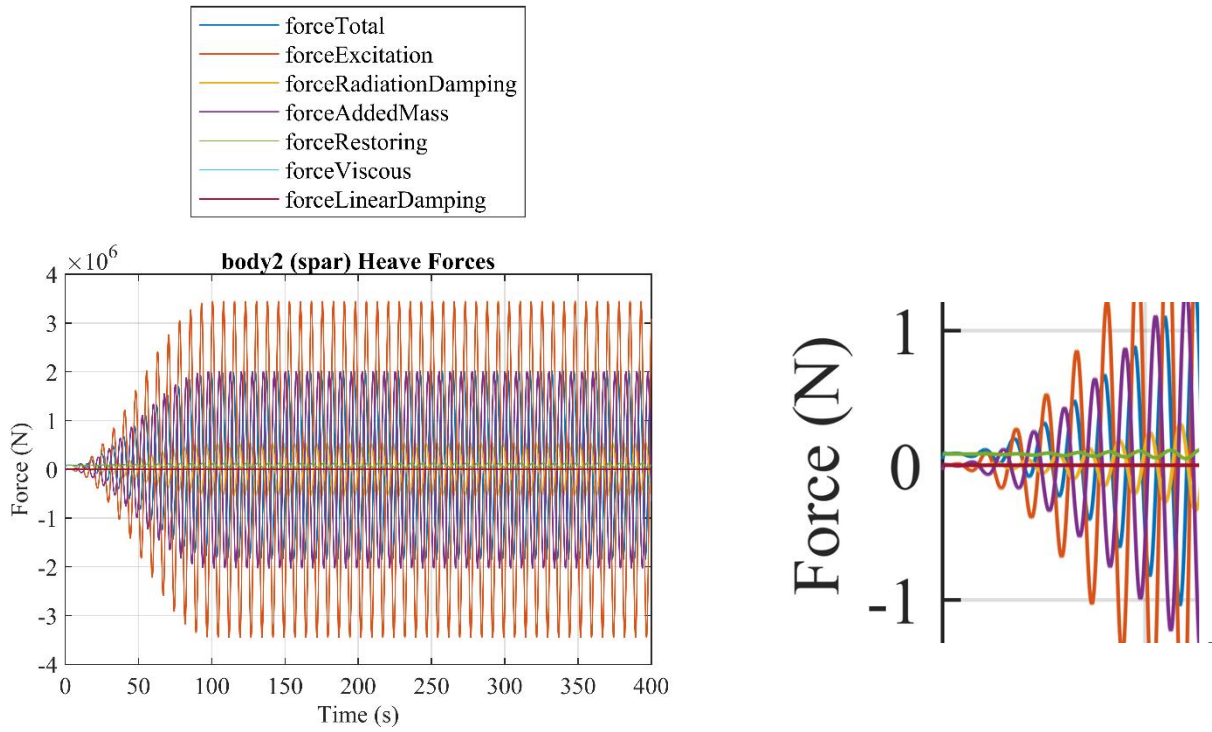
Figure 7.25: Spar heave forces in regular wave state for moored case
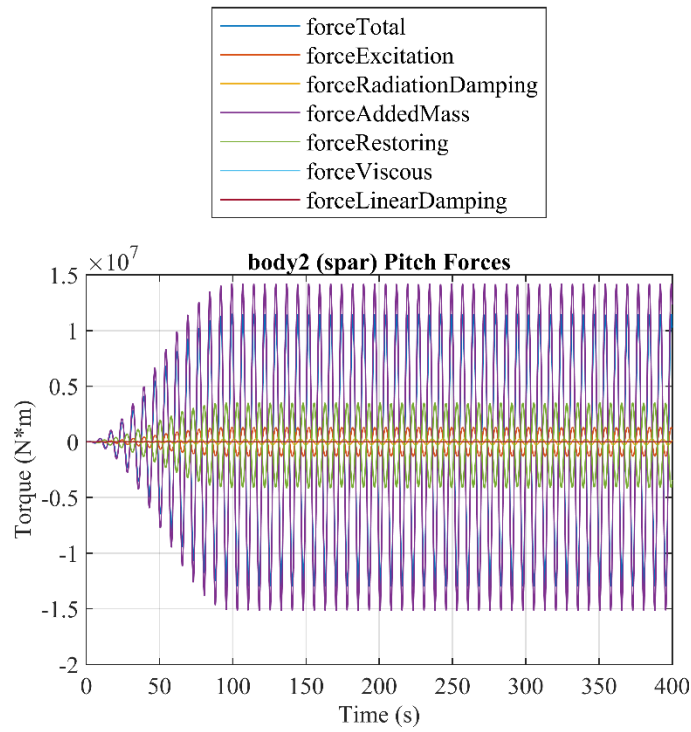
Figure 7.26: Spar pitch forces in regular wave state for moored case
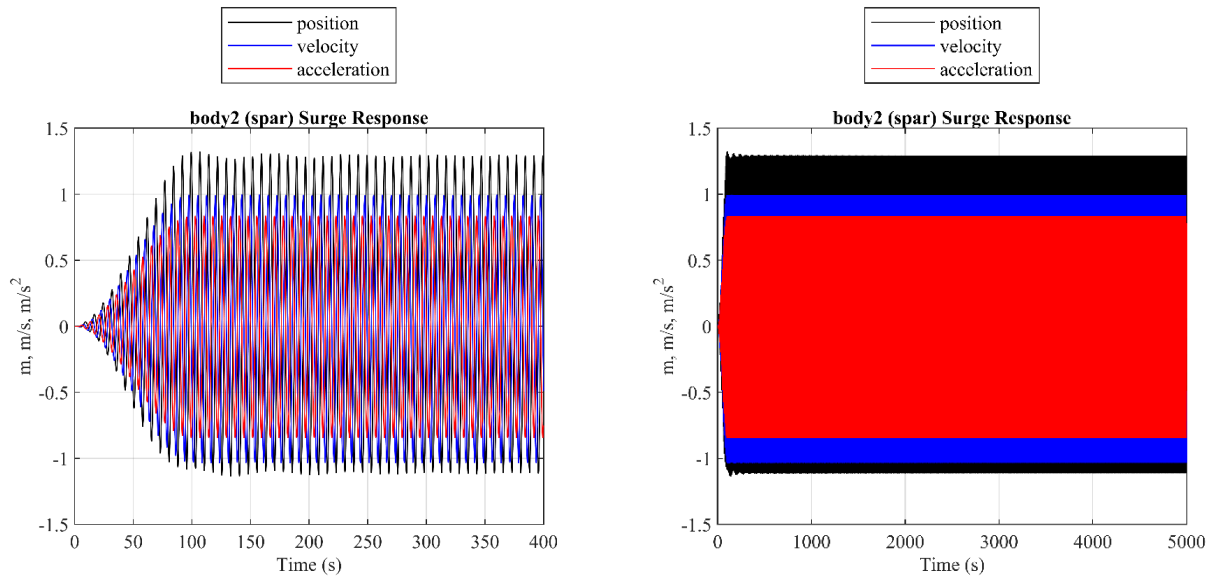
Figure 7.27: Moored case: Spar surge response in regular wave state for 400 seconds of simulation (left) and spar surge response in regular wave state for 500 seconds of simulation (right)
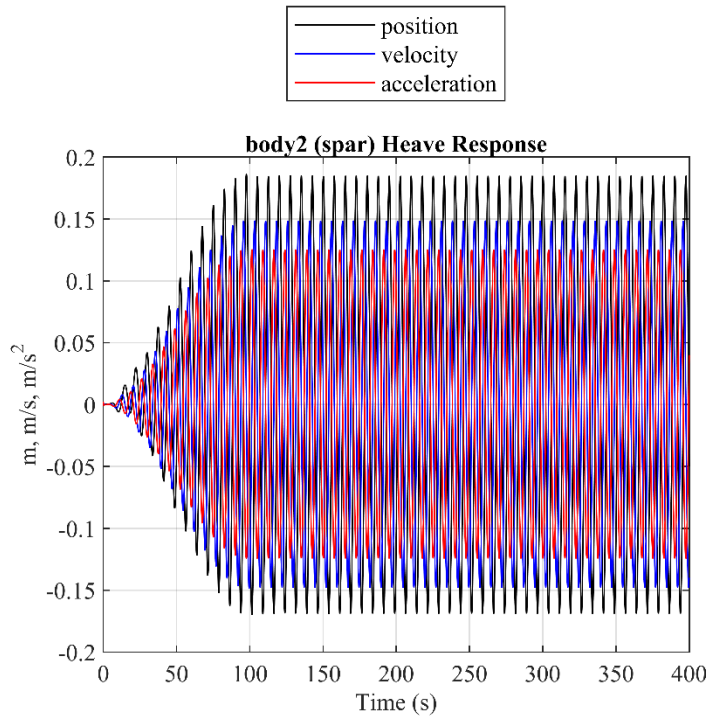
Figure 7.28: Spar heave response in regular wave state for moored case
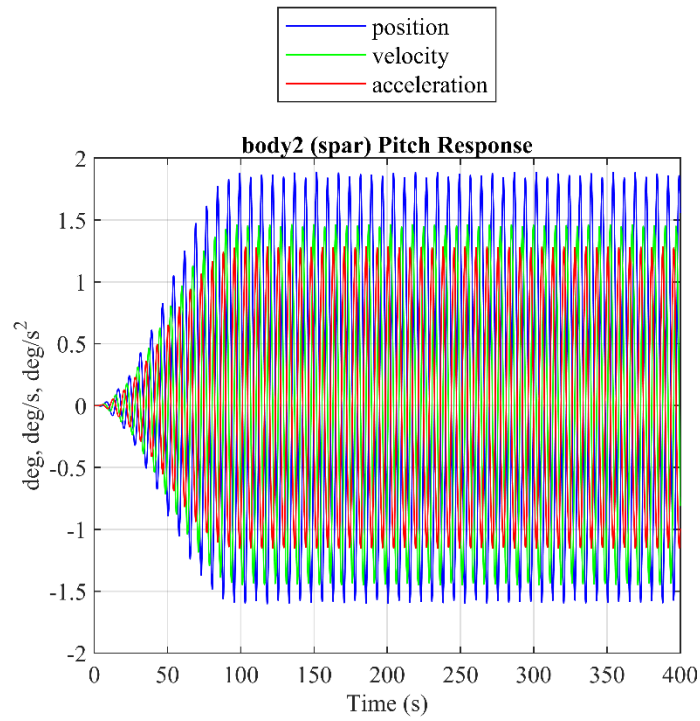
Figure 7.29: Spar pitch response in regular wave state for moored case
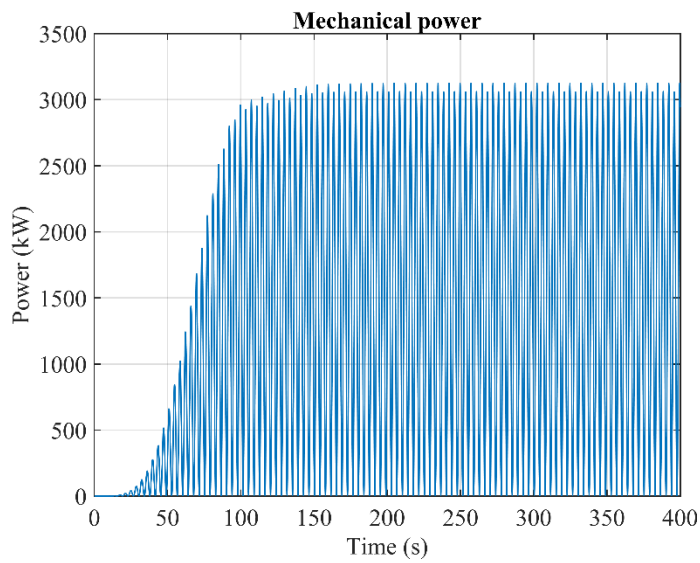
Figure 7.30: 2BPA mechanical power in regular wave state for moored case
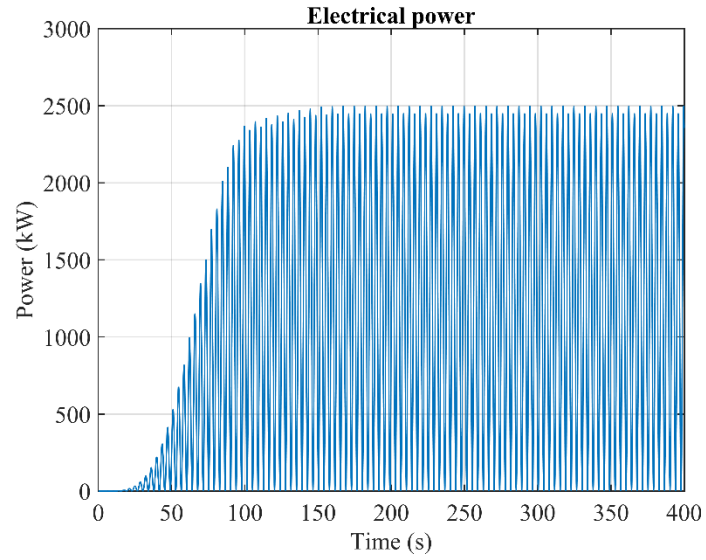
Figure 7.31: 2BPA electrical power in regular wave state for moored case
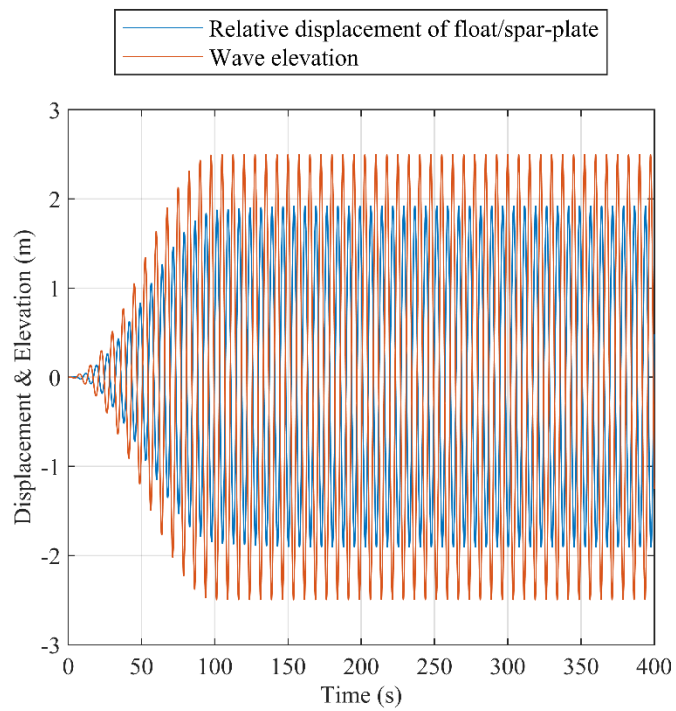
Figure 7.32: Relative displacement of float/spar-plate and wave elevation in regular wave state for moored case
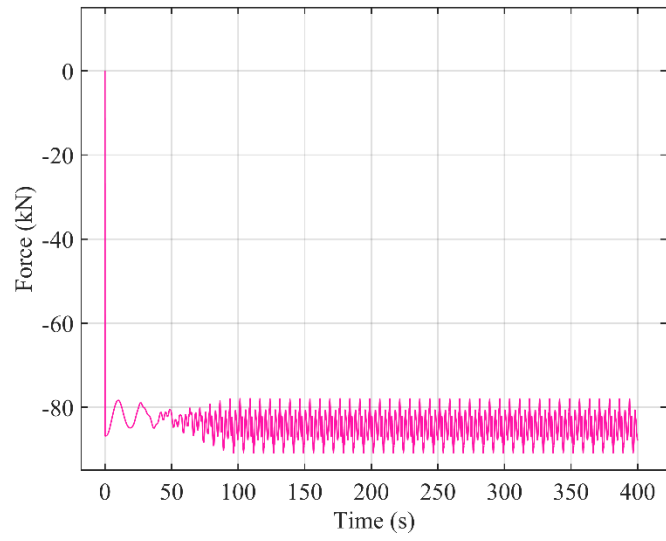
Figure 7.33: Mooring heave force in regular wave state
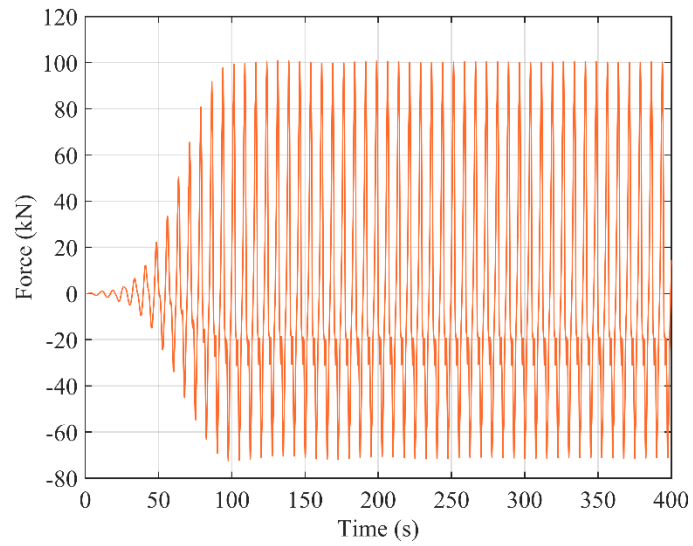
Figure 7.34: Mooring surge force in regular wave state
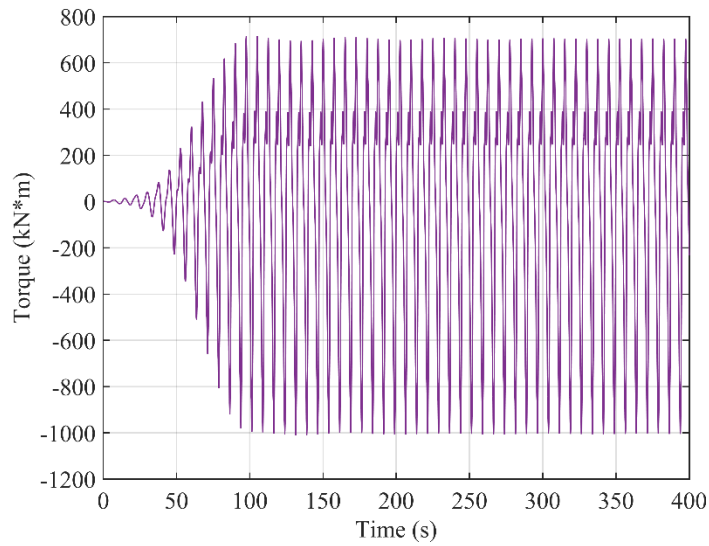
Figure 7.35: Mooring pitch force in regular wave state

7.2.3 Dynamic Response of OSWEC in Regular Wave State

The wave height and the wave period defined for the OSWEC were 2 m and 10 seconds, respectively. The simulation ending time was set to 400 seconds. The results are shown in Figures 7.36-7.40.
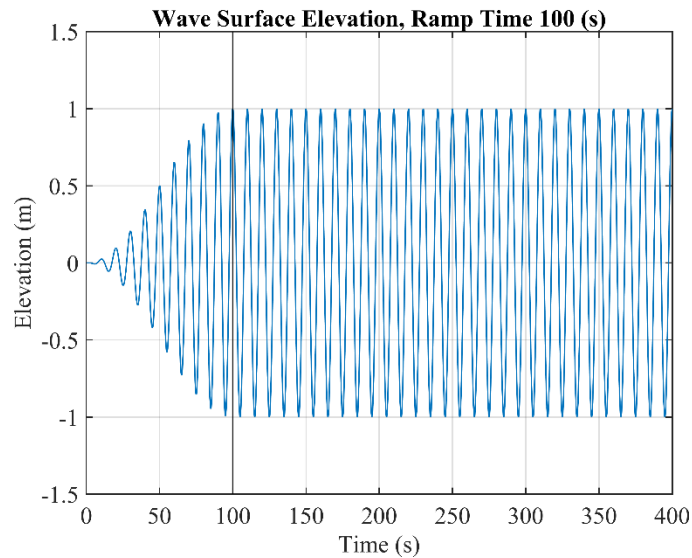
Figure 7.36: Regular wave surface elevation in OSWEC simulation
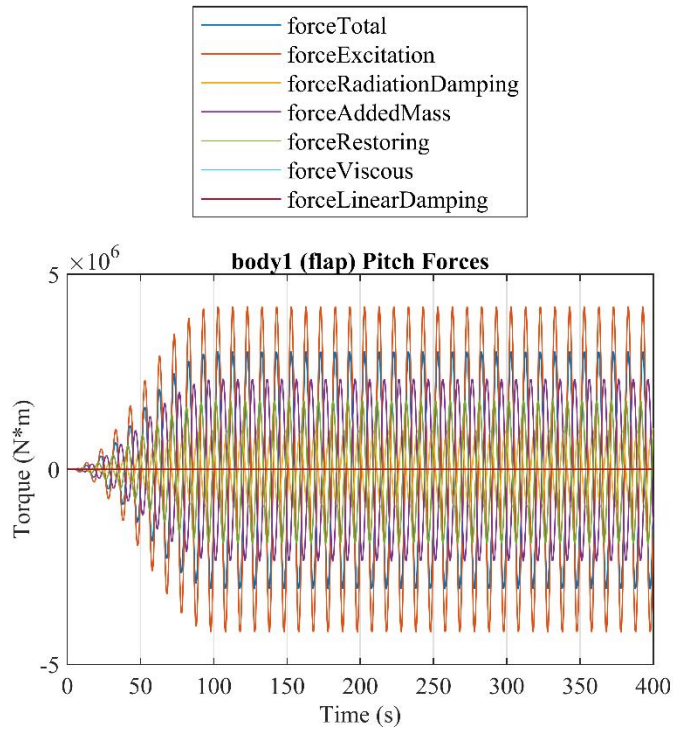
Figure 7.37: Flap pitch forces in regular wave state
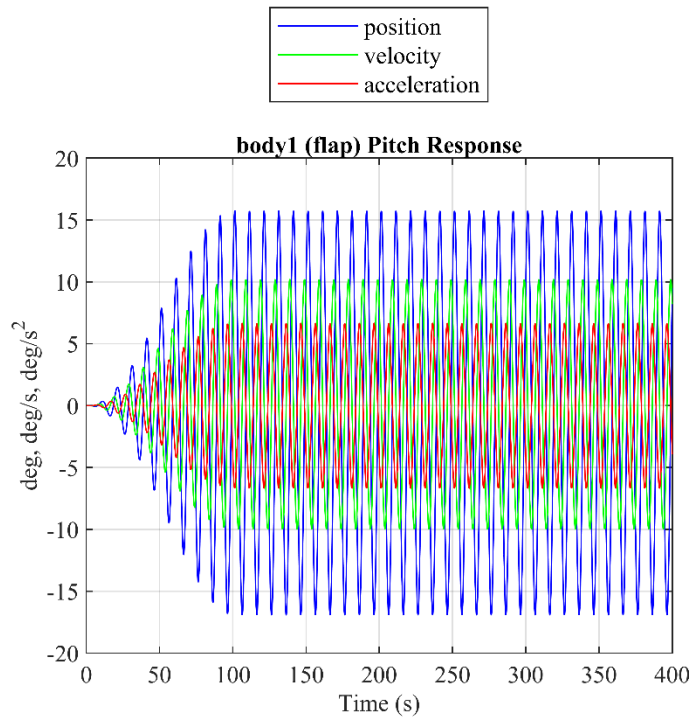
Figure 7.38: Flap pitch response in regular wave state
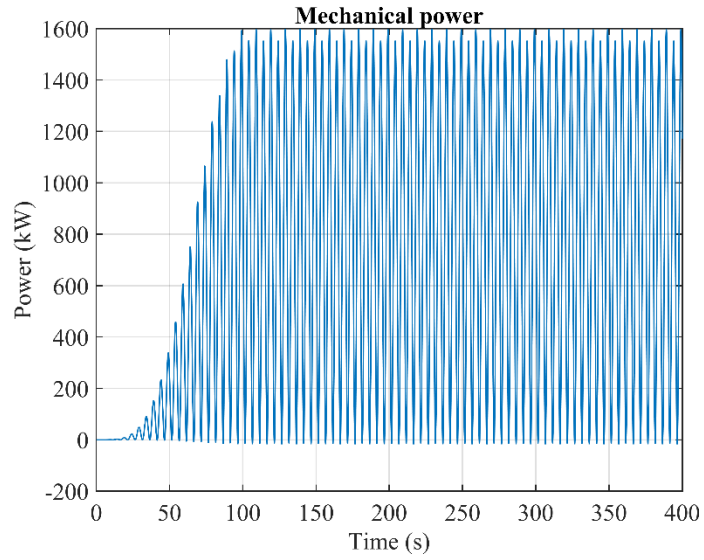
Figure 7.39: OSWEC mechanical power in regular wave state
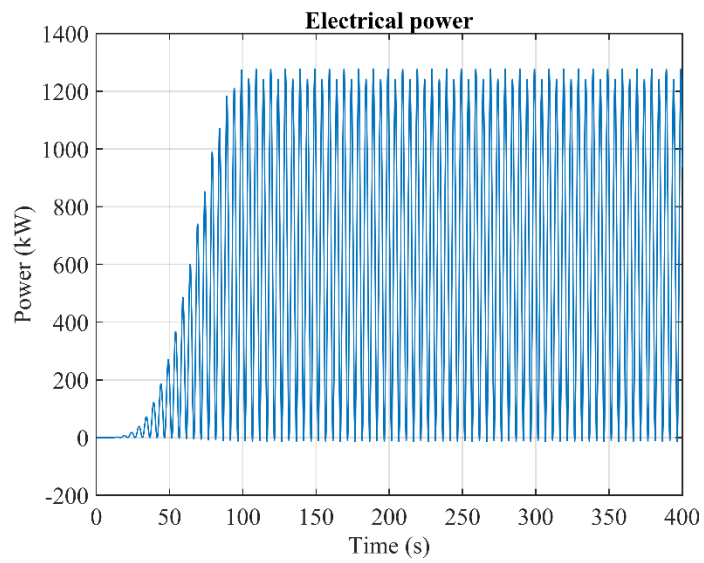
Figure 7.40: OSWEC electrical power in regular wave state

7.2.4 Dynamic Response of 2BPA in Irregular Wave State

For 2BPA in irregular wave case, three possible points were chosen in the Mediterranean Sea in Italy and one in the North Sea to calculate the power matrix for each of those points. Table 7.1 shows the information regarding those three points.

Tables 7.2, 7.10, 7.18, and 7.26 are the probability of occurrence of sea states for sites No. 1-4. Tables 7.3, 7.11, 7.19, and 7.27 indicate the number of occurrence of sea states recorded during 20 years for sites No. 1-4. Tables 7.4, 7.12, 7.20, and 7.28 are the mechanical power matrix of 2BPA calculated by WEC-Sim for sites No. 1-4. Tables 7.5, 7.13, 7.21, and 7.29 are the electrical power matrix of 2BPA obtained by WEC-Sim for sites No. 1-4.

Tables 7.6, 7.14, 7.22, and 7.30 are the electrical power matrices combined with the probability of occurrence for 2BPA at sites No. 1-4. Tables 7.7, 7.15, 7.23, and 7.31 are electrical power matrices for the 2BPA device (rated power with a capacity factor of 30%) estimated at sites No. 1-4.

Tables 7.8, 7.16, 7.24, and 7.32 are the scatter tables of the significant wave height versus mean wave direction for sites Nos. 1-4. Tables 7.9, 7.17, 7.25, and 7.33 are the scatter tables of the significant wave height versus principal wave direction at spectral peak for sites No. 1-4.

Note that the data are recorded every 1 hour for the Mediterranean Sea for 20 years from 2001-05-31 23:00:00 to 2022-01-01 00:00:00 extracted from Copernicus Monitoring Environment Marine Service (CMEMS) for Mediterranean Sea waves analysis and forecast [51, 52]. However, for the North Sea, the data are recorded every 3 hours for 20 years from 2001-09-30 21:00:00 to 2021-09-30 21:00:00 extracted from CMEMS for Atlantic- European North West Shelf- Wave Physics Reanalysis [53].

The files downloaded from the CMEMS are in NC format. Hence, Script 7.8 was used to extract the data from the files in MATLAB software and export the data from MATLAB to EXCEL. The user must first indicate the location of the NC files downloaded from the CMEMS (see lines 21 and 22). Line 21 reads the data from a folder where the significant wave height (Hs) and wave peak period (T_p) are saved. On the other hand, line 22 reads data from a folder where the mean wave direction (VMDR) and principal wave direction at spectral peak (VPED) are saved. Also, the script written below obtains the latitude and longitude of each site in terms of radians. Finally, the data extracted from each NC file in MATLAB were exported to the EXCEL file to form scatter tables (see lines 68-72).

```
1    clc
2    clear all
3
4    close all
5    M=[];
6      %cd C:\Users\Babak Shafiei\Documents\MATLAB\nctoolbox-nctoolbox-20130305
7      setup_nctoolbox
8
```

```matlab
 9  %cd C:\Users\Babak Shafiei\Desktop\OSWEC
10
11  %for
12  km=2020;%[2007,2008,2009,2010,2011,2012,2013,2014,2015,2016,2017,2018,2019];%
13  ,2020];
14      clear Hm0 Hm01 Tp Dm Tp1 Dm1 YEAR
15  %ds =
16  ncdataset(['C:\Users\mariagabriella.gaet2\Dropbox\Gobbino\Dati\Onde\sv03-med-
17  hcmr-wav-hi-h_' num2str(km) '.nc']);%%file da leggere
18  %ds =
19  ncdataset(['C:\Users\mariagabriella.gaet2\Dropbox\RER\Dati\CMEMS\Wav\wav_'
20  num2str(km) ]);%%file da leggere
21  %ds = ncdataset(['C:\Users\Babak Shafiei\Desktop\site6\dir\2.nc']);
22  ds = ncdataset(['C:\Users\Babak Shafiei\Desktop\site6\2.nc']);
23  %SST_MED_SST_L4_REP_OBSERVATIONS_010_021_a_1539768580484.nc')
24  ds.variables
25  %clear all;
26
27  time = ds.time('time');
28  lon = ds.data('longitude');
29  lat = ds.data('latitude');
30  lon=deg2rad(lon);
31  lat=deg2rad(lat);
32
33  Hmt = ds.data('VHM0');
34  Hm0 = Hmt(:,:,:);
35  H=round (Hm0);
36  clear Hmt
37
38  Tpt = ds.data('VTPK');
39  Tp = Tpt(:,:,:);
40  T=round (Tp);
41  clear Tpt
42
43  %WPDt=ds.data('VPED');
44  %WPD=WPDt(:,:,:);
45  %clear WPDt
46
47  %WMDRt=ds.data('VMDR');
48  %WMDR=WMDRt(:,:,:);
49  %clear WMDRt
50
51  %%clear ds
52  LAT=ones(length(lat),length(lon));
53  LON=ones(length(lat),length(lon));
54
55  for k=1:length(lat)
56      LAT2(k,:)=LAT(k,:)*lat(k);
57    end
58
59  for k=1:length(lon)
60  LON2(:,k)=LON(:,k)*lon(k);
61  end
62
63  figure(1)
64  plot(LON2,LAT2,'b.')
65  ylabel('lat [rad]')
```

140

```
66   xlabel('lon [rad]')
67
68   xlswrite('Hm0.xlsx',H)
69   xlswrite('Tp.xlsx',T)
70
71   %xlswrite('VMDR.xlsx',WMDR)
72   %xlswrite('VPED.xlsx',WPD)
```

Script 7.8: The MATLAB code to read CMEMS data

1

The first step to calculate the electrical power matrix for each site is to create a mechanical power matrix of the 2BPA for each sea state. Then, the electrical power matrix was obtained by multiplying the mechanical power matrix with a PCC conversion efficiency, η_1 which in this study is assumed to be 0.80(80%) [15].

The second step is to limit the maximum electrical power output at the rated power. So, the annual average electrical power, P_{ae} was obtained by summing the product of the electrical power matrix and the probability of occurrence of sea states for the reference site. Note that the sum of all numbers indicated in Tables 7.2, 7.10, 7.18, and 7.26 must be equal to 100. However, during the calculation of the P_{ae}, the numbers indicated in the earlier mentioned tables must be divided by 100 before multiplying each number by the electrical power for each sea state. Then, the rated power was calculated by dividing the P_{ae} by a capacity factor which was assumed to be 0.30(30%) [15].

The third step is to find the electrical powers higher than the rated power calculated earlier and replace them with the rated power. In this case, the maximum electrical power output is limited at the rated power [17].

Site No.	Geographical Area	Lat (°)	Long (°)	Water Depth (m)	Nearest port to the WEC location
1	Sea of Sicily-Italy	37°46'52.69"N	12°19'55.11"E	-70	Port of Marsala-Sicily
2	Sea of Sardinia-Italy	39°13'18.03"N	8°17'9.15"E	-70	Port of Portovesme-Sardinia
3	Tyrrhenian Sea-Italy	41°25'0.02"N	12°31'56.05"E	-70	Port of Anzio
4	North Sea-Norway	58°10'22.52"N	2°25'0.96"E	-70	Port of Tananger

Table 7.1: Sites considered to place the 2BPA

Hs (m)/Tp (s)	1	2	3	4	5	6	7	8	9	10	11	12	13	14	15	16	17
<0.5	0.008	1.87	4.297	8.8734	8.04223	3.61631	0.79464	0.78632	0.13964	0.0604	0.01829	0.004433	0	0.000554	0	0	0
1	0	0.002	1.079	5.4727	11.0002	16.4602	7.43489	7.59171	1.17034	0.609	0.22055	0.062064	0	0.014962	0.001108	0.000554	0
2	0	0	0	0.0006	0.2006	2.95301	3.32594	6.40751	1.32439	0.53142	0.15959	0.054306	0	0.016624	0.002771	0	0
3	0	0	0	0	0	0.01939	0.21279	2.20603	0.99579	0.33027	0.10418	0.024382	0.000554	0.004433	0.001662	0	0
4	0	0	0	0	0	0	0	0.20337	0.48598	0.38679	0.08201	0.011083	0	0	0	0	0
5	0	0	0	0	0	0	0	0.00166	0.04655	0.15627	0.0665	0.004987	0	0	0	0	0
6	0	0	0	0	0	0	0	0	0	0.00887	0.02604	0.014408	0	0	0	0	0
7	0	0	0	0	0	0	0	0	0	0	0	0	0	0	0	0	0
8	0	0	0	0	0	0	0	0	0	0	0	0	0	0	0	0	0
9	0	0	0	0	0	0	0	0	0	0	0	0	0	0	0	0	0

Table 7.2: Probability of occurrence of sea states (%) at site No. 1 for 2BPA

Hs (m)/Tp (s)	1	2	3	4	5	6	7	8	9	10	11	12	13	14	15	16	17
<0.5	15	3374	7754	16013	14513	6526	1434	1419	252	109	33	8	0	1	0	0	0
1	0	3	1947	9876	19851	29704	13417	13700	2112	1099	398	112	0	27	2	1	0
2	0	0	0	1	362	5329	6002	11563	2390	959	288	98	0	30	5	0	0
3	0	0	0	0	0	35	384	3981	1797	596	188	44	1	8	3	0	0
4	0	0	0	0	0	0	0	367	877	698	148	20	0	0	0	0	0
5	0	0	0	0	0	0	0	3	84	282	120	9	0	0	0	0	0
6	0	0	0	0	0	0	0	0	0	16	47	26	0	0	0	0	0
7	0	0	0	0	0	0	0	0	0	0	0	0	0	0	0	0	0
8	0	0	0	0	0	0	0	0	0	0	0	0	0	0	0	0	0
9	0	0	0	0	0	0	0	0	0	0	0	0	0	0	0	0	0

Table 7.3: Occurrence of sea events at site No. 1 for 2BPA

Hs (m)/Tp (s)	1	2	3	4	5	6	7	8	9	10	11	12	13	14	15	16	17
<0.5	1.87538E-05	0.0499	0.1221	0.44963	1.00113	1.5185	1.76763	1.7575	1.72813	1.55613	1.382	1.1975	0	0.89988	0	0	0
1	0	0.2829	1.3774	5.0995	11.1056	16.5923	19.1968	20.0761	20.5878	18.4099	15.7546	13.2765	0	9.887	8.9641	0	0
2	0	0	0	19.8551	43.3174	65.5139	81.8643	86.3548	78.9911	70.2669	63.4399	54.78288	0	40.8536	36.932	29.313	0
3	0	0	0	0	0	148.752	189.407	187.317	188.456	163.049	144.878	126.4098	102	97.8916	73.529	0	0
4	0	0	0	0	0	0	0	342.637	315.221	289.056	255.316	218.3334	0	0	0	0	0
5	0	0	0	0	0	0	0	526.515	517.964	448.446	385.97	336.0656	0	0	0	0	0
6	0	0	0	0	0	0	0	0	0	618.459	523.973	461.4825	0	0	0	0	0
7	0	0	0	0	0	0	0	0	0	0	0	0	0	0	0	0	0
8	0	0	0	0	0	0	0	0	0	0	0	0	0	0	0	0	0
9	0	0	0	0	0	0	0	0	0	0	0	0	0	0	0	0	0

Table 7.4: Mechanical power matrix in terms of kilowatts for 2BPA obtained by WEC-Sim for site No. 1

Hs (m)/Tp (s)	1	2	3	4	5	6	7	8	9	10	11	12	13	14	15	16	17
<0.5	1.50E-05	0.0399	0.0977	0.3597	0.8009	1.2148	1.4141	1.406	1.3825	1.2449	1.1056	0.958	0	0.7199	0	0	0
1	0	0.2263	1.1019	4.0796	8.8845	13.2738	15.3574	16.0609	16.4702	14.7279	12.6037	10.6212	0	7.9096	7.1713	0	0
2	0	0	0	15.8841	34.6539	52.4111	65.4914	69.0838	63.1929	56.2135	50.7519	43.8263	0	32.6829	29.5455	23.45	0
3	0	0	0	0	0	119.002	151.526	149.853	150.765	130.439	115.902	101.128	81.2827	78.3133	58.8235	0	0
4	0	0	0	0	0	0	0	274.11	252.177	231.245	204.253	174.667	0	0	0	0	0
5	0	0	0	0	0	0	0	421.212	414.371	358.757	308.776	268.853	0	0	0	0	0
6	0	0	0	0	0	0	0	0	0	494.767	419.178	369.186	0	0	0	0	0
7	0	0	0	0	0	0	0	0	0	0	0	0	0	0	0	0	0
8	0	0	0	0	0	0	0	0	0	0	0	0	0	0	0	0	0
9	0	0	0	0	0	0	0	0	0	0	0	0	0	0	0	0	0

Table 7.5: Electrical power matrix in terms of kilowatts for 2BPA obtained by WEC-Sim for site No. 1

Hs (m)/Tp (s)	1	2	3	4	5	6	7	8	9	10	11	12	13	14	15	16	17
<0.5	1.25E-09	0.0007	0.0042	0.03192	0.06441	0.04393	0.01124	0.01106	0.00193	0.00075	0.0002	4.2E-05	0	4E-06	0	0	0
1	0	4E-06	0.0119	0.22326	0.97731	2.18489	1.14181	1.2193	0.19276	0.08969	0.0278	0.00659	0	0.00118	7.9E-05	0	0
2	0	0	0	8.8E-05	0.06952	1.5477	2.17821	4.42655	0.83692	0.29873	0.081	0.0238	0	0.00543	0.00082	0	0
3	0	0	0	0	0	0.02308	0.32243	3.30581	1.5013	0.4308	0.12075	0.02466	0.00045	0.00347	0.00098	0	0
4	0	0	0	0	0	0	0	0.55745	1.22553	0.89443	0.16751	0.01936	0	0	0	0	0
5	0	0	0	0	0	0	0	0.007	0.19288	0.56062	0.20533	0.01341	0	0	0	0	0
6	0	0	0	0	0	0	0	0	0	0.04387	0.10917	0.05319	0	0	0	0	0
7	0	0	0	0	0	0	0	0	0	0	0	0	0	0	0	0	0
8	0	0	0	0	0	0	0	0	0	0	0	0	0	0	0	0	0
9	0	0	0	0	0	0	0	0	0	0	0	0	0	0	0	0	0

Table 7.6: Electrical power matrix combined with the probability of occurrence for 2BPA at site No. 1

Hs (m)/Tp (s)	1	2	3	4	5	6	7	8	9	10	11	12	13	14	15	16	17
<0.5	1.50E-05	0.0399	0.0977	0.3597	0.8009	1.2148	1.4141	1.406	1.3825	1.2449	1.1056	0.958	0	0.7199	0	0	0
1	0	0.2263	1.1019	4.0796	8.8845	13.2738	15.3574	16.0609	16.4702	14.7279	12.6037	10.6212	0	7.9096	7.1713	0	0
2	0	0	0	15.8841	34.6539	52.4111	65.4914	69.0838	63.1929	56.2135	50.7519	43.8263	0	32.6829	29.5455	23.45	0
3	0	0	0	0	0	85	85	85	85	85	85	85	81.2827	78.3133	58.8235	0	0
4	0	0	0	0	0	0	0	85	85	85	85	85	0	0	0	0	0
5	0	0	0	0	0	0	0	85	85	85	85	85	0	0	0	0	0
6	0	0	0	0	0	0	0	0	0	85	85	85	0	0	0	0	0
7	0	0	0	0	0	0	0	0	0	0	0	0	0	0	0	0	0
8	0	0	0	0	0	0	0	0	0	0	0	0	0	0	0	0	0
9	0	0	0	0	0	0	0	0	0	0	0	0	0	0	0	0	0

Table 7.7: Electrical power matrix in terms of kilowatts for the 2BPA device (rated power with a capacity factor of 30% estimated at site No. 1)

Hs (m)/VMDR (deg)	0-30	30-60	60-90	90-120	120-150	150-180	180-210	210-240	240-270	270-300	300-330	330-360
<0.5	3301	627	474	585	1666	6487	7191	3413	3122	8668	8507	7410
1	2191	414	267	478	2369	20263	8434	4054	8435	30099	10555	4690
2	193	31	28	21	342	4980	1653	800	3075	13072	2212	620
3	18	1	1	0	40	654	212	93	998	4303	635	81
4	0	0	0	0	7	135	40	14	363	1398	153	0
5	0	0	0	0	0	16	2	10	80	389	1	0
6	0	0	0	0	0	0	0	0	0	89	0	0
7	0	0	0	0	0	0	0	0	0	0	0	0
8	0	0	0	0	0	0	0	0	0	0	0	0
9	0	0	0	0	0	0	0	0	0	0	0	0

Table 7.8: Scatter table of significant wave height-mean wave direction for site No. 1

Hs (m)/VPED (deg)	0-30	30-60	60-90	90-120	120-150	150-180	180-210	210-240	240-270	270-300	300-330	330-360
<0.5	6680	3	0	0	3984	7180	4960	2968	1476	15308	1431	7461
1	3827	0	0	0	5552	20655	5219	1728	6606	40171	2794	5697
2	448	0	0	0	545	5526	863	271	2484	14937	1163	790
3	35	0	0	0	31	750	121	44	864	4621	348	222
4	0	0	0	0	6	163	13	2	287	1513	96	30
5	0	0	0	0	0	18	0	0	56	423	1	0
6	0	0	0	0	0	0	0	0	1	88	0	0
7	0	0	0	0	0	0	0	0	0	0	0	0
8	0	0	0	0	0	0	0	0	0	0	0	0
9	0	0	0	0	0	0	0	0	0	0	0	0

Table 7.9: Scatter table of significant wave height - principal wave direction at spectral peak for site No. 1

Hs (m)/Tp (s)	1	2	3	4	5	6	7	8	9	10	11	12	13	14	15	16	17
<0.5	0.022166	4.2497	6.5854	8.93494	7.97739	5.08257	1.04455	0.7032	0.08312	0.02771	0.02272	0.04766	0	0.07924	0.04101	0.0399	0
1	0	0.0022	2.3922	2.83719	3.4667	11.0335	7.73967	11.2069	1.03624	0.24493	0.05098	0.00554	0	0	0	0	0
2	0	0	0	0.0061	0.00942	0.52532	1.21301	7.55237	4.5046	1.48676	0.11249	0.01275	0	0.00222	0	0	0
3	0	0	0	0	0	0	0.01385	1.09055	2.14341	2.33681	0.69544	0.04211	0.00055	0.00055	0	0	0
4	0	0	0	0	0	0	0	0.05264	0.29591	1.0235	0.75973	0.13521	1.1E-05	0.01164	0	0	0
5	0	0	0	0	0	0	0	0	0.01773	0.17123	0.36296	0.15239	0	0.0072	0	0	0
6	0	0	0	0	0	0	0	0	0	0.0061	0.0931	0.11582	0	0.00166	0	0	0
7	0	0	0	0	0	0	0	0	0	0	0.0072	0.02992	0	0.00222	0	0	0
8	0	0	0	0	0	0	0	0	0	0	0	0.00277	0	0	0	0	0
9	0	0	0	0	0	0	0	0	0	0	0	0	0	0.00166	0	0	0

Table 7.10: Probability of occurrence of sea states (%) at site No. 2 for 2BPA

7. WEC-Sim

Hs (m)/Tp (s)	1	2	3	4	5	6	7	8	9	10	11	12	13	14	15	16	17
<0.5	40	7669	11884	16124	14396	9172	1885	1269	150	50	41	86	0	143	74	72	0
1	0	4	4317	5120	6256	19911	13967	20224	1870	442	92	10	0	0	0	0	0
2	0	0	0	11	17	948	2189	13629	8129	2683	203	23	0	4	0	0	0
3	0	0	0	0	0	0	25	1968	3868	4217	1255	76	1	1	0	0	0
4	0	0	0	0	0	0	0	95	534	1847	1371	244	2	21	0	0	0
5	0	0	0	0	0	0	0	0	32	309	655	275	0	13	0	0	0
6	0	0	0	0	0	0	0	0	0	11	168	209	0	3	0	0	0
7	0	0	0	0	0	0	0	0	0	0	13	54	0	4	0	0	0
8	0	0	0	0	0	0	0	0	0	0	0	5	0	0	0	0	0
9	0	0	0	0	0	0	0	0	0	0	0	0	0	3	0	0	0

Table 7.11: Occurrence of sea events at site No. 2 for 2BPA

Hs (m)/Tp (s)	1	2	3	4	5	6	7	8	9	10	11	12	13	14	15	16	17
<0.5	1.87538E-05	0.0499	0.1221	0.44963	1.00113	1.5185	1.76763	1.7575	1.72813	1.55613	1.382	1.1975	0	0.89988	0.7741	0.6474	0
1	0	0.2829	1.3774	5.0995	11.1056	16.5923	19.1968	20.0761	20.5878	18.4099	15.7546	13.2765	0	0	0	0	0
2	0	0	0	19.8551	43.3174	65.5139	81.8643	86.3548	78.9911	70.2669	63.4399	54.78288	0	40.8536	0	0	0
3	0	0	0	0	0	0	189.407	187.317	188.456	163.049	144.878	126.4098	102	97.8916	0	0	0
4	0	0	0	0	0	0	0	342.637	315.221	289.056	255.316	218.3334	193	164.333	0	0	0
5	0	0	0	0	0	0	0	0	517.964	448.446	385.97	336.0656	0	252.087	0	0	0
6	0	0	0	0	0	0	0	0	0	618.459	523.973	461.4825	0	365.198	0	0	0
7	0	0	0	0	0	0	0	0	0	0	732.534	658.1968	0	493.367	0	0	0
8	0	0	0	0	0	0	0	0	0	0	0	818.3794	0	0	0	0	0
9	0	0	0	0	0	0	0	0	0	0	0	0	0	804.084	0	0	0

Table 7.12: Mechanical power matrix in terms of kilowatts for 2BPA obtained by WEC-Sim for site No. 2

Hs (m)/Tp (s)	1	2	3	4	5	6	7	8	9	10	11	12	13	14	15	16	17
<0.5	1.50E-05	0.0399	0.0977	0.3597	0.8009	1.2148	1.4141	1.406	1.3825	1.2449	1.1056	0.958	0	0.7199	0.6193	0.5179	0
1	0	0.2263	1.1019	4.0796	8.8845	13.2738	15.3574	16.0609	16.4702	14.7279	12.6037	10.6212	0	0	0	0	0
2	0	0	0	15.8841	34.6539	52.4111	65.4914	69.0838	63.1929	56.2135	50.7519	43.8263	0	32.6829	0	0	0
3	0	0	0	0	0	0	151.526	149.853	150.765	130.439	115.902	101.128	81.2827	78.3133	0	0	0
4	0	0	0	0	0	0	0	274.11	252.177	231.245	204.253	174.667	154.416	131.467	0	0	0
5	0	0	0	0	0	0	0	0	414.371	358.757	308.776	268.853	0	201.67	0	0	0
6	0	0	0	0	0	0	0	0	0	494.767	419.178	369.186	0	292.158	0	0	0
7	0	0	0	0	0	0	0	0	0	0	586.027	526.557	0	394.693	0	0	0
8	0	0	0	0	0	0	0	0	0	0	0	654.704	0	0	0	0	0
9	0	0	0	0	0	0	0	0	0	0	0	0	0	643.267	0	0	0

Table 7.13: Electrical power matrix in terms of kilowatts for 2BPA obtained by WEC-Sim for site No. 2

Hs (m)/Tp (s)	1	2	3	4	5	6	7	8	9	10	11	12	13	14	15	16	17
<0.5	3.33E-09	0.0017	0.0064	0.03214	0.06389	0.06174	0.01477	0.00989	0.00115	0.00034	0.00025	0.00046	0	0.00057	0.00025	0.0002	0
1	0	5E-06	0.0264	0.11575	0.308	1.46456	1.18861	1.79993	0.17067	0.03607	0.00643	0.00059	0	0	0	0	0
2	0	0	0	0.00097	0.00326	0.27533	0.79442	5.21746	2.84659	0.83576	0.05709	0.00559	0	0.00072	0	0	0
3	0	0	0	0	0	0	0.02099	1.63422	3.23151	3.0481	0.80604	0.04259	0.00045	0.00043	0	0	0
4	0	0	0	0	0	0	0	0.1443	0.74622	2.36678	1.55176	0.23617	1.7E-05	0.0153	0	0	0
5	0	0	0	0	0	0	0	0	0.07348	0.6143	1.12074	0.4097	0	0.01453	0	0	0
6	0	0	0	0	0	0	0	0	0	0.03016	0.39024	0.42757	0	0.00486	0	0	0
7	0	0	0	0	0	0	0	0	0	0	0.04222	0.15756	0	0.00875	0	0	0
8	0	0	0	0	0	0	0	0	0	0	0	0.01814	0	0	0	0	0
9	0	0	0	0	0	0	0	0	0	0	0	0	0	0.01069	0	0	0

Table 7.14: Electrical power matrix combined with the probability of occurrence for 2BPA at site No. 2

Hs (m)/Tp (s)	1	2	3	4	5	6	7	8	9	10	11	12	13	14	15	16	17
<0.5	1.50E-05	0.0399	0.0977	0.3597	0.8009	1.2148	1.4141	1.406	1.3825	1.2449	1.1056	0.958	0	0.7199	0.6193	0.5179	0
1	0	0.2263	1.1019	4.0796	8.8845	13.2738	15.3574	16.0609	16.4702	14.7279	12.6037	10.6212	0	0	0	0	0
2	0	0	0	15.8841	34.6539	52.4111	65.4914	69.0838	63.1929	56.2135	50.7519	43.8263	0	32.6829	0	0	0
3	0	0	0	0	0	0	108.333	108.333	108.333	108.333	108.333	101.128	81.2827	78.3133	0	0	0
4	0	0	0	0	0	0	0	108.333	108.333	108.333	108.333	108.333	108.333	108.333	0	0	0
5	0	0	0	0	0	0	0	0	108.333	108.333	108.333	108.333	0	108.333	0	0	0
6	0	0	0	0	0	0	0	0	0	108.333	108.333	108.333	0	108.333	0	0	0
7	0	0	0	0	0	0	0	0	0	0	108.333	108.333	0	108.333	0	0	0
8	0	0	0	0	0	0	0	0	0	0	0	108.333	0	0	0	0	0
9	0	0	0	0	0	0	0	0	0	0	0	0	0	108.333	0	0	0

Table 7.15: Electrical power matrix in terms of kilowatts for the 2BPA device (rated power with a capacity factor of 30% estimated at site No. 2)

Hs (m)/VMDR (deg)	0-30	30-60	60-90	90-120	120-150	150-180	180-210	210-240	240-270	270-300	300-330	330-360
<0.5	402	290	415	1868	4278	2258	1580	2201	6664	8289	27781	7109
1	260	148	345	1683	3159	964	657	1153	11751	10520	36759	4814
2	62	46	84	309	496	225	102	181	4757	3865	16786	923
3	13	11	43	209	241	121	40	88	1483	1301	7601	259
4	2	4	8	73	108	16	20	20	433	527	2840	61
5	2	2	7	34	35	6	6	8	121	116	919	28
6	0	0	0	11	11	1	1	3	31	36	291	6
7	0	0	0	2	0	0	0	0	7	15	47	0
8	0	0	0	0	0	0	0	0	0	0	5	0
9	0	0	0	0	0	0	0	0	0	0	3	0

Table 7.16: Scatter table of significant wave height-mean wave direction for site No. 2

Hs (m)/VPED (deg)	0-30	30-60	60-90	90-120	120-150	150-180	180-210	210-240	240-270	270-300	300-330	330-360
<0.5	6	10	35	1106	3736	4196	255	1555	9611	1996	23318	17311
1	1	7	40	599	3601	1682	79	1122	15514	2339	34366	12863
2	0	3	23	166	542	370	14	309	5848	720	15250	4591
3	0	0	19	122	227	211	1	123	1842	307	6966	1592
4	0	0	0	43	111	57	4	19	575	122	2766	415
5	0	0	0	20	52	10	5	10	130	55	881	121
6	0	0	0	0	20	2	0	2	44	10	276	37
7	0	0	0	0	2	0	0	0	7	14	43	5
8	0	0	0	0	0	0	0	0	0	0	5	0
9	0	0	0	0	0	0	0	0	0	0	3	0

Table 7.17: Scatter table of significant wave height - principal wave direction at spectral peak for site No. 2

Hs (m)/Tp (s)	1	2	3	4	5	6	7	8	9	10	11	12	13	14	15	16	17
<0.5	0.018841	2.9746	9.7346	17.9353	10.1435	4.21091	1.05674	0.88718	0.16569	0.0931	0.02383	0.00942	0	0	0	0	0
1	0	0.0028	0.5946	4.76172	10.164	16.883	6.58595	3.3204	0.3408	0.10917	0.02882	0.00776	0	0	0	0	0
2	0	0	0	0	0.07425	1.00743	2.17943	4.36884	0.18342	0.05264	0.01718	0.00111	0	0.00111	0	0	0
3	0	0	0	0	0	0.00499	0.07869	1.30278	0.27153	0.02715	0.00222	0.00111	0.00055	0	0	0	0
4	0	0	0	0	0	0	0	0.13798	0.15682	0.03768	0	0	0	0	0	0	0
5	0	0	0	0	0	0	0	0.00332	0.01773	0.01552	0.00222	0	0	0	0	0	0
6	0	0	0	0	0	0	0	0	0.00166	0.00055	0	0	0	0	0	0	0
7	0	0	0	0	0	0	0	0	0	0	0	0	0	0	0	0	0
8	0	0	0	0	0	0	0	0	0	0	0	0	0	0	0	0	0
9	0	0	0	0	0	0	0	0	0	0	0	0	0	0	0	0	0

Table 7.18: Probability of occurrence of sea states (%) at site No. 3 for 2BPA

Hs (m)/Tp (s)	1	2	3	4	5	6	7	8	9	10	11	12	13	14	15	16	17
<0.5	34	5368	17567	32366	18305	7599	1907	1601	299	168	43	17	0	0	0	0	0
1	0	5	1073	8593	18342	30467	11885	5992	615	197	52	14	0	0	0	0	0
2	0	0	0	0	134	1818	3933	7884	331	95	31	2	0	2	0	0	0
3	0	0	0	0	0	9	142	2351	490	49	4	2	1	0	0	0	0
4	0	0	0	0	0	0	0	249	283	68	0	0	0	0	0	0	0
5	0	0	0	0	0	0	0	6	32	28	4	0	0	0	0	0	0
6	0	0	0	0	0	0	0	0	3	1	0	0	0	0	0	0	0
7	0	0	0	0	0	0	0	0	0	0	0	0	0	0	0	0	0
8	0	0	0	0	0	0	0	0	0	0	0	0	0	0	0	0	0
9	0	0	0	0	0	0	0	0	0	0	0	0	0	0	0	0	0

Table 7.19: Occurrence of sea events at site No. 3 for 2BPA

Hs (m)/Tp (s)	1	2	3	4	5	6	7	8	9	10	11	12	13	14	15	16	17
<0.5	1.87538E-05	0.0499	0.1221	0.44963	1.00113	1.5185	1.76763	1.7575	1.72813	1.55613	1.382	1.1975	0	0	0	0	0
1	0	0.2829	1.3774	5.0995	11.1056	16.5923	19.1968	20.0761	20.5878	18.4099	15.7546	13.2765	0	0	0	0	0
2	0	0	0	0	43.3174	65.5139	81.8643	86.3548	78.9911	70.2669	63.4399	54.78288	0	40.8536	0	0	0
3	0	0	0	0	0	138.686	189.407	187.317	188.456	163.049	144.878	126.4098	102	0	0	0	0
4	0	0	0	0	0	0	0	342.637	315.221	289.056	0	0	0	0	0	0	0
5	0	0	0	0	0	0	0	525.299	517.964	448.446	385.97	0	0	0	0	0	0
6	0	0	0	0	0	0	0	0	742.636	618.459	0	0	0	0	0	0	0
7	0	0	0	0	0	0	0	0	0	0	0	0	0	0	0	0	0
8	0	0	0	0	0	0	0	0	0	0	0	0	0	0	0	0	0
9	0	0	0	0	0	0	0	0	0	0	0	0	0	0	0	0	0

Table 7.20: Mechanical power matrix in terms of kilowatts for 2BPA obtained by WEC-Sim for site No. 3

Hs (m)/Tp (s)	1	2	3	4	5	6	7	8	9	10	11	12	13	14	15	16	17
<0.5	1.50E-05	0.0399	0.0977	0.3597	0.8009	1.2148	1.4141	1.406	1.3825	1.2449	1.1056	0.958	0	0	0	0	0
1	0	0.2263	1.1019	4.0796	8.8845	13.2738	15.3574	16.0609	16.4702	14.7279	12.6037	10.6212	0	0	0	0	0
2	0	0	0	0	34.6539	52.4111	65.4914	69.0838	63.1929	56.2135	50.7519	43.8263	0	32.6829	0	0	0
3	0	0	0	0	0	110.948	151.526	149.853	150.765	130.439	115.902	101.128	81.2827	0	0	0	0
4	0	0	0	0	0	0	0	274.11	252.177	231.245	0	0	0	0	0	0	0
5	0	0	0	0	0	0	0	420.24	414.371	358.757	308.776	0	0	0	0	0	0
6	0	0	0	0	0	0	0	0	594.109	494.767	0	0	0	0	0	0	0
7	0	0	0	0	0	0	0	0	0	0	0	0	0	0	0	0	0
8	0	0	0	0	0	0	0	0	0	0	0	0	0	0	0	0	0
9	0	0	0	0	0	0	0	0	0	0	0	0	0	0	0	0	0

Table 7.21: Electrical power matrix in terms of kilowatts for 2BPA obtained by WEC-Sim for site No. 3

Hs (m)/Tp (s)	1	2	3	4	5	6	7	8	9	10	11	12	13	14	15	16	17
<0.5	2.83E-09	0.0012	0.0095	0.06451	0.08124	0.05115	0.01494	0.01247	0.00229	0.00116	0.00026	9E-05	0	0	0	0	0
1	0	6E-06	0.0066	0.19426	0.90302	2.24101	1.01143	0.53329	0.05613	0.01608	0.00363	0.00082	0	0	0	0	0
2	0	0	0	0	0.02573	0.528	1.42734	3.01816	0.11591	0.02959	0.00872	0.00049	0	0.00036	0	0	0
3	0	0	0	0	0	0.00553	0.11923	1.95226	0.40937	0.03542	0.00257	0.00112	0.00045	0	0	0	0
4	0	0	0	0	0	0	0	0.37822	0.39547	0.08714	0	0	0	0	0	0	0
5	0	0	0	0	0	0	0	0.01397	0.07348	0.05566	0.00684	0	0	0	0	0	0
6	0	0	0	0	0	0	0	0	0.00988	0.00274	0	0	0	0	0	0	0
7	0	0	0	0	0	0	0	0	0	0	0	0	0	0	0	0	0
8	0	0	0	0	0	0	0	0	0	0	0	0	0	0	0	0	0
9	0	0	0	0	0	0	0	0	0	0	0	0	0	0	0	0	0

Table 7.22: Electrical power matrix combined with the probability of occurrence for 2BPA at site No. 3

Hs (m)/Tp (s)	1	2	3	4	5	6	7	8	9	10	11	12	13	14	15	16	17
<0.5	1.50E-05	0.0399	0.0977	0.3597	0.8009	1.2148	1.4141	1.406	1.3825	1.2449	1.1056	0.958	0	0	0	0	0
1	0	0.2263	1.1019	4.0796	8.8845	13.2738	15.3574	16.0609	16.4702	14.7279	12.6037	10.6212	0	0	0	0	0
2	0	0	0	0	34.6539	46.3333	46.3333	46.3333	46.3333	46.3333	46.3333	43.8263	0	32.6829	0	0	0
3	0	0	0	0	0	46.3333	46.3333	46.3333	46.3333	46.3333	46.3333	46.3333	46.3333	0	0	0	0
4	0	0	0	0	0	0	0	46.3333	46.3333	46.3333	0	0	0	0	0	0	0
5	0	0	0	0	0	0	0	46.3333	46.3333	46.3333	46.3333	0	0	0	0	0	0
6	0	0	0	0	0	0	0	0	46.3333	46.3333	0	0	0	0	0	0	0
7	0	0	0	0	0	0	0	0	0	0	0	0	0	0	0	0	0
8	0	0	0	0	0	0	0	0	0	0	0	0	0	0	0	0	0
9	0	0	0	0	0	0	0	0	0	0	0	0	0	0	0	0	0

Table 7.23: Electrical power matrix in terms of kilowatts for the 2BPA device (rated power with a capacity factor of 30% estimated at site No. 3)

Hs (m)/VMDR (deg)	0-30	30-60	60-90	90-120	120-150	150-180	180-210	210-240	240-270	270-300	300-330	330-360
<0.5	51	40	20	63	2527	7937	12598	17113	21366	21235	2039	285
1	39	24	28	56	4532	11759	13768	10060	23476	8824	4119	550
2	0	0	0	0	399	2083	2167	2084	6600	525	364	8
3	0	0	0	0	44	270	487	462	1667	109	8	0
4	0	0	0	0	0	36	111	112	315	26	0	0
5	0	0	0	0	0	3	14	12	41	0	0	0
6	0	0	0	0	0	2	2	0	0	0	0	0
7	0	0	0	0	0	0	0	0	0	0	0	0
8	0	0	0	0	0	0	0	0	0	0	0	0
9	0	0	0	0	0	0	0	0	0	0	0	0

Table 7.24: Scatter table of significant wave height-mean wave direction for site No. 3

Hs (m)/VPED (deg)	0-30	30-60	60-90	90-120	120-150	150-180	180-210	210-240	240-270	270-300	300-330	330-360
<0.5	4	9	4	9	9263	2133	14820	15631	14476	20581	8300	44
1	0	2	0	6	8492	3735	15829	10545	21149	12341	5123	13
2	0	0	0	0	814	856	3274	1579	4953	2537	217	0
3	0	0	0	0	121	82	674	382	1234	554	0	0
4	0	0	0	0	4	23	157	71	254	91	0	0
5	0	0	0	0	0	2	14	13	23	18	0	0
6	0	0	0	0	0	2	0	2	0	0	0	0
7	0	0	0	0	0	0	0	0	0	0	0	0
8	0	0	0	0	0	0	0	0	0	0	0	0
9	0	0	0	0	0	0	0	0	0	0	0	0

Table 7.25: Scatter table of significant wave height - principal wave direction at spectral peak for site No. 3

Hs (m)/Tp (s)	1	2	3	4	5	6	7	8	9	10	11	12	13	14	15	16	17	18	19	20
<0.5	0	0.003	0.075	0.38	0.325	0.224	0.18	0.151	0.207	0.137	0.125	0.074	0.046	0.029	0.014	0.005	0	0	0	0
1	0	0	0.108	1.472	6.169	7.705	4.416	4.341	3.64	2.141	1.348	1.27	0.876	0.508	0.335	0.127	0.043	0.014	0.005	0.003
2	0	0	0	0	0.626	6.848	9.281	5.046	3.29	3.561	2.45	1.181	0.744	0.599	0.412	0.175	0.06	0.019	0.002	0
3	0	0	0	0	0	0.123	2.685	7.649	2.514	1.239	1.389	1.004	0.431	0.24	0.152	0.082	0.033	0.017	0	0
4	0	0	0	0	0	0	0.009	1.53	3.727	0.943	0.537	0.383	0.27	0.166	0.074	0.019	0.002	0.002	0	0
5	0	0	0	0	0	0	0	0.003	0.787	1.148	0.356	0.183	0.127	0.113	0.015	0.01	0.002	0.002	0	0
6	0	0	0	0	0	0	0	0	0.005	0.378	0.364	0.11	0.034	0.029	0.01	0	0	0.003	0	0
7	0	0	0	0	0	0	0	0	0	0.003	0.062	0.055	0.033	0.029	0.027	0.003	0	0	0	0
8	0	0	0	0	0	0	0	0	0	0	0.003	0.019	0.022	0.012	0.009	0.014	0	0	0	0
9	0	0	0	0	0	0	0	0	0	0	0	0.003	0.003	0.007	0.003	0.005	0	0	0	0

Table 7.26: Probability of occurrence of sea states (%) at site No. 4 for 2BPA

Hs (m)/Tp (s)	1	2	3	4	5	6	7	8	9	10	11	12	13	14	15	16	17	18	19	20
<0.5	0	2	44	222	190	131	105	88	121	80	73	43	27	17	8	3	0	0	0	0
1	0	0	63	860	3605	4503	2581	2537	2127	1251	788	742	512	297	196	74	25	8	3	2
2	0	0	0	0	366	4002	5424	2949	1923	2081	1432	690	435	350	241	102	35	11	1	0
3	0	0	0	0	0	72	1569	4470	1469	724	812	587	252	140	89	48	19	10	0	0
4	0	0	0	0	0	0	5	894	2178	551	314	224	158	97	43	11	1	1	0	0
5	0	0	0	0	0	0	0	2	460	671	208	107	74	66	9	6	1	1	0	0
6	0	0	0	0	0	0	0	0	3	221	213	64	20	17	6	0	0	2	0	0
7	0	0	0	0	0	0	0	0	0	2	36	32	19	17	16	2	0	0	0	0
8	0	0	0	0	0	0	0	0	0	0	2	11	13	7	5	8	0	0	0	0
9	0	0	0	0	0	0	0	0	0	0	0	2	2	4	2	3	0	0	0	0

Table 7.27: Occurrence of sea events at site No. 4 for 2BPA

Hs (m)/Tp (s)	1	2	3	4	5	6	7	8	9	10	11	12	13	14	15	16	17	18	19	20
<0.5	0	0.05	0.12	0.45	1.001	1.5185	1.7676	1.7575	1.7281	1.5561	1.382	1.1975	1.0331	0.8533	0.7345	0.6398	0	0	0	0
1	0	0	1.38	5.1	11.11	16.592	19.197	20.076	20.588	18.41	15.755	13.2765	11.171	10.704	8.8101	7.739	6.2233	5.4736	4.669	4.46
2	0	0	0	0	43.32	65.514	81.864	86.355	78.991	70.267	63.44	54.7829	50.582	40.854	36.568	32.252	27.003	21.803	20.7	0
3	0	0	0	0	0	138.69	189.41	187.32	188.46	163.05	144.88	126.41	101.6	91.746	83.639	70.169	56.562	52.168	0	0
4	0	0	0	0	0	0	311.87	342.64	315.22	289.06	258.37	201.859	198.41	163.53	143.49	117.98	104.18	94.465	0	0
5	0	0	0	0	0	0	0	525.3	506.61	448.45	385.97	346.037	281.24	265.53	228.35	184.24	170.73	146.35	0	0
6	0	0	0	0	0	0	0	0	742.64	618.46	550.79	494.357	444.56	355.58	315.75	0	0	215.34	0	0
7	0	0	0	0	0	0	0	0	0	851.88	771.1	673.333	607.96	518.49	438.38	405.18	0	0	0	0
8	0	0	0	0	0	0	0	0	0	0	937.18	845.087	769.52	647.53	561.15	491.82	0	0	0	0
9	0	0	0	0	0	0	0	0	0	0	0	1075.81	974.59	883.14	725.77	613.68	0	0	0	0

Table 7.28: Mechanical power matrix in terms of kilowatts for 2BPA obtained by WEC-Sim for site No. 4

Hs (m)/Tp (s)	1	2	3	4	5	6	7	8	9	10	11	12	13	14	15	16	17	18	19	20
<0.5	0	0	0.1	0.4	0.8	1.215	1.414	1.406	1.383	1.245	1.106	0.958	0.827	0.683	0.588	0.512	0	0	0	0
1	0	0	1.1	4.1	8.88	13.27	15.36	16.06	16.47	14.73	12.6	10.62	8.937	8.563	7.048	6.191	4.979	4.379	3.73	3.6
2	0	0	0	0	34.7	52.41	65.49	69.08	63.19	56.21	50.75	43.83	40.47	32.68	29.25	25.8	21.6	17.44	16.6	0
3	0	0	0	0	0	110.9	151.5	149.9	150.8	130.4	115.9	101.1	81.28	73.4	66.91	56.14	45.25	41.73	0	0
4	0	0	0	0	0	0	249.5	274.1	252.2	231.2	206.7	161.5	158.7	130.8	114.8	94.39	83.35	75.57	0	0
5	0	0	0	0	0	0	0	420.2	405.3	358.8	308.8	276.8	225	212.4	182.7	147.4	136.6	117.1	0	0
6	0	0	0	0	0	0	0	0	594.1	494.8	440.6	395.5	355.7	284.5	252.6	0	0	172.3	0	0
7	0	0	0	0	0	0	0	0	0	681.5	616.9	538.7	486.4	414.8	350.7	324.1	0	0	0	0
8	0	0	0	0	0	0	0	0	0	0	749.7	676.1	615.6	518	448.9	393.5	0	0	0	0
9	0	0	0	0	0	0	0	0	0	0	0	860.7	779.7	706.5	580.6	490.9	0	0	0	0

Table 7.29: Electrical power matrix in terms of kilowatts for 2BPA obtained by WEC-Sim for site No. 4

Hs (m)/Tp (s)	1	2	3	4	5	6	7	8	9	10	11	12	13	14	15	16	17	18	19	20
<0.5	0	0	0	0	0	0.003	0.003	0.002	0.003	0.002	0.001	7E-04	4E-04	2E-04	8E-05	3E-05	0	0	0	0
1	0	0	0	0.1	0.55	1.023	0.678	0.697	0.599	0.315	0.17	0.135	0.078	0.044	0.024	0.008	0.002	6E-04	0	0
2	0	0	0	0	0.22	3.589	6.078	3.486	2.079	2.002	1.244	0.517	0.301	0.196	0.121	0.045	0.013	0.003	0	0
3	0	0	0	0	0	0.137	4.068	11.46	3.79	1.616	1.61	1.016	0.35	0.176	0.102	0.046	0.015	0.007	0	0
4	0	0	0	0	0	0	0.021	4.193	9.398	2.18	1.111	0.619	0.429	0.217	0.084	0.018	0.001	0.001	0	0
5	0	0	0	0	0	0	0	0.014	3.19	4.119	1.099	0.507	0.285	0.24	0.028	0.015	0.002	0.002	0	0
6	0	0	0	0	0	0	0	0	0.03	1.871	1.606	0.433	0.122	0.083	0.026	0	0	0.006	0	0
7	0	0	0	0	0	0	0	0	0	0.023	0.38	0.295	0.158	0.121	0.096	0.011	0	0	0	0
8	0	0	0	0	0	0	0	0	0	0	0.026	0.127	0.137	0.062	0.038	0.054	0	0	0	0
9	0	0	0	0	0	0	0	0	0	0	0	0.029	0.027	0.048	0.02	0.025	0	0	0	0

Table 7.30: Electrical power matrix combined with the probability of occurrence for 2BPA at site No. 4

Hs (m)/Tp (s)	1	2	3	4	5	6	7	8	9	10	11	12	13	14	15	16	17	18	19	20
<0.5	0	0	0.1	0.4	0.8	1.215	1.414	1.406	1.383	1.245	1.106	0.958	0.827	0.683	0.588	0.512	0	0	0	0
1	0	0	1.1	4.1	8.88	13.27	15.36	16.06	16.47	14.73	12.6	10.62	8.937	8.563	7.048	6.191	4.979	4.379	3.73	3.6
2	0	0	0	0	34.7	52.41	65.49	69.08	63.19	56.21	50.75	43.83	40.47	32.68	29.25	25.8	21.6	17.44	16.6	0
3	0	0	0	0	0	110.9	151.5	149.9	150.8	130.4	115.9	101.1	81.28	73.4	66.91	56.14	45.25	41.73	0	0
4	0	0	0	0	0	0	249.5	274.1	252.2	231.2	206.7	161.5	158.7	130.8	114.8	94.39	83.35	75.57	0	0
5	0	0	0	0	0	0	0	274.4	274.4	274.4	274.4	274.4	225	212.4	182.7	147.4	136.6	117.1	0	0
6	0	0	0	0	0	0	0	0	274.4	274.4	274.4	274.4	274.4	274.4	252.6	0	0	172.3	0	0
7	0	0	0	0	0	0	0	0	0	274.4	274.4	274.4	274.4	274.4	274.4	274.4	0	0	0	0
8	0	0	0	0	0	0	0	0	0	0	274.4	274.4	274.4	274.4	274.4	274.4	0	0	0	0
9	0	0	0	0	0	0	0	0	0	0	0	274.4	274.4	274.4	274.4	274.4	0	0	0	0

Table 7.31: Electrical power matrix in terms of kilowatts for the 2BPA device (rated power with a capacity factor of 30% estimated at site No. 4)

Hs (m)/VMDR (deg)	0-30	30-60	60-90	90-120	120-150	150-180	180-210	210-240	240-270	270-300	300-330	330-360
<0.5	125	24	27	54	53	125	102	90	64	92	152	246
1	1944	361	368	1078	1355	1324	1817	1578	1323	2113	2486	4420
2	1406	322	337	1395	1478	1194	1661	1677	1607	2210	2493	4254
3	613	135	173	787	696	581	772	882	839	1256	1387	2137
4	219	65	87	347	289	295	349	395	360	585	606	879
5	70	28	30	125	123	96	151	150	149	233	182	266
6	20	12	5	60	41	23	49	50	38	80	69	99
7	6	2	1	9	11	2	16	17	15	13	14	18
8	2	0	0	0	1	0	4	16	5	8	4	6
9	2	0	0	0	0	0	1	3	1	1	3	2

Table 7.32: Scatter table of significant wave height-mean wave direction for site No. 4

Hs (m)/VPED (deg)	0-30	30-60	60-90	90-120	120-150	150-180	180-210	210-240	240-270	270-300	300-330	330-360
<0.5	201	9	20	39	70	129	116	74	37	54	156	249
1	3296	164	167	1032	1250	1443	2170	1557	702	1119	2824	4441
2	2187	103	144	1307	1449	1362	2030	1621	879	896	3117	4933
3	978	34	76	733	727	643	995	872	462	552	1656	2525
4	381	24	37	326	305	306	430	378	196	216	811	1064
5	107	12	9	125	122	117	164	156	69	106	277	340
6	31	1	0	55	43	26	57	46	29	38	96	124
7	6	0	0	10	12	7	16	19	5	8	18	23
8	0	0	0	0	1	0	9	11	3	4	9	9
9	0	0	0	0	0	0	3	1	1	2	1	5

Table 7.33: Scatter table of significant wave height - principal wave direction at spectral peak for site No. 4

In order to estimate the annual energy production (AEP) for the 2BPA at site No. 1, 2, and 3, the following equation was used [17]:

$$AEP = P_{ae} \times 8766(hours) \times \beta \tag{7.1}$$

where $\beta = \eta_2 \times \eta_3$ is the parameter that accounts for the losses caused by transmission efficiency $\eta_3 = 0.98$ (98%) and device availability $\eta_2 = 0.95(95\%)$. Table 7.34 shows a summary of the power performance for the 2BPA at sites listed in Table 7.1. As can be seen from the table given below, the estimated rated power and AEP at site No. 2 (Sea of Sardinia) for 2BPA are higher compared to site No. 1 (Sea of Sicily) and site No. 3 (Tyrrhenian Sea). Hence, it was concluded that in the Mediterranean Sea of Italy, the Sea of Sardinia is the best location to deploy the 2BPA since the power performance at this site is higher compared to the power performance at the Sea of Sicily and the Tyrrhenian Sea. However, at site No. 4 (North Sea), the power performance is even higher compared to the sites No. 1-3 because in the North Sea, the annual average electrical power, P_{ae} is 82.31 kW while at site No. 1 is 25.5 kW, at site No. 2 is 32.5 kW, and at site No. 3 is 13.9 kW.

Site No.	Rated Power kW	Annual Energy Production (AEP) MWh
1	85 kW	208.10 MWh
2	108.33 kW	265.23 MWh
3	46.33 kW	113.44 MWh
4	274.4 kW	671.7439 MWh

Table 7.34: 2BPA rated power and AEP

The dynamic response of the 2BPA device was simulated for sea state $H_s = 2\ m$ and $T_p = 8\ sec$, and for water depth -70 m and shown in Figures 7.41-7.60. For 2BPA, three mooring lines were considered to keep the device in its location. The type of the mooring lines is chain. Mooring lines are of the chain type. All mooring lines data are given in the MoorDyn input file lines.txt. This file is located inside the MoorDyn\mooring folder. In this thesis, the mooring lines data in lines.txt were not changed and remained the default. The WEC-Sim input file used to simulate the moored 2BPA was previously given in Script 7.4.
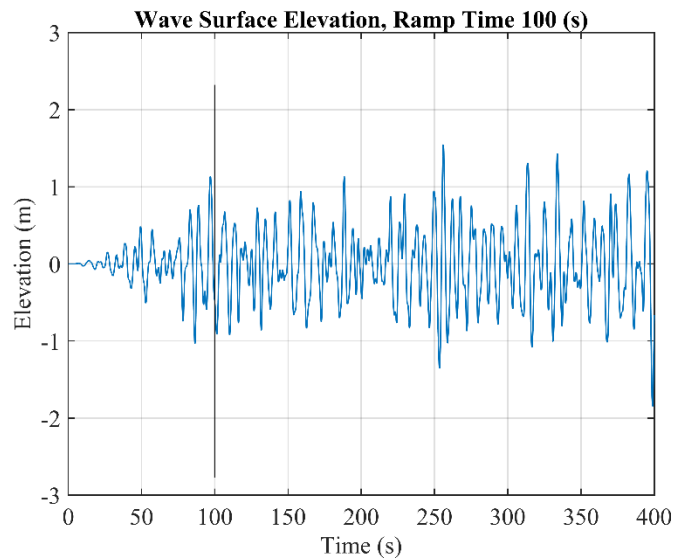
Figure 7.41: Irregular wave surface elevation in moored 2BPA simulation
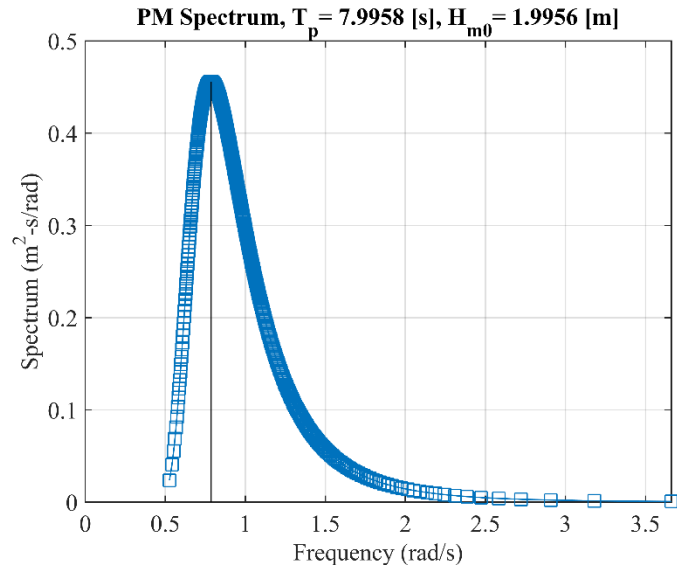
Figure 7.42: Pierson Moskowitz (PM) spectrum in moored 2BPA simulation for irregular wave state
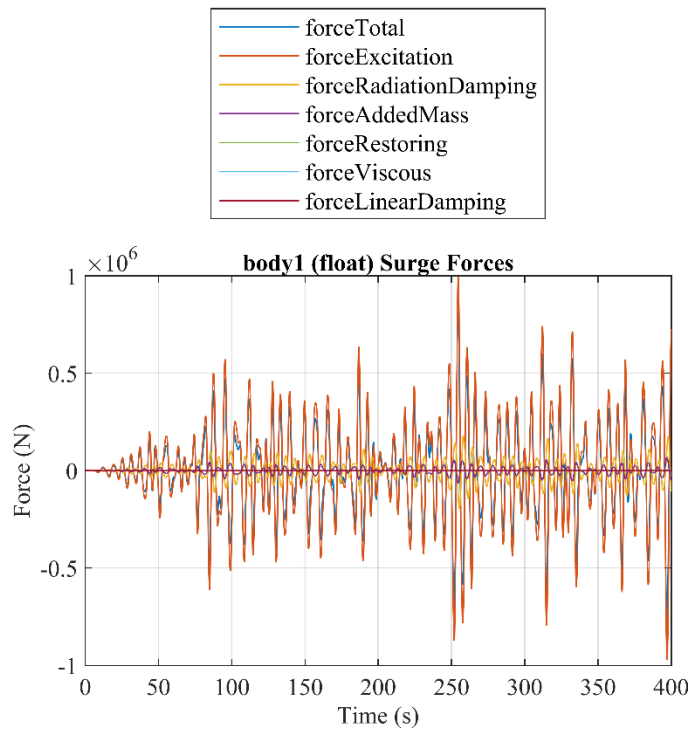
Figure 7.43: Float surge forces in irregular wave state for moored case
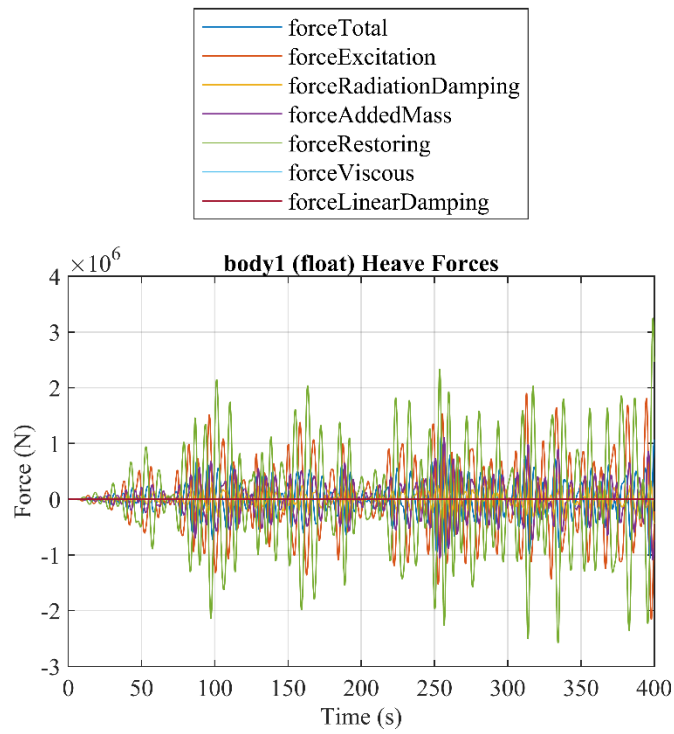
Figure 7.44: Float heave forces in irregular wave state for moored case
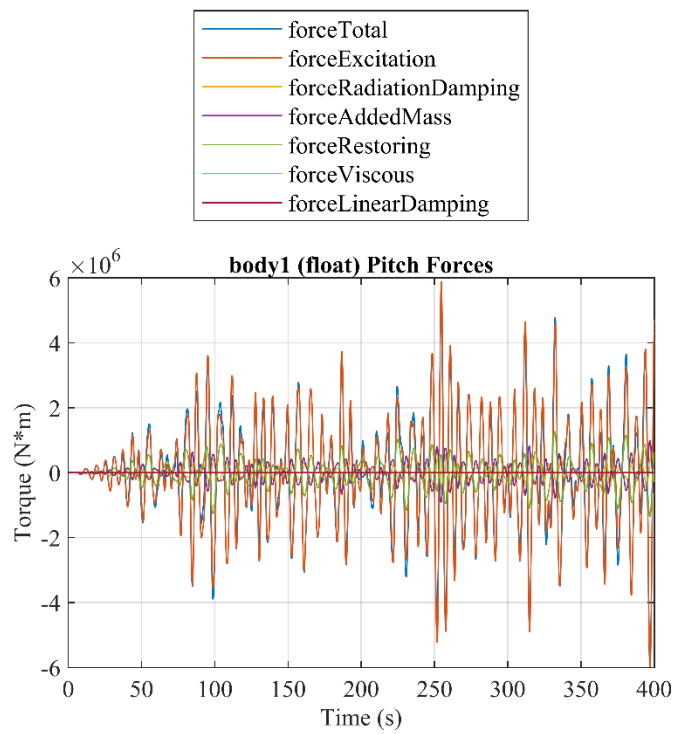
Figure 7.45: Float pitch forces in irregular wave state for moored case
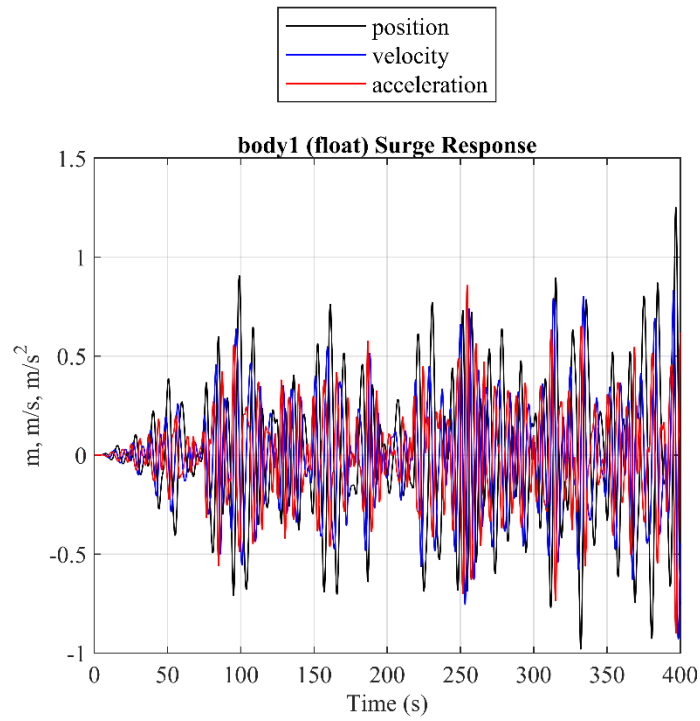
Figure 7.46: Float surge response in irregular wave state for moored case
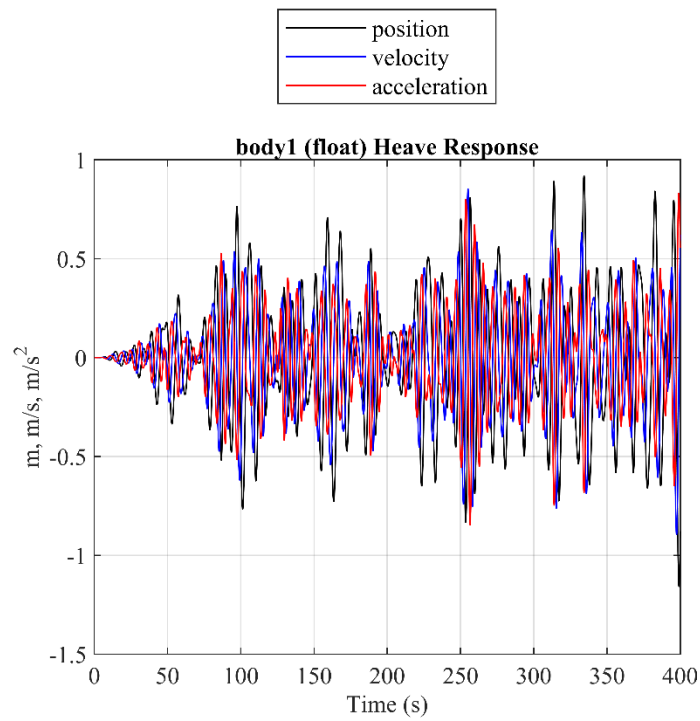
Figure 7.47: Float heave response in irregular wave state for moored case
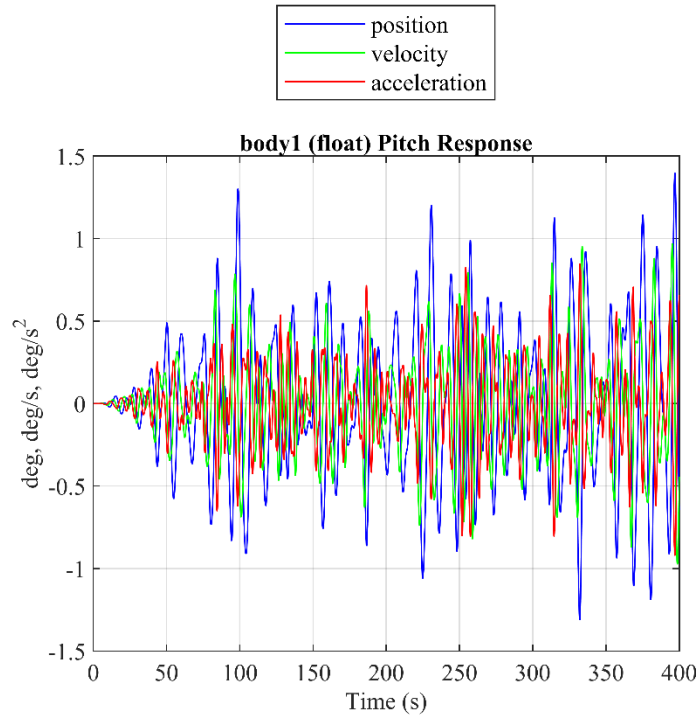
Figure 7.48: Float pitch response in irregular wave state for moored case
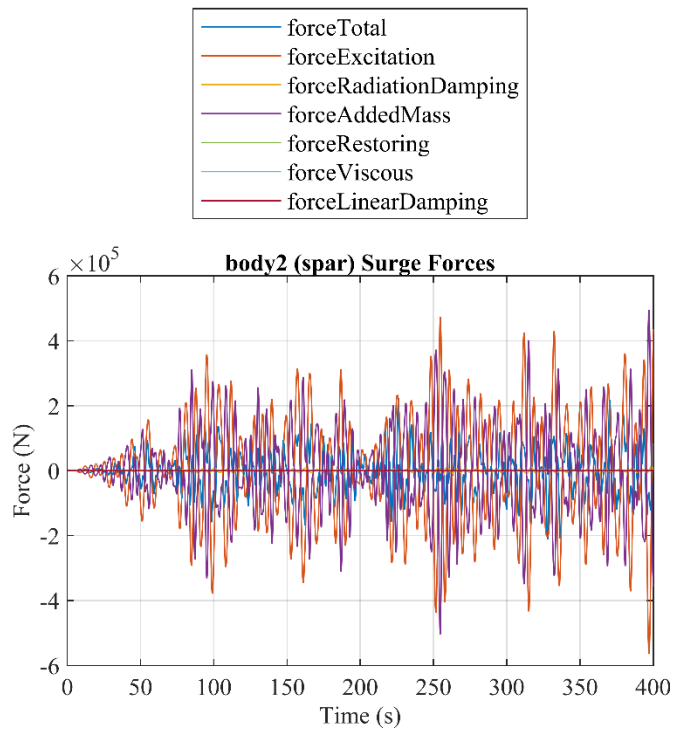
Figure 7.49: Spar surge forces in irregular wave state for moored case
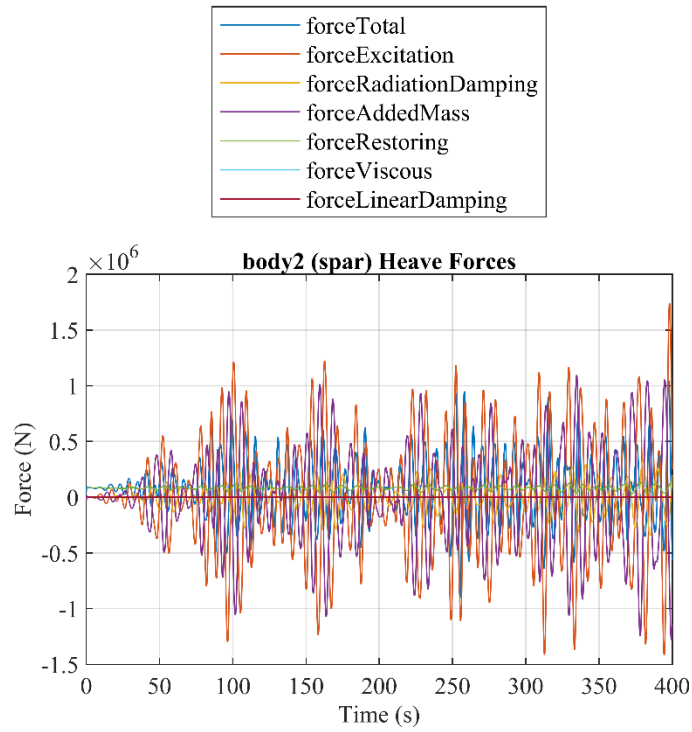
Figure 7.50: Spar heave forces in irregular wave state for moored case
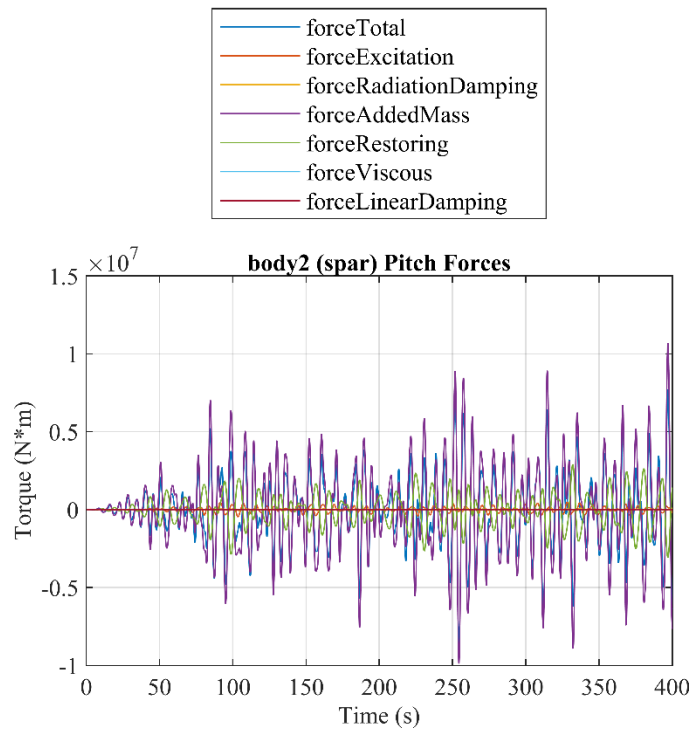
Figure 7.51: Spar pitch forces in irregular wave state for moored case
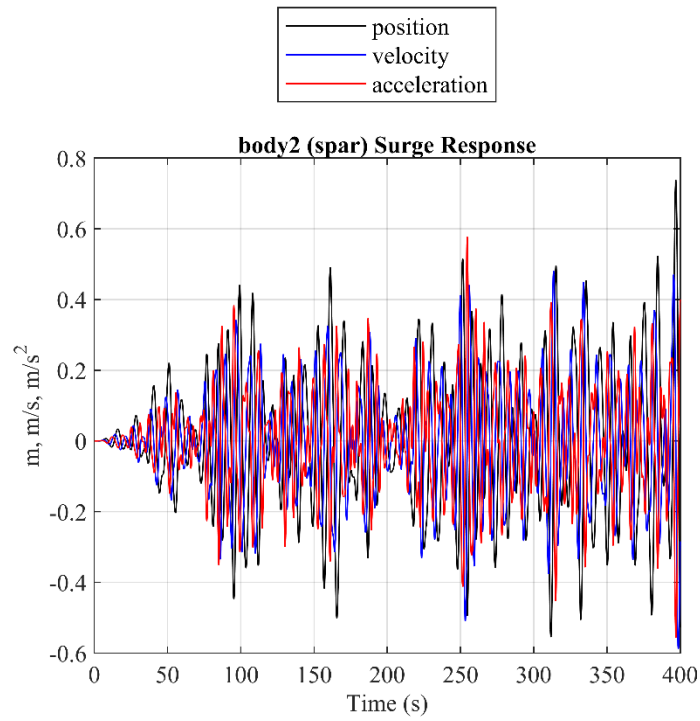
Figure 7.52: Spar surge response in irregular wave state for moored case
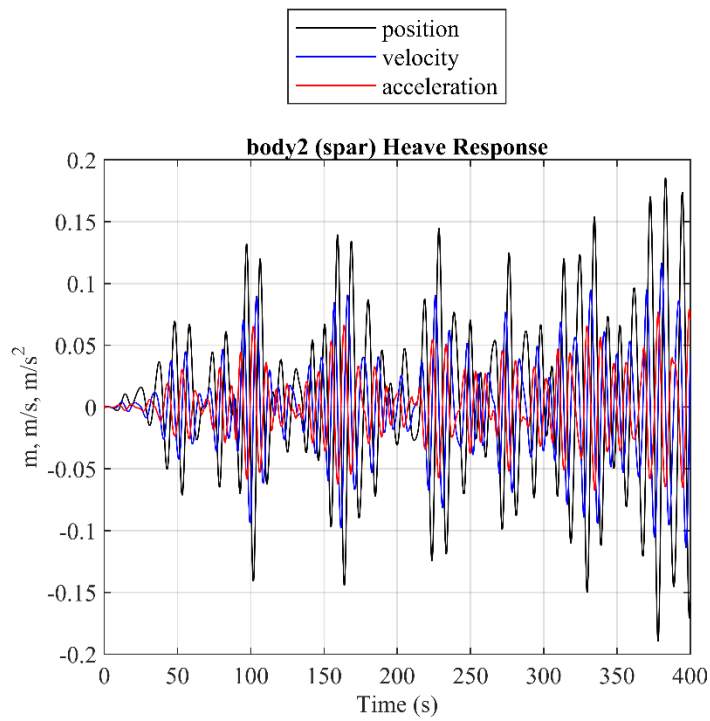
Figure 7.53: Spar heave response in irregular wave state for moored case

159
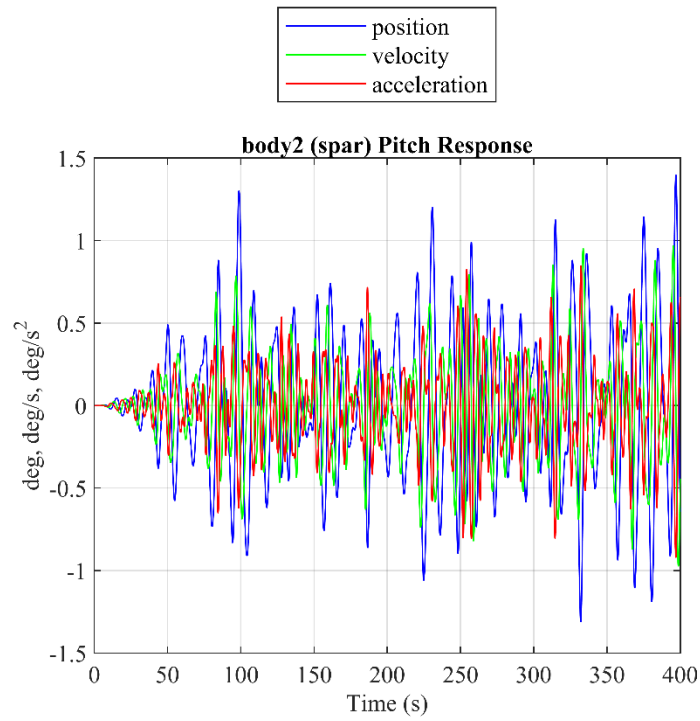
Figure 7.54: Spar pitch response in irregular wave state for moored case
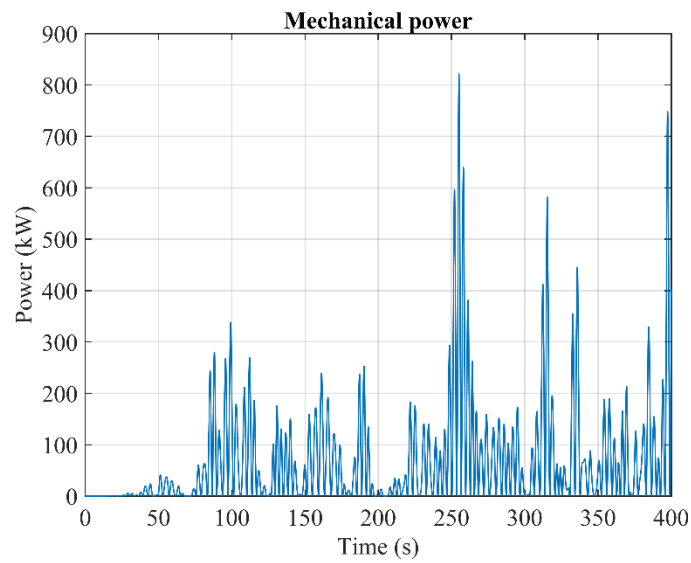
Figure 7.55: 2BPA mechanical power in irregular wave state for moored case
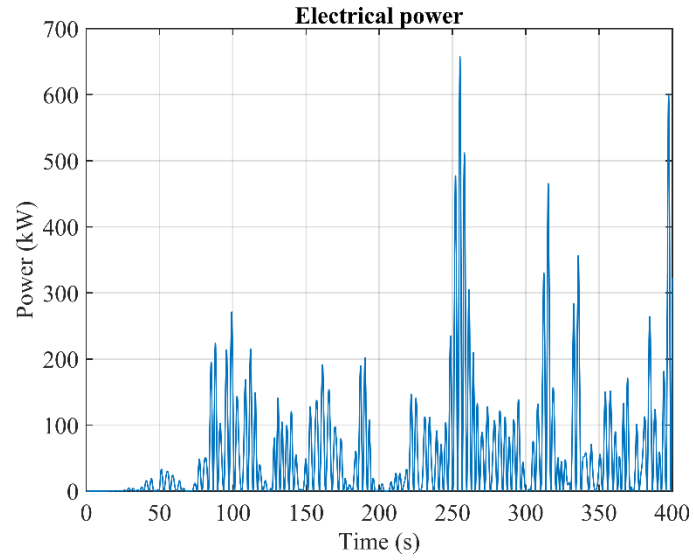
Figure 7.56: 2BPA electrical power in irregular wave state for moored case
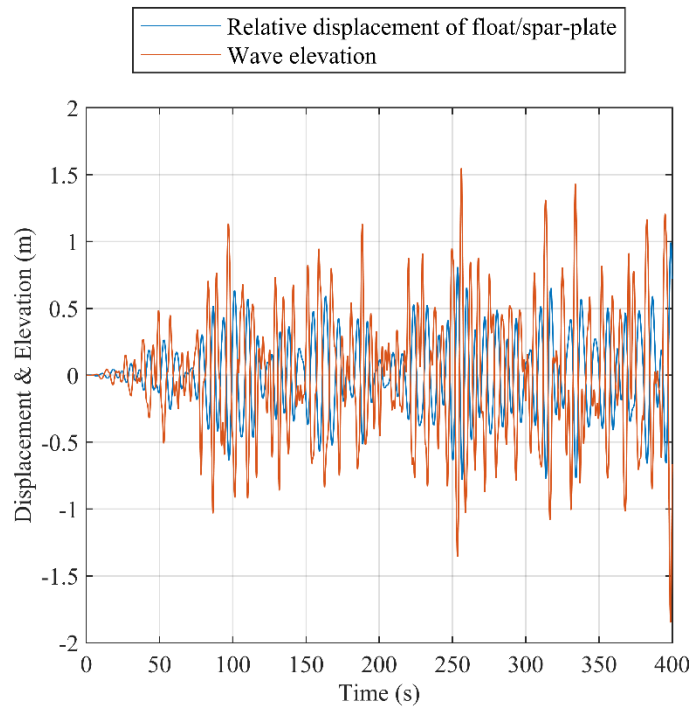
Figure 7.57: Relative displacement of float/spar-plate and wave elevation in irregular wave state for moored case
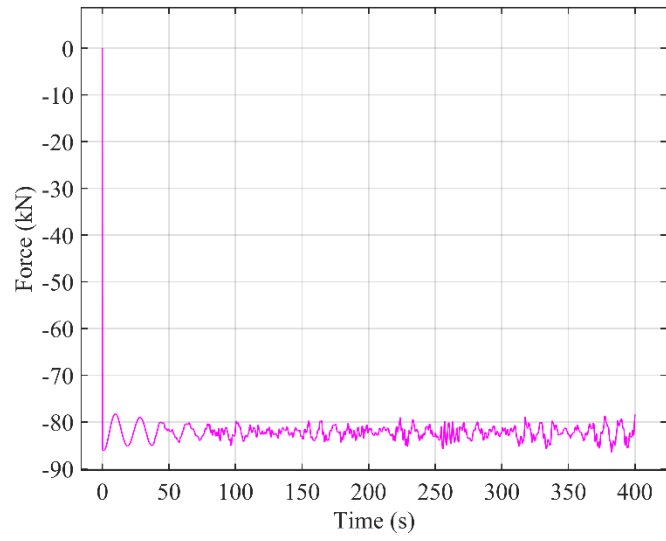
Figure 7.58: Mooring heave force in irregular wave state
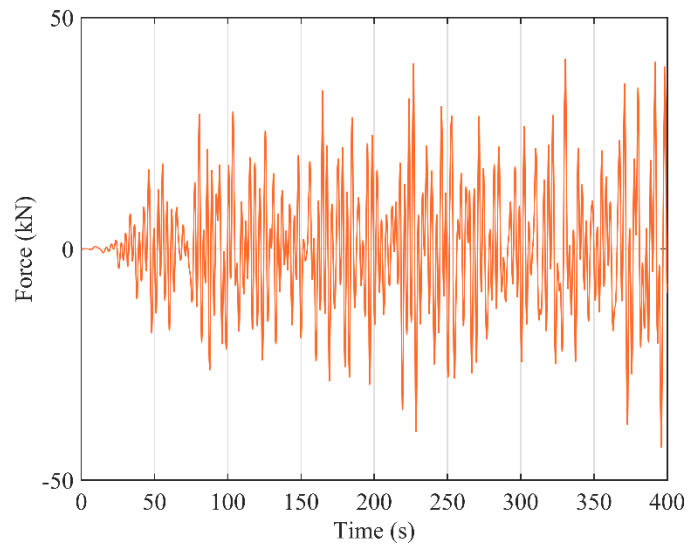
Figure 7.59: Mooring surge force in irregular wave state
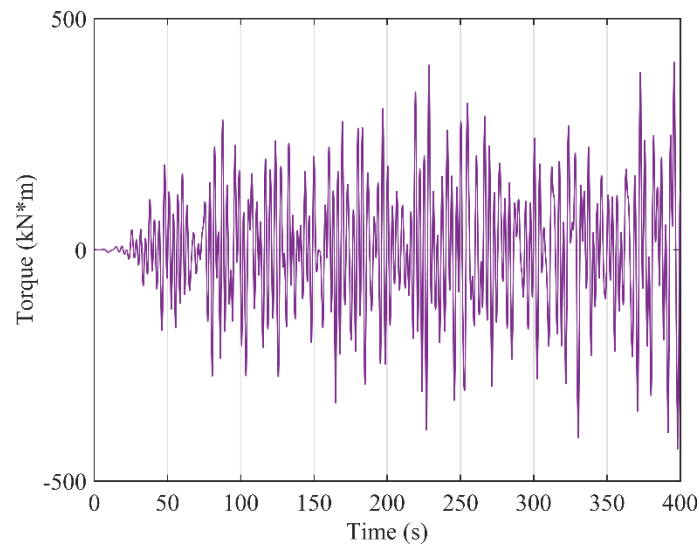
Figure 7.60: Mooring pitch force in irregular wave state

7.2.5 Dynamic Response of OSWEC in Irregular Wave State

In order to estimate the OSWEC device's power performance, two sites were assumed; one in the Sea of Sicily and another in the Adriatic Sea. Table 7.35 shows the site's data in which the fifth and sixth sites are defined for the deployment of the OSWEC device.

Tables 7.36 and 7.44 indicate the probability of occurrence of sea states for sites No. 5 and 6. Tables 7.37 and 7.45 indicate the occurrence of sea states recorded during 20 years for sites No. 5 and 6.

Tables 7.38 and 7.46 are the mechanical power matrix of OSWEC calculated by WEC-Sim for sites No. 5 and 6. Tables 7.39 and 7.47 are the electrical power matrix of OSWEC obtained by WEC-Sim for sites No. 5 and 6.

Tables 7.40 and 7.48 are the electrical power matrices combined with the probability of occurrence for 2BPA at sites No. 5 and 6. Tables 7.41 and 7.49 are electrical power matrices for the OSWEC device (rated power with a capacity factor of 30%) estimated at sites No. 5 and 6.

Tables 7.42 and 7.50 are the scatter tables of the significant wave height versus mean wave direction for sites No. 5 and 6. Tables 7.43 and 7.51 are the scatter tables of significant wave height versus principal wave direction at the spectral peak for sites No. 5 and 6.

Note that the data are recorded every 1 hour for 20 years from 2001-05-31 23:00:00 to 2022-01-01 00:00:00 extracted from Copernicus Monitoring Environment Marine Service (CMEMS) for Mediterranean Sea waves analysis and forecast [51, 52].

163

7. WEC-Sim

Site No.	Geographical Area	Lat (°)	Long (°)	Water Depth (m)	Nearest port to the WEC location
5	Sea of Sicily-Italy	37°46'48.01"N	12°24'5.38"E	-13	Port of Marsala-Sicily
6	Adriatic Sea-Italy	40°40'3.97"N	17°59'33.06"E	-13	Port of Brindisi-Brindisi

Table 7.35: Sites considered to place the OSWEC

Hs (m)/Tp (s)	1	2	3	4	5	6	7	8	9	10	11	12	13	14	15	16	17
<0.5	0.0089	1.5638	4.58883	11.3709	9.721822	4.606007	1.129336	0.968082	0.15128	0.080904	0.026599	0.012745	0	0.004433	0.000554	0	0
1	0	0.0017	0.6622	3.76704	9.965643	17.04644	7.644353	8.002882	1.330489	0.658318	0.260446	0.084229	0	0.029924	0.002217	0.000554	0
2	0	0	0	0	0.062064	1.542724	2.711958	5.952012	1.206916	0.498171	0.14463	0.058739	0	0.018287	0.006096	0.000554	0
3	0	0	0	0	0	0.003879	0.082013	1.588164	0.945362	0.350216	0.101408	0.023274	0.000554	0.003325	0	0	0
4	0	0	0	0	0	0	0	0.068159	0.294248	0.360745	0.080904	0.00942	0	0	0	0	0
5	0	0	0	0	0	0	0	0.002771	0.014962	0.09365	0.055968	0.008866	0	0	0	0	0
6	0	0	0	0	0	0	0	0	0	0.002217	0.008866	0.008866	0	0	0	0	0
7	0	0	0	0	0	0	0	0	0	0	0	0	0	0	0	0	0
8	0	0	0	0	0	0	0	0	0	0	0	0	0	0	0	0	0
9	0	0	0	0	0	0	0	0	0	0	0	0	0	0	0	0	0

Table 7.36: Probability of occurrence of sea states (%) at site No. 5 for OSWEC

Hs (m)/Tp (s)	1	2	3	4	5	6	7	8	9	10	11	12	13	14	15	16	17
<0.5	16	2822	8281	20520	17544	8312	2038	1747	273	146	48	23	0	8	1	0	0
1	0	3	1195	6798	17984	30762	13795	14442	2401	1188	470	152	0	54	4	1	0
2	0	0	0	0	112	2784	4894	10741	2178	899	261	106	0	33	11	1	0
3	0	0	0	0	0	7	148	2866	1706	632	183	42	1	6	0	0	0
4	0	0	0	0	0	0	0	123	531	651	146	17	0	0	0	0	0
5	0	0	0	0	0	0	0	5	27	169	101	16	0	0	0	0	0
6	0	0	0	0	0	0	0	0	0	4	16	16	0	0	0	0	0
7	0	0	0	0	0	0	0	0	0	0	0	0	0	0	0	0	0
8	0	0	0	0	0	0	0	0	0	0	0	0	0	0	0	0	0
9	0	0	0	0	0	0	0	0	0	0	0	0	0	0	0	0	0

Table 7.37: Occurrence of sea events at site No. 5 for OSWEC

Hs (m)/Tp (s)	1	2	3	4	5	6	7	8	9	10	11	12	13	14	15	16	17
<0.5	0.02475	0.863	3.046	3.3608	3.5256	4.1643	5.0415	5.7041	6.79025	6.9015	7.412	8.202	0	8.17288	7.54275	0	0
1	0	9.578	33.88	37.433	38.717	45.744	54.916	65.839	75.90025	82.926	94.36	93.842	0	88.3973	87.4541	81.6265	0
2	0	0	0	0	158.03	187.11	232.11	260.21	295.024625	339.67	355.6	355.54	0	390.509	358.03	698.541	0
3	0	0	0	0	0	426.82	497.97	592.13	713.35925	739.65	795.7	826.65	802.69	788.655	0	0	0
4	0	0	0	0	0	0	0	1117.6	1260.5	1328.6	1504	1462.1	0	0	0	0	0
5	0	0	0	0	0	0	0	1792.9	1970	2367.5	2505	2329	0	0	0	0	0
6	0	0	0	0	0	0	0	0	0	3128.9	3251	3555.8	0	0	0	0	0
7	0	0	0	0	0	0	0	0	0	0	0	0	0	0	0	0	0
8	0	0	0	0	0	0	0	0	0	0	0	0	0	0	0	0	0
9	0	0	0	0	0	0	0	0	0	0	0	0	0	0	0	0	0

Table 7.38: Mechanical power matrix in terms of kilowatts for OSWEC obtained by WEC-Sim for site No. 5

Hs (m)/Tp (s)	1	2	3	4	5	6	7	8	9	10	11	12	13	14	15	16	17
<0.5	0.0198	0.6902	2.4368	2.6886	2.8205	3.3314	4.0332	4.5633	5.4322	5.5212	5.9296	6.5616	0	6.5383	6.0342	0	0
1	0	7.6621	27.1001	29.9461	30.9737	36.5952	43.9328	52.6713	60.7202	66.3407	75.4842	75.0736	0	70.7178	69.9633	65.3012	0
2	0	0	0	0	126.4203	149.6884	185.6916	208.1707	236.0197	271.7338	284.4922	284.4303	0	312.4069	286.4241	558.8324	0
3	0	0	0	0	0	341.4562	398.3778	473.706	570.6874	591.716	636.5516	661.3185	642.1519	630.9236	0	0	0
4	0	0	0	0	0	0	0	894.1045	1008.4	1062.9	1202.8	1169.7	0	0	0	0	0
5	0	0	0	0	0	0	0	1434.3	1576	1894	2004.1	1863.2	0	0	0	0	0
6	0	0	0	0	0	0	0	0	0	2503.1	2601	2844.6	0	0	0	0	0
7	0	0	0	0	0	0	0	0	0	0	0	0	0	0	0	0	0
8	0	0	0	0	0	0	0	0	0	0	0	0	0	0	0	0	0
9	0	0	0	0	0	0	0	0	0	0	0	0	0	0	0	0	0

Table 7.39: Electrical power matrix in terms of kilowatts for OSWEC obtained by WEC-Sim for site No. 5

Hs (m)/Tp (s)	1	2	3	4	5	6	7	8	9	10	11	12	13	14	15	16	17
<0.5	2E-06	0.0108	0.11182	0.30572	0.274204	0.153445	0.045548	0.044176	0.008218	0.004467	0.001577	0.000836	0	0.00029	3.34E-05	0	0
1	0	0.0001	0.17946	1.12808	3.086728	6.238178	3.358378	4.215222	0.807875	0.436733	0.196595	0.063234	0	0.021161	0.001551	0.000362	0
2	0	0	0	0	0.078461	2.309279	5.035879	12.39034	2.848559	1.3537	0.411462	0.167071	0	0.057129	0.017459	0.003097	0
3	0	0	0	0	0	0.013245	0.32672	7.523226	5.395061	2.072285	0.645511	0.153914	0.003558	0.020977	0	0	0
4	0	0	0	0	0	0	0	0.609414	2.967197	3.834356	0.973118	0.11019	0	0	0	0	0
5	0	0	0	0	0	0	0	0.03974	0.235797	1.773723	1.121656	0.165196	0	0	0	0	0
6	0	0	0	0	0	0	0	0	0	0.055483	0.230611	0.252209	0	0	0	0	0
7	0	0	0	0	0	0	0	0	0	0	0	0	0	0	0	0	0
8	0	0	0	0	0	0	0	0	0	0	0	0	0	0	0	0	0
9	0	0	0	0	0	0	0	0	0	0	0	0	0	0	0	0	0

Table 7.40: Electrical power matrix combined with the probability of occurrence for OSWEC at site No. 5

Hs (m)/Tp (s)	1	2	3	4	5	6	7	8	9	10	11	12	13	14	15	16	17
<0.5	0.0198	0.6902	2.4368	2.6886	2.8205	3.3314	4.0332	4.5633	5.4322	5.5212	5.9296	6.5616	0	6.5383	6.0342	0	0
1	0	7.6621	27.1001	29.9461	30.9737	36.5952	43.9328	52.6713	60.7202	66.3407	75.4842	75.0736	0	70.7178	69.9633	65.3012	0
2	0	0	0	0	126.4203	149.6884	185.6916	208.1707	236.0197	246.3333	246.3333	246.3333	0	246.3333	246.3333	246.3333	0
3	0	0	0	0	0	246.3333	246.3333	246.3333	246.3333	246.3333	246.3333	246.3333	246.3333	246.3333	0	0	0
4	0	0	0	0	0	0	0	246.3333	246.3333	246.3333	246.3333	246.3333	0	0	0	0	0
5	0	0	0	0	0	0	0	246.3333	246.3333	246.3333	246.3333	246.3333	0	0	0	0	0
6	0	0	0	0	0	0	0	0	0	246.3333	246.3333	246.3333	0	0	0	0	0
7	0	0	0	0	0	0	0	0	0	0	0	0	0	0	0	0	0
8	0	0	0	0	0	0	0	0	0	0	0	0	0	0	0	0	0
9	0	0	0	0	0	0	0	0	0	0	0	0	0	0	0	0	0

Table 7.41: Electrical power matrix in terms of kilowatts for the OSWEC device (rated power with a capacity factor of 30% estimated at site No. 5)

Hs (m)/VMDR (deg)	0-30	30-60	60-90	90-120	120-150	150-180	180-210	210-240	240-270	270-300	300-330	330-360
<0.5	641	138	71	106	317	8471	7721	3576	6947	19940	8112	5739
1	867	134	114	147	404	10324	12047	5479	10543	28703	12420	8067
2	149	33	25	24	73	2013	2959	1491	2262	7121	3382	2488
3	20	6	2	3	18	512	904	358	490	1632	870	775
4	16	1	0	1	6	136	175	107	133	420	294	179
5	15	0	0	0	0	18	31	16	28	51	118	41
6	0	0	0	0	0	2	9	2	0	3	19	1
7	0	0	0	0	0	0	0	0	0	0	0	0
8	0	0	0	0	0	0	0	0	0	0	0	0
9	0	0	0	0	0	0	0	0	0	0	0	0

Table 7.42: Scatter table of significant wave height-mean wave direction for site No. 5

Hs (m)/VPED (deg)	0-30	30-60	60-90	90-120	120-150	150-180	180-210	210-240	240-270	270-300	300-330	330-360
<0.5	1706	0	0	0	487	9734	6736	1931	5619	25775	1104	8687
1	2339	0	0	0	697	11933	11080	3058	8227	37867	1489	12559
2	567	0	0	0	149	2427	2690	883	1983	9136	315	3870
3	100	0	0	0	49	671	713	254	411	2103	64	1225
4	35	0	0	0	24	134	169	50	149	546	14	347
5	26	0	0	0	0	20	26	5	35	120	6	80
6	4	0	0	0	0	6	6	0	4	12	4	0
7	0	0	0	0	0	0	0	0	0	0	0	0
8	0	0	0	0	0	0	0	0	0	0	0	0
9	0	0	0	0	0	0	0	0	0	0	0	0

Table 7.43: Scatter table of significant wave height - principal wave direction at spectral peak for site No. 5

Hs (m)/Tp (s)	1	2	3	4	5	6	7	8	9	10	11	12	13	14	15	16	17
<0.5	0.1956	8.3448	12.9863	20.4743	7.979054	2.489194	0.768591	1.072814	0.166796	0.042669	0.011637	0.000554	0	0	0	0	0
1	0	0.0044	0.50427	8.62629	15.48044	11.64524	1.890724	1.447412	0.22886	0.088662	0.030478	0.004433	0	0.001108	0	0	0
2	0	0	0	0	0.053752	2.412169	1.662418	0.624515	0.029924	0.013853	0.004987	0	0.001108	0	0	0	0
3	0	0	0	0	0	0.005541	0.165688	0.446082	0.003325	0	0	0	0.000554	0	0	0	0
4	0	0	0	0	0	0	0	0.068713	0.018287	0.002217	0	0	0	0	0	0	0
5	0	0	0	0	0	0	0	0	0.003325	0.000554	0	0	0	0	0	0	0
6	0	0	0	0	0	0	0	0	0	0	0	0	0	0	0	0	0
7	0	0	0	0	0	0	0	0	0	0	0	0	0	0	0	0	0
8	0	0	0	0	0	0	0	0	0	0	0	0	0	0	0	0	0
9	0	0	0	0	0	0	0	0	0	0	0	0	0	0	0	0	0

Table 7.44: Probability of occurrence of sea states (%) at site No. 6 for OSWEC

Hs (m)/Tp (s)	1	2	3	4	5	6	7	8	9	10	11	12	13	14	15	16	17
<0.5	353	15059	23435	36948	14399	4492	1387	1936	301	77	21	1	0	0	0	0	0
1	0	8	910	15567	27936	21015	3412	2612	413	160	55	8	0	2	0	0	0
2	0	0	0	0	97	4353	3000	1127	54	25	9	0	2	0	0	0	0
3	0	0	0	0	0	10	299	805	6	0	0	0	1	0	0	0	0
4	0	0	0	0	0	0	0	124	33	4	0	0	0	0	0	0	0
5	0	0	0	0	0	0	0	0	6	1	0	0	0	0	0	0	0
6	0	0	0	0	0	0	0	0	0	0	0	0	0	0	0	0	0
7	0	0	0	0	0	0	0	0	0	0	0	0	0	0	0	0	0
8	0	0	0	0	0	0	0	0	0	0	0	0	0	0	0	0	0
9	0	0	0	0	0	0	0	0	0	0	0	0	0	0	0	0	0

Table 7.45: Occurrence of sea events at site No. 6 for OSWEC

Hs (m)/Tp (s)	1	2	3	4	5	6	7	8	9	10	11	12	13	14	15	16	17
<0.5	0.02475	0.863	3.046	3.3608	3.5256	4.1643	5.0415	5.7041	6.79025	6.9015	7.412	8.202	0	0	0	0	0
1	0	9.578	33.88	37.433	38.717	45.744	54.916	65.839	75.90025	82.926	94.36	93.842	0	88.3973	0	0	0
2	0	0	0	0	158.03	187.11	232.11	260.21	295.024625	339.67	355.6	0	395.55	0	0	0	0
3	0	0	0	0	0	426.82	497.97	592.13	713.35925	0	0	0	802.69	0	0	0	0
4	0	0	0	0	0	0	0	1117.6	1260.5	1328.6	0	0	0	0	0	0	0
5	0	0	0	0	0	0	0	0	1970	2367.5	0	0	0	0	0	0	0
6	0	0	0	0	0	0	0	0	0	0	0	0	0	0	0	0	0
7	0	0	0	0	0	0	0	0	0	0	0	0	0	0	0	0	0
8	0	0	0	0	0	0	0	0	0	0	0	0	0	0	0	0	0
9	0	0	0	0	0	0	0	0	0	0	0	0	0	0	0	0	0

Table 7.46: Mechanical power matrix in terms of kilowatts for OSWEC obtained by WEC-Sim for site No. 6

Hs (m)/Tp (s)	1	2	3	4	5	6	7	8	9	10	11	12	13	14	15	16	17
<0.5	0.0198	0.6902	2.4368	2.6886	2.8205	3.3314	4.0332	4.5633	5.4322	5.5212	5.9296	6.5616	0	0	0	0	0
1	0	7.6621	27.1001	29.9461	30.9737	36.5952	43.9328	52.6713	60.7202	66.3407	75.4842	75.0736	0	70.7178	0	0	0
2	0	0	0	0	126.4203	149.6884	185.6916	208.1707	236.0197	271.7338	284.4922	0	316.4423	0	0	0	0
3	0	0	0	0	0	341.4562	398.3778	473.706	570.6874	0	0	0	642.1519	0	0	0	0
4	0	0	0	0	0	0	0	894.1045	1008.4	1062.9	0	0	0	0	0	0	0
5	0	0	0	0	0	0	0	0	1576	1894	0	0	0	0	0	0	0
6	0	0	0	0	0	0	0	0	0	0	0	0	0	0	0	0	0
7	0	0	0	0	0	0	0	0	0	0	0	0	0	0	0	0	0
8	0	0	0	0	0	0	0	0	0	0	0	0	0	0	0	0	0
9	0	0	0	0	0	0	0	0	0	0	0	0	0	0	0	0	0

Table 7.47: Electrical power matrix in terms of kilowatts for OSWEC obtained by WEC-Sim for site No. 6

Hs (m)/Tp (s)	1	2	3	4	5	6	7	8	9	10	11	12	13	14	15	16	17
<0.5	4E-05	0.0576	0.31645	0.55047	0.225049	0.082925	0.030999	0.048956	0.009061	0.002356	0.00069	3.64E-05	0	0	0	0	0
1	0	0.0003	0.13666	2.58324	4.794865	4.261599	0.830648	0.762371	0.138964	0.058819	0.023006	0.003328	0	0.000784	0	0	0
2	0	0	0	0	0.067953	3.610737	3.086971	1.300058	0.070625	0.037645	0.014188	0	0.003506	0	0	0	0
3	0	0	0	0	0	0.018921	0.660063	2.113118	0.018974	0	0	0	0.003558	0	0	0	0
4	0	0	0	0	0	0	0	0.614369	0.184402	0.02356	0	0	0	0	0	0	0
5	0	0	0	0	0	0	0	0	0.052399	0.010495	0	0	0	0	0	0	0
6	0	0	0	0	0	0	0	0	0	0	0	0	0	0	0	0	0
7	0	0	0	0	0	0	0	0	0	0	0	0	0	0	0	0	0
8	0	0	0	0	0	0	0	0	0	0	0	0	0	0	0	0	0
9	0	0	0	0	0	0	0	0	0	0	0	0	0	0	0	0	0

Table 7.48: Electrical power matrix combined with the probability of occurrence for OSWEC at site No. 6

Hs (m)/Tp (s)	1	2	3	4	5	6	7	8	9	10	11	12	13	14	15	16	17
<0.5	0.0198	0.6902	2.4368	2.6886	2.8205	3.3314	4.0332	4.5633	5.4322	5.5212	5.9296	6.5616	0	0	0	0	0
1	0	7.6621	27.1001	29.9461	30.9737	36.5952	43.9328	52.6713	60.7202	66.3407	75.4842	75.0736	0	70.7178	0	0	0
2	0	0	0	0	89.3333	89.3333	89.3333	89.3333	89.3333	89.3333	89.3333	0	89.3333	0	0	0	0
3	0	0	0	0	0	89.3333	89.3333	89.3333	89.3333	0	0	0	89.3333	0	0	0	0
4	0	0	0	0	0	0	0	89.3333	89.3333	89.3333	0	0	0	0	0	0	0
5	0	0	0	0	0	0	0	0	89.3333	89.3333	0	0	0	0	0	0	0
6	0	0	0	0	0	0	0	0	0	0	0	0	0	0	0	0	0
7	0	0	0	0	0	0	0	0	0	0	0	0	0	0	0	0	0
8	0	0	0	0	0	0	0	0	0	0	0	0	0	0	0	0	0
9	0	0	0	0	0	0	0	0	0	0	0	0	0	0	0	0	0

Table 7.49:   Electrical power matrix in terms of kilowatts for the OSWEC device (rated power with a capacity factor of 30% estimated at site No. 6)

Hs (m)/VMDR (deg)	0-30	30-60	60-90	90-120	120-150	150-180	180-210	210-240	240-270	270-300	300-330	330-360
<0.5	8953	6030	5708	13979	15896	2384	796	505	405	578	7785	35390
1	6366	3365	1566	6363	11998	610	159	74	78	171	11245	30103
2	1708	708	127	353	513	0	0	0	0	0	1476	3780
3	296	106	0	4	7	0	0	0	0	0	122	585
4	19	29	0	0	0	0	0	0	0	0	11	102
5	0	0	0	0	0	0	0	0	0	0	0	7
6	0	0	0	0	0	0	0	0	0	0	0	0
7	0	0	0	0	0	0	0	0	0	0	0	0
8	0	0	0	0	0	0	0	0	0	0	0	0
9	0	0	0	0	0	0	0	0	0	0	0	0

Table 7.50: Scatter table of significant wave height-mean wave direction for site No. 6

Hs (m)/VPED (deg)	0-30	30-60	60-90	90-120	120-150	150-180	180-210	210-240	240-270	270-300	300-330	330-360
<0.5	3403	5455	3415	8483	25127	358	347	358	112	141	35185	16025
1	2764	5698	319	3645	16063	4	31	74	12	36	27050	16402
2	1002	962	39	46	840	0	0	0	0	0	3426	2350
3	163	117	0	0	11	0	0	0	0	0	350	479
4	9	29	0	0	0	0	0	0	0	0	36	87
5	0	0	0	0	0	0	0	0	0	0	0	7
6	0	0	0	0	0	0	0	0	0	0	0	0
7	0	0	0	0	0	0	0	0	0	0	0	0
8	0	0	0	0	0	0	0	0	0	0	0	0
9	0	0	0	0	0	0	0	0	0	0	0	0

Table 7.51: Scatter table of significant wave height - principal wave direction at spectral peak for site No. 6

In order to estimate the annual energy production (AEP) for the OSWEC at sites No.5 and 6, the same procedure explained for 2BPA in section 7.2.4 was carried out. The PCC conversion efficiency is $\eta_1 = 0.80$ (80%), the capacity factor is 0.30(30%), transmission efficiency is $\eta_3 = 0.98$ (98%), and device availability is $\eta_2 = 0.95(95\%)$ for OSWEC.

Table 7.52 represents the power performance of the OSWEC at sites No. 5 and No. 6. It was concluded that at site No. 4 (Sea of Sicily), the rated power and AEP of the OSWEC is higher than the site No. 5 (Adriatic Sea) because, in the Adriatic Sea, most of the wave heights are less than 0.50 meters while at the Sea of Sicily most of the wave heights are equal or more than 1 meter. In addition, the annual average electrical power, P_{ae} at site No. 4 is 73.9 kW, while at site No. 5 is 26.8 kW.

Site No.	Rated Power kW	Annual Energy Production (AEP) MWh
4	246.33 kW	603.1087 MWh
5	89.33 kW	218.7187 MWh

Table 7.52: OSWEC rated power and AEP

Moreover, by running the WEC-Sim, the dynamic response of the OSWEC was obtained for sea state $H_s = 2\ m$ and $T_p = 8\ sec$, and for water depth -13 m and shown in Figures 61-66. The WEC-Sim input file used to run the simulation of the OSWEC was given in Script 7.6.
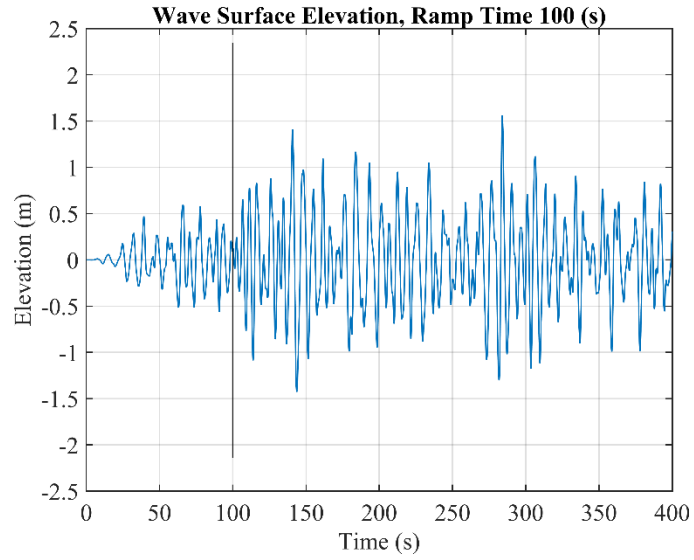
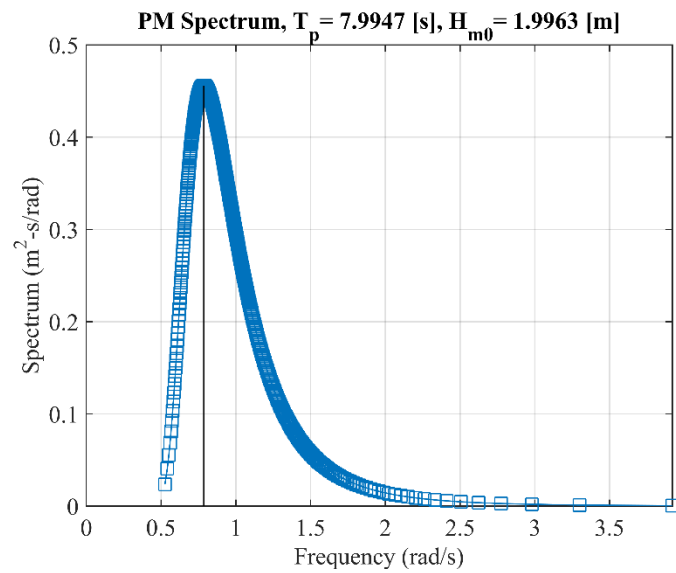Figure 7.61: Irregular wave surface elevation in OSWEC simulation

Figure 7.62: Pierson Moskowitz (PM) spectrum in OSWEC simulation for irregular wave state
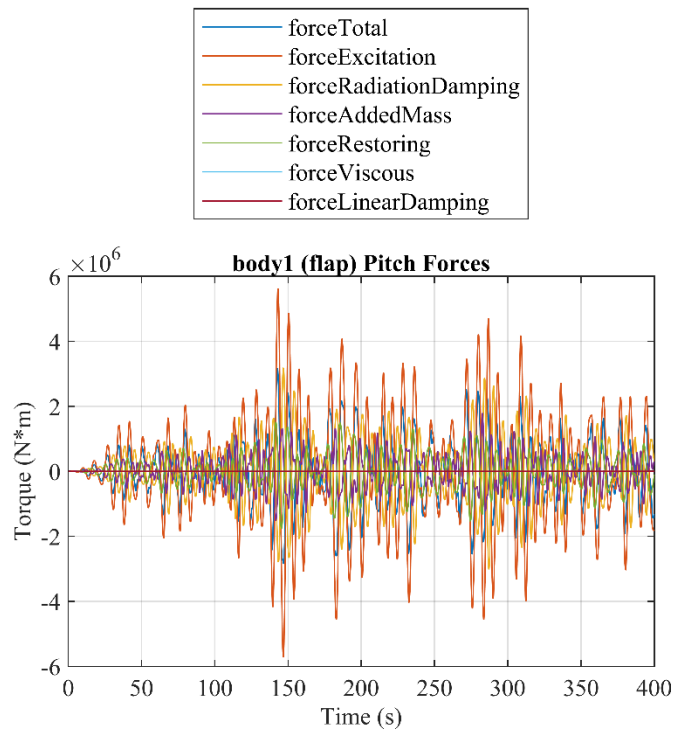
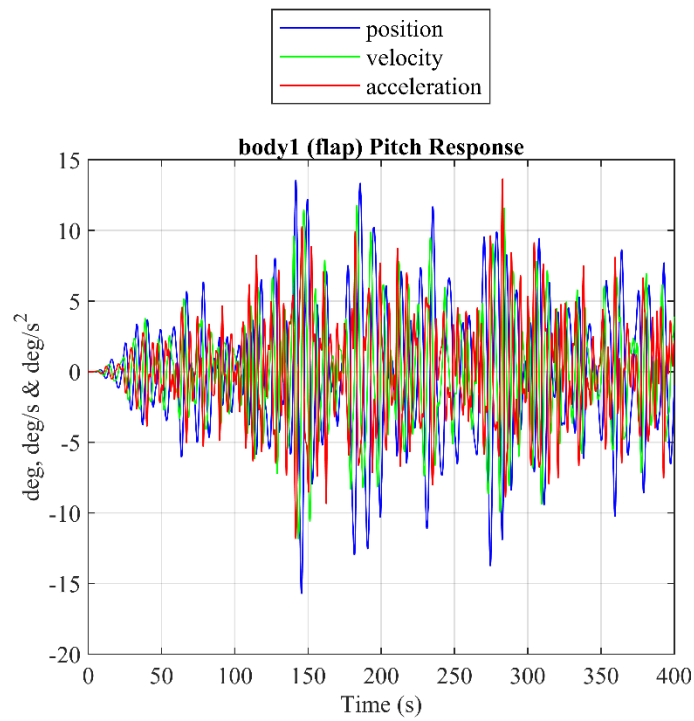Figure 7.63: Flap pitch forces in irregular wave state

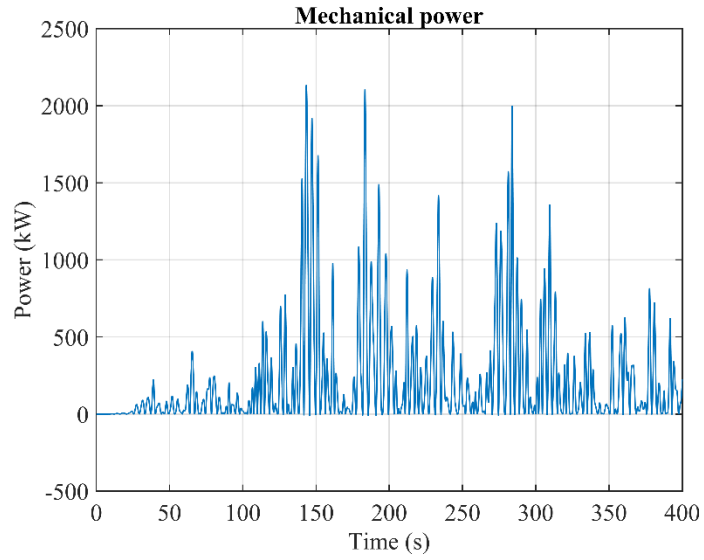Figure 7.64: Flap pitch response in irregular wave state

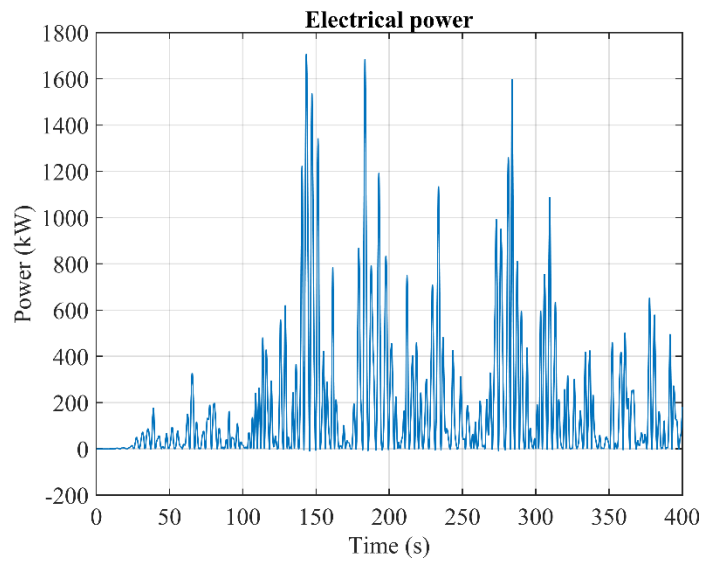Figure 7.65: OSWEC mechanical power in irregular wave state

Figure 7.66: OSWEC electrical power in irregular wave state

8.

Conclusions and Recommendations

8.1 Conclusions

In this thesis, the first step was to mesh the 2BPA and OSWEC using axiMesh.m and Mesh.m functions for the use of NEMOH. For the RM3 2BPA, the axiMesh.m function and for the OSWEC, Mesh.m function were used to mesh the bodies. The hydrostatic properties of the devices such as coordinates of the center of buoyancy (COB) and center of mass (COG), hydrostatic stiffness matrix of the body, water displacement, waterplane area, and the information relative to the number of points and panels in the mesh file for NEMOH were obtained at the end of meshing process. Also, at the end of the meshing process, Nemoh.cal files were created by axiMesh.m and Mesh,m functions which include data for environmental conditions, description of bodies, load cases that have to be solved, and post-processing. It was concluded that the Nemoh MATLAB functions are very user-friendly to mesh the offshore structures and obtain the hydrostatic properties.

The second step was to use Nemoh as a MATLAB wrapper to calculate the hydrodynamic coefficients of 2BPA and OSWEC. The first-order hydrodynamic coefficients, including added mass coefficient, radiation damping coefficient, excitation force, and excitation force phase response, are numerically obtained by running the NEMOH preprocessor successfully. For the 2BPA case, it was concluded that the radiation damping coefficient shows a negative value for specific wave frequencies. These irregular frequencies are related to singularities in the system of equations solved by NEMOH BEM solver. NEMOH 2.03 is the version of the solver used in this thesis, which does not have the additional equations required for removing these singularities. However, the ability to remove these singularities will be available in a future version of NEMOH. Nevertheless, for the OSWEC case, it was concluded that there were no significant irregular frequencies in the radiation damping coefficient obtained by NEMOH.

The third step was to generate a *.h5 file for 2BPA and OSWEC devices. The *.h5 files were created via BEMIO, a pre-and post-processing tool developed by WEC-Sim. Further, the output data for 2BPA and OSWEC resulting from BEMIO were plotted. It was concluded that for 2BPA, the normalized radiation damping was negative in specific wave frequencies because the radiation damping coefficient $B(\omega)$ was negative in those frequencies due to a fundamental error in the formulation of the NENOH BEM solver. It was also concluded that the normalized excitation force magnitude curve did not regularly descend when the wave frequency was increased. The reason

8. Conclusions and Recommendations

for having such an irregular curve for normalized excitation force magnitude was the irregular spikes that NEMOH could not remove. Nevertheless, for OSWEC, it was concluded that there were no significant irregular frequencies in normalized added mass, normalized radiation damping, and normalized excitation force, which indicates that the NEMOH works well calculating hydrodynamic coefficients for OSWEC devices.

In the 7th step, the dynamic responses of the 2BPA and OSWEC were obtained using WEC-Sim. The dynamic responses of the 2BPA for unmoored and moored installation types were studied. For the unmoored case, it was concluded that after 5000 seconds, the device moved 100 meters along the negative direction of the x-axis in a regular wave state. Hence, the surge response of the device had to be controlled using mooring lines. Then, the 2BPA with three mooring lines was simulated by coupling the WEC-Sim and MoorDyn external code. The simulation results showed identical float and spar-plate pitch responses and pitch forces in both moored and unmoored cases. Also, the heave responses of the float and spar-plate and their surge forces were identical in both unmoored and moored cases. However, in the spar heave forces, the restoring force gained an initial value because of the initial displacement of the spar. Moreover, by simulating the surge response of the device for 5000 seconds, it was concluded that the mooring lines fixed the device in its location so that it was not moving along the x-axis. It was also denoted that by comparing the power performances in both unmoored and moored cases, there were no changes in the mechanical and electrical power magnitudes. Finally, it was concluded that the mooring lines did not affect the resonance phenomena of the system since the relative displacement of the float/spar-plate in both moored and unmoored cases remained unchanged.

In the 7th step, the rated power and annual energy production (AEP) of 2BPA and OSWEC were estimated using the 20 years of wave state record gathered for different sites in the Mediterranean Sea and the North Sea. For 2BPA in the Italian Mediterranean Sea, it was concluded that the Sea of Sardinia is the best location to deploy the 2BPA since the power performance at this site is higher than the power performance at the Sea of Sicily and the Tyrrhenian Sea. To deploy the 2BPA at Sardinia Sea, the manufacturer has to design the device so that its rated power should be 108.33 kW. The AEP estimated at the Sea of Sardinia was 265.23 MWh. However, for the North Sea, the estimated AEP was 671.7439 MWh, and it was the highest AEP that can be obtained among other sites. The reason is that there are higher waves at the North Sea with a higher probability of occurrence. The estimated rated power that the manufacturer has to design for 2BPA at the North Sea was 274.4 kW. The rated power estimated for all sites was obtained by assuming a capacity factor equal to 30%, which is the optimal value. In addition to 2BPA, two sites were considered for OSWEC deployment. It was concluded that the AEP of the device at the Sea of Sicily was 603.1087 MWh which was higher than the AEP estimated for the Adriatic Sea because, in the Adriatic Sea, most of the wave heights are less than 0.50 meters.

In contrast, most waves' heights are equal to or more than 1 meter at the Sea of Sicily. The rated power estimated for the Sea of Sicily was 246.33 kW assuming the capacity factor equal to 30%. So, for deploying the OSWEC in the Sea of Sicily, the manufacturer has to limit the device's rated power to 246.33 kW.

8. Conclusions and Recommendations

Overall, the NEMOH tool is capable of meshing the floating structures and calculating the hydrodynamic coefficients. The NEMOH has been demonstrated to be a useful tool for the simulation of WECs and the estimation of AEP. NEMOH and WEC-Sim can be used by engineers to simulate the dynamic behavior of a floating body without using more sophisticated tools such as ANSYS and WAMIT. The NEMOH code is more user-friendly compared to WAMIT. However, at this moment, unlike WAMIT, NEMOH cannot remove irregular frequencies created during calculating the hydrodynamic coefficients. The future versions of NEMOH will have additional equations required for removing the singularities, which in this case this tool will be the priority of any engineer who wants to have the most accurate and real results.

8.2 Recommendations

For future work on this subject, there is still room for improvement. In order to help the researchers to make improvements to the research, the following suggestions are given:

Better Meshes for the Models

The meshes for the 2BPA and OSWEC can be refined using alternative methods such as WAMIT and ANSYS-AQWA. The WAMIT can remove the irregular frequencies created during the calculation of the hydrodynamic coefficients, but in NEMOH, it is not possible at this time.

Perform Tests in the Laboratory

The author strongly suggests performing laboratory tests to validate the numerical simulation results obtained by WEC-Sim. In science, experiments play many roles, and testing theories and providing new scientific knowledge are two of its essential functions. Alternatively, it can indicate that an accepted theory is incorrect, or it can be an indication that a new phenomenon needs to be explained.

Bibliography

[1] C. Miller, "A brief history of wave and tidal energy experiments in San Francisco and Santa Cruz," *Western Neighborhoods Projects. Western Neighborhoods Project,* vol. 3, 2004

[2] O. E. Europe, "Ocean Energy: Key Trends and Statistics 2020," ed: OEE Brussles, Belgium, 2021

[3] S. Barstow, G. Mørk, D. Mollison, and J. Cruz, "The wave energy resource," in *Ocean wave energy*, ed: Springer, 2008, pp. 93-132

[4] IRENA, "Ocean Energy Technology Brief 4," *www.irena.org*, 2014

[5] R. Pelc and R. M. Fujita, "Renewable energy from the ocean," *Marine Policy,* vol. 26, pp. 471-479, 2002

[6] A. Babarit, J. Hals, M. J. Muliawan, A. Kurniawan, T. Moan, and J. Krokstad, "Numerical benchmarking study of a selection of wave energy converters," *Renewable energy,* vol. 41, pp. 44-63, 2012

[7] J. van Rij, Y.-H. Yu, K. Edwards, and M. Mekhiche, "Ocean power technology design optimization," *International Journal of Marine Energy,* vol. 20, pp. 97-108, 2017

[8] T. Whittaker and M. Folley, "Nearshore oscillating wave surge converters and the development of Oyster," *Philosophical Transactions of the Royal Society A: Mathematical, Physical and Engineering Sciences,* vol. 370, pp. 345-364, 2012

[9] K. Ruehl, C. Michelen, S. Kanner, M. Lawson, and Y.-H. Yu, "Preliminary verification and validation of WEC-Sim, an open-source wave energy converter design tool," in *International conference on offshore mechanics and arctic engineering*, 2014, p. V09BT09A040

[10] S. Sirnivas, Y.-H. Yu, M. Hall, and B. Bosma, "Coupled mooring analyses for the WEC-Sim wave energy converter design tool," in *International Conference on Offshore Mechanics and Arctic Engineering*, 2016, p. V006T09A023

[11] B. Bosma, W. Sheng, and F. Thiebaut, "Performance assessment of a floating power system for the galway bay wave energy test site," in *International Conference on Ocean Energy (ICOE), Halifax, NS, Canada, Nov*, 2014, pp. 4-6

[12] V. S. Neary, M. Lawson, M. Previsic, A. Copping, K. C. Hallett, A. Labonte, *et al.*, "Methodology for design and economic analysis of marine energy conversion (MEC) technologies," 2014

[13] J. C. Berg, "Extreme ocean wave conditions for northern California wave energy conversion device," *Sandia Natl. Lab. Doc. SAND,* vol. 9304, p. 2011, 2011

Bibliography

[14] M. Previsic and J. Berg, "Reference Model Development Wave Energy Resource and Site Characterization," *Report by ReVision. Report for US Department of Energy (DOE)*, 2010

[15] V. S. Neary, M. Previsic, R. A. Jepsen, M. J. Lawson, Y.-H. Yu, A. E. Copping*, et al.*, "Methodology for Design and Economic Analysis of Marine Energy Conversion (MEC) Technologies."

[16] Y.-H. Yu, Y. Li, K. Hallett, and C. Hotimsky, "Design and analysis for a floating oscillating surge wave energy converter," in *International Conference on Offshore Mechanics and Arctic Engineering*, 2014, p. V09BT09A048

[17] Y.-H. Yu, D. Jenne, R. Thresher, A. Copping, S. Geerlofs, and L. Hanna, "Reference model 5 (rm5): Oscillating surge wave energy converter," National Renewable Energy Lab.(NREL), Golden, CO (United States)2015

[18] B. P. Dooher, E. Cheslak, R. Booth, D. Davy, A. Faraglia, I. Caliendo*, et al.*, "PG&E WaveConnect Program Final Report," Pacific Gas and Electric Company2011

[19] M. Lawson, Y.-H. Yu, K. Ruehl, and C. Michelen, "Development and demonstration of the WEC-Sim wave energy converter simulation tool," 2014

[20] J. van't Hoff, M. Folley, and T. Whittaker, "Numerical Modelling of an Oscillating Wave Surge Converter Using Volterra Theory," in *Proceedings of the 11th European Wave and Tidal Energy Conference, Nantes, France*, 2015, pp. 6-11

[21] IEA-OES, "Annual Report—An Overview of Ocean Energy Activities in 2020," ed: The Executive Committee of Ocean Energy Systems Lisbon, Portugal, 2021

[22] S. Bozzi, A. M. Miquel, A. Antonini, G. Passoni, and R. Archetti, "Modeling of a point absorber for energy conversion in Italian seas," *Energies,* vol. 6, pp. 3033-3051, 2013

[23] A. Viola, V. Franzitta, D. Curto, M. Trapanese, V. Di Dio, G. Cipriani*, et al.*, "Design of wave energy converter (WEC): A prototype installed in Sicily," in *OCEANS 2015-Genova*, 2015, pp. 1-5

[24] S. Bozzi, A. M. Miquel, F. Scarpa, A. Antonini, R. Archetti, G. Passoni*, et al.*, "Wave energy production in Italian offshore: Preliminary design of a point absorber with tubular linear generator," in *2013 International Conference on Clean Electrical Power (ICCEP)*, 2013, pp. 203-208

[25] C. H. Lee and J. N. Newman, "Wamit user manual," *WAMIT, Inc,* p. 42, 2006

[26] A. ANSYS, "Users Manual (ver. 14.0)," *ANSYS Incorporated, Canonsburg, PA,* 2012

[27] M. Penalba, T. Kelly, and J. Ringwood, "Using NEMOH for modelling wave energy converters: A comparative study with WAMIT," 2017

[28] T. S. Mckie, "Optimization of Point Absorber Design in Ocean Wave Energy," 2019

[29] M. Amini-Afshar and H. B. Bingham, "Added resistance using Salvesen–Tuck–Faltinsen strip theory and the Kochin function," *Applied Ocean Research,* vol. 106, p. 102481, 2021

[30] G. Giorgi and J. V. Ringwood, "Comparing nonlinear hydrodynamic forces in heaving point absorbers and oscillating wave surge converters," *Journal of Ocean Engineering and Marine Energy,* vol. 4, pp. 25-35, 2018

Bibliography

[31] A. Babarit and G. Delhommeau, "Theoretical and numerical aspects of the open source BEM solver NEMOH," in *11th European wave and tidal energy conference (EWTEC2015)*, 2015

[32] B. Guo, R. Patton, S. Jin, J. Gilbert, and D. Parsons, "Nonlinear modeling and verification of a heaving point absorber for wave energy conversion," *IEEE transactions on sustainable energy,* vol. 9, pp. 453-461, 2017

[33] A. Pecher and J. P. Kofoed, *Handbook of ocean wave energy*: Springer Nature, 2017

[34] J. N. Newman, *Marine hydrodynamics*: The MIT press, 2018

[35] E. M. Lewandowski, *The dynamics of marine craft: maneuvering and seakeeping* vol. 22: World scientific, 2004

[36] M. Folley, T. Whittaker, and J. Van't Hoff, "The design of small seabed-mounted bottom-hinged wave energy converters," in *Proceedings of the 7th European wave and tidal energy conference*, 2007, p. 312

[37] C. Bergin, C. Beringer, D. Brandt, M. Carlson-Funk, C. Dizon, D. Gaebele*, et al.*, "Lightning: A Wave Energy Converter to Power the Future of Ocean Observation by Obseaver Marine Energy."

[38] G. Kanagaraj, "Modelling of the Novi Ocean Wave Energy Converter using WEC-Sim," ed, 2021

[39] P. McIver and D. Evans, "The occurrence of negative added mass in free-surface problems involving submerged oscillating bodies," *Journal of engineering mathematics,* vol. 18, pp. 7-22, 1984

[40] S. Mavrakos and P. Koumoutsakos, "Hydrodynamic interaction among vertical axisymmetric bodies restrained in waves," *Applied Ocean Research,* vol. 9, pp. 128-140, 1987

[41] T. F. Ogilvie, "First-and second-order forces on a cylinder submerged under a free surface," *Journal of Fluid Mechanics,* vol. 16, pp. 451-472, 1963

[42] J. S. Chung, "Forces on submerged cylinders oscillating near a free surface," *Journal of Hydronautics,* vol. 11, pp. 100-106, 1977

[43] J. N. Newman, "The motions of a floating slender torus," *Journal of Fluid Mechanics,* vol. 83, pp. 721-735, 1977

[44] S. Wang and R. Wahab, "Heaving oscillations of twin cylinders in a free surface," *Journal of Ship Research,* 1971

[45] M. Srokosz and D. Evans, "A theory for wave-power absorption by two independently oscillating bodies," *Journal of Fluid Mechanics,* vol. 90, pp. 337-362, 1979

[46] K. Ruehl, C. Michelen, B. Bosma, and Y.-H. Yu, "WEC-Sim phase 1 validation testing: Numerical modeling of experiments," in *International Conference on Offshore Mechanics and Arctic Engineering*, 2016, p. V006T09A026

[47] K. M. Ruehl and C. Michelen, "WEC-Sim Training Course," Sandia National Lab.(SNL-NM), Albuquerque, NM (United States)2015

[48] M. Bonfanti, A. Hillis, S. A. Sirigu, P. Dafnakis, G. Bracco, G. Mattiazzo*, et al.*, "Real-time wave excitation forces estimation: An application on the ISWEC device," *Journal of Marine Science and Engineering,* vol. 8, p. 825, 2020

Bibliography

[49] Y. Li and Y.-H. Yu, "A synthesis of numerical methods for modeling wave energy converter-point absorbers," *Renewable and Sustainable Energy Reviews,* vol. 16, pp. 4352-4364, 2012

[50] M. Hall, "MoorDyn user's guide," *Department of Mechanical Engineering, University of Maine: Orono, ME, USA,* vol. 15, 2015

[51] Korres, G., Ravdas, M., Zacharioudaki, A., Denaxa, D., & Sotiropoulou, M. (2021). Mediterranean Sea Waves Reanalysis (CMEMS Med-Waves, MedWAM3 system) (Version 1) set. Copernicus Monitoring Environment Marine Service (CMEMS). https://doi.org/10.25423/CMCC/MEDSEA_MULTIYEAR_WAV_006_012

[52] Korres, G., Ravdas, M., Zacharioudaki, A., Denaxa, D., & Sotiropoulou, M. (2021). Mediterranean Sea Waves Analysis and Forecast (CMEMS MED-Waves, MedWAM3 system) (Version 1) set. Copernicus Monitoring Environment Marine Service (CMEMS). https://doi.org/10.25423/CMCC/MEDSEA_ANALYSISFORECAST_WAV_006_017_MEDWAM3

[53] https://doi.org/10.48670/moi-00060